ASSESSMENT OF NONLINEAR STATIC (PUSHOVER) ANALYSIS PROCEDURES USING FIELD EXPERIENCE

A THESIS SUBMITTED TO
THE GRADUATE SCHOOL OF NATURAL AND APPLIED SCIENCES
OF
MIDDLE EAST TECHNICAL UNIVERSITY

BY

ABDULLAH DİLSİZ

IN PARTIAL FULFILLMENT OF THE REQUIREMENTS
FOR
THE DEGREE OF DOCTOR OF PHILOSOPHY
IN
CIVIL ENGINEERING

NOVEMBER 2013

Approval of the thesis:

ASSESSMENT OF NONLINEAR STATIC (PUSHOVER) ANALYSIS PROCEDURES USING FIELD EXPERIENCE

submitted by **ABDULLAH DİLSİZ** in partial fulfillment of the requirements for the degree of **Doctor of Philosophy in Civil Engineering Department, Middle East Technical University** by,

Prof. Dr. Canan Özgen ______________________
Dean, Graduate School of **Natural and Applied Sciences**

Prof. Dr. Ahmet Cevdet Yalçıner ______________________
Head of Department, **Civil Engineering**

Prof. Dr. Polat Gülkan ______________________
Supervisor, **Civil Engineering Dept., METU**

Prof. Dr. Ahmet Yakut ______________________
Co-Supervisor, **Civil Engineering Dept., METU**

Examining Committee Members:

Prof. Dr. Haluk Sucuoğlu ______________________
Civil Engineering Dept., METU

Prof. Dr. Polat Gülkan ______________________
Civil Engineering Dept., METU

Prof. Dr. Kurtuluş Soyluk ______________________
Civil Engineering Dept., Gazi University

Prof. Dr. Güney Özcebe ______________________
Civil Engineering Dept., TED University

Assoc. Prof. Dr. M. Altuğ Erberik ______________________
Civil Engineering Dept., METU

Date: ______________________

I hereby declare that all information in this document has been obtained and presented in accordance with academic rules and ethical conduct. I also declare that, as required by these rules and conduct, I have fully cited and referenced all material and results that are not original to this work.

Name, Last Name: Abdullah Dilsiz

Signature :

ABSTRACT

ASSESSMENT OF NONLINEAR STATIC (PUSHOVER) ANALYSIS PROCEDURES USING FIELD EXPERIENCE

Dilsiz, Abdullah
Ph.D., Department of Civil Engineering
Supervisor: Prof. Dr. Polat Gülkan
Co-Supervisor: Prof. Dr. Ahmet Yakut

November 2013, 310 pages

Recently, many nonlinear analysis procedures have been proposed for earthquake response determination of the structures. Although, the nonlinear response history analysis (NRHA) is accepted as the most accurate source of information for nonlinear seismic response, nonlinear static procedures (NSP) may also provide reasonable estimates of seismic demand and inelastic behavior. However, all proposed NSPs have limitations, due to the certain approximations and simplifications, such as invariable load pattern and single mode consideration.

This study is concentrated on the “NSPs” which are generally compared with the “exact results” of NRHA. The current widely used NSPs’ results were compared with the results of both NRHA and the “real” results (real building performance records or experimental results). The results of observations of real structures which

are subjected to strong ground motions were used for the assessment. In addition, the buildings were evaluated using nonlinear static and nonlinear dynamic detailed assessment procedures of the current codes.

Considering “If I had known that this Earthquake would happen 1 day before the occurrence of the earthquake, could I estimate the damage states, using the widely used NSPs?” moderately and heavily damaged building samples have been collected from Adapazarı and analytical models formed.

According to the results of NSPs and NRHA of studied buildings, there is no clear result that any of the procedures used can identify the performance point suitably for each condition.

Most of the analyses results could not predict the level of damage accurately. Using these results it is not possible to determine the seismic response and the damage of the buildings before the occurrence of earthquake. The expectations obtained from the NSPs also do not comply with the results of NRHA. Thus; there is no safety for the compatibility of pushover procedures as well as the code specifications with field observations, yet.

Considering the high effort given for the computation and post-process of the analyses results, global seismic performance of the buildings were assessed by preliminary assessment procedures. In contrary with the detailed assessment results, the vulnerable buildings studied could be evaluated successfully and qualified according to moderate or severe damage experienced during the earthquake by some preliminary assessment procedures.

The valuable information about the seismic behavior of RC buildings obtained from the tests should be supported with more data obtained from the field. This strikes a pessimistic tone because if the inconsistencies between field data and assessment procedures described in guidelines on account of fluctuations of material properties, geometries, ground motion variations and many other parameters considered then a clear need exists to be sanguine about the predictive powers of these methods.

Keywords: Pushover Analysis, Nonlinear Static Procedures, Nonlinear Response, Approximate Procedures, Detailed Assessment Procedures**...**

ÖZ

DOĞRUSAL OLMAYAN STATİK İTKİ HESAP YÖNTEMLERİNİN SAHA TECRÜBESİ KULLANILARAK DEĞERLENDİRİLMESİ

Dilsiz, Abdullah
Doktora, İnşaat Mühendisliği Bölümü
Tez Yöneticisi: Prof. Dr. Polat Gülkan
Ortak Tez Yöneticisi: Prof. Dr. Ahmet Yakut

Kasım 2013, 310 sayfa

Son yıllarda yapıların deprem davranışını belirlemek için birçok doğrusal olmayan yöntem yayınlanmıştır. Doğrusal olmayan davranış geçmişi hesabı (NRHA), doğrusal olmayan deprem davranışı konusunda en doğru bilgi kaynağı olarak kabul edilse de, doğrusal olmayan statik yöntemler (NSP) ile de deprem talebi ve elastik ötesi davranış konusunda güvenilir tahminler yapılabilir. Fakat her NSP'nin belirli kabul ve basitleştirmelerden (değişmeyen yükleme modeli ve tek modun hesaba katılması) dolayı kısıtlamaları vardır.

Bu çalışma genellikle NRHA'nın "doğru sonuçları" ile karşılaştırılan NSP'ler üzerine yoğunlaşmaktadır. Halen çok kullanılan NSP sonuçlarının hem NRHA ve hem de "gerçek" sonuçlar (gerçek bina performans kayıtları) ile karşılaştırılmıştır.

Değerlendirme için depremlere maruz kalmış gerçek bina gözlemleri kullanılmıştır. Ayrıca, bu binalar mevcut kodlarca tanımlanan doğrusal olmayan statik ve doğrusal olmayan dinamik yöntemler kullanılarak değerlendirilmiştir.

“Eğer 1 gün öncesinde bu depremin olacağını bilseydim, eldeki hesap yöntemleri (NSP) ile bu hasar mertebesini tahmin edebilir miydim?” sualinden hareketle 17 Ağustos Marmara Depremi’ne maruz kalmış Adapazarı’ndan orta ve ağır hasarlı bina örnekleri alınmış ve analitik modelleri oluşturulmuştur.

Toplanan bina örnekleri üzerinde yapılan çalışmalarda NSP ve NRHA sonuçlarına bakıldığında, kullanılan yaklaşık yöntemler ile performans noktası tahminlerinin doğruya yakın olarak tahmin edildiğine dair açık bir sonuç yoktur.

Yaklaşık hesap sonuçlarına göre bu hasar seviyeleri doğru bir şekilde belirlenememiştir. Bu sonuçlara göre, depremin meydana gelişinden önce deprem davranışı ve hasarın belirlenmesi mümkün olmamıştır. Ayrıca, NSP ile elde edilen yaklaşık performans tahminleri NRHA sonuçları ile de uyum sağlamamıştır. Çalışmanın bu kısmı sonucuna göre, statik itki hesap yöntemlerinin ve ayrıca yönetmelik şartlarının arazi gözlemleriyle uyumu konusunda yeterli güvenilirlik henüz yoktur.

Bilgisayar hesaplamaları ve sonrasındaki değerlendirme için harcanan yoğun çaba düşünülerek, seçilen binalar üzerinde ön değerlendirme yöntemleri de uygulanmıştır. Detaylı değerlendirme yöntemleri sonuçlarının aksine, hassas binaların depremde gözlenen orta ve ağır hasar durumları yeterli seviyede nitelenebilmiştir.

Betonarme binaların deprem davranışı hakkında deneysel sonuçlardan elde edilen çok kıymetli bilgilerin çok daha fazla arazi bilgisi ile desteklenmesi gereklidir. Buradaki karamsar vurgu şartnamelerce tanımlanan değerlendirme yöntemleri ile arazi verisi arasındaki uyumsuzluk nedeni iledir ki; bu malzeme özellikleri, geometri, yer hareketindeki değişiklikler ve daha başka değişkenlerin hesabındaki tereddütlerden kaynaklanmaktadır. Bu yöntemlerin tahmin gücü konusunda umutlu olabilmek için bunların aşılmasına ihtiyaç vardır.

Anahtar Kelimeler: İtme Analizi, Elastik Ötesi Statik Yöntemler, Elastik Ötesi Davranış, Yaklaşık Yöntemler, Detaylı Değerlendirme Yöntemleri**...**

To my family…

ACKNOWLEDGEMENTS

First of all, I would like to express my deepest appreciation to my supervisor Prof. Dr. Polat Gülkan for his supervision, support and encouragement and to my co-supervisor Prof. Dr. Ahmet Yakut for his guidance, advice and criticism throughout the study. Furthermore, I would like to thank to Dr. Gülkan for providing me the opportunity to make research at UC Berkeley for one year.

I would also like to thank Drs. Halûk Sucuoğlu, Kurtuluş Soyluk, Güney Özcebe, and M. Altuğ Erberik for serving on my dissertation committee. Suggestions and discussions by Dr. Sucuoğlu at various stages of the study and his keen insight are acknowledged.

I would like to thank to Dr. Khalid M. Mosalam for hosting me at UC Berkeley as a visiting scholar for one year and providing me the opportunity of the research in Berkeley. I would also like to extend my thanks to Dr. M Selim Günay for his help and support during the research at UC Berkeley, comments and advice on my thesis, and for his invaluable friendship.

Especially, my dear friend Dr. Özgür Avşar deserves special thank for his friendship, help, kindness and willingness to answer my extended questions. His continuous encouragement is greatly appreciated.

I want to thank all my friends and colleagues at Structural Mechanics Laboratory, especially Dr. İlker Kazaz, Vesile H Akansel, Dr. Tuba Eroğlu Azak, Özkan Kale, Dr. B. Özer Ay, Aida Azari, Dr. Beyhan Bayhan for their help and friendship during my assistantship. Moreover, I cannot forget Mr. Sebay Durul; he was always patient and helpful.

I also want to thank to Dr. Naci Çağlar (Sakaya Uni.), Naci Çelik and Nigar Coşar Bal (Adapazarı Municipality), Sadi Şentürk (Directorate of Public Works and Resettlement in Adapazarı), Ahmet Erdem (former head of the Chamber of the Civil Engineers Branch in Adapazarı) and the other designer and constructer engineers of the buildings studied, for their help, information provided and discussions on the damaged buildings studied.

This study was supported by the State Planning Organization (DPT) Grant No: BAP-09-11-DPT-2002K125/510, and the visiting scholarship at UC Berkeley was supported by TÜBİTAK 2214-Grant, which are also gratefully acknowledged.

Last but not the least, my great family… I wish to dedicate this dissertation to my wife Şeyda Sevde and to my beloved daughter Zeynep Betül. I am thankful to my parents Cemil and Şerife, to my brothers Ahmet, Mustafa Şükrü and Muhammed Ali, to my mother-in-law Betül, to my sister-in-law Büşra S., her husband Muhammed Lütfü and her daughter Bahar Erva, to my nieces Dilara and Elif, and to my nephew Cemil. Their enduring love and unconditional support and encouragement have been the real inspiration that I always felt during the course of this study.

TABLE OF CONTENTS

ABSTRACT v
ÖZ.......... viii
ACKNOWLEDGEMENTS xii
TABLE OF CONTENTS xiv
LIST OF TABLES xix
LIST OF FIGURES.......... xxi
CHAPTERS
1. INTRODUCTION 1
   1.1 GENERAL, BACKGROUND, STATEMENT OF THE PROBLEM 1
   1.2 Review of Previous Works / Literature Survey 8
   1.3 Objective and Scope.......... 13
   1.4 Organization of the Dissertation 15
2. NONLINEAR ASSESSMENT PROCEDURES 17
   2.1 Introduction 17
   2.2 Inelastic Response Prediction Methods Using Nonlinear Static Procedures (NSP) 21
      2.2.1 Displacement Coefficient Method (DCM) of FEMA-356 (FEMA 2000).......... 22
      2.2.2 Displacement Coefficient Method (DCM) of FEMA-440 (ATC 2005) 26
      2.2.3 Capacity Spectrum Method (CSM) of ATC-40 (ATC 1996) 28
      2.2.4 Capacity Spectrum Method (CSM) of FEMA-440 (ATC 2005) 33

2.2.5 Nonlinear Analysis of Equivalent SDOF System (Eq. SDOF) (Fajfar and Fischinger 1987) 36
2.2.6 Modified Modal Pushover Analysis (MMPA) (Chopra et al. 2004) 37
2.3 Building Performance Definitions 39
2.3.1 Performance Definitions of ASCE/SEI-41 (ASCE 2007) 41
2.3.2 Performance Definitions of TEC-2007 (TEC 2007) 42
2.3.3 Performance Definitions of EC8-3 (EC 2005) 42
2.3.4 Performance Definitions of ATC-40 (ATC 1996) 44
2.4 Acceptability Limits / Performance Criteria 44
2.4.1 Response Limits of ATC-40 (ATC 1996) 45
2.4.2 Response Limits of ASCE/SEI-41 and Supplement-1 (ASCE 2007, ASCE 2008) 46
2.4.3 Response Limits of TEC-2007 (TEC 2007) 49
2.4.4 Response Limits of EC8-3 (EC 2005) 51
3. THE AUGUST 17, 1999, MARMARA EARTHQUAKE 55
3.1 Introduction 55
3.2 August 17, 1999, Marmara Earthquake 56
3.3 Strong Ground Motion Record and Derived Site Specific Ground Motion 58
3.4 Seismicity and Geotechnical Description of Adapazarı 62
3.5 Post Earthquake Damage Assessment 65
3.6 Description of Damage in Adapazarı 66
4. DESCRIPTION OF THE SELECTED BUILDINGS 75
4.1 Selection of the Damaged Buildings 75
4.2 General Properties of Selected Buildings for the Study 76
4.3 Adapazarı Survey Using GIS Tools 81
5. ANALYSIS OF THE BUILDINGS 83
5.1 Introduction 83
5.2 OpenSees as a Modeling Tool and Analysis Environment 84
5.2.1 Elements 85

5.2.2 Materials 87
5.3 Analytical Models 90
5.3.1 Building Models 90
5.3.2 Modeling Assumptions 99
5.4 Eigenvalue Analysis and Modal Properties 99
5.5 Nonlinear Response History Analysis of the Buildings 100
5.5.1 Results of Nonlinear Response History Analysis (NRHA) 100
5.5.2 Examination of Incomplete NRHA Results 112
5.6 Nonlinear Static Analysis of the Buildings 116
5.6.1 Building #1 118
5.6.2 Building #2 119
5.6.3 Building #3 120
5.6.4 Building #4 121
5.6.5 Building #5 122
5.6.6 Building #6 123
5.6.7 Building #7 124
5.6.8 Building #8 125
5.6.9 Building #9 126
5.6.10 Building #10 127
5.6.11 Discussion of the NSP Results 128
6. PERFORMANCE ASSESSMENT OF THE BUILDINGS 131
6.1 Introduction 131
6.2 Shear Check (Demand / Capacity) 132
6.3 Detailed Assessment according to ASCE/SEI-41 142
6.3.1 Building #1 144
6.3.2 Building #2 147
6.3.3 Building #3 150
6.3.4 Building #4 153
6.3.5 Building #5 156
6.3.6 Building #6 159
6.3.7 Building #7 162

6.3.8 Building #8 164
6.3.9 Building #9 168
6.3.10 Building #10 172
6.4 Detailed Assessment according to TEC-2007 174
6.4.1 Building #1 177
6.4.2 Building #2 180
6.4.3 Building #3 182
6.4.4 Building #4 185
6.4.5 Building #5 187
6.4.6 Building #6 190
6.4.7 Building #7 193
6.4.8 Building #8 195
6.4.9 Building #9 198
6.4.10 Building #10 201
6.5 Detailed Assessment according to EC8-3 203
6.5.1 Building #1 205
6.5.2 Building #2 208
6.5.3 Building #3 210
6.5.4 Building #4 213
6.5.5 Building #5 215
6.5.6 Building #6 218
6.5.7 Building #7 221
6.5.8 Building #8 223
6.5.9 Building #9 226
6.5.10 Building #10 229
6.6 Discussion of the Assessment Results and Comparisons 232
7. EVALUATION USING PRELIMINARY ASSESSMENT PROCEDURES 235
7.1 Introduction 235
7.2 Preliminary Assessment Procedures 236
7.2.1 Hassan and Sözen (1997) Procedure 236
7.2.2 Yakut (2004) Procedure 240

7.2.3 Özcebe et al. (2004) Procedure 245
7.3 Interpretations and Discussions 253
8. SUMMARY AND CONCLUSIONS 255
8.1 Summary 255
8.2 Conclusions 260
8.3 Recommendations for Future Studies 263
REFERENCES 265
APPENDICES
APPENDIX A 277
APPENDIX B 279
APPENDIX C 293
APPENDIX D 305
CURRICULUM VITAE 309

LIST OF TABLES

TABLES

Table 1.1 Levels for Design and Verification 5

Table 2.1 Values for modification factor C_0 25

Table 2.2 Damping modification factor, κ 32

Table 2.3 Lateral deformation limits (ATC-40) 45

Table 2.4 Classification of columns by ASCE/SEI 41 Supplement 1 47

Table 2.5 Numerical acceptance criteria for nonlinear procedures – RC columns (adapted from ASCE/SEI-41 Supplement-1, 2008) 49

Table 2.6 Interstory drift limits (TEC-2007) 50

Table 4.1 General information of selected buildings 77

Table 4.2 Geotechnical information of selected buildings 82

Table 5.1 Contribution of infill walls to initial stiffness and initial fundamental period 98

Table 5.2 Fundamental mode periods in orthogonal directions and torsion 99

Table 5.3 Calculated and normalized NRHA results for the buildings studied 107

Table 5.4 Comparison of moment demands with the capacities of Building #1 columns (mezzanine and 1st stories), for NRHA in the X direction of the building 113

Table 5.5 Comparison of moment demands with the capacities of Building #2 columns (ground story), for NRHA in X and Y directions of the building...... 114

Table 5.6 Comparison of moment demands with the capacities of Building #7 columns (ground and 2nd stories), for NRHA in X and Y directions of the building 115

Table 5.7 Comparison of moment demands with the capacities of Building #10 columns (ground story), for NRHA in the X direction of the building 116
Table 6.1 Comparison of shear force capacities with corresponding demands for the ground story (incl. mezzanine) columns of Building #1 133
Table 6.2 Comparison of shear force capacities with corresponding demands for the ground story columns of building #2 134
Table 6.3 Comparison of shear force capacities with corresponding demands for the ground story columns of building #3 135
Table 6.4 Comparison of shear force capacities with corresponding demands for the ground story columns of building #4 136
Table 6.5 Comparison of shear force capacities with corresponding demands for the ground story columns of building #5 136
Table 6.6 Comparison of shear force capacities with corresponding demands for the ground story columns of building #6 137
Table 6.7 Comparison of shear force capacities with corresponding demands for the ground story and 2nd story columns of building #7 138
Table 6.8 Comparison of shear force capacities with corresponding demands for the first, second and third story columns of building #8 139
Table 6.9 Comparison of shear force capacities with corresponding demands for the ground story columns of building #9 140
Table 6.10 Comparison of shear force capacities with corresponding demands for the ground story columns of building #10.. 141
Table 7.1 Hassan and Sözen (1997) preliminary assessment on the buildings studied.. 238
Table 7.2 Yakut (2004) preliminary assessment on the buildings studied............. 243
Table 7.3 Number of story based cut-off values (*CVR*) 249
Table 7.4 Cut-off modification coefficients, *CMC*, for $M_w = 7.4$. 251
Table 7.5 Damage inducing parameters and corresponding Damage Indices 252
Table 7.6 The cut-off values and the evaluation results... 252

LIST OF FIGURES

FIGURES

Figure 1.1 Recommended Performance Objectives for Buildings (SEAOC 1999)... 5
Figure 2.1 Bilinearization of capacity curve (FEMA 2000) 23
Figure 2.2 The notation for determining limitation on strength.............................. 28
Figure 2.3 Graphic representation of capacity and demand curves (adopted from ATC-40) 30
Figure 2.4 Illustration of the energy terms (adopted from ATC-40) 31
Figure 2.5 Damage States and Corresponding Damage Limits of a Ductile Member.. 43
Figure 2.6 Plastic (hinge) rotation and chord rotation (figure from ATC-40, 1996).. 44
Figure 2.7 Chord rotation in a beam member supported by axially rigid columns . 52
Figure 3.1 Map of northwestern Turkey, affected by 1999 Marmara Earthquake (adopted from GDDA, 2000) 57
Figure 3.2 5% damped elastic response spectra of horizontal components of the two prominent aftershocks (figures adapted from Bakır et al. 2002)................. 60
Figure 3.3 Site specific strong ground motion record (soft soil, bedrock depth: 150 m)... 61
Figure 3.4 Response spectra (original record, site-specific, and TEC design spectrum for Z4) 62
Figure 3.5 Justinianus Bridge (Beşköprü)... 64
Figure 3.6 Front page view of the Damage Assessment Report Form 67
Figure 3.7 Back page view of the Damage Assessment Report Form..................... 68

Figure 3.8 Failure due to the soft story irregularity (photo courtesy of METU-DMC) 70
Figure 3.9 Ground floor destruction due to high ductility demands (photos courtesy of METU-DMC) 70
Figure 3.10 Tilting and/or settlement of the buildings (photos courtesy of METU-DMC) 71
Figure 3.11 Nonductile detailing (photos courtesy of METU-DMC) 72
Figure 3.12 Anchorage problems at beam-column connections (photo courtesy of METU-DMC) 73
Figure 5.1 Beam-with-hinges element 86
Figure 5.2 The fiber section of a circular column and quadrilateral definition for fibers 87
Figure 5.3 Concrete 01 material 88
Figure 5.4 Concrete 02 material 88
Figure 5.5 Reinforcing Steel material (Chang and Mander, 1994) 89
Figure 5.6 Steel 01 material 89
Figure 5.7 Steel 02 material (Filippou, et al. 1983) 89
Figure 5.8 The *Vr / Ve* ratios for ground story columns of building #1 93
Figure 5.9 The *Vr / Ve* ratios for ground story columns of building #2 93
Figure 5.10 The *Vr / Ve* ratios for ground story columns of building #3 94
Figure 5.11 The *Vr / Ve* ratios for ground story columns of building #4 94
Figure 5.12 The *Vr / Ve* ratios for ground story columns of building #5 94
Figure 5.13 The *Vr / Ve* ratios for ground story columns of building #6 95
Figure 5.14 The *Vr / Ve* ratios for ground story columns of building #7 95
Figure 5.15 The *Vr / Ve* ratios for ground story columns of building #8 95
Figure 5.16 The *Vr / Ve* ratios for ground story columns of building #9 96
Figure 5.17 The *Vr / Ve* ratios for ground story columns of building #10 96
Figure 5.18 Normalized roof drift response history of moderately damaged buildings, (a) X direction and (b) Y direction 101
Figure 5.19 Normalized roof drift response history of severely damaged buildings, (a) X direction and (b) Y direction 102

Figure 5.20 Normalized total base shear response history of moderately damaged buildings, (a) X direction and (b) Y direction.. 103
Figure 5.21 Normalized total base shear response history of severely damaged buildings, (a) X direction and (b) Y direction.. 104
Figure 5.22 The normalized base shear–roof drift hysteresis plots of the NRHA for moderately damaged buildings, (a) X direction and (b) Y direction 105
Figure 5.23 The normalized base shear–roof drift hysteresis plots of the NRHA for severely damaged buildings, (a) X direction and (b) Y direction................ 106
Figure 5.24 ISDRs for moderately damaged buildings according to NRHA, (a) X direction and (b) Y direction 109
Figure 5.25 ISDRs for severely damaged buildings according to NRHA, (a) X direction and (b) Y direction 110
Figure 5.26 Arias Intensity (percent) of Sakarya site-specific ground motion 112
Figure 5.27 Pushover curves and the performance estimations for building #1 119
Figure 5.28 Pushover curves and the performance estimations for building #2 120
Figure 5.29 Pushover curves and the performance estimations for building #3 121
Figure 5.30 Pushover curves and the performance estimations for building #4 122
Figure 5.31 Pushover curves and the performance estimations for building #5 123
Figure 5.32 Pushover curves and the performance estimations for building #6 124
Figure 5.33 Pushover curves and the performance estimations for building #7 125
Figure 5.34 Pushover curves and the performance estimations for building #8 126
Figure 5.35 Pushover curves and the performance estimations for building #9 127
Figure 5.36 Pushover curves and the performance estimations for building #10 128
Figure 6.1 Plastic Hinge Rotation, θ_{pl}, results for Building 1 columns, computed by NRHA in X and Y directions 145
Figure 6.2 Plastic Hinge Rotation, θ_{pl}, results for Building 1 columns, computed at ultimate roof displacement of the pushover curve in the X direction............ 146
Figure 6.3 Plastic Hinge Rotation, θ_{pl}, results for Building 1 columns, computed by Eq.SDOF, FEMA356-DCM, FEMA440-DCM and MMPA in the Y direction 147

Figure 6.4 Plastic Hinge Rotation, θ_{pl}, results for Building 2 columns, computed by NRHA in X and Y directions 149

Figure 6.5 Plastic Hinge Rotation, θ_{pl}, results for Building 2 columns, computed at ultimate roof displacement of the pushover curve in X and Y directions....... 149

Figure 6.6 Plastic Hinge Rotation, θ_{pl}, results for Building 3 columns, computed by NRHA in X and Y directions 151

Figure 6.7 Plastic Hinge Rotation, θ_{pl}, results for Building 3 columns, computed by Eq.SDOF, FEMA356-DCM, FEMA440-DCM and MMPA in the X direction 152

Figure 6.8 Plastic Hinge Rotation, θ_{pl}, results for Building 3 columns, computed by FEMA356-DCM, and FEMA440-DCM in the Y direction 152

Figure 6.9 Plastic Hinge Rotation, θ_{pl}, results for Building 4 columns, computed by NRHA in X and Y directions 154

Figure 6.10 Plastic Hinge Rotation, θ_{pl}, results for Building 4 columns, computed by FEMA356-DCM, and FEMA440-DCM in the X direction 155

Figure 6.11 Plastic Hinge Rotation, θ_{pl}, results for Building 4 columns, computed by FEMA440-DCM in the Y direction........ 155

Figure 6.12 Plastic Hinge Rotation, θ_{pl}, results for Building 5 columns, computed by NRHA in X and Y directions 157

Figure 6.13 Plastic Hinge Rotation, θ_{pl}, results for Building 5 columns, computed by FEMA356-DCM, and FEMA440-DCM in the X direction 158

Figure 6.14 Plastic Hinge Rotation, θ_{pl}, results for Building 5 columns, computed by FEMA356-DCM, and FEMA440-DCM in the Y direction 158

Figure 6.15 Plastic Hinge Rotation, θ_{pl}, results for Building 6 columns, computed by NRHA in X and Y directions 160

Figure 6.16 Plastic Hinge Rotation, θ_{pl}, results for Building 6 columns, computed by Eq. SDOF, FEMA356-DCM, FEMA440-DCM and MMPA in the X direction 161

Figure 6.17 Plastic Hinge Rotation, θ_{pl}, results for Building 6 columns, computed by FEMA356-DCM and FEMA440-DCM in the Y direction 161

Figure 6.18 Plastic Hinge Rotation, θ_{pl}, results for Building 7 columns, computed by NRHA in X and Y directions 163

Figure 6.19 Plastic Hinge Rotation, θ_{pl}, results for Building 7 columns, computed at ultimate roof displacement of the pushover curve in X and Y directions....... 163

Figure 6.20 Plastic Hinge Rotation, θ_{pl}, results for Building 8 columns, computed by NRHA in X and Y directions 165

Figure 6.21 Plastic Hinge Rotation, θ_{pl}, results for Building 8 columns, computed by Eq. SDOF, FEMA356-DCM, FEMA440-DCM, MMPA and CSM of ATC-40 in the X direction........ 167

Figure 6.22 Plastic Hinge Rotation, θ_{pl}, results for Building 8 columns, computed by Eq. SDOF in the Y direction 168

Figure 6.23 Plastic Hinge Rotation, θ_{pl}, results for Building 9 columns, computed by NRHA in X and Y directions 169

Figure 6.24 Plastic Hinge Rotation, θ_{pl}, results for Building 9 columns, computed by Eq. SDOF, FEMA356-DCM, FEMA440-DCM and MMPA in the X direction 171

Figure 6.25 Plastic Hinge Rotation, θ_{pl}, results for Building 9 columns, computed by FEMA356-DCM and FEMA440-DCM in the Y direction........ 171

Figure 6.26 Plastic Hinge Rotation, θ_{pl}, results for Building 10 columns, computed by NRHA in X and Y directions........ 173

Figure 6.27 Plastic Hinge Rotation, θ_{pl}, results for Building 10 columns, computed at ultimate roof displacement of the pushover curve in the X direction 174

Figure 6.28 Plastic Hinge Rotation, θ_{pl}, results for Building 10 columns, computed by FEMA356-DCM and FEMA440-DCM in the Y direction 174

Figure 6.29 Max Strain, $\varepsilon_{c,max}$ and $\varepsilon_{s,max}$ results for Building 1 columns, computed by NRHA in X and Y directions 178

Figure 6.30 Max Strain, $\varepsilon_{c,max}$ and $\varepsilon_{s,max}$ results for Building 1 columns, computed at ultimate roof displacement of the pushover curve in the X direction........ 179

Figure 6.31 Max Strain, $\varepsilon_{c,max}$ and $\varepsilon_{s,max}$, results for Building 1 columns, computed by Eq. SDOF, FEMA356-DCM, FEMA440-DCM and MMPA in the Y direction 179
Figure 6.32 Max Strain, $\varepsilon_{c,max}$ and $\varepsilon_{s,max}$ results for Building 2 columns, computed by NRHA in X and Y directions 181
Figure 6.33 Max Strain, $\varepsilon_{c,max}$ and $\varepsilon_{s,max}$ results for Building 2 columns, computed at ultimate roof displacement of the pushover curve in X and Y directions....... 181
Figure 6.34 Max Strain, $\varepsilon_{c,max}$ and $\varepsilon_{s,max}$ results for Building 3 columns, computed by NRHA in X and Y directions 183
Figure 6.35 Max Strain, $\varepsilon_{c,max}$ and $\varepsilon_{s,max}$, results for Building 3 columns, computed by Eq. SDOF, FEMA356-DCM, FEMA440-DCM and MMPA in the X direction 184
Figure 6.36 Max Strain, $\varepsilon_{c,max}$ and $\varepsilon_{s,max}$, results for Building 3 columns, computed by FEMA356-DCM and FEMA440-DCM in the Y direction........................... 184
Figure 6.37 Max Strain, $\varepsilon_{c,max}$ and $\varepsilon_{s,max}$ results for Building 4 columns, computed by NRHA in X and Y directions 186
Figure 6.38 Max Strain, $\varepsilon_{c,max}$ and $\varepsilon_{s,max}$, results for Building 4 columns, computed by FEMA356-DCM and FEMA440-DCM in the X direction........................... 186
Figure 6.39 Max Strain, $\varepsilon_{c,max}$ and $\varepsilon_{s,max}$, results for Building 4 columns, computed by FEMA440-DCM in the Y direction.. 187
Figure 6.40 Max Strain, $\varepsilon_{c,max}$ and $\varepsilon_{s,max}$ results for Building 5 columns, computed by NRHA in X and Y directions 188
Figure 6.41 Max Strain, $\varepsilon_{c,max}$ and $\varepsilon_{s,max}$, results for Building 5 columns, computed by FEMA356-DCM and FEMA440-DCM in the X direction........................... 189
Figure 6.42 Max Strain, $\varepsilon_{c,max}$ and $\varepsilon_{s,max}$, results for Building 5 columns, computed by FEMA356-DCM and FEMA440-DCM in the Y direction........................... 190
Figure 6.43 Max Strain, $\varepsilon_{c,max}$ and $\varepsilon_{s,max}$ results for Building 6 columns, computed by NRHA in X and Y directions 191

Figure 6.44 Max Strain, $\varepsilon_{c,max}$ and $\varepsilon_{s,max}$, results for Building 6 columns, computed by Eq. SDOF, FEMA356-DCM, FEMA440-DCM and MMPA in the X direction 192

Figure 6.45 Max Strain, $\varepsilon_{c,max}$ and $\varepsilon_{s,max}$, results for Building 6 columns, computed by FEMA356-DCM and FEMA440-DCM in the Y direction.......................... 192

Figure 6.46 Max Strain, $\varepsilon_{c,max}$ and $\varepsilon_{s,max}$ results for Building 7 columns, computed by NRHA in X and Y directions 194

Figure 6.47 Max Strain, $\varepsilon_{c,max}$ and $\varepsilon_{s,max}$ results for Building 7 columns, computed at ultimate roof displacement of the pushover curve in X and Y directions....... 194

Figure 6.48 Max Strain, $\varepsilon_{c,max}$ and $\varepsilon_{s,max}$ results for Building 8 columns, computed by NRHA in X and Y directions 196

Figure 6.49 Max Strain, $\varepsilon_{c,max}$ and $\varepsilon_{s,max}$, results for Building 8 columns, computed by Eq. SDOF, FEMA356-DCM, FEMA440-DCM, MMPA and ATC40-CSM in the X direction.. 197

Figure 6.50 Max Strain, $\varepsilon_{c,max}$ and $\varepsilon_{s,max}$, results for Building 8 columns, computed by Eq. SDOF in the Y direction 198

Figure 6.51 Max Strain, $\varepsilon_{c,max}$ and $\varepsilon_{s,max}$ results for Building 9 columns, computed by NRHA in X and Y directions 199

Figure 6.52 Max Strain, $\varepsilon_{c,max}$ and $\varepsilon_{s,max}$, results for Building 9 columns, computed by Eq. SDOF, FEMA356-DCM, FEMA440-DCM and MMPA in the X direction 200

Figure 6.53 Max Strain, $\varepsilon_{c,max}$ and $\varepsilon_{s,max}$, results for Building 9 columns, computed by FEMA356-DCM and FEMA440-DCM in the Y direction.......................... 201

Figure 6.54 Max Strain, $\varepsilon_{c,max}$ and $\varepsilon_{s,max}$ results for Building 10 columns, computed by NRHA in X and Y directions.. 202

Figure 6.55 Max Strain, $\varepsilon_{c,max}$ and $\varepsilon_{s,max}$ results for Building 10 columns, computed at ultimate roof displacement of the pushover curve in the X direction 203

Figure 6.56 Max Strain, $\varepsilon_{c,max}$ and $\varepsilon_{s,max}$, results for Building 10 columns, computed by FEMA356-DCM and FEMA440-DCM in the Y direction 203

Figure 6.57 Chord Rotation, θ, results for Building 1 columns, computed by NRHA in X and Y directions 206
Figure 6.58 Chord Rotation, θ, results for Building 1 columns, computed at ultimate roof displacement of the pushover curve in the X direction................. 207
Figure 6.59 Chord Rotation, θ, results for Building 1 columns, computed by Eq. SDOF, FEMA356-DCM, FEMA440-DCM and MMPA in the Y direction...... 207
Figure 6.60 Chord Rotation, θ, results for Building 2 columns, computed by NRHA in X and Y directions 208
Figure 6.61 Chord Rotation, θ, results for Building 2 columns, computed at ultimate roof displacement of the pushover curve in X and Y directions........... 209
Figure 6.62 Chord Rotation, θ, results for Building 3 columns, computed by NRHA in X and Y directions 211
Figure 6.63 Chord Rotation, θ, results for Building 3 columns, computed by Eq. SDOF, FEMA356-DCM, FEMA440-DCM and MMPA in the X direction...... 212
Figure 6.64 Chord Rotation, θ, results for Building 3 columns, computed by FEMA356-DCM, and FEMA440-DCM in the Y direction.............................. 212
Figure 6.65 Chord Rotation, θ, results for Building 4 columns, computed by NRHA in X and Y directions 214
Figure 6.66 Chord Rotation, θ, results for Building 4 columns, computed by FEMA356-DCM, and FEMA440-DCM in the X direction.............................. 214
Figure 6.67 Chord Rotation, θ, results for Building 4 columns, computed by FEMA440-DCM in the Y direction... 215
Figure 6.68 Chord Rotation, θ, results for Building 5 columns, computed by NRHA in X and Y directions 216
Figure 6.69 Chord Rotation, θ, results for Building 5 columns, computed by FEMA356-DCM, and FEMA440-DCM in the X direction.............................. 217
Figure 6.70 Chord Rotation, θ, results for Building 5 columns, computed by FEMA356-DCM, and FEMA440-DCM in the Y direction.............................. 217
Figure 6.71 Chord Rotation, θ, results for Building 6 columns, computed by NRHA in X and Y directions 219

Figure 6.72 Chord Rotation, θ, results for Building 6 columns, computed by Eq. SDOF, FEMA356-DCM, FEMA440-DCM and MMPA in the X direction...... 220
Figure 6.73 Chord Rotation, θ, results for Building 6 columns, computed by FEMA356-DCM and FEMA440-DCM in the Y direction............................... 220
Figure 6.74 Chord Rotation, θ, results for Building 7 columns, computed by NRHA in X and Y directions 222
Figure 6.75 Chord Rotation, θ, results for Building 7 columns, computed at ultimate roof displacement of the pushover curve in X and Y directions 222
Figure 6.76 Chord Rotation, θ, results for Building 8 columns, computed by NRHA in X and Y directions 224
Figure 6.77 Chord Rotation, θ, results for Building 8 columns, computed by Eq. SDOF, FEMA356-DCM, FEMA440-DCM, MMPA and ATC40-CSM in the X direction 225
Figure 6.78 Chord Rotation, θ, results for Building 8 columns, computed by Eq. SDOF in the Y direction.. 226
Figure 6.79 Chord Rotation, θ, results for Building 9 columns, computed by NRHA in X and Y directions 227
Figure 6.80 Chord Rotation, θ, results for Building 9 columns, computed by Eq. SDOF, FEMA356-DCM, FEMA440-DCM and MMPA in the X direction...... 228
Figure 6.81 Chord Rotation, θ, results for Building 9 columns, computed by FEMA356-DCM and FEMA440-DCM in the Y direction............................... 229
Figure 6.82 Chord Rotation, θ, results for Building 10 columns, computed by NRHA in X and Y directions 230
Figure 6.83 Chord Rotation, θ, results for Building 10 columns, computed at ultimate roof displacement of the pushover curve in the X direction................ 231
Figure 6.84 Chord Rotation, θ, results for Building 10 columns, computed by FEMA356-DCM and FEMA440-DCM in the Y direction............................... 231
Figure 7.1 Preliminary assessment results of Hassan and Sözen (1997) procedure 238
Figure 7.2 Preliminary assessment results of Yakut (2004) procedure 244

CHAPTER 1

INTRODUCTION

1.1 GENERAL, BACKGROUND, STATEMENT OF THE PROBLEM

In Earthquake Engineering research area which has been significantly improved especially in the last 40-50 years, recent researches have been significantly concentrated on the idea of “performance based earthquake engineering (PBEE)”. Especially after the two large earthquakes on two shores of the Pacific (1994 Northridge and 1995 Kobe Earthquakes), performance-based design and assessment approaches have gained more popularity. The main objective of the PBEE is to answer the question of “what would be the performance (dynamic response and resulting damage) of a structure during the “expected earthquakes” at the site?” Performance based methods require reasonably accurate estimates of inelastic deformation and resulting structural damage.

In spite of its application difficulties, performance based approaches provide important economical contribution in long term, since they provide the rational usage of sources. The basic problem of the performance based approaches is to respond to “Under which level of loadings and at which performance level can a structure serve reliably?” Thus, “performance based approaches” are being investigated on a vast scale by structural and earthquake engineers.

In this research area, many new linear and nonlinear analysis procedures have been proposed for earthquake response determination of the structures. The main aim of these researches is to obtain the adequate knowledge level for a proper structural design for a stated objective of performance. The control of nonlinear displacements is necessary in order to control the structural damage (Shibata and Sözen, 1976). The nonlinear displacements, on the other hand, should be determined using nonlinear analysis (Saiidi and Sözen, 1981). Therefore, Nonlinear Static Procedures (NSPs) come into prominence as a practical seismic response determination tool within these proposals, due to the complexities of Nonlinear Response History Analysis (NRHA).

The seismic performance of buildings is determined by linear static, linear dynamic, nonlinear static and nonlinear dynamic analysis procedures. The value of information related with the dynamic response of the building increases from first to the last. Thus, nonlinear dynamic (nonlinear response history) analysis (NRHA) is accepted as the most accurate source of information for nonlinear response, i.e. the inelastic deformations. In general, the reliability of NSP's has been evaluated comparing their expectations with the results of Nonlinear Response History Analyses (NRHA), which have been accepted as the "exact results". However, the application of NRHA is not as standard as the linear elastic analysis methods. Due to its complexity, stability or convergence problems occur, frequently. Moreover, NRHA requires significant run-time and post-processing efforts. Nevertheless, linear analysis tools have limited capacity in simulating inelastic seismic behavior.

Nonlinear static pushover analysis may provide reasonable estimates of location of inelastic behavior. However, all the proposed pushover analysis procedures have limitations in prediction of seismic demand exactly, due to the certain approximations and simplifications. Thus, many improved pushover analysis procedures have been proposed in literature.

On the other hand, pushover analysis is not fully capable of providing estimates of maximum deformation, alone. Additional analysis must be performed for this purpose. The fundamental issue is: “How far to push?”

This fundamental issue is related with the expected “damage index” of the structure, for a performance level determined for design and the predicted strong ground motion intensity. Different damage indices are proposed in literature. As an example, recently published Turkish Earthquake Code (2007) has specified the following maximum interstory drift check for the Life Safety damage state, while applying the linear elastic assessment procedure of the code, as;

$$\delta_{\max} / h_i \leq 0.03$$

where, δ_{max} : maximum interstory (relative) displacement,

h_i : the story height.

It is important to recognize that the purpose of pushover analysis is not to predict the actual response of a structure to an earthquake (but, nonlinear dynamic analysis can predict the response to an earthquake). The minimum requirement for any method of analysis, including pushover analysis, is that it must be “good enough for design”.

The assumptions of nonlinear static pushover analyses must be emphasized here:

- dynamic effects are ignored,
- duration effects are ignored,
- choice of lateral load pattern,
- only first mode response is included,
- elastic response spectrum is used,
- use of equivalent viscous damping,
- modification of response spectrum for higher damping.

Due to the drawbacks originated from these assumptions, researchers have proposed several procedures which are classified as "improved pushover analysis". In these studies,

- use of inelastic response spectrum,
- adaptive load patterns,
- use of SDOF response history analysis,
- inclusion of higher mode effects, are taken into account.

In the case of "nonlinear dynamic response history analysis (NRHA)", principally all problems with pushover analysis are eliminated. And, the principal concerns in NRHA are;

- modeling of hysteretic behavior,
- modeling the inherent damping,
- selection and scaling of ground motions,
- interpretation of results,
- results may be very sensitive to seemingly minor perturbations.

"Which analysis procedures should be used?" The issues related with this question are; (i) which performance level, (ii) geometry of the structure, (iii) the approximation in analysis. Generally, for high performance levels the response of structure should remain elastic. However, when lower performance levels are considered the inelastic region of structural response (ductility capacity) is important. For these conditions; nonlinear static pushover procedures (NSPs) provide reliable approximation for the structural response governed by the first mode, where nonlinear response history analysis (NRHA) is needed for the structures for which the higher modes effects are important.

Most earthquake codes in use in the world are strength based codes, not performance based codes. Traditional strength based codes consider only a single performance level and also a single level of earthquake loading. On the other hand, in performance based approaches, the expected performance levels of the structure are considered according to the expected seismic loading. The researches on improvement of seismic codes using performance based design (limit states design) approaches are interested in "coupling the expected performance levels with the expected levels of seismic ground motion" that is recently accepted as the main seismic design philosophy (SEAOC 1999). In Figure 1.1, performance objectives for buildings which are recommended by the Blue Book (SEAOC 1999) are shown.

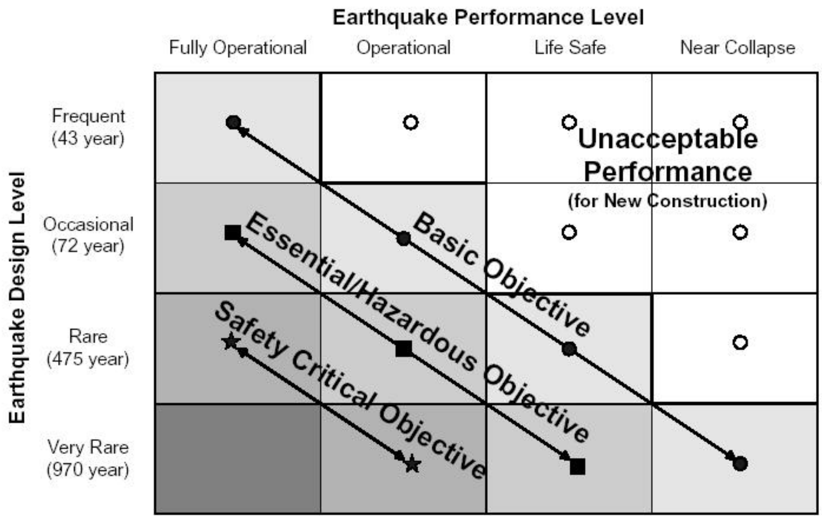

Figure 1.1 Recommended Performance Objectives for Buildings (SEAOC 1999)

The probable expected earthquake values are also important parameters for performance based approaches as strength capacities of the structure and its members. In the Blue Book, four "Earthquake Design Levels" according to their probability of occurrence has been proposed, as given in Table 1.1.

Table 1.1 Levels for Design and Verification

Event	Recurrence Interval	Probability of Exceedance
Frequent	43 years	50% in 30 years
Occasional	72 years	50% in 50 years
Rare	475 years	10% in 50 years
Very Rare	970 years	10% in 100 years

The response of the structure is related with the features of the ground motion, as well as structural characteristics, i.e. material and geometric features. There are many uncertainties to determine the level of ground motion for a specific site and to determine the response of a structure due to the specified ground motion. As a consequence of these uncertainties in both “capacity” and “demand”, quantification of the “risk” is generally not possible to be determined for an existing structure (Priestley et al. 2007).

In this study, however, expected earthquake level is not considered. This study is focused on the procedures which are proposed for investigation of the structural response due to specific ground motions. The principal modality is to compare observed performance of buildings on the basis of field observations with estimates using nonlinear static procedures. This way a calibration of these procedures may be possible.

On August 17, 1999, Turkey experienced an un-planned large scale testing of buildings during the Marmara Earthquake. The 7.4 magnitude earthquake struck Marmara Region of Turkey and a large number of buildings were damaged. The vulnerable reinforced concrete buildings, which create the majority of buildings with moment-resisting-frame systems in Turkey, experienced various damages (moderate, severe) while many of them collapsed. It would appear that, using building response observations from this earthquake and performing “back calculations” for selected structures, it might be possible to assess the “global” performance of performance assessment procedures that have been developed.

The rhetorical question, “had we known one day in advance that this earthquake would occur, could we have estimated their global performance (the damage states) using the widely used NSPs?” deserves an informed answer. Aiming to answer this question, which is the "core" of this study, moderately and heavily damaged buildings were sampled from Adapazarı / Sakarya and their models built.

For the study, five moderately and five heavily damaged buildings were selected from the archives of Adapazarı Merkez Municipality and a number of analysis procedures were applied to them. For the performance assessment of buildings, the following analysis procedures were used: NSPs of ATC-40, FEMA-356, FEMA-440, Nonlinear Analysis of SDOF System (Eq. SDOF), Modified Modal Pushover Analysis (MMPA), and NRHA. The study has concentrated on NSPs that were compared with the global building performance of selected buildings. Because global damage states for buildings are known, comparing them with predictions from analyses using NSPs is done. This way, the NSP Methods were evaluated and checked whether they have estimated the global damages suitably.

In addition to these global comparisons were conducted, the buildings were also examined using the detailed evaluation procedures of ASCE/SEI-41/06 (ASCE 2007), and its Supplement-1 (ASCE 2008), Turkish Earthquake Code (TEC 2007) and EuroCode-8-3 (EC 2005). The buildings were evaluated in detail, using both Nonlinear Static (NSA) and Nonlinear Dynamic (NDP) Assessment Procedures of the codes. The linear assessment procedures proposed by the codes were not considered in this study.

Considering the high effort given for the computation and post-process of the analyses, global seismic performance of the buildings were also assessed to determine their likely performance under the given ground motion effects, by preliminary assessment procedures proposed by Hassan and Sözen (1997), Yakut (2004) and Özcebe et al. (2004).

1.2 REVIEW OF PREVIOUS WORKS / LITERATURE SURVEY

It can be seen that the research area of the "nonlinear analysis procedures" is rapidly developing, when the related literature surveyed. There are many studies in literature related with all the details of procedures. Some of them are summarized in this section.

It is suitable to start a review about the nonlinear analysis of the buildings, nonlinear static (pushover) analysis, and the approximate nonlinear static procedures (NSPs) for the performance estimation of the buildings with the studies on "equivalent linearization".

After the proposal of "equivalent viscous damping" by Jacobsen (1930 and 1960) for the solutions of steady state vibration of SDOF systems with linear and nonlinear force – deformation relationships, "equivalent linearization method" was developed for elasto-plastic SDOF systems under harmonic loading by Rosenblueth and Herrera (1964). The equivalent damping is computed as equal to the energy dissipated in the hysteresis loop at resonance, while the equivalent stiffness is taken as the secant stiffness in this loop. In this way, approximate solutions for the elasto-plastic SDOF systems are obtained. Different equivalent damping approximations were evaluated by Jennings (1968), and the use of initial stiffness was suggested with the equivalent damping, due to the conservative results.

The importance of estimating the maximum displacement as the response to strong earthquake motions was indicated first by Gülkan and Sözen (1974) that underlies the concept of "nonlinear static analysis". Based on the experimental investigation on one bay – one story frames, they emphasized that the response of the RC structures is influenced by reduction in stiffness and increase in energy-dissipation capacity. At larger displacement demand values, the stiffness of the structure decreases while the energy-dissipating capacity increases, and both parameters can be related with the ductility ratio. The maximum dynamic response, on the other hand, can be approximated by linear response analysis with a reduced stiffness and a “substitute damping” of “substitute” SDOF system. They formulized the relation between the substitute damping and the ductility, according to their test results. Their objective was to satisfy the maximum displacement limit providing sufficient strength to the structure, from the design point of view. Corresponding design base shear to the maximum displacement is also estimated with this simplified procedure.

The Capacity Spectrum Method (CSM) was developed by Freeman et al. (1975), for the purpose of the maximum displacement demand calculation of the SDOF systems, based on the “equivalent linearization method” (Rosenblueth and Herrera, 1964). The CSM was used in ATC-40 (ATC, 1996) taking some imperfections of the dynamic characteristics of SDOF system, i.e. degradation and pinching, into consideration.

Shibata and Sözen (1976) proposed the “Substitute-Structure Method” for seismic design of the RC buildings, extending the design force determination concept for SDOF structures of Gülkan and Sözen (1974) to MDOF structures. They emphasized that the nonlinear displacement demands of a structure should be controlled for limiting the seismic damage during an earthquake.

Arising from the thought that the nonlinear displacements should be determined by nonlinear analysis but the difficulties of computation, Saiidi and Sözen (1981) proposed the “Q-Model”, which is the first idea of nonlinear static analysis in order to determine the force-deformation relationship of the SDOF System. The nonlinear analysis can be conducted using the simple numerical model (Q-Model) of the structure, and displacement history of the reinforced concrete structures can be estimated. In order to model the stiffness changes in structure which are subjected to strong ground motions, SDOF representation of the MDOF system is proposed. The Q-Model was modified and applied the model to the analysis of vertically irregular buildings by Saiidi and Hudson (1982), Moehle (1984), and Moehle and Alarcon (1986).

In 1987, Fajfar and Fischinger introduced the N2 Method which is an extension of Q-Model. In order to obtain accurate results especially in nonlinear range, nonlinear dynamic analysis of the buildings is preferred. Hence, the N2 method was proposed as an accurate but less complicated nonlinear method, especially for structures oscillating predominantly in a single mode. This method is a combination of a nonlinear static analysis of the MDOF system under a monotonically increasing lateral load and NRHA of the SDOF representation of the system that is obtained from the nonlinear static analysis. The maximum displacement demand of the earthquake ground motion is computed for the SDOF system. Then, maximum roof displacement demand of the MDOF system is computed from the max displacement demand of the SDOF system. A force distribution proportional to the mass matrix multiplied by an assumed displacement shape was used by Fajfar and Gaspersic (1996).

The concept of the nonlinear static analysis and corresponding SDOF representation of the N2 method was used by FEMA 273 (FEMA 1997), FEMA 356 (FEMA, 2000), and ATC 40 (ATC, 1996), with differences in the lateral load force vector.

The drawbacks of the proposed nonlinear static procedures are evaluated by several researchers. Chopra and Goel (2000) have examined the CSM procedure in detail to point out that, under an unfavorable set of conditions the procedure may not converge, or otherwise lead to unrealistic displacement estimates. According to their evaluation, the CSM generally underestimated the displacement demands compared to the results of NRHA, due to the overestimation of equivalent damping.

Different methods proposed for estimating the maximum deformation demands are evaluated by Miranda and Ruiz-Garcia (2002), and Akkar and Miranda (2005). The former study evaluated the approximate methods for the preliminary design of the structures, while the existing structures were considered by the latter one. The ductility ratio is a known parameter for the new designs and it is unknown for existing structures. The accuracy of these methods was shown statistically for varying period ranges in comparison with the NRHA results.

Krawinkler, H., and Seneviratna, (1998), discussed the applicability of nonlinear static analysis as a seismic performance evaluation tool. Besides its sufficient features as a nonlinear analysis, the deficiencies of the nonlinear static analysis were noted such as the effect of higher modes, lateral load pattern, and capability to identify all possible structural mechanisms.

The deficiencies of the nonlinear static procedures were attempted to overwhelm by adaptive procedures in the more recent researches. Paret et al. (1996) proposed the idea of conducting several pushover analyses with force distributions proportional to the multiplication of the mass matrix and the elastic mode shapes corresponding to different modes. They proposed the Modal Criticality Index (MCI) in order to identify the vibration mode that is the most likely to cause structural failure. The MCI was extended by Sasaki et al. (1998) and the Multi-Mode Pushover (MMP) Procedure was proposed that account for the effects of higher modes.

Many other researchers studied on adaptive pushover procedures, considering the higher mode effects and different lateral load patterns (i.e. Gupta and Kunnath 2000, Aydınoğlu 2003, Antoniou and Pinho 2004a and 2004b).

Based on the structural dynamics theory, the Modal Pushover Analysis (MPA) was proposed by Chopra and Goel (2002). According to MPA, pushover analyses are carried out for each vibration period of the building by applying the lateral loads proportional to the corresponding mode shape. The pushover curves are idealized in order to obtain the equivalent SDOF system. The inelastic peak response is computed for each mode conducting the NRHA. The appropriate modal combination rule is used in order to compute the overall structural response, including all significant modes of vibration. Dealing with the height-wise regular generic frames, P-Δ effects and vertically irregular generic frames, improvements were proposed for the MPA procedure (Chintanapakdee and Chopra 2003 and 2004, Goel and Chopra 2004.

The modified version of MPA, as MMPA, was proposed in which the inelastic response obtained from first-mode pushover analysis has been combined with the elastic contribution of higher modes by Chopra et al. (2004). In MMPA the effect of higher modes is assumed to be linear elastic, and hence pushover analysis is not needed for the higher modes of vibration. Therefore, the inelastic response of the fundamental mode combined with the elastic contribution of higher modes, which are computed by individual linear response history analysis. This simplification reduces the computational effort.

Another pushover analysis procedure proposed which is derived through adaptive modal combinations (AMC) by Kalkan and Kunnath (2006) utilizes an energy based scheme. The procedure eliminates the need to pre-estimate the target displacement using constant-ductility inelastic spectra.

Vamvatsikos and Cornell (2002) developed the incremental dynamic analysis procedure (IDA), based on nonlinear response history analyses applying the scaled ground motion records.

In order to improve the NSPs, Aschheim et al. (2007) also used the multiple scaled nonlinear dynamic analyses in order to match the target displacement computed by NSPs.

1.3 OBJECTIVE AND SCOPE

This study is concentrated on the procedures which are proposed for investigation of the structural response due to specific ground motions. The study has initiated from the question of “had we known one day in advance that this earthquake would occur, could we have estimated their global performance using the widely used NSPs?” The principal modality will be to compare observed performance of buildings on the basis of field observations with estimates using NSPs. This way a calibration of these procedures may be possible.

In the research, the current widely used nonlinear static (pushover) analysis procedures are compared with the results of both nonlinear dynamic procedures (nonlinear response history analysis - NRHA) and the “real results” (real building performance during the earthquake).

Since, the objective of this study is to assess the nonlinear seismic response estimations of NSPs, linear analyses are not applied in this study as well as linear assessment procedures.

The procedures used for nonlinear analysis of structures result in different outcomes due to the uncertainties and assumptions included. Generally, these procedures are compared with each other (and nonlinear response history analysis) to investigate the differences thoroughly. However, since it is impossible to model all uncertainties simultaneously, more accurate solution methods can only be discovered by comparing these analytical results with the real observation and/or experimental measurement results. Since the calibration of the NSPs would be possible this research is concentrated on the comparison of the observed performance of buildings on the basis of field observations with estimates using NSPs.

For this purpose, direct observations from 1999 Marmara Earthquake are used in the study. Some selected building's – which are located at city center and very close to each other – information was collected from Archives of Adapazarı Merkez Municipality / Sakarya (one of the most affected cities during the earthquake). Project blueprints of five heavily damaged and five moderately damaged buildings were copied from the archives and modeled in computer.

In order to compare the estimations of the NSPs with the results of NRHA and the observed global damage, a number of analysis procedures were applied to these moderately and severely damaged buildings, with different structural and geotechnical attributes. For the performance assessment of buildings, the following analysis procedures were used: NSPs of Capacity Spectrum Method (ATC-40 and FEMA-440) (ATC 1996, ATC 2005), Displacement Coefficients Method (FEMA-356 and FEMA-440) (ASCE 2000, ATC 2005), Nonlinear Analysis of SDOF Systems (Eq. SDOF) (Fajfar and Fischinger 1987) and Modified Modal Pushover Analysis (MMPA) (Chopra et al. 2004). In addition to the NSPs, NRHA was carried out as well. According to the review of detailed assessment result, preliminary assessment procedures were also carried out.

This study is considered to be useful for;

- determination of the sensitivity, superiority and shortcomings of nonlinear analysis procedures,
- improvement of the analysis procedures by investigation of procedures throughout the real observation and measurement data.

When the conclusions are available to the use of researchers, it is considered to help;

- the comprehensive understanding of nonlinear analysis procedures,
- the interpretation of both the analysis procedures and their results.

The study was concentrated on the application of NSPs to the large building stocks in Turkey. The approximate assessment procedures were applied to the selected buildings, which reflect the general structural features of the RC building inventory in Turkey, in order to evaluate the global building performance during the earthquake. The known global damage states of the buildings were compared with predictions from NSP analyses. This way, the NSP methods were evaluated and checked whether they have estimated the global damages suitably.

1.4 ORGANIZATION OF THE DISSERTATION

This thesis is composed of seven main chapters. The contents can be briefed as follows:

Chapter 1: General overview and statement of the study and literature survey on the development of approximate nonlinear static procedures.

Chapter 2: An extended review of approximate nonlinear static procedures and investigation of the existing standards and provisions by means of the "seismic performance" of the existing ordinary reinforced concrete structures. The corresponding acceptance criteria for different performance levels are also defined.

Chapter 3: Description of the hazardous 1999 Marmara Earthquake and the structural damage in Adapazarı.

Chapter 4: Selection of the damaged reinforced concrete buildings for the study, general structural properties and the GIS investigation in order to obtain the geotechnical features.

Chapter 5: After describing the analytical models of the buildings constituted, and corresponding modeling tools, the results of the nonlinear response history analyses are presented.

Chapter 6: Application of the seismic performance assessment procedures including both approximate nonlinear static procedures and detailed nonlinear assessment procedures is presented. The results of each assessment are discussed, comparing each of the procedure with one another.

Chapter 7: Evaluation of the buildings by preliminary assessment procedures is presented.

Chapter 8: A brief summary and the conclusions are given with recommendations for future studies.

In addition to the main chapters, complementary information is given in four sections of the appendices, as follows;

Appendix A: The scanned copies of the blueprints of the buildings studied. Due to the electronic file type and their storage size, the documents are burned on the DVD enclosed.

Appendix B: The geotechnical maps of Adapazarı that are obtained by GIS survey.

Appendix C: Ground story plans and 3D views of the analytical models of the buildings studied.

Appendix D: Available technical reports of the buildings.

CHAPTER 2

NONLINEAR ASSESSMENT PROCEDURES

2.1 INTRODUCTION

Seismically vulnerable reinforced concrete (RC) frame systems are commonly constructed structural systems worldwide, including, of course, in seismic regions. Recent earthquakes in many countries have caused significant damage and collapse to these buildings, including the earthquakes that struck Turkey (GDDA 2000, IMO 2000, Sezen et al. 2003, Mosalam and Günay 2010). According to the latest building inventory census of Turkey (SIS, 2000), 48 percent of all buildings has been constructed as reinforced concrete systems, while 51 percent are masonry. Moment-resisting-frame systems consist of 98 percent of all RC systems.

Besides their vulnerable seismic behavior, considering the construction practice in Turkey, reinforced concrete buildings usually have different configurations and detailing than their design drawings (Yakut et al., 2006). Therefore, evaluation of existing buildings is one of the most challenging tasks in seismic mitigation efforts. Nonlinear dynamic analysis of buildings is difficult and needs time consuming applications. Thus, simpler but accurate methods for building response estimation are needed.

The evaluation procedures for existing buildings can be classified into three categories, according to details of information that are used and reliability of their results; as walk-down, preliminary and detailed assessment procedures. The walk-down (street) survey procedures are proposed as rapid screening procedures in urban areas and take limited data into consideration, i.e. number of stories, plan and vertical irregularities, structural system, and material and workmanship quality observed (FEMA 1988, Ohkubo 1991, Sucuoğlu et al. 2007). The walk-down procedures are not investigated in this study because they involve no analytical modeling or computation.

Using walk-down procedures only ranking of vulnerable buildings against the earthquake expected at the site can be determined. However, since the evaluation results are not reliable, the preliminary assessment procedures, which are more detailed assessment procedures, are needed. The preliminary assessment procedures are more quick methods than the detailed procedures, in order to determine the priority of detailed assessment for the building inventories using the limited data of general properties and/or irregularities of the buildings (FEMA 1989, FEMA 1998, Hassan and Sözen 1997, Gülkan and Sözen 1999, Yakut 2004, Özcebe et al. 2004). For the aim of ranking buildings at a site, preliminary assessment procedures are efficient, considering their practicality and time required for the application. Information about the structural system (size and orientation of structural members, layout and material characteristics) is also needed for more reliable assessment results than street survey. For a reliable assessment result, the data supplied must be realistic and as detailed as possible.

Detailed assessment procedures examine buildings using comprehensive information about the building and the force-resisting frame system (design information on geometrical properties of the members, material properties and detailing information, as well as as-built features). Thus, these procedures rely on sophisticated and time consuming analysis. In general, in order to put a decision for rehabilitation needs, detailed procedures are applied to individual buildings. In recent years, the detailed assessment procedures have been considered in many standardization attempts (ATC 1996, FEMA 1997, FEMA 1998, FEMA 2000, ATC 2005, EC 2005, TEC 2007, ASCE 2007, ASCE 2008).

The main concern for the performance-based evaluation of the existing buildings is estimation of the "demand" of a certain ground motion or a presumed intensity level. The demand parameters can be defined as global (i.e. max roof displacement, max drift ratio, max interstory drift) or local (i.e. deformation of structural elements such as drifts, plastic rotation and chord rotation, or strain values at critical sections). The detailed assessment procedures use the local demand parameters, as well as global parameters. Most of the provisions and standards, i.e. ATC-40 (ATC 1996), FEMA 356 (FEMA 2000), ASCE/SEI-41 (ASCE 2007) and EC8-3 (EC 2005), define performance criteria using "plastic rotation" and "chord rotation", while TEC 2007 specifies the limit "strain" values at critical sections in order to determine the seismic performance level.

These demand parameters can be calculated using either linear or nonlinear structural analyses (static or dynamic). However, typically, the actual response of the buildings to earthquakes is nonlinear. Therefore, it is expected that nonlinear analysis procedures provide the actual response and performance of a building during the earthquake. On the other hand, generally, the acceptance criteria defined for linear procedures are more conservative than for the nonlinear procedures. Thus, performing a nonlinear analysis is recommended by the provisions. From this point of view, the demand results obtained from nonlinear analyses were compared with the performance acceptance criteria, and linear procedures were not taken into consideration, in this study.

In order to apply the detailed assessment procedures of the codes, firstly, inelastic response should be predicted. The global inelastic response of a building is also called as "performance point" or "target displacement". In this study, inelastic response of the selected buildings were predicted using the Nonlinear Static

Procedures (NSPs) in conjunction with the Displacement Coefficients Method (DCM) (FEMA-356 and FEMA-440) (ASCE 2000, ATC 2005) and Capacity Spectrum Method (CSM) (ATC-40 and FEMA-440) (ATC 1996, ATC 2005), Nonlinear Analysis of Equivalent SDOF Systems (Eq. SDOF) (Fajfar and Fischinger 1987), and Modified Modal Pushover Analysis (MMPA) (Chopra et al. 2004), as well as Nonlinear Response History Analysis (NRHA). The global roof displacement value was used as the global performance parameter. The predictions of the NSPs were compared with the predictions of NRHA and with the observed damage level of the selected buildings. After this global comparison, the local deformations and strains of structural members at performance points predicted by NSPs and NRHA, were checked and compared with the acceptance criteria defined by NSA (Nonlinear Static Assessment Procedure) and NDP (Nonlinear Dynamic Assessment Procedure) of ASCE/SEI-41/06 (ASCE 2007) and its Supplement-1 (ASCE 2008), Turkish Earthquake Code (TEC 2007), and Eurocode 8 – Part 3 (EC 2005).

The nonlinear assessment procedures are classified as NSA (Nonlinear Static Assessment Procedure) and NDP (Nonlinear Dynamic Assessment Procedure), according to the method used for inelastic response prediction of the building. The assessment procedure is named as NSA when the performance point is predicted using pushover (nonlinear static) methods. If the NRHA is conducted, then the assessment procedure is called as NDP.

The ASCE/SEI-41 standard is intended to serve as the US national tool for the seismic rehabilitation of existing buildings. The provisions and commentary of the standard are primarily based on the FEMA 356 (FEMA 2000) which was based on FEMA 273 (FEMA 1997), and it is intended to supersede FEMA 356. The standard uses the performance-based methodology, as well.

From the performance-based assessment point of view, the recent supplement of TEC 2007 for assessment and rehabilitation of the existing buildings has similar approaches with FEMA 356 and EC8-3. TEC 2007, however, specifies maximum strain values for each performance levels of RC members, rather than plastic rotation or chord rotation. The strain demands at performance point of the buildings are calculated from the deformation demands at that stage. The calculated strain demands are compared with the given strain acceptance limits for each performance level. The assembly of member performances in order to obtain the global performance level of the building is another difference between TEC 2007 and the other two prominent standards (Sucuoğlu 2006).

In this chapter, the NSPs used in the study are reviewed in an extent of the objectives, and then performance definitions and acceptance criteria of the detailed assessment documents of ASCE/SEI-41/06 and its Supplement-1, TEC 2007, and EC8-3 are given.

2.2 INELASTIC RESPONSE PREDICTION METHODS USING NONLINEAR STATIC PROCEDURES (NSP)

The initial step of the detailed assessment of the existing buildings is the prediction of inelastic response (performance point, target displacement) against the earthquake intensity expected at the site. For this purpose, although NRHA is accepted as the most reliable tool in order to estimate the nonlinear seismic response of structures, application of NSPs is also possible, as a more practical way of nonlinear analysis. Thus, these methods have also been recommended by current civil engineering guidelines and specifications (ATC40, FEMA356, ASCE/SEI-41, EC8-3, TEC 2007).

In general, all NSP methods proposed in literature consist of four sequent steps. First of all, nonlinear static pushover analysis is carried out on the building model, under a monotonically increasing lateral load vector. All structural elements of the building should be modeled assigning appropriate nonlinear force-deformation relationships. Selection of the lateral load vector distribution, i.e. triangular, uniform, or proportional to the multiplication of the mass matrix and the first mode shape, may differ for different methods, considering the post yield mechanism of the building. The capacity (pushover) curve (force-deformation relationship) is obtained for the multi-degree-of-freedom (MDOF) system modeled, which represents the characteristics of strength, stiffness and ductility. In the second step, the capacity curve is bilinearized in order to represent the equivalent single-degree-of-freedom (SDOF) system. For bilinearization, the procedure proposed by either FEMA356 or ATC40 is used. Thirdly, maximum displacement demand of SDOF system is computed, using the procedure proposed by the method. In this sense, the NRHA (nonlinear response history analysis) of SDOF system can be carried out, or displacement coefficient method (multiplication by a number of modification factors) can be applied. In the fourth step, the roof displacement of MDOF system is computed, converting the maximum SDOF displacement. At this pushover step, the deformation and force demands are computed locally, in order to represent the inelastic behavior of the structural elements.

In this section, the nonlinear static analysis procedures (NSPs) based on Displacement Coefficient Method (DCM) (FEMA356 and FEMA440), Capacity Spectrum Method (CSM) (ATC40 and FEMA440), Nonlinear Analysis of SDOF Systems (Eq. SDOF), and Modified Modal Pushover Analysis (MMPA) will be reviewed.

2.2.1 Displacement Coefficient Method (DCM) of FEMA-356 (FEMA 2000)

According to FEMA356, in order to carry out the nonlinear static analysis, the mathematical model of building should be constituted, incorporating the nonlinear load-deformation characteristics of individual structural elements. This model is analyzed under the monotonically increasing lateral loads that represent the inertia forces in an earthquake, besides the already assigned gravity loads. The lateral loads are increased until a target displacement or onset of a structural mechanism. The structural response parameters, such as nodal displacements, element deformations, and strains, are recorded for each load step.

The capacity (pushover) curve is computed as the relationship between base shear force and lateral displacement of the "control" node that is assigned as the center of mass at the roof. For the lateral load patterns, at least two vertical distributions should be applied, i.e. proportional to the shape of the fundamental mode, proportional to the design story shears, a uniform distribution consisting of lateral forces at each level proportional to the story mass. In this study, the lateral load pattern was assigned only proportional to the shape of the fundamental mode in the direction of consideration.

The capacity curve computed is idealized using the bilinearization process as shown in Figure 2.1, in order to represent the equivalent SDOF system. The effective lateral stiffness, K_e, and the effective yield strength, V_y, values are calculated. Here, the initial slope of the bilinear curve is K_e and post-yield slope is αK_e. The areas under the capacity curve and bilinearized curve should be approximately balanced. On the other hand, the bilinearized curve intersects the capacity curve approximately at 60 percent of the effective yield strength, $0.6 \cdot V_y$.

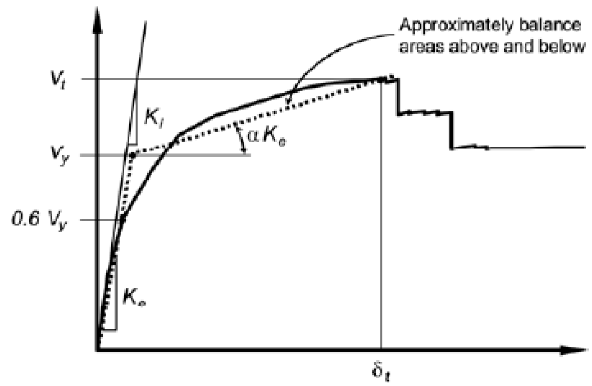

Figure 2.1 Bilinearization of capacity curve (FEMA 2000)

Based on the idealized curve, the effective fundamental period, T_e, is given in Equation (2.1).

$$T_e = T_i \sqrt{\frac{K_i}{K_e}} \quad \textbf{(2.1)}$$

where T_i is the elastic fundamental period calculated by elastic dynamic analysis, K_i is the elastic lateral stiffness of the building and K_e is the effective lateral stiffness in the direction under consideration.

The target displacement, δ_t, is calculated using the multiplication of spectral displacement, S_d, by a series of empirically derived modification factors as shown in Equation (2.2).

$$\delta_t = C_0 C_1 C_2 C_3 S_d \quad ; \quad S_d = S_a \frac{T_e^{\,2}}{4\pi^2} g \quad \textbf{(2.2)}$$

Where;

S_a is the response spectrum acceleration at the effective fundamental period and damping ratio and g is the acceleration of gravity.

C_0 is the modification factor to relate spectral displacement of the equivalent SDOF system to the roof displacement of the MDOF system. This value can be calculated as the first modal participation factor at the level of the control node or the appropriate value can be selected from Table 2.1.

C_1 is the modification factor to relate expected maximum inelastic displacements to displacements calculated for linear elastic response, and calculated by Equation (2.3). This value cannot exceed 1.5 and cannot be less than 1.0, according to FEMA356.

Table 2.1 Values for modification factor C_0

	Shear Buildings		Other Buildings
No of Stories	Triangular Load Pattern	Uniform Load Pattern	Any Load Pattern
1	1.0	1.0	1.0
2	1.2	1.15	1.2
3	1.2	1.2	1.3
5	1.3	1.2	1.4
10+	1.3	1.2	1.5

$$C_1 = 1.0 \quad \text{for} \quad T_e \geq T_S$$
$$C_1 = [1.0 + (R-1)\, T_S / T_e] / R \quad \text{for} \quad T_e < T_S \qquad \textbf{(2.3)}$$

T_e is the effective fundamental period of the building.
T_S is the characteristic corner period of the response spectrum that is defined as the transition period between constant acceleration and constant velocity segments of the spectrum.
R is the ratio of elastic strength demand to calculated yield strength coefficient calculated by Equation (2.4).

$$R = \frac{S_a}{V_y / W} \cdot C_m \qquad \textbf{(2.4)}$$

where, W is the effective seismic weight, V_y is the yield strength of idealized curve, and C_m is the effective mass factor that is given as 0.9 for the concrete moment frame systems with stories more than 3.

C_2 is the modification factor to represent the effect of pinched hysteretic shape, stiffness degradation and strength deterioration on maximum displacement response. For the nonlinear procedures, C_2 is permitted to be taken as 1.0.

C_3 is the modification factor to represent increased displacements due to P-Δ effects. This value is taken as 1.0 for the buildings having positive post-yield stiffness; otherwise, it is computed by Equation (2.5).

$$C_3 = 1.0 + \frac{|\alpha| \cdot (R-1)^{3/2}}{T_e} \qquad \textbf{(2.5)}$$

where α is the ratio of post-yield stiffness to effective elastic stiffness (Figure 2.1).

After obtaining the target displacement of the structure using DCM as explained above, the response of each structural member is computed at corresponding pushover step.

2.2.2 Displacement Coefficient Method (DCM) of FEMA-440 (ATC 2005)

Following the publication of FEMA273 and ATC-40 documents, the NSPs gained widespread use for seismic demand estimation. According to the diverse displacement demand results reported by engineers for the same building, however, improvement of these two methods was needed. Hence the ATC-55 Project (ATC 2005) was conducted and guidance for improved applications was provided by the final report, FEMA440.

FEMA440 suggests improved relationships for coefficients C_1 and C_2. In addition, the coefficient C_3 is eliminated and replaced with the minimum strength limit, which is proposed by the value of R_{max}.

The improved modification factor, C_1, that relates the expected max inelastic displacements to displacements calculated for linear elastic response, is given in Equation (2.6). The limitation allowed for C_1 by FEMA356 for relatively short-period structures is suggested not to be used by FEMA440.

$$C_1 = 1.0 + \frac{R-1}{aT_e^{\,2}} \qquad \textbf{(2.6)}$$

where T_e is the effective fundamental period and R is the strength ratio. The constant value, *a,* is equal to 130, 90, and 60 for site classes B, C, and D, respectively.

The C_1 value at 0.2 s is allowed to be used for lower periods, and can be taken as 1.0 for the periods greater than 1.0 s.

The modification factor, C_2, which represents the effect of stiffness degradation on max displacement response, is given in Equation (2.7). The C_2 value can be taken as 1.0 for the periods greater than 0.7 s. The C_2 value at 0.2 s is allowed to be used for the periods less than 0.2 s.

$$C_2 = 1 + \frac{1}{800}\left(\frac{R-1}{T_e}\right)^2 \qquad \textbf{(2.7)}$$

According to the improvement studies of FEMA440, it is indicated that global displacement demands are not significantly amplified by degrading strength, unless dynamic instability occurs. In order to avoid dynamic instability, C_3 factor is suggested to be eliminated and replaced with the limit on minimum strength (max R) that is given in Equation (2.8).

$$R_{\max} = \frac{\Delta_d}{\Delta_y} + \frac{\alpha_2^{\,-1}}{4} \qquad \textbf{(2.8)}$$

The notation of Equation (2.8) is shown in Figure 2.2.

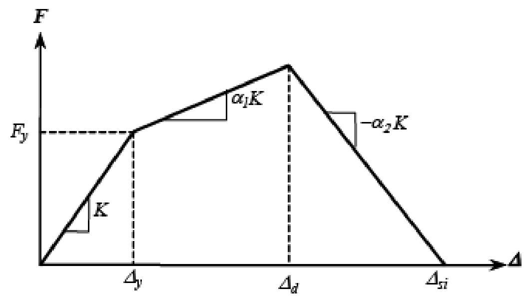

Figure 2.2 The notation for determining limitation on strength

2.2.3 Capacity Spectrum Method (CSM) of ATC-40 (ATC 1996)

The capacity spectrum method (CSM) was originally developed by Freeman et al. (1975), as part of a rapid evaluation procedure. The CSM of ATC-40 is based on equivalent linearization that is similar to the approach defined by Rosenblueth and Herrera (1964), rather than a displacement modification method of FEMA356. In equivalent linearization techniques, it is assumed that the max inelastic deformation of a nonlinear SDOF system is approximately equal to the maximum deformation of a linear elastic SDOF system that has larger values of period and damping ratio than the values of the nonlinear system.

CSM also requires the pushover analysis and computation of the pushover curve that represents the inelastic force-deformation behavior of the structure. The nonlinear displacement demand of the building under a given earthquake ground motion is determined from the intersection of the capacity curve of the building with the response spectrum of the ground motion which represents the demand curve. The capacity curve is the converted form of the pushover curve (base shear vs. roof displacement), using dynamic properties of the structure. The demand curve is a modified response spectrum of the design ground motion, accounting for hysteretic damping effects. The effective period and effective damping values of the structure, which are the functions of ductility, are computed using the empirically derived relationships. But, since equivalent viscous damping is a function of the ductility, an iterative solution is carried out.

Both the capacity curve and the demand curve are plotted in ADRS (acceleration-displacement response spectrum) format, as shown in Figure 2.3. The global displacement demand parameter is "spectral displacement (S_d)" and that is termed as "Performance Point" by ATC-40. In ADRS format, the period is represented by radial lines originating from the origin. The demand curve is converted to ADRS format by means of Equation (2.9). Similarly, for the conversion of pushover curve into capacity curve in ADRS format Equation (2.10) is used.

$$S_d = \frac{T^2}{4\pi^2} \cdot S_a \cdot g \tag{2.9}$$

$$S_a = \frac{V / W}{\alpha_1} \quad ; \quad S_d = \frac{\Delta_{roof}}{PF_1 \times \phi_{1,roof}} \tag{2.10}$$

where, S_a is the spectral acceleration, S_d is spectral displacement, T is the period, g is the acceleration of gravity, V is the base shear, W is the total weight of the building, α_1 is the modal mass coefficient for the fundamental (first natural) mode, PF_1 is the modal participation factor for the first mode, Δ_{roof} is the roof displacement and $\phi_{1,roof}$ is the amplitude of the first mode at roof level.

This iterative process is standardized and simplified by ATC-40, proposing three alternative procedures that are all based on same concepts, except that the application of either analytical or graphical techniques. In this study, the Procedure A, which is iterative and direct application of the concepts, was used. Procedure A is summarized in the following paragraphs.

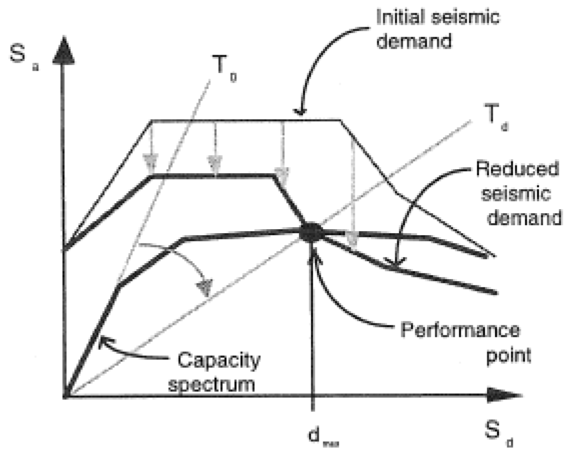

Figure 2.3 Graphic representation of capacity and demand curves (adopted from ATC-40)

The total amount of damping during an earthquake is simply the combination of the inherent viscous damping of the structure and hysteretic damping that is related with the energy dissipation capacity inside the hysteresis loops formed under earthquake excitation. The damping can be represented as equivalent viscous damping, β_{eq}, (Chopra 2007), as given in Equation (2.11).

$$\beta_{eq} = \beta_0 + 0.05 \quad ; \quad \beta_0 = \frac{1}{4\pi}\frac{E_D}{E_{So}} \qquad \textbf{(2.11)}$$

where β_0 is the hysteretic damping represented as equivalent viscous damping, E_D is energy dissipated by one cycle of the inelastic system and E_{So} is the max strain energy of the equivalent system. Note that the inherent viscous damping in the structure is assumed to be constant and 5 percent. The two energy terms, i.e. E_D and E_{So}, in the given equation are shown in Figure 2.4. However, the max equivalent damping value is limited as 45 percent.

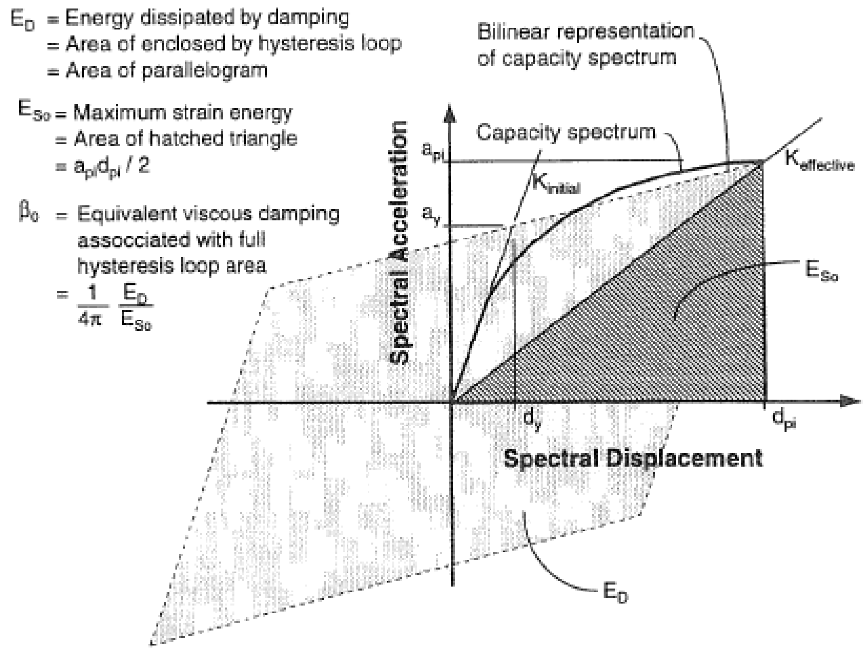

Figure 2.4 Illustration of the energy terms (adopted from ATC-40)

The equivalent viscous damping is computed for bilinear systems and elasto-plastic systems, as given in Equations (2.12) and (2.13), respectively.

$$\beta_0 = \frac{2}{\pi}\frac{(\mu - 1)(1-\alpha)}{\mu(1+\alpha\mu-\alpha)} \tag{2.12}$$

$$\beta_0 = \frac{2}{\pi}\frac{\mu - 1}{\mu} \tag{2.13}$$

where μ is ductility ($\mu = d_{pi}/d_y$) and α is the post-yield slope of the idealized curve.

Although the equivalent damping calculation using Equation (2.11) is reasonable for ductile buildings with equivalent viscous damping less than 30 percent, the damping level of the existing buildings that are not ductile might be overestimated. Therefore, the damping modification factor, κ, is introduced, which depends on the structural behavior, in order to compute the effective damping, β_{eff}, as given in Equation (2.14).

$$\beta_{eff} = \kappa \cdot \beta_0 + 0.05 \tag{2.14}$$

The structural behavior is affected by the quality of the seismic resisting system and duration of the ground motion. ATC-40 designated three categories of behavior as stable (type A), moderate (type B) and poor (type C) hysteretic behavior. The corresponding modification factors for each behavior type are given in Table 2.2. In this study, the buildings investigated were assumed to have moderate hysteretic behavior (type B).

Table 2.2 Damping modification factor, κ

Structural Behavior	β_0 **(%)**	κ
Type A	≤ 16.25	1.0
	> 16.25	$1.13 - \frac{0.51(\mu-1)(1-\alpha)}{\mu(1+\alpha\mu-\alpha)}$
Type B	≤ 25	2 / 3
	> 25	$0.845 - \frac{0.446(\mu-1)(1-\alpha)}{\mu(1+\alpha\mu-\alpha)}$
Type C	any value	1 / 3

Based on the secant stiffness at maximum displacement, the equivalent period (of the equivalent SDOF system), T_{eq}, can be computed by Equation (2.15), where T_0 is the elastic period of nonlinear system.

$$T_{eq} = T_0 \sqrt{\frac{\mu}{1 + \alpha\mu - \alpha}} \tag{2.15}$$

The iterative procedure of CSM (procedure A) is summarized as follows;

1. Plot the capacity curve and demand curve (elastic response spectra with 5 percent damping),
2. Select a trial performance point (equal displacement rule may be used for the first trial),
3. Compute the ductility, $\mu = d_{pi} / d_y$
4. Compute the equivalent damping ratio by Equation (2.14),
5. Plot the demand curve for β_{eff}, and read the spectral displacement at intersection of capacity and demand curves,
6. Check the convergence (should be less than 0.05). If the computed spectral displacement is close with a tolerance less than 0.05, the analysis is terminated. Otherwise, the steps 2 – 6 are repeated setting the spectral displacement read in fifth step as initial estimate.

Chopra and Goel (2000) have examined the CSM procedure in detail to point out that, under an unfavorable set of conditions the procedure may not converge, or otherwise lead to unrealistic displacement estimates.

2.2.4 Capacity Spectrum Method (CSM) of FEMA-440 (ATC 2005)

In the light of extensive evaluation of CSM, FEMA440 suggests improved empirical expressions for effective period, T_{eff}, and effective damping ratio, β_{eff}, computation. On the other hand, much of the process remains the same. However, the upper limit for the effective damping designated by ATC-40 is eliminated by FEMA 440.

The improved expressions were developed taking the hysteretic behavior types into consideration, such as bilinear (elastic perfectly plastic), stiffness-degrading and strength-degrading hysteretic behavior. The relationships for T_{eff} and β_{eff} are developed using the coefficients A to K that depends on the ductility level and hysteretic behavior type of the model. The coefficients A to K are designated in a tabulated format. Furthermore, these equations are optimized for application to any capacity curve, independent of the hysteretic behavior, but for the $T_0 = 0.2 \sim 2.0$ s. Since the elastic periods of the buildings studied were within the given range, the optimized approximate equations were used.

The proposed expressions for the effective period, T_{eff}, are given in Equations (2.16) - (2.18), for three different levels of ductility.

For $\mu < 4$: $$T_{eff} = \left[0.20(\mu-1)^2 - 0.038(\mu-1)^3 + 1\right] \cdot T_0 \qquad \textbf{(2.16)}$$

For $4.0 \le \mu \le 6.5$: $$T_{eff} = \left[0.28 + 0.13(\mu-1) + 1\right] \cdot T_0 \qquad \textbf{(2.17)}$$

For $\mu > 6.5$: $$T_{eff} = \left[0.89 \cdot \left(\sqrt{\frac{\mu-1}{1+0.05\cdot(\mu-2)}} - 1\right) + 1\right] \cdot T_0 \qquad \textbf{(2.18)}$$

The proposed expressions for the effective damping, β_{eff}, are given in Equations (2.19) - (2.21), for three different levels of ductility. Note that the constant value of 5 percent as the inherent viscous damping in the structure is included in the given optimized β_{eff} equations.

For $\mu < 4$: $$\beta_{eff} = 4.9 \cdot (\mu-1)^2 - 1.1 \cdot (\mu-1)^3 + 0.05 \qquad \textbf{(2.19)}$$

For $4.0 \le \mu \le 6.5$: $$\beta_{eff} = 14.0 + 0.32 \cdot (\mu-1) + 0.05 \qquad \textbf{(2.20)}$$

For $\mu > 6.5$: $$\beta_{eff} = 19 \cdot \left[\frac{0.64\cdot(\mu-1)-1}{[0.64\cdot(\mu-1)]^2}\right] \cdot \left(\frac{T_{eff}}{T_0}\right) + 0.05 \qquad \textbf{(2.21)}$$

Soil-structure interaction (SSI) is also considered by FEMA440, proposing simplified procedures. On the purpose, FEMA440 addresses the reduction of the shaking demand on the structure relative to the free-field motion caused by kinematic interaction and the foundation damping effect. In this study, due to the modeling assumption of fixed building foundations, the foundation damping was neglected, while the kinematic effects were considered.

Kinematic interaction effects that are related with the foundation size and embedment may be important especially for the buildings with relatively short fundamental periods, large plan dimensions, and deep basement embedment in soil materials.

In order to represent the kinematic interaction effects, the ratio of response spectra, *RRS*, is used, considering base slab averaging and foundation embedment. The *RRS* is calculated by multiplication of the ratios RRS_{bsa} and RRS_e that are related with the base slab averaging and embedment, respectively. The RRS_{bsa} can be computed using the Equation (2.22), for the periods greater than 0.2s.

$$RRS_{bsa} = 1 - \frac{1}{14100}\left(\frac{b_e}{T}\right)^{1.2} \qquad \textbf{(2.22)}$$

where $b_e = \sqrt{ab} =$ effective foundation size, where a and b values are the full footprint dimensions (in feet) of the building.

The RRS_e can be computed as the maximum value of the Equation (2.23), 0.453 or the RRS_e value for the period 0.2s.

$$RRS_e = \cos\left(\frac{2\pi e}{Tnv_s}\right) \qquad \textbf{(2.23)}$$

where e is the foundation embedment, v_s is shear wave velocity for site soil conditions, taken as average value of velocity to a depth of b_e below foundation, and n is shear wave velocity reduction factor for the expected PGA.

The improved CSM procedure of FEMA440 also requires an iterative process, since both the effective period and effective damping values depend on the ductility demand. The iterative procedure (procedure A) can be summarized as follows;

1. Plot the capacity curve and demand curve (elastic response spectra with 5 percent damping),
2. Modify the selected spectrum, applying the SSI related factor, *RRS*,
3. Select a trial performance point (equal displacement rule may be used for the first trial),
4. Compute the ductility, $\mu = d_{pi} / d_y$
5. Compute the equivalent period (T_{eff}) and equivalent damping ratio (β_{eff}) through the Equations (2.16) to (2.21),
6. Plot the demand curve for β_{eff}, and read the spectral displacement at intersection of capacity and demand curves,
7. Check the convergence (should be less than 0.05).

If the computed spectral displacement is close with a tolerance less than 0.05, the analysis is terminated. Otherwise, the steps 2 – 7 are repeated setting the spectral displacement read in sixth step as initial estimate.

2.2.5 Nonlinear Analysis of Equivalent SDOF System (Eq. SDOF) (Fajfar and Fischinger 1987)

Due to the large inelastic deformations of the buildings subjected to strong ground motions, nonlinear dynamic analysis of the buildings are preferred for accurate results. The N2 method was proposed by Fajfar and Fischinger (1987) as an accurate but less complicated nonlinear method, especially for structures oscillating predominantly in a single mode. Although, the N2 method was proposed mainly for the seismic design of the buildings, the method can also be applied for the evaluation of existing buildings. This analysis method is an extension of the Q-Model by Saiidi and Sözen (1981).

The N2 method is summarized in four steps. In the first step, a nonlinear static pushover analysis is carried out on the MDOF system model under a monotonically increasing lateral load. The resulting capacity curve that represents the stiffness, strength and supplied ductility characteristics of the building, is converted into an equivalent SDOF system, in the second step. Then, in third step, the equivalent SDOF system is analyzed by nonlinear response history analysis, in order to compute the maximum displacement demand of the earthquake ground motion. Inelastic response spectra can also be used as a simpler way of the dynamic analysis. Lastly, maximum roof displacement demand of the MDOF system is computed from the max displacement demand of the SDOF system. The structural response parameters, i.e. local force and deformation demands, plastic hinges, interstory drifts, etc., are computed at the pushover step corresponding to the max roof displacement obtained. Furthermore, the structural behavior is predicted, comparing the ductility demand and supply.

2.2.6 Modified Modal Pushover Analysis (MMPA) (Chopra et al. 2004)

One of the major drawbacks of conventional pushover analysis procedures is discussed as the higher mode effects that are generally ignored (Sasaki et al., 1998; Gupta and Kunnath, 2000). In order to take the higher mode effects into consideration for the inelastic demand calculation, the MMPA (modified modal pushover analysis) procedure was proposed (Chopra et al., 2004), as an improved version of the MPA (Chopra and Goel, 2002), which are both based on the structural dynamics theory (Chopra, 2007).

The MPA procedure computes the inelastic displacement demand combining the contribution of all significant (first two or three) modes of vibration. Independent pushover analyses are carried out for each of the significant modes in the direction of loading, and equivalent SDOF representation of each modal pushover curve is obtained. Then, inelastic modal displacement demands are calculated by individual NRHA of equivalent SDOF systems. The modal response quantities computed are combined using either SRSS or CQC combination rules.

In MMPA, on the other hand, the effect of higher modes is assumed to be linear elastic, and hence pushover analysis is not needed for the higher modes of vibration. Therefore, the inelastic response of the fundamental mode combined with the elastic contribution of higher modes, which are computed by individual linear response history analysis. Although, the results of MMPA are not more accurate than MPA, this simplification reduces the computational effort. Since the seismic demand results of MMPA are slightly larger, its conservatism is improved.

The application of MMPA procedure is summarized in a series of steps, as follows;

1. Carry out the linear elastic modal analysis of the building.
2. For the fundamental (first) mode in the direction of consideration, develop the pushover curve (base shear, V_{b1}, vs. roof displacement, u_{r1}) for the lateral load vector proportional to the product of mass times fundamental mode shape. The gravity loads should be initially applied, and lateral roof displacement due to gravity loads, u_{rg}, is computed.
3. Idealize the pushover curve as a bilinear curve.
4. Convert the idealized curve to the force-displacement (F_{s1}/L_1 - D_1) relation for the first-mode inelastic SDOF system by Equation (2.24).

$$\frac{F_{s1}}{L_1} = \frac{V_{b1y}}{M_1^*} \quad ; \quad D_{1y} = \frac{u_{r1y}}{\Gamma_1 \phi_{r1}} \tag{2.24}$$

where M_1^* is the effective modal mass, ϕ_{r1} is the value of ϕ_1 at roof, and $\Gamma_1 = \dfrac{\phi_1^T m 1}{\phi_1^T m \phi_1}$.

5. Compute the peak deformation, D_1, for the SDOF system defined in step 4 with the damping ratio, ζ_1. Either NRHA or inelastic design spectrum can be used for this purpose.
6. Calculate the peak roof displacement, u_{r1}, using the relation $u_{r1} = \Gamma_1 \phi_{r1} D_1$.
7. Compute the desired responses, r_{1+g}, due to the combined effect of gravity and lateral loads at roof diplacement value of u_{r1}+u_{rg}.
8. Dynamic response due to first-mode, r_1, can be computed by $r_1 = r_{1+g} - r_g$, where r_g is the contribution of gravity loads.
9. Compute the dynamic responses due to higher modes, r_n, assuming that system remains elastic. Either linear RHA or elastic design spectrum can be used for this purpose.

Subsequently, the total dynamic response quantity is computed using SRSS rule as given in Equation (2.25).

$$r \approx \max\left[r_g \pm \sqrt{\sum_n r_n^2} \right] \qquad \textbf{(2.25)}$$

Of course, Equation (2.25) is not mathematically correct because nonlinear systems do not obey the SRSS rule, but the authors show that the errors lie on the safe side.

2.3 BUILDING PERFORMANCE DEFINITIONS

Seismic performance definitions for the reinforced concrete buildings given by the seismic provisions and standards, i.e. ASCE/SEI-41, EC8-3, and TEC2007, are described in this section.

The expected or intended seismic performance of a building against a given earthquake ground motion is specified by the “performance objective”. In order to qualify the seismic performance, maximum allowable damage states (performance levels) are designated, for certain levels of seismic hazard of the site. For this purpose, different performance levels have been defined by provisions and standardization attempts based on the observed damage states of the building. In the Blue Book (SEAOC 1999), for instance, four different performance levels are designated as follows;

- **Level 1: Fully Operational.** In this level, since the damage is negligible, facility continues in operation.
- **Level 2: Operational.** There is minor damage on structural members and limited disruption in nonessential services. Immediate occupancy of the structure is allowed.
- **Level 3: Life Safe.** Although, the damage is moderate to extensive, life safety is substantially protected.
- **Level 4: Near Collapse.** Damage is severe, and thus, life safety is at risk. Structural collapse, however, is prevented.

As it can be seen from the performance levels by Blue Book, limiting condition of the building is described by means of the physical damage and threat to the life safety in building due to the damage that occurred, as well as building serviceability after the damage.

The earthquake performance levels are defined for different levels of probable expected earthquake intensity at the site. According to the objective of the building, different seismic performance levels can be selected considering different levels of strong ground motion which corresponds to the seismic hazard of the site (Figure 1.1). If necessary, more than one damage state for different levels of ground motion might be included in the desired performance objective.

This general philosophy on qualification of the performance levels is generally followed by the recent provisions and standards which are discussed in the following sections.

2.3.1 Performance Definitions of ASCE/SEI-41 (ASCE 2007)

In ASCE/SEI-41 (ASCE 2007), three discrete “Structural Performance Levels” and two intermediate “Structural Performance Ranges” are identified as performance levels of a building. These performance levels are Immediate Occupancy (IO), Life Safety (LS), and Collapse Prevention (CP); while the intermediate structural performance ranges are defined as Damage Control Range and the Limited Safety Range. ASCE/SEI-41 also designates the “Non-structural Performance Levels”, however, the non-structural performance of the buildings were not taken into consideration in this study.

Immediate Occupancy (IO) is defined as the post-earthquake damage state in which the structure remains safe to occupy, and essentially retains its design strength and stiffness, since very limited structural damage has occurred. However, some minor structural repair might be needed.

At Life Safety (LS) damage state significant structural damage has occurred, but some margin against onset of either partial or total structural collapse remains. Even though there is possibility of injuries during the earthquake, the expected overall risk of life-threatening injuries is low. It is possible to repair the structure, unless it may not be practical regarding economic reasons.

The structure is severely damaged at Collapse Prevention (CP) damage state. However, it continues to support the gravity loads, is on the verge of partial or total collapse. There is significant risk of injury due to falling hazards of structural debris.

The structural performance ranges of Damage Control Range and Limited Safety Range are also identified between IO-LS and LS-CP, respectively. The aim of structural performance range definition is to permit users to customize their building rehabilitation objectives.

2.3.2 Performance Definitions of TEC-2007 (TEC 2007)

The Chapter 7 of TEC-2007 standard proposes two different procedures as linear and nonlinear evaluation of existing buildings. The linear evaluation procedure is not considered in this study.

According to TEC-2007, the “ductile” and “brittle” modes of failure are considered in order to classify the structural members, and the corresponding damage limits are determined. Three damage limits are defined for ductile members, as minimum damage limit (MN), safety limit (SF) and collapse limit (CL). The damage states of a member and corresponding damage limits have been shown in Figure 2.5. Brittle members are not permitted to exceed the MN limit that defines the beginning of plastic behavior.

2.3.3 Performance Definitions of EC8-3 (EC 2005)

Similar to ASCE/SEI-41 and TEC-2007, EC8 also defines damage limitation states as well as ultimate limit state of the building. While ultimate limit state is associated with the collapse or other forms of structural failure, damage limitation states are defined in order to check whether the specified service requirements are met. At ultimate limit state, the whole building should be stable under the design seismic action.

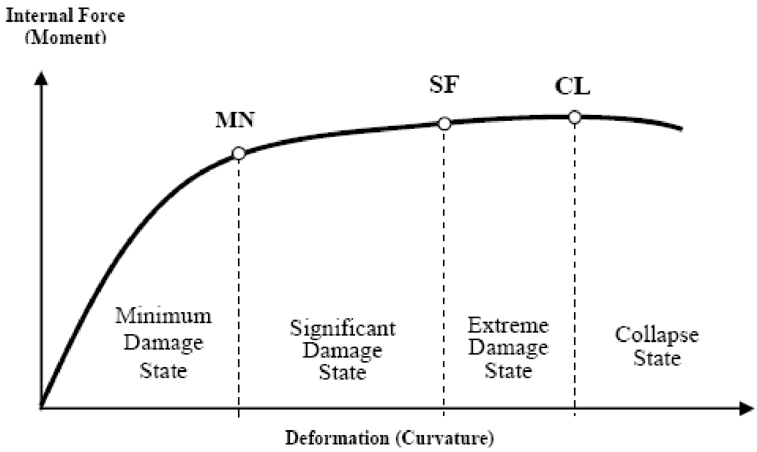

Figure 2.5 Damage States and Corresponding Damage Limits of a Ductile Member

The three limit states are Near Collapse (NC), Significant Damage (SD), and Damage Limitation (DL). The structure is heavily damaged at NC limit state, with small residual strength and stiffness. The vertical elements, however, are still capable of sustaining vertical loads, but large permanent drifts might be present. The structure would not survive another earthquake.

The structure is significantly damaged at SD limit state, with some residual strength and stiffness, and vertical elements are capable of sustaining vertical loads. Moderate permanent drifts might be present. In general, the structure is likely to be uneconomic to repair.

At DL limit state, very light damage occurs. There are no permanent drifts in the building, and any repair is not needed.

The damage interval between DL and SD is designated as "damage control range", while the damage interval between SD and NC is designated as "limited safety range", implying the moderate and severe damage states, respectively.

2.3.4 Performance Definitions of ATC-40 (ATC 1996)

Performance definitions of ATC-40 for different performance levels are the same as the definitions of the subsequent document of ASCE/SEI-41 (Section 2.3.1). The ultimate damage state of "Collapse Prevention" given in ASCE/SEI-41 is designated as "Structural Stability" in ATC-40, but the level of structural damage is the same.

2.4 ACCEPTABILITY LIMITS / PERFORMANCE CRITERIA

In many standards, each of the performance or damage levels (Section 2.3) is quantified by corresponding acceptance criteria, which are described in this section. When the acceptance criteria of discrete documents viewed, it can be seen that global acceptance criteria are only available by ATC-40 and TEC-2007, defining the maximum allowable interstory drift ratios. ATC-40 was superseded by ASCE/SEI-41 and the subsequent standard does not propose any global acceptance criteria. Structural element based criteria are given by means of plastic (hinge) rotation, chord rotation and strain, by ASCE/SEI-41, EC8-3 and TEC-2007, respectively. The definitions of the component deformation parameters of plastic rotation and chord rotation are shown in Figure 2.6.

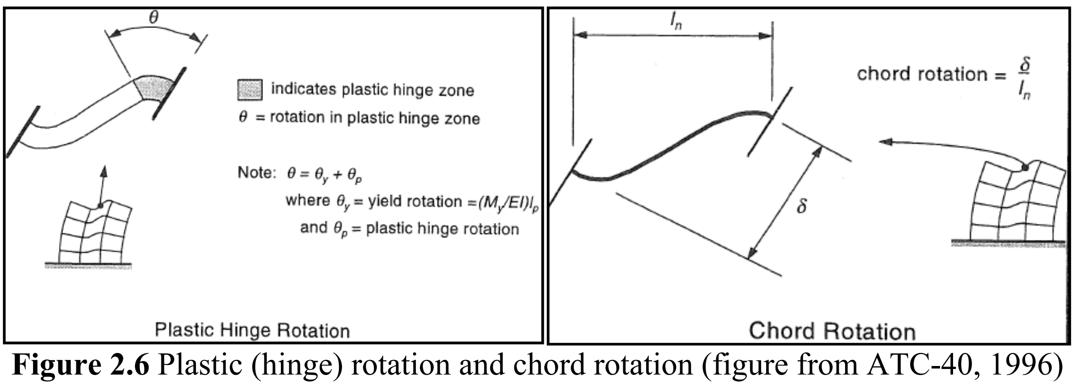

Figure 2.6 Plastic (hinge) rotation and chord rotation (figure from ATC-40, 1996)

2.4.1 Response Limits of ATC-40 (ATC 1996)

Global Building Acceptability Limits: Gravity Loads

Since, the loss of gravity load carrying capacity in frame elements or connections has been the primary cause of collapse in past earthquakes; ATC-40 document makes sure that the gravity load capacity of the building must remain intact at any performance level.

Global Building Acceptability Limits: Lateral Loads

Some of the structural components may degrade over multiple load cycles as strong ground motions. Due to the degrading components, overall load resistance of the structure may be affected. The requirement of ATC-40 for the case of degrading is "the lateral load resistance of the building system, including resistance to the effects of gravity loads acting through lateral displacements, should not degrade by more than 20 percent of the max resistance of the structure".

Global Building Acceptability Limits: Lateral Deformations

The global lateral deformation limits of the ATC-40 are given in Table 2.3. The max total drift is defined as the interstory drift at performance point and max inelastic drift is the portion of the max total drift beyond the effective yield point. For the structural stability (SS) performance level, max total drift is limited by 1/3 of the base shear coefficient ($0.33*V_i/P_i$), where the V_i is the story shear force at i^{th} story, and P_i is the total gravity load at that story.

Table 2.3 Lateral deformation limits (ATC-40)

Interstory Drift Limit	Performance Level			
	IO	DC	LS	SS
Maximum Total Drift (%)	1	1 – 2	2	$33 * V_i / P_i$
Maximum Inelastic Drift (%)	0.5	0.5 – 1.5	no limit	no limit

Element Acceptability Limits:

In ATC-40, element and component acceptance criteria are given, as well as global acceptance criteria, which are summarized above. "Plastic hinge rotation" is used as the member deformation parameter. The calculated values of structural component deformations are not permitted to exceed deformation limits for each performance level. These deformation limits given by ATC-40, however, superseded by subsequent documents, i.e. FEMA-356, ASCE/SEI-41.

2.4.2 Response Limits of ASCE/SEI-41 and Supplement-1 (ASCE 2007, ASCE 2008)

ASCE/SEI-41 standard proposes assessment procedures as “linear (static and dynamic)” and “nonlinear (static and dynamic)”. It also designates the corresponding acceptance criteria for structural and non-structural members. The linear assessment procedures are out of the scope of this study. On the other hand, component acceptance criteria for nonlinear analysis procedures are defined for columns, beams, beam-column connections and structural walls by means of plastic hinge rotation, for each of the structural performance levels. The deformation capacities of the structural components should not be less than the maximum deformation demands calculated by nonlinear analysis procedures at the target displacement.

ASCE/SEI-41 standard does not propose any global acceptance criteria similar to the given in ATC-40 and TEC-2007.

The RC columns were classified according to whether they are “controlled by flexure,” “controlled by inadequate development or splicing,” or subjected to high axial loads by the former prestandard of seismic rehabilitation of buildings, FEMA-356. There was no plastic deformation permission for the shear controlled columns. Moreover, the flexure controlled columns were also categorized as “conforming” or “nonconforming”, according to spacing of hoops ($\leq d/3$), and the level of the strength provided by hoops (whether it is at least three-fourths of the design shear for conforming columns) if the ductility demand is moderate or high (ASCE 2008). The same classification was also followed by the successor standard, ASCE/SEI-41.

Some recent experimental research results (e.g., Sezen and Moehle, 2006; Yoshimura et al., 2004; Ousalem et al., 2004) have demonstrated that the FEMA 356 assessment model predicted the column strengths well, but underestimated the displacements. According to these researches, many older type columns are capable of sustaining limited plastic deformation due to flexural yielding prior to shear failure (flexure-shear failure mode). Especially for low axial loads, such columns may be capable of sustaining axial loads well beyond the point of apparent shear failure. Thus, based on these experimental evidences, the acceptance criteria have been liberalized (ASCE 2008).

Consequently, in the ASCE/SEI 41 Supplement 1 (ASCE 2008), the revisions for classification of the columns have been proposed. The proposed classification is given in Table 2.4.

Table 2.4 Classification of columns by ASCE/SEI 41 Supplement 1

	Transverse Reinforcement Details		
	ACI conforming details with 135° hooks	Closed hoops with 90° hooks	Other (including lap spliced transverse reinforcement)
Vp/(Vn/k) ≤ 0.6	Condition i	Condition ii	Condition ii
1.0 ≥ Vp/(Vn/k) > 0.6	Condition ii	Condition ii	Condition iii
Vp/(Vn/k) > 1.0	Condition iii	Condition iii	Condition iii

The classification into three conditions is based on the ratio of nominal shear strength (V_n) to the plastic shear demand (V_p) of the column and the detailing of transverse reinforcement. Here, the "*k*" value is the modifier based on ductility demand (according to ASCE/SEI-41). The three conditions of the classification can be defined as follows;

- Condition i: Flexure failure (flexural yielding without shear failure)
- Condition ii: Flexure-shear failure (where yielding in flexure is expected prior to shear failure)
- Condition iii: Shear failure (shear failure before flexural yielding)

According to the classification of columns, poor transverse detailing directly affects the performance level limits for the columns. In order to avoid unconservatively misclassifying a column as flexure-critical, the upper bound of the $V_p/(V_n/k)$ ratio for condition i has been set as 0.6 rather than 0.7, which is the equivalent corresponding value from ASCE/SEI-41 shear strength model. The acceptance criteria have been designated for each of the conditions defined in the ASCE/SEI 41 Supplement 1 (ASCE 2008).

The stirrups of RC sections have a closing angle of 90° instead of 135° of the buildings selected for this study (according to their blue prints). On the other hand, the shear responses of the buildings were analyzed separately (Section 5.3.1 and Section 6.2). Therefore, the columns of the buildings studied were classified as in "Condition ii". The corresponding numerical acceptance criteria for nonlinear procedures defined in ASCE/SEI 41 Supplement 1, for RC columns, are given in Table 2.5 (in an extent of the relation to buildings of this study). It is permitted to use linear interpolation between the values listed in table.

Similar to the acceptance criteria designated for the columns as discussed in the preceding paragraphs, the acceptance criteria also defined for the other structural components, as beams, structural walls or connections. Since the evaluation of columns is preferential and sufficient for the overall building evaluation in this study, the acceptance criteria of the other structural components are not given here for the brevity.

Table 2.5 Numerical acceptance criteria for nonlinear procedures – RC columns (adapted from ASCE/SEI-41 Supplement-1, 2008)

Condition ii:			**Acceptance Criteria**		
			Plastic Rotations Angle, radians		
			Performance Level		
$\dfrac{P}{A_g \cdot f'_c}$	$\rho = \dfrac{A_v}{b_w \cdot s}$	$\dfrac{V}{b_w \cdot d \cdot \sqrt{f'_c}}$	**IO**	**LS**	**CP**
≤ 0.1	≥ 0.006	≤ 0.25	0.005	0.024	0.032
≤ 0.1	≥ 0.006	≥ 0.50	0.005	0.019	0.025
≥ 0.6	≥ 0.006	≤ 0.25	0.003	0.008	0.009
≥ 0.6	≥ 0.006	≥ 0.50	0.003	0.006	0.007
≤ 0.1	≤ 0.0005	≤ 0.25	0.005	0.009	0.010
≤ 0.1	≤ 0.0005	≥ 0.50	0.004	0.005	0.005
≥ 0.6	≤ 0.0005	≤ 0.25	0.002	0.003	0.003
≥ 0.6	≤ 0.0005	≥ 0.50	0.0	0.0	0.0

2.4.3 Response Limits of TEC-2007 (TEC 2007)

The element acceptance criteria for three performance levels have been defined similarly as in ASCE/SEI-41, but the "material strain" parameter has been used rather than "plastic hinge rotation". The compressive strains for concrete and tensile strain demands for steel, which are calculated from curvature demands (which are calculated from plastic rotation demands) at the plastic regions are used for the comparison with the given acceptance criteria.

Concrete and steel strain limits at the fibers of a cross section for minimum damage limit (MN), safety limit (SF) and collapse limit (CL) are given in the Equations (2.26) to (2.28), respectively.

$$(\varepsilon_{cu})_{MN} = 0.0035 \quad ; \quad (\varepsilon_s)_{MN} = 0.010 \qquad \textbf{(2.26)}$$

$$\left(\varepsilon_{cg}\right)_{SF} = 0.0035 + 0.01 \cdot \left(\rho_s / \rho_{sm}\right) \leq 0.0135 \quad ; \quad \left(\varepsilon_s\right)_{SF} = 0.040 \tag{2.27}$$

$$\left(\varepsilon_{cg}\right)_{CL} = 0.004 + 0.014 \cdot \left(\rho_s / \rho_{sm}\right) \leq 0.018 \quad ; \quad \left(\varepsilon_s\right)_{CL} = 0.060 \tag{2.28}$$

In Equations (2.26) to (2.28), ε_{cu} is the concrete strain at the outer fiber, ε_{cg} is the concrete strain at the outer fiber of the confined core, ε_s is the steel strain and (ρ_s/ρ_{sm}) is the ratio of existing confinement reinforcement at the section to the confinement required by the Code.

For assessment of the existing buildings, transverse reinforcement of the structural members should be designed and built according to the rules given by the Code. Nonconforming transverse reinforcement shall be neglected in assessment process (TEC-2007).

The damage state of any structural member is determined by the most critical fiber section, having the most severe damage state. The overall structural performance is then obtained by accounting for the distribution of member damages over the building. The limits in Equations (2.26) - (2.28) have been shown to lie on the unsafe side by Kazaz et al. (2012a, 2012b).

The acceptability limits of the interstory drift ratio (ISDR) are given in Table 2.6, for each performance level of the RC members (columns and structural walls). Although it is given in the section for linear procedures in TEC-2007, the ISDR limits are also valid as a global check of the building for nonlinear assessment procedure of TEC-2007 (Sucuoğlu 2006).

Table 2.6 Interstory drift limits (TEC-2007)

Interstory Drift Ratio	Performance Level		
	Immediate Occupancy	Life Safety	Collapse Prevention
$\delta_{i,max} / h_i$ (%)	1	3	4

2.4.4 Response Limits of EC8-3 (EC 2005)

The European Standard, EC8-3, does not propose any global acceptance criteria, except for the limitation of interstory drift (for seismic design of buildings[1]), which is given by Equation (2.29). This limitation for the lateral displacement is also valid for the rehabilitated buildings according to the EC8-3.

$$dr \cdot v \leq 0.01 \cdot h \qquad \textbf{(2.29)}$$

where dr is design interstory drift, v is reduction factor, and h is the story height.

The structural elements are classified as "ductile" or "brittle". The ductile elements are verified by checking deformation demands, while the brittle elements are verified in comparison of the demands with the strength capacities.

The component evaluation is done using the parameter of element chord rotation (θ), i.e., the angle between the tangent to the axis at the yielding end and the chord connecting that end with the end of the shear span ($L_V = M / V$ = moment/shear). The chord rotation is also equal to the element drift ratio ($\theta = \Delta / L$). The chord rotation parameter is graphically shown in Figure 2.7 for a beam member. The demand values calculated by the nonlinear analysis are compared with the given limitations by a few expressions that define the yield and ultimate plastic rotations for each performance level, i.e. near collapse (NC), severe damage (SD) and damage limitation (DL).

The ultimate chord rotation capacity for concrete structural members is defined as given in Equation (2.30). The ultimate chord rotation limit designates the Near Collapse (NC) limit state, which is the upper-bound of limited safety performance range.

[1] Section 4.4.3.2 of the EC8-1

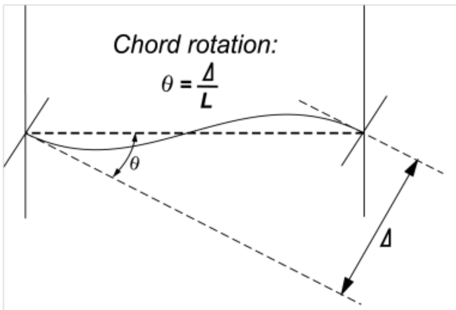

Figure 2.7 Chord rotation in a beam member supported by axially rigid columns

$$\theta_{um} = \frac{1}{\gamma_{el}} 0.0172 \cdot \left(0.3^{\nu}\right) \cdot \left[\frac{\max(0.01, \omega')}{\max(0.01, \omega)} f_c\right]^{0.175} \left(\frac{L_V}{h}\right)^{0.4} 25^{\left(\alpha \rho_{sx} \frac{f_{yw}}{f_c}\right)} \left(1.3^{100\rho_d}\right) \qquad \textbf{(2.30)}$$

Where;

γ_{el} = 1.5 (primary elements) and γ_{el} = 1.0 (secondary elements),

h is depth of cross-section,

$\nu = N / bhf_c$ (b is width of compression zone, N is axial force positive for compression),

ω and ω' are mechanical reinforcement ratios of the tension and compression (respectively) longitudinal reinforcement,

f_c is the estimated value of the concrete compressive strength (MPa),

$\rho_{sx} = A_{sx} / b_w s_h$ = ratio of transverse steel parallel to the direction x of loading (s_h = stirrup spacing),

ρ_d = steel ratio of diagonal reinforcement (if any), in each diagonal direction,

α is the confinement effectiveness factor that may be calculated by Equation (2.31).

$$\alpha = \left(1 - \frac{s_h}{2b_c}\right)\left(1 - \frac{s_h}{2h_c}\right)\left(1 - \frac{\sum b_i^2}{6h_c b_c}\right) \qquad \textbf{(2.31)}$$

where b_c and h_c are the dimensions of confined core, b_i is centerline spacing of longitudinal bars (indexed by i) laterally restrained by a stirrup corner or a cross-tie along the perimeter of the cross-section.

According to the EC8-3, if the members were not detailed for earthquake resistance, the ultimate chord rotation capacity should be divided by the factor of 1.2. Moreover, α should taken as "zero", if stirrups are not closed with 135° hoops.

The ultimate chord rotation capacity, defined by Equation (2.30) is the total rotation of the member, including both the elastic and inelastic (plastic) rotation. The plastic chord rotation of the structural member may be calculated by Equation (2.32).

$$\theta_{um}{}^{pl} = \frac{1}{\gamma_{el}} 0.0129 \cdot \left(0.2^{\nu}\right)\left[\frac{\max(0.01,\omega')}{\max(0.01,\omega)} f_c\right]^{0.225} \left(\frac{L_V}{h}\right)^{0.375} 25^{\left(\alpha \rho_{sx} \frac{f_{yw}}{f_c}\right)} \left(1.3^{100\rho_d}\right) \quad \textbf{(2.32)}$$

The chord rotation relative to Severe Damage (SD) limit state (the upper-bound of the damage control performance range), θ_{SD}, is also designated using ultimate chord rotation capacity, assuming that it is 75 percent of the ultimate chord rotation (Equation (2.33)).

$$\theta_{SD} = \frac{3}{4} \cdot \theta_{um} \quad \textbf{(2.33)}$$

The deformation limit for the Damage Limitation (DL) limit state is designated by the chord rotation at yield, which is given in Equation (2.34). In this equation, flexural and shear contributions are taken into consideration by first and second terms, respectively, and the third term accounts for the anchorage slip of bars.

$$\theta_y = \phi_y \frac{L_V}{3} + \alpha_{el} + \alpha_{el} \frac{0.2 \cdot \varepsilon_{sy} \cdot d_b f_y}{(d - d')\sqrt{f_c}} \quad \textbf{(2.34)}$$

Where;

φ_y is the yield curvature,

α_{el} = 0.00275 (beams and columns) and α_{el} = 0.0025 (walls: rectangular, T- or barbelled section),

d and d' are the depth to the tension and compression reinforcement, respectively,

f_y and f_c are the estimated values of the steel tensile and concrete compressive strength, respectively.

CHAPTER 3

THE AUGUST 17, 1999, MARMARA EARTHQUAKE

3.1 INTRODUCTION

On August 17, 1999, Turkey experienced an un-planned large scale testing of buildings during the Marmara Earthquake. The 7.4 magnitude earthquake struck Marmara Region of Turkey and a large number of buildings were damaged, thousands of people died.

This strong earthquake was another lesson that clearly indicates again the vulnerability of the existing building stocks against seismic hazard. The vulnerable reinforced concrete buildings, which represent over 48 percent of the building stock (98 percent of buildings with moment-resisting-frame systems) in Turkey (SIS, 2000) experienced various degrees of damage (moderate, severe) while many of them collapsed. The buildings in Adapazarı were not exempt and exposed to various levels of structural damage during the earthquake.

Several reasons come together which result in the increase of seismic risks as in this case. First, Marmara Region is among those most seismically active regions in Turkey, sitting on the well-known North Anatolian Fault (NAF), second, rapid industrialization and urbanization of the region, third, improper practices of the construction sector, such as inadequate practices of earthquake resistant design and construction of frame systems, inadequate detailing, and poor material quality.

In this chapter, seismic issues related with the Marmara Earthquake are reviewed. At first, general characteristics of the strong ground motion are given. Then, the recorded ground motion in Adapazarı as well as the site-specific ground motion is presented. After describing the seismic and geotechnical characteristics of Adapazarı, overall damage observed after the earthquake is discussed.

It should be mentioned that the buildings investigated in detail in this study are presented in Chapter 4. Geotechnical features of each building site are also given there, using the results of a GIS-supported investigation described in Section 4.3.

3.2 AUGUST 17, 1999, MARMARA EARTHQUAKE

The northwestern region of Turkey was strongly shaken by the Marmara Earthquake on August 17th, 1999. The 7.4 magnitude earthquake occurred on the western part of the 1200 km long North Anatolian Fault (NAF) that lies through the whole north Anatolia. A segment of approximately 140 km of the NAF ruptured between İzmit Bay (Gölcük) and Melen (Eften) Lake (Düzce) (Bakır et al. 2002, Sezen et al. 2003). The map of the affected region is given in Figure 3.1 where the peak ground acceleration values measured are shown as percentage of acceleration of gravity.

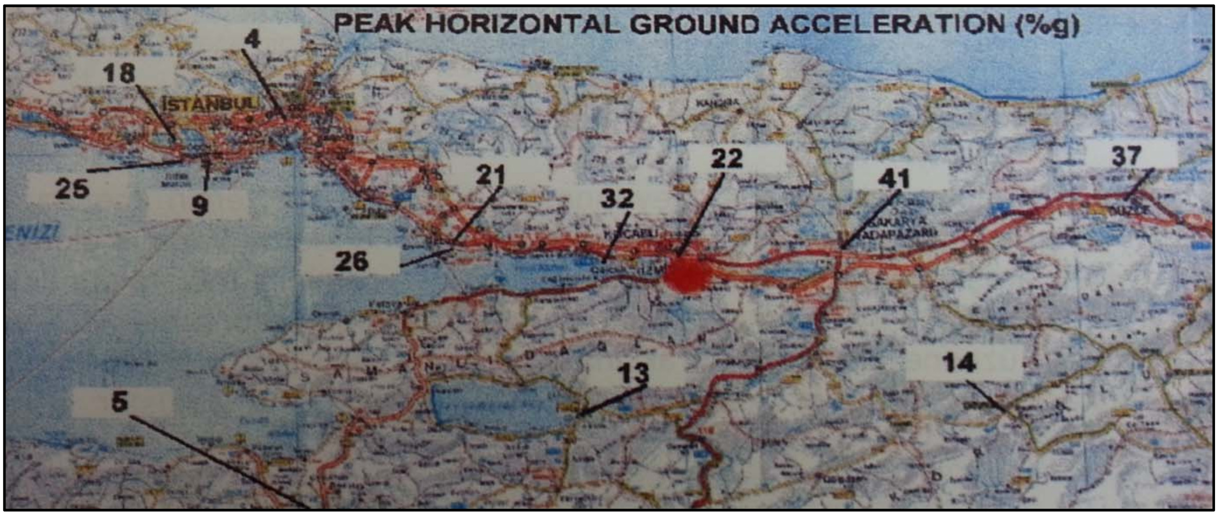

Figure 3.1 Map of northwestern Turkey, affected by 1999 Marmara Earthquake (adopted from GDDA, 2000)

Right-lateral strike-slip on NAF caused an average displacement offset of 2.60 m and triggered several ground motion recording instruments, though unfortunately not in the most heavily affected cities. A once-in-a-century chance was thus missed. The highest PGA values were recorded at Sakarya and Düzce stations, as 396.03 cm/s^2 and 356.52 cm/s^2, respectively, (Elnashai 2000, Sucuoğlu 2002).

Although the recorded PGA (peak ground acceleration) values are about 0.3~0.4 g and the acceleration response spectra of recorded ground motions were comparable with the design spectra in TEC, total number of collapsed and heavily damaged buildings was about 20000, apart from the buildings that suffered other grades of damage. According to official counts approximately 17500 people were killed and 44000 people were injured due to the widespread damage of the structures in several cities in the region. Kocaeli, Sakarya (Adapazarı), Düzce and Yalova, however, were the foremost provinces of deaths and injuries. Economic losses estimated were about 20 billion US dollars, including the indirect effects (Sezen et al. 2000, Bakır et al. 2002, Sezen et al. 2003).

As a sequel, on 12 November 1999, Düzce earthquake struck the region again with a moment magnitude of 7.2. An additional 40 km part of NAF was ruptured from the east end of Marmara Earthquake rupture. The max PGA values were recorded at Bolu and Düzce stations, as 790.03 cm/s^2 and 507.03 cm/s^2, respectively (Sucuoğlu 2002). There were additional deaths and injuries.

3.3 STRONG GROUND MOTION RECORD AND DERIVED SITE SPECIFIC GROUND MOTION

One of the permanent strong ground motion stations in Marmara Region, where the August 17, 1999, earthquake triggered, was located in Sakarya/Adapazarı. The Sakarya strong ground motion station (SKR) is operated by Earthquake Research Department of Disaster and Emergency Management Presidency (formerly Earthquake Research Department of the Ministry of Public Works and Resettlement). The instrument is located in the Sakarya Construction Department (40°44.212'N, 30°22.719'E) that is located 3.3 km north of the NAF rupture (Bakır et al. 2002, Sancio et al. 2002). Since the one-storey building (with no basement) structure where the instrument located is very light and small, the Sakarya strong ground motion record was probably the least affected by the structure among other stations triggered during Marmara Earthquake (Sucuoğlu 2002).

The Sakarya station is located on a shallow stiff soil deposit on the bedrock. In upper 30 m of the soil, the shear wave velocity (V_s) is measured as 470 m/s. The horizontal east–west (approximately fault parallel) component of the main event of the 1999 Marmara earthquake was recorded as well as its vertical component. The peak ground acceleration (PGA), velocity (PGV), and displacement values of horizontal east–west component were recorded as 0.41g, 81 cm/s, and 220 cm, respectively (Sancio et al. 2002). The north–south (fault normal) component, however, was not recorded due to the malfunction of the instrument.

The damage intensity in the neighborhoods where the Sakarya station is located was low during the earthquake. The apparent disaster, however, was observed in downtown Adapazarı, which is located on soft soils at a distance of approximately 7-8 km north of the fault rupture. There were no instruments in that area. The geotechnical aspects of the 1999 Marmara Earthquake were investigated by many researchers (e.g., Bakır et al. 2002, Sancio et al. 2002, Bakır et al. 2005), including the study of amplification and de-amplification factors of the site specific soil conditions. The inconsistency between the recorded ground motion and the severe damage observed was investigated under considerable uncertainty.

Although amplification of the ground motion would be expected, nonlinear soil response was applied by some engineers who investigated the event as a seismic demand reduction factor in Adapazarı. Attenuation of the seismic waves for similar site-source distances was also taken into consideration. Eventually, the PGA value in downtown Adapazarı was estimated to be in the order of 0.3–0.4g (Bakır et al. 2002, Sancio et al. 2002). Hence, considerable judgment must be exercised in evaluating the re-construction of the ground motion in downtown Adapazarı.

After the 17 August mainshock, the aftershocks were monitored using the temporary stations ("İmar" temporary station on stiff soil and close to the Sakarya station, and "Hastane" temporary station on soft soil at the city center that are shown in Figure B.3 in Appendix B) (Beyen and Erdik, 2004). According to the N-S and E-W components of the aftershocks recorded, and corresponding response spectra in both directions, it is observed that the spectral acceleration responses were similar to each other. The comparisons of the response spectra with 5 percent damping of horizontal components of the two prominent aftershocks recorded on August 31, 1999 (M5.2), and September 13, 1999 (M5.8) are given in Figure 3.2. Hence, it was interpreted that there was no dominant direction of the mainshock, and both horizontal components of the mainshock had similar effects on building damage (Bakır et al. 2002). The studies on the aftershock records also showed that the amplification factor for the soft soils was varying between 2 and 6 compared to the rock sites, especially for the period range of 0.3–1.0 s that is significant from the structural point of view.

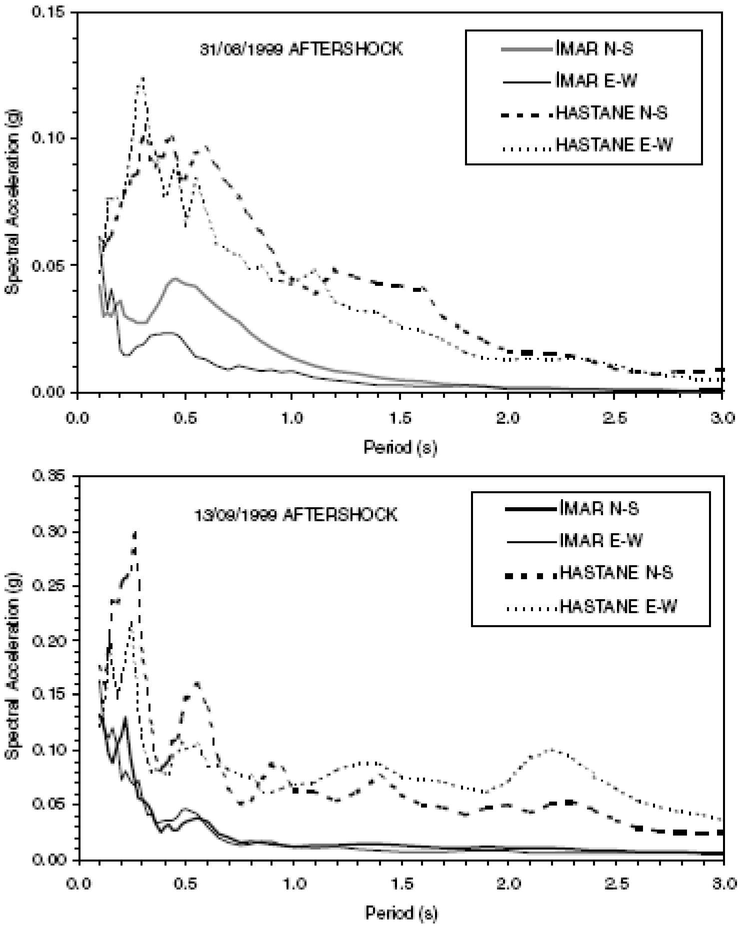

Figure 3.2 5% damped elastic response spectra of horizontal components of the two prominent aftershocks (figures adapted from Bakır et al. 2002)

The representative site-specific strong ground motions were developed by Bakır et al. (2002) for various depths of alluvium deposits in the entire Adapazarı basin, using the available E-W component of the Sakarya record of the mainshock. The buildings evaluated in this dissertation were analyzed under the site-specific ground motion which was obtained for 150 m thickness of soft soil. The bedrock depth of 150 m was taken as an average value for all buildings located close to downtown Adapazarı, according to the available information in the literature (Bakır et al. 2002, DRM 2003, GDDA 2004, Bakır et al. 2005), and the spatial investigation as given in Section 4.3.

The site-specific ground motion record which is used for the analyses of all buildings in this dissertation is shown in Figure 3.3, and the corresponding response spectrum for 5-percent damping is shown in Figure 3.4. The site specific response spectrum is compared with the response spectrum of original ground motion record and design spectrum of TEC-2007 in Figure 3.4.

According to the comparison given in Figure 3.4, the derived site specific response spectrum exceeds the code specified design spectrum for loose soils (Z4) for the buildings within the fundamental period range of 0.8 s – 2.3 s, due to soil amplification.

On the other hand, if the response spectrum of original ground motion record is compared with the site-specific ground motion response spectrum between the periods of 0.5 s and 1.0 s, it can be seen that the spectral acceleration (S_a) demands were amplified by factors of 2~3. In other words, soft soil characteristics of Adapazarı amplified the elastic seismic demands 2 or 3 times considering S_a.

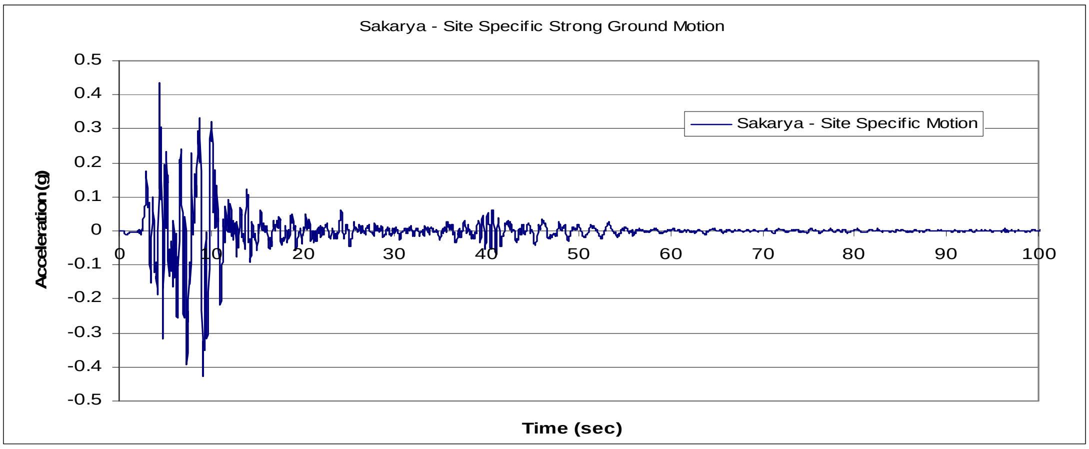

Figure 3.3 Site specific strong ground motion record (soft soil, bedrock depth: 150 m)

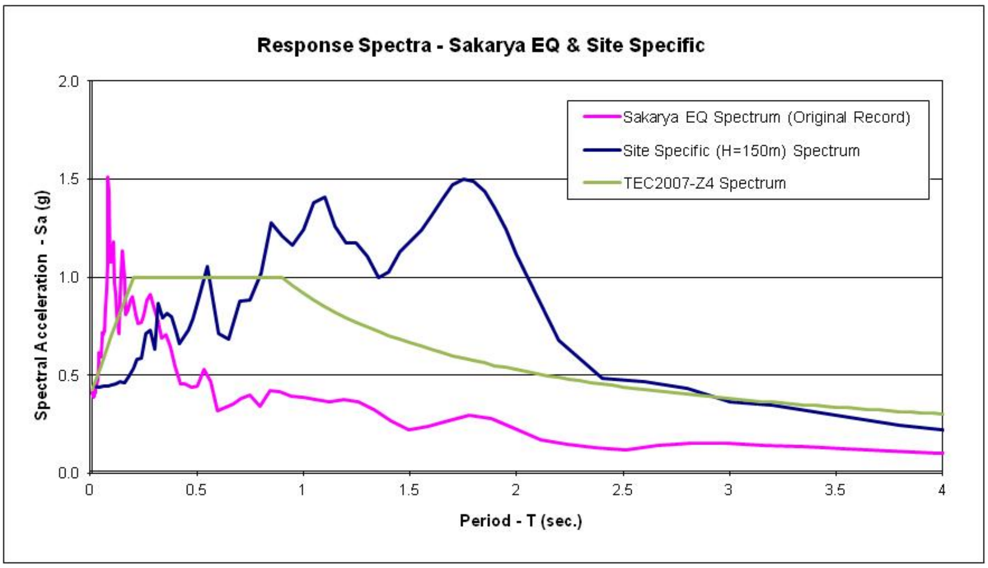

Figure 3.4 Response spectra (original record, site-specific, and TEC design spectrum for Z4)

3.4 SEISMICITY AND GEOTECHNICAL DESCRIPTION OF ADAPAZARI

The city of Adapazarı is located on a deep alluvial basin in the near field of the NAF that ruptured during the August 17, 1999, Marmara Earthquake. Hence, Adapazarı was significantly affected by the poorly understood close-field effects of the earthquake.

The city of Adapazarı was strongly shaken by two other strong earthquakes that occurred on NAF since 1940s; 26 June 1943 Adapazarı Earthquake, and 22 July 1967 Mudurnu Valley Earthquake, with magnitudes of 6.6 and 7.1, respectively (Bakır et al. 2005). The epicenters of the 1943 and 1967 earthquakes were 10 km (east) and 27 km (southeast) away, respectively, from Adapazarı city center.

Adapazarı is situated on a sedimentary basin, which was a former lake bed. Primary materials of the Quaternary alluvial sediments of the basin are silt and fine sand, which are transported by Sakarya and Çark Rivers and their tributaries. The thickness of alluvial soft soils of the basin is highly variable, and it exceeds 300 m at several locations in the city (Bakır et al. 2002). Variation of bedrock depth is shown in Figure B.6 in Appendix B. Thickness of alluvium is relatively less on the south, where it reaches 250 m on the northwest of Adapazarı city center. The bedrock depth in the downtown area is about 150 – 200 m.

The groundwater depth, on the other hand, ranges about 0.5–2.0 m throughout the Adapazarı basin (Bakır et al. 2005). Due to the high groundwater level that is consistent with the high thickness of soft soils, the foundations of the buildings have been built as shallow rigid mats and no basements built. The groundwater depth measurement results for Adapazarı are shown in Figure B.13 in Appendix B. Similar to the other geotechnical information, the groundwater depth values are obtained from the results of the microzonation studies held by DRM and GDDA (DRM 2003, GDDA 2004). These studies were used as one of the main layers for the GIS study which will be described in Section 4.3, in detail.

As a consequence of the loose sandy soil characteristics and high groundwater table of Adapazarı, extensive liquefaction and loss of soil bearing capacity occurred during the earthquake, especially in central districts of the city. These effects and corresponding damages, such as tilting of the buildings and building penetration relative to adjacent ground level, eruption of sand boils, were also investigated by several researchers (Bakır et al. 2002, Sancio et al. 2002, DRM 2003, GDDA 2004, Bray et al. 2004, Bakır et al. 2005, Bray and Sancio 2006), which are not considered in this study.

The site condition of Adapazarı has been created by the Sakarya and Çark rivers and their tributaries depositing the alluvium materials. The current situation of "Justinianus Bridge (Beşköprü)" is an interesting sign of the geotechnical evolution of the basin, when the current river stream is considered. The 430 meter long Justinianus Bridge was built spanning Çark Stream, which flows from Sapanca

Lake to Sakarya River, at about 553-561 AD. Since then, the stream bed has been displaced by natural tectonic effects; however, the Bridge itself is deeply embedded in the ground today, and the geometry of the piers indicates that when the bridge was built, the stream flowed in the opposite direction. The Justinianus Bridge (Beşköprü) is shown in Figure 3.5.

Figure 3.5 Justinianus Bridge (Beşköprü)

The investigations on local site effects and the correlation of site conditions and structural damage by Bakır et al. (2002) and Bakır et al. (2005) have concluded that due to the soil amplification the seismic forces during Marmara Earthquake on the buildings with three or more stories (especially those of five to six stories) located on the alluvial soils in Adapazarı were larger than the buildings located on the firm sites of the city. The amplification ratio is estimated to vary between 1.5 and 3.0 within the period range of 0.5-0.6 s. The amplification of demand within the period range of 0.5-1.0 s strongly influences the mid-rise buildings. Consistent with this, the structural damage was concentrated at central districts of Adapazarı rather than the outskirt districts. However, the collapse rates were reduced in the central districts, where surface deposits are predominantly either liquefaction prone or classified as soft sites, as a result of seismic demand reduction due to nonlinear soil response. It is very difficult to take into account quantitatively the reduced effects, if any, of the ground shaking on buildings. This is open to much conjecture, and serves only to underline the difficulty in making post-de-facto analyses of building response in urban settings.

3.5 POST EARTHQUAKE DAMAGE ASSESSMENT

In the regions affected from the 1999 Marmara Earthquake, the survey teams inspected the damage immediately after the disaster. The aim of these inspection surveys was to determine the damaged buildings as soon as possible. It was also intended to determine the distribution of “damage” within the cities affected by the earthquake.

The survey teams used post-earthquake rapid screening methods only, in order to define the global damage states. The damages are decided according to the “Damage Assessment Report Form” prepared by the General Directorate of Disaster Affairs (GDDA) of Turkey. These damage states are determined as slight/none, moderate or severe/heavy in the form in order to determine the global damage, however, the forms do not have enough engineering details for the RC buildings and their damages. The plan geometry, the number of stories and type of the load carrying system were the only parameters which are directly related with the RC buildings. The front and back sides of the Damage Assessment Report Form are shown in Figure 3.6 and Figure 3.7, respectively. Although an updated version of the form which is more detailed was available at the date, due to the practical considerations and urgent need of information on damaged buildings the forms given in Figure 3.6 and Figure 3.7 were used for the post earthquake damage assessment.

The post-earthquake damage assessment surveys were also carried out in Adapazarı by GDDA and Adapazarı Municipality, independently of one another. Only the damaged buildings were covered by the survey of GDDA. The survey by Adapazarı Municipality, on the other hand, was more comprehensive, and covered the municipal area of approximately 20 km^2 and 26 districts. A total of 23 914 buildings were investigated and classified according to their damage states (light/moderate damage and severe damage/collapse) observed. The primary objective of the survey was to determine whether a feasible repair of the building is possible or not. According to the results of this survey, 2844 buildings collapsed or were severely damaged, while 2076 buildings experienced light or moderate damage. In other words, 12 percent of the buildings in municipal area of Adapazarı were beyond the limits of a feasible repair, and approximately 9 percent of the buildings were judged to be repairable (Bakır et al. 2002, Bakır et al. 2005, Yakut et al. 2005).

The detailed damage distribution information for each of the buildings was not collected during these rapid and superficial post-earthquake inspections, unless some of the damaged buildings were investigated by expert teams, especially from the universities, immediately after the earthquake. Hence, the detailed damage information could not be obtained for the buildings which are selected and assessed; this study has concentrated on the global damage states only, not prediction of the damage distribution.

3.6 DESCRIPTION OF DAMAGE IN ADAPAZARI

In Adapazarı, as one of the worst affected cities during the August 17, 1999, Marmara Earthquake, 3694 people (approximately 2 percent of the total city population) were killed, a shameful result by any current measure. The damage distribution in Adapazarı is shown in Figure B.4 in Appendix B**,** as the ratio of collapsed and heavily damaged buildings to the total number of buildings.

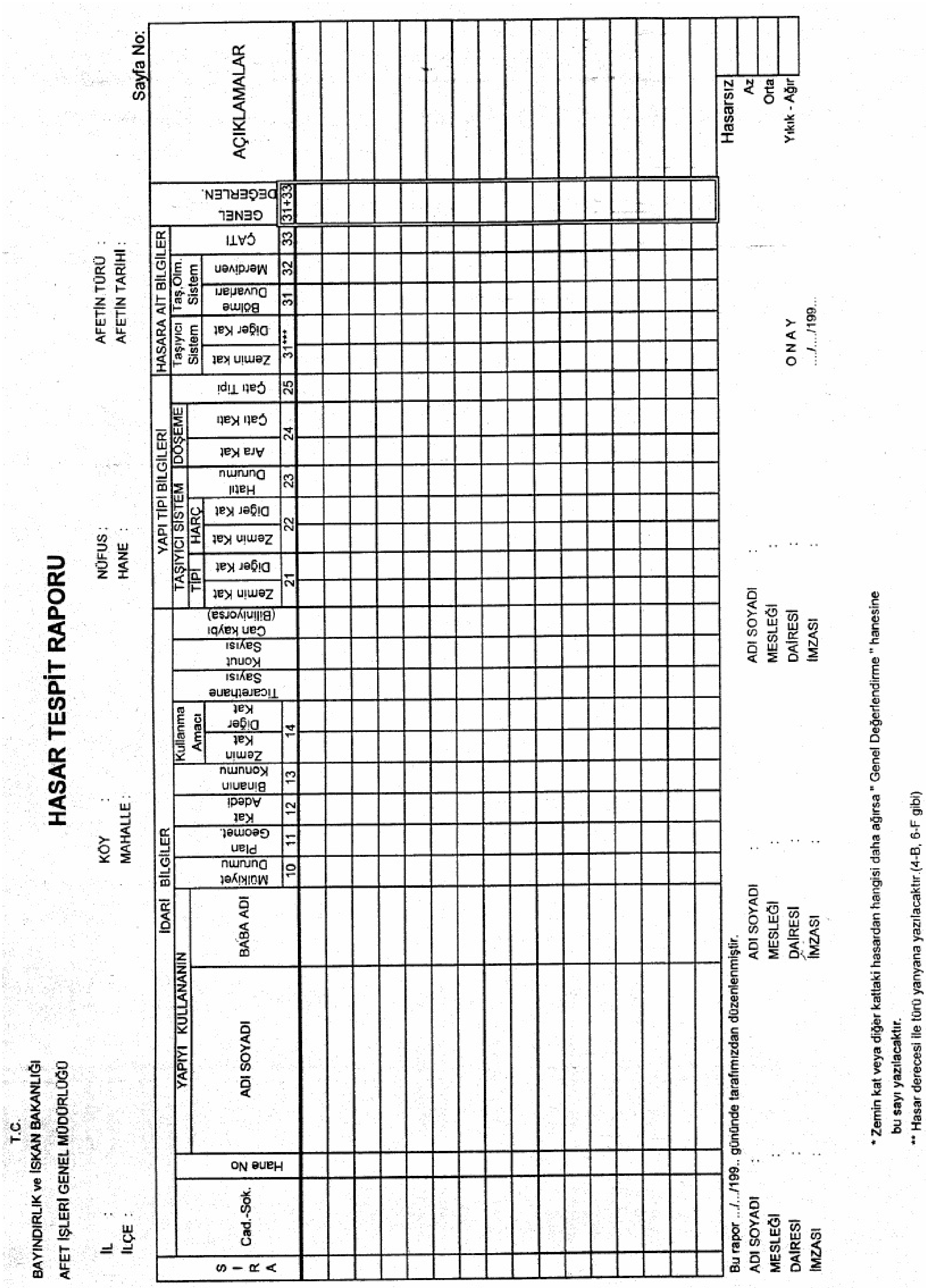

T.C.
BAYINDIRLIK ve İSKAN BAKANLIĞI
AFET İŞLERİ GENEL MÜDÜRLÜĞÜ

HASAR TESPİT RAPORU

İL :
İLÇE :
KÖY :
MAHALLE :
NÜFUS :
HANE :
AFETİN TÜRÜ :
AFETİN TARİHİ :
Sayfa No:

SIRA	İDARİ BİLGİLER													YAPI TİPİ BİLGİLERİ									HASARA AİT BİLGİLER					GENEL DEĞERLEN.	AÇIKLAMALAR
	Cad.-Sok.	Hane No	YAPIYI KULLANANIN		Mülkiyet Durumu	Plan Geomet.	Kat Adedi	Binanın Konumu	Kullanma Amacı		Ticarethane Sayısı	Konut Sayısı	Can kaybı (Biliniyorsa)	TAŞIYICI SİSTEM					DÖŞEME		Çatı Tipi		Taşıyıcı Sistem		Taş.Olm. Sistem		ÇATI		
														TİPİ		HARÇ													
			ADI SOYADI	BABA ADI					Zemin Kat	Diğer Kat				Zemin Kat	Diğer Kat	Zemin Kat	Diğer Kat	Hatıl Durumu	Ara Kat	Çatı Katı			Zemin kat	Diğer Kat	Bölme Duvarları	Merdiven			
					10	11	12	13	14					21		22		23	24		25		31***		31	32	33	31+33	

Bu rapor .../.../199.. gününde tarafımızdan düzenlenmiştir.

ADI SOYADI :
MESLEĞİ :
DAİRESİ :
İMZASI :

ADI SOYADI :
MESLEĞİ :
DAİRESİ :
İMZASI :

ADI SOYADI :
MESLEĞİ :
DAİRESİ :
İMZASI :

ONAY
..../..../199...

Hasarsız
Az
Orta
Yıkık - Ağır

* Zemin kat veya diğer kattaki hasardan hangisi daha ağırsa " Genel Değerlendirme " hanesine bu sayı yazılacaktır.

** Hasar derecesi ile türü yanyana yazılacaktır.(4-B, 6-F gibi)

Figure 3.6 Front page view of the Damage Assessment Report Form

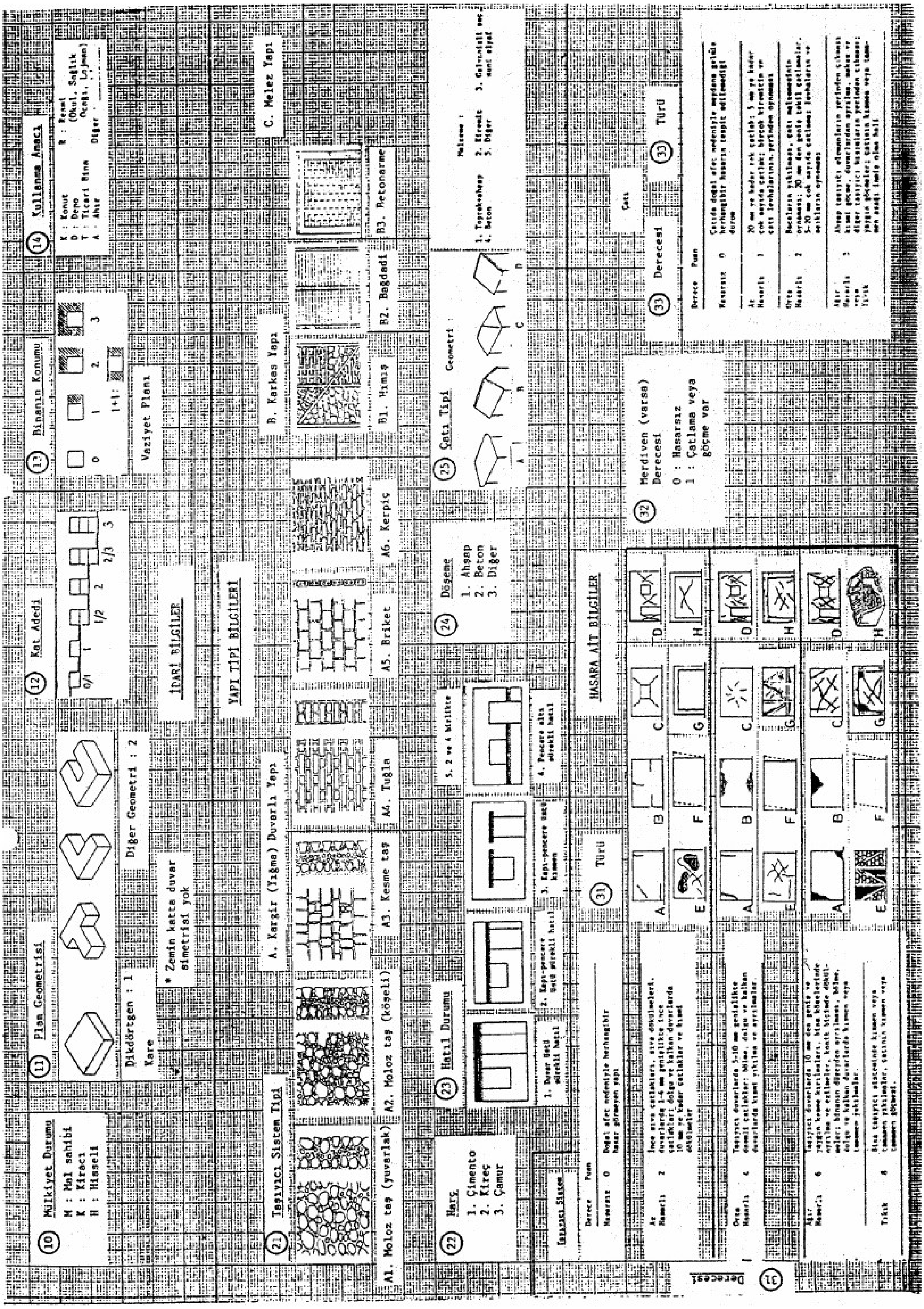

Figure 3.7 Back page view of the Damage Assessment Report Form

Due to the soil modification, the significant structural damage was concentrated especially in the city center that is located on thick soft soil layers, as discussed in Sections 3.3 and 3.4. The seismic effects driving the five to six story buildings were amplified possibly by a factor of 1.5 to 3.0. In the southern districts that are located on firm grounds, the damage level was low even though the fault line is closer (~3.5km). Besides the local site effects, this situation can also be explained by the effective peak acceleration (EPA) calculated as 287 cm/s^2 (~0.29g) for the Sakarya mainshock record (Sucuoğlu, 2002). This low value of EPA compared to the PGA (0.41g) indicates that the damage potential of this strong ground motion record is lower than expected for such a near-field record of M7.4 earthquake.

The building inventory of downtown Adapazarı consisted of mid-rise buildings with three or more stories. The majority of these buildings were four to six story RC buildings. The ground stories of the buildings were commonly used for commercial businesses. For this purpose these commercial stories were built higher than the upper stories. Moreover, the infill (partition) walls that increase the lateral strength and stiffness were usually less than the upper stories. These common building traditions lead to the occurrence of weak and soft stories. The building shown in Figure 3.8 which was under construction during the earthquake, experienced severe damage due to high lateral drift demands that caused the soft story mechanism.

In addition to the weak/soft story irregularity, especially for the near field sites (such as Adapazarı during Marmara Earthquake), ductility demands increase in ground floors. Thus the buildings should satisfy the ductile detailing. The illustration of such damage is given in Figure 3.9.

As mentioned in Section 3.4, due to the high groundwater level in the basin, the foundations of the buildings have been built as shallow rigid mats, with basements.

Figure 3.8 Failure due to the soft story irregularity (photo courtesy of METU-DMC)

Figure 3.9 Ground floor destruction due to high ductility demands (photos courtesy of METU-DMC)

During the Marmara Earthquake, approximately 22 percent of the buildings located in central districts were severely damaged or completely collapsed. Additionally, about 14–15 percent of these buildings experienced moderate damage within the limits of economic repair. Most of the buildings that experienced moderate structural damage had simultaneously foundation displacements (settlement and/or tilting). The significantly damaged or collapsed buildings, however, rarely experienced such foundation bearing failures (Bakır et al. 2002). The buildings shown in Figure 3.10 were tilted and/or settled during the earthquake in consequence of the loss of soil bearing capacity.

Figure 3.10 Tilting and/or settlement of the buildings (photos courtesy of METU-DMC)

Nonductile detailing of the structural members, as spacing of the transverse reinforcement, 90-degree hooks, and poor detailing in joint regions, were emphasized as the major reasons of the structural damage of earthquake in PEER reconnaissance report (Sezen et al. 2000). The examples are shown in Figure 3.11. As shown in Figure 3.11, the spacing of the transverse reinforcement is approximately 250 mm in the region close to column ends.

Figure 3.11 Nonductile detailing (photos courtesy of METU-DMC)

Another reason for the structural damage was the poor construction quality observed (e.g. material strength, workmanship), especially for the residential buildings. According to the investigations on damaged buildings, an average value of concrete strength was found to be 15 MPa, although the specified values were 20 MPa in design documents (Yakut et al. 2005). The building shown in Figure 3.12 has strong columns; however, due to the lack of anchorage reinforcement of beams to the columns, beam mechanisms occurred.

Figure 3.12 Anchorage problems at beam-column connections (photo courtesy of METU-DMC)

The structural irregularities were also emphasized as the reasons of increasing structural vulnerability and damage (Yakut et al. 2005). In addition to formation of soft story mechanism, mentioned above, the plan irregularity forms, such as torsional irregularity and overhanging (projections in plan), were observed frequently. Short columns were created, especially if the mezzanines were built. Even for the taller buildings, shear walls were not designed and built, and thus, structural damage level was increased.

CHAPTER 4

DESCRIPTION OF THE SELECTED BUILDINGS

4.1 SELECTION OF THE DAMAGED BUILDINGS

As one of the worst affected cities during the August 17, 1999, Marmara Earthquake, Adapazarı (Sakarya) was selected as the study area. It is natural that there would be the largest number of buildings with design blueprints available in the city that would enable the evaluation of building performance evaluation techniques.

For that purpose, ten buildings which are located at city center and very close to each other that experienced damage during the August 17, 1999, Marmara Earthquake, were selected for the assessment, considering the general features of the RC building inventory in Turkey. Since the representation of the general characteristics of the RC buildings in Turkey was important, the buildings with vertical and plan irregularities, as well as the similar material quality shortfalls were selected. The selected projects/blue prints of five heavily damaged and five moderately damaged buildings were copied, and available information on these buildings was collected from the archives of Adapazarı Municipality. The locations of the buildings selected are shown in Figure B.2 in Appendix B.

After the inspections of the survey teams (Section 3.5), the ruins of the heavily damaged buildings were removed and the moderately damaged buildings were strengthened, as quickly as possible. Thus, only the moderately damaged buildings could be visited for preliminary inspections of this study. The computer models of the damaged buildings were generated assuming the information obtained from the blueprints represent as built properties. Actually, this assumption is consistent with the author's observations on the strengthened (moderately damaged) buildings. It is observed that the information of the plan and vertical dimensions of the building, as well as the dimensions of the structural members, were consistent with the blueprints on moderately damaged buildings.

4.2 GENERAL PROPERTIES OF SELECTED BUILDINGS FOR THE STUDY

This study is concentrated on the application of NSPs to the large building stocks in Turkey. Thus, the approximate assessment procedures are applied to the selected buildings, which reflect the general structural features of the RC building inventory in Turkey, in order to evaluate the global building performance during the earthquake. As the general properties of the selected buildings defined in this section, the selected buildings have certain irregularities and average material quality which is valid for the general building inventory. Thus, these selected buildings are accepted to reflect the general characteristics of the RC building inventory of Turkey.

While the information related with the buildings was being collected, all the possible sources were used. Blue prints of the building design drawings were obtained. The design layouts of the selected buildings and their photos are given in Appendix A. The general information about these selected buildings is given in Table 4.1 where it can be seen that the design strength values of the construction materials are available for six (out of ten) buildings. The structural system for all the buildings is reinforced concrete frame system. A basement story below the surface had never been built for these sample buildings, due to the reason of high water table level of the basin (Section 3.4). The amount of infill walls were decreased whenever the ground floor is used for commercial purposes. Considering these features, the sample models reflect the general characteristics of building stock in Adapazarı city, as well as the entire country.

The building ID numbers, given in the second column of Table 4.1, will be used as reference identification numbers for the selected buildings, in the rest of the study. Furthermore, the X and Y orthogonal directions of these buildings were selected based on the plans given in blueprints (Appendix A).

Table 4.1 General information of selected buildings

	ID	District	Section	City Block	Parsel	Construction Year	Number of Stories	Concrete f_{cd} (kg/cm^2)	Steel f_{yd} (kg/cm^2)	Coordinates x ^{0} x ' x''	Footprint area (m * m)
Moderate Damage	1	Semerciler	57	210	69	1988	4 + Mezzanine	95	1910	40 46 27 N 30 24 08 E	13.5 * 20
	2	Yağcılar	50	955	438	1988	5	95	1910	40 46 42 N 30 25 02 E	24.8 * 17
	3	Yahyalar	6	72	83		4			40 46 43 N 30 24 37 E	22 * 17
	4	Akıncılar	69	764	181	1988	4	95	1910	40 46 02 N 30 24 13 E	12.5 * 10
	5	Tekeler	107	783	442	1994	5	95	1910		11.5 * 16.5
Severe Damage	6	Semerciler	54	388	30	1990	5				11.5 * 9.7
	7	Semerciler	54	388	32	1993	6	95	1910		11 * 11
	8	İstiklal	15	607	768	1987	5				8.8 * 12.1
	9	Semerciler	55	203	9		6	95	1910		25.3 * 9
	10	Cumhuriyet	35	130	101	1990	5				21.2 * 15

All the buildings selected were built in late eighties and early nineties, thus all buildings are expected to comply with the requirements of the 1975 Turkish Earthquake Code. However, the weak enforcement of the code provisions, especially those for the ductile detailing, was stated as the major reason of the destruction (Gülkan 2000, Sezen at al. 2000).

Many studies showed that, the material and the construction quality is poor for the Adapazarı region. This is not different from the general situation of Turkey, unfortunately. According to the tests on drilling core samples taken, the average compressive strength of the concrete was reported as 25 percent lower than the used values in projects (Yakut at al. 2005).

The lack of data about the actual strength values of structural materials of the buildings damaged (e.g. cored concrete sample test results, technical reports, etc.) was mentioned in Section 3.5. For the buildings selected in this study, there are only two technical reports for Building 2 and Building 5, among the 10 buildings studied. These reports were prepared prior to the strengthening of the moderately damaged buildings after the earthquake. However, they are superficial, and include the information about location and total number of the stories, original concrete grade of the buildings. According to these available reports, buildings have not experienced any ground failure. In addition to the ground failure information, there is specific information on Building 2 that there is no structural failure on RC frame members. On the other hand, cored concrete test results are only available for Building 2, as an appendix to the technical report. The available technical reports are given in Appendix D.

However, the outcome of the cored concrete results of Building 2 should be discussed. The average strength result for the concrete was measured as 160 kg/cm^2. According to this value, the concrete class was set as C16 (BS16). However, the given concrete class does not seem to be suitable, considering the measured strength values for concrete. According to the Cored Concrete Standard (TS10465) in Turkey, the concrete class should have been set as C14[2]. Moreover, according to the other limited technical report for Building 5, the concrete class was also given as C16 (BS16), but without any cored concrete sample test details.

[2] TS10465 (Cored Concrete Standard), Table 3.

Considering these limited information about the concrete strength, and other deficiencies for modeling and construction, as well as reliability of available data, the design values were used for the compressive strength of the concrete (f_{cd}) and tensile strength of the reinforcing steel (f_{yd}) in this study. Additionally, the plain reinforcement steel was used, in the buildings. This assumption is consistent with the studies which consider the material quality of the region. The design strength values of the concrete and reinforcing steel were given as 9.5 MPa ($f_{cd} = f_{ck} / 1.5$) and 191 MPa ($f_{yd} = f_{yk} / 1.15$) (Table 4.1).

During the preliminary investigation visits to Adapazarı, in order to collect more detailed information about the building damages, some knowledgeable people were met, including the engineers of the buildings, former and current presidents of the Sakarya Branch of the Chamber of Civil Engineers, and an experienced civil engineer from the Directorate of Public Works and Resettlement in Sakarya. The general damage database for entire Sakarya was obtained. Although this database contains a lot of information about the global damage states of the buildings for Adapazarı, it was not possible to find the detailed information on the distribution of damage within the building. Moreover, some of the buildings were visited by surveillance of the design engineers of the buildings. According to the records and the information from the people met, it is stated that there was no major soil damage beneath the buildings. However, in some of the buildings shear damage might have occurred in a few structural members.

In Adapazarı, tall ground stories are often designed and constructed for commercial (shop) purposes. Furthermore, out of the commercial districts of the city, the ground stories are used as warehouses with lower story heights, since basement stories have never been built due to the high groundwater level. The upper stories have been used as either apartments or offices, with typical story heights that range between 2.7 and 2.9 m. For the buildings studied, the ground story heights range between 2.4 to 4.7 m, while the typical story height for the upper stories is 2.8 m (Appendix A).

In order to obtain larger showcases at the front sides of the ground stories, columns are usually designed and constructed in such a way that their strong axes in flexure are located parallel to the street. Hence in general, the frame systems of the buildings are stiffer and stronger in the direction that perpendicular to the street against the lateral loading. Eventually, the buildings are more vulnerable in one of their orthogonal directions. Various column plan dimensions were used ranging between 300 mm x 600 mm and 400 mm x 900 mm, with the aspect ratios ranging between 1.0 and 3.0. Column plan dimensions were decreased by decreasing gravity loads in upper stories. 12 to 20 mm and 6 to 10 mm diameter smooth rebars were used as the longitudinal and transverse reinforcement of structural members, respectively. The longitudinal reinforcement ratio ranges between 1 percent and 2 percent for the columns. Ductile transverse reinforcement details were not satisfied, due to the application of 90-degree hooks and spacing ranging between 200 mm and 250 mm of transverse ties.

Structural walls were rarely designed and constructed in the buildings studied, but generally are placed perpendicular to the front street as columns. Moreover, the structural walls that are parallel to the street were located in a manner that increases the torsional irregularity of the building.

The beams, connecting the columns, were designed with the widths between 200 mm and 250 mm, and the depths between 500 mm and 600 mm. When the floor plans are examined (Appendix A), it can be observed that the buildings were designed with irregularities in plan, i.e. imperfect frames in each principle axes of the building, projections in plan. Thus, the vulnerability levels of the buildings were high.

Although there are no comprehensive structural damage reports, it is thought that it is possible to use nonlinear static procedures for the assessment of these buildings. Since the detailed damage distribution information throughout the buildings could not be obtained for the buildings assessed from the available resources, the assessment of NSP's was done considering the global damage states in general, not prediction of the damage distribution within the buildings.

4.3 ADAPAZARI SURVEY USING GIS TOOLS

The special features of soil in Adapazarı basin were discussed in Section 3.4. The city is entirely built on a deep alluvium deposit. Therefore, for the Adapazarı study stage, some issues related with the soil effect must be considered. Consequently, at the beginning, a survey for the soil conditions in city was done, using the GIS tools. Some of the maps obtained from this brief study are given in Appendix B. The mapped spatial information was obtained primarily from the results of the microzonation studies held by DRM and GDDA (DRM 2003, GDDA 2004). The other available sources were also used, e.g. Bakır et al. (2002). The locations of the buildings selected are also shown on the maps in Appendix B.

The geotechnical information for the buildings studied was filtered from this GIS survey, and given in Table 4.2. The bedrock depth at locations of the buildings ranges between 150 m and 200 m, consistent with Section 3.4. The soft soils at these locations were classified as D or E by NEHRP, and Z3 or Z4 by TEC. Due to the soft soil characteristics; these sites had low shear wave velocities and large predominant periods.

The increasing values of Liquefaction Severity Index (LSI) given in the last column of Table 4.2, indicates the increasing risk of liquefaction, and scaled 0 to 10. Thus, the buildings had moderate or lower liquefaction risk. According to the available studies in literature, on the other hand, no ground failure was reported for the locations of these selected buildings, i.e. Sancio et al. (2002), Bakır et al. (2005). Also, experts and engineers (met in Adapazarı) did not report any ground failure for any of these buildings.

Table 4.2 Geotechnical information of selected buildings

	ID	District	Bedrock Depth	NEHRP Site Class	Turkish Site Class	Distance to NAF (km)	PGA (g)	Vs (m/s)	T (s) Pred. Per.	Groundwater Depth (m)	Liquefaction Severity Index
Moderate Damage	1	Semerciler	175	E	Z4	11.3	< 0.21	< 263	> 1.23	0 - 5	1
	2	Yağcılar	175	D	Z3	12	< 0.21	< 263	> 1.23	0 - 5	3
	3	Yahyalar	175	E	Z3	12	< 0.21	< 263	0.82 - 1.23	0 - 5	2
	4	Akıncılar	175	D	Z3	10.6	< 0.21	< 263	0.82 - 1.23	10 - 15	5
	5	Tekeler	150	E	Z4	13.7	< 0.21	< 263	< 0.82	> 15	0
Severe Damage	6	Semerciler	175	E	Z3	12	< 0.21	263<Vs< 371	> 1.23	0 - 5	2
	7	Semerciler	175	E	Z3	12	< 0.21	263<Vs< 372	> 1.23	0 - 5	2
	8	İstiklal	175	E	Z4	12.1	< 0.21	< 263	< 0.82	0 - 5	5
	9	Semerciler	200	E	Z4	11.6	< 0.21	263<Vs< 371	> 1.23	0 - 5	3
	10	Cumhuriyet	200	E	Z4	11.6	< 0.21	> 371	> 1.23	0 - 5	3

In order to take the site effects into consideration, the buildings of this study were analyzed under the representative site-specific ground motion that was developed by Bakır et al. (2002), as discussed in Section 3.3, assuming the bedrock depth to be 150 m and equal for each building. Moreover, the modifications for site effects designated by the NSPs such as FEMA440 (Section 2.2.4) were applied to the spectra.

None of the buildings selected from Adapazarı for this study, has an embedment below the ground surface. Thus, while applying the NSPs of FEMA440, RRS_e value for each of the buildings is computed as unity. On the other hand, kinematic interaction effects should be neglected for Site Class E, according to FEMA440. Therefore, RRS_{bsa} value is computed for the buildings if the corresponding soil type is not of type E (i.e. for buildings #2 and #4).

CHAPTER 5

ANALYSIS OF THE BUILDINGS

5.1 INTRODUCTION

In order to obtain a comprehensive seismic evaluation of the buildings studied, as a back calculation after the earthquake, nonlinear analyses were carried out on the analytical models built. Since the nonlinear assessment of the buildings is of concern in this study, nonlinear static (pushover) and nonlinear dynamic analyses have been conducted.

In this chapter, firstly, the OpenSEES software will be described. This has been used as the general structural modeling and analysis environment. The tools for material and structural element models will also be included in this description. Second, modeling of the buildings studied will be given. Third, the results of linear Eigenvalue analyses will be summarized. Then, the nonlinear response history analysis (NRHA) and its results that were carried out on each building model will be presented. Finally, the nonlinear static (pushover) analysis and the corresponding results were presented.

5.2 OPENSEES AS A MODELING TOOL AND ANALYSIS ENVIRONMENT

The analytical models of the selected buildings were constituted using the OpenSees software (Mazzoni et al. 2009). OpenSees® is an open source software for Earthquake Engineering is also used for running the nonlinear analyses and simulating the seismic response and structural performance of the buildings (OpenSees 2010). On the other hand, similar software like SAP 2000 Nonlinear, were used, generally for verification purposes.

In order to examine the seismic response of selected buildings, nonlinear static analysis (pushover) and nonlinear response history analysis (NRHA) were conducted using OpenSees.

OpenSees (Open System for Earthquake Engineering Simulation) has been developed as a software platform for research and application of simulation for structural and geotechnical systems by the Pacific Earthquake Engineering Research Center (PEER) at UC Berkeley, with the support of the National Science Foundation.

OpenSees has features for linear and nonlinear modeling. The component behavior is represented by defining the nonlinear force–deformation relations (i.e. moment-curvature, moment-rotation, etc.) as well as defining the force–deformation relations of the materials to be assigned to fiber sections. Fiber sections are powerful in automatically setting the N–M and N–M–M interactions for 2D and 3D models. Nonlinear force–deformation or stress–strain relations of the materials are assigned to fiber sections.

In the light of preliminary exercises (2D and previously studied frames, etc.) with OpenSees, the model related parameters (e.g. parameters for structural elements and material) and modeling techniques were decided. Using these element and material models, which are given in the following sections, the buildings were modeled representing the linear and nonlinear force-deformation relationships for the structural components.

5.2.1 Elements

The options for nonlinear structural element models for beams and columns were investigated in OpenSEES library. There are basically two types of "Nonlinear Beam–Column Elements";

i. force-based elements

- Distributed plasticity (nonlinearBeamColumn)

This element considers the spread of plasticity along the element.

- Concentrated plasticity with elastic interior (beamWithHinges)

This element considers plasticity to be concentrated over specified hinge lengths at the element ends.

ii. displacement-based element

- Distributed plasticity with linear curvature distribution (dispBeamColumn)

This is a displacement beam element which is based on the displacement formulation, and considers the spread of plasticity along the element.

The RC Frame Systems that consist of beams (and girders), and columns (and structural walls if they exist) are modeled using "beam with hinges element" of OpenSees library. This type of element divides the element in three parts: two hinges at the ends, and a linear-elastic region in the middle. The hinges are defined by assigning to each a previously-defined section. The length of the each hinge is also specified by the user. The element is shown in Figure 5.1.

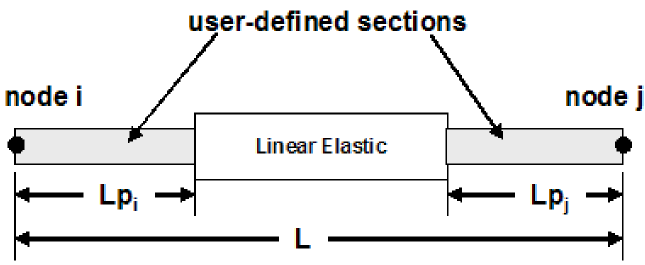

Figure 5.1 Beam-with-hinges element

Since the middle region of the structural element is assumed to be elastic, nonlinear behavior is confined to the integration points at the element ends and the computational time is reduced. This element only needs the hinge length to be specified, that is useful for modeling. Some other advantages of this formulation can be given as follows:

- It captures largest bending moment values at the ends,
- It represents linear curvature distributions exactly,
- Characteristic length is equal to Lp when deformations localize,
- It is possible to model the different amount of reinforcing at two joints of RC members.

If structural walls exist in the building as the elements of the structural frame, rigid links were used in order to represent the rigid end zones of the structural members.

Fiber sections were used in order to assign the nonlinear force-deformation relationships of structural components for modeling beam-with-hinges elements. Using fiber sections, a composite model of various material types can be defined within the section of element. Thus, sectional M-φ analyses were unnecessary in order to obtain M-θ relationships. The fiber section is shown in Figure 5.2 schematically.

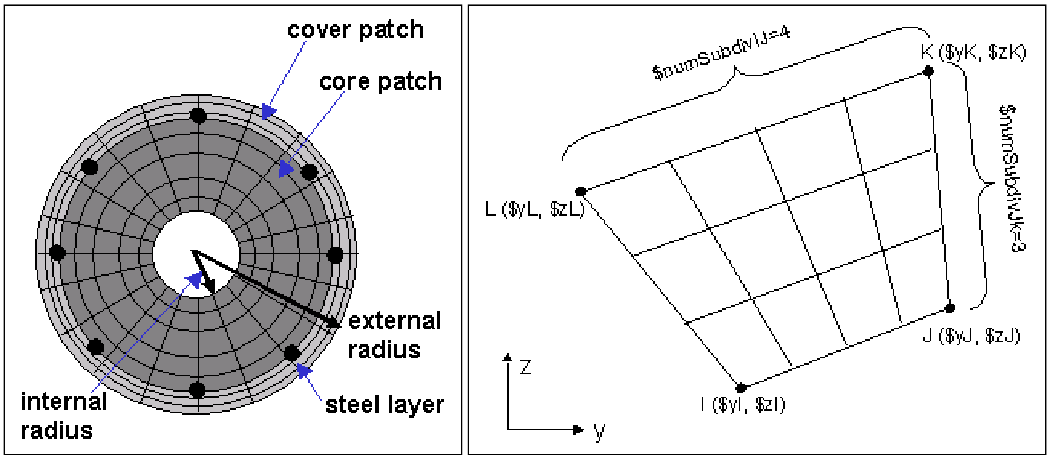

Figure 5.2 The fiber section of a circular column and quadrilateral definition for fibers

Modeling with fiber sections provides the direct representation of the distributed plasticity along the structural member and the cross section as well. Another advantageous feature of OpenSees is the possibility of reading the strain outputs for each fiber section, as well as section forces and deformations.

5.2.2 Materials

Using fibers, the RC column sections were constructed considering three types of materials; unconfined concrete, confined concrete and reinforcing steel. In OpenSEES, the Kent-Scott-Park concrete model (Kent and Park 1971, Scott et al. 1982, Mander et al. 1988) is defined as "Concrete01" material, which neglects the tensile strength of the concrete. The uniaxial concrete model of Concrete01 is shown in Figure 5.3.

The "Concrete02" material is also available in order to consider the tensile strength of the concrete. This feature is sometimes very useful to overcome the convergence problems of large and irregular building models. The uniaxial concrete model of Concrete02 is shown in Figure 5.4.

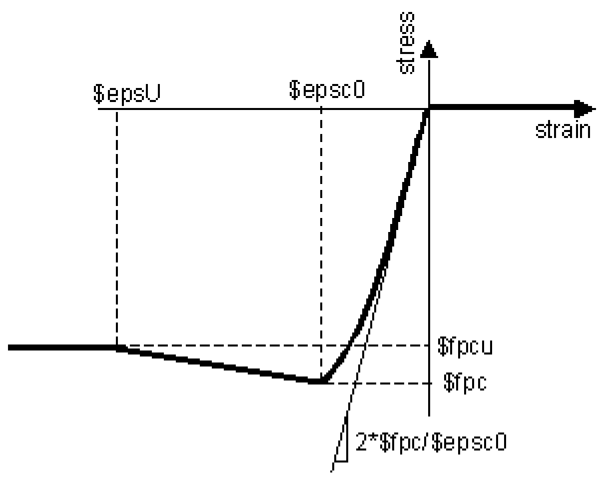

Figure 5.3 Concrete 01 material

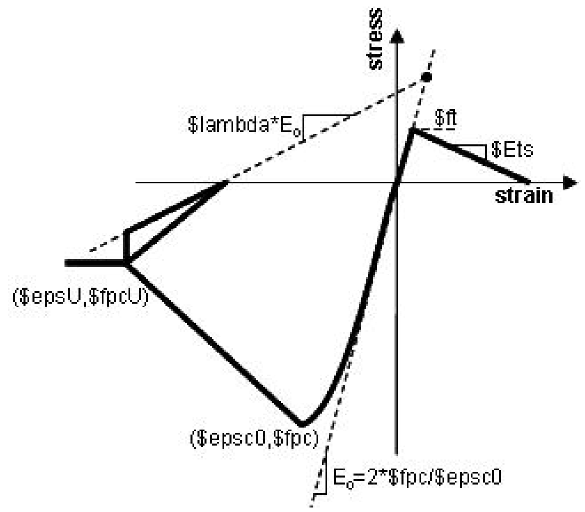

Figure 5.4 Concrete 02 material

The reinforcement steel in RC sections were modeled using the pre-defined "Reinforcing Steel" (which is based on the Chang and Mander (1994) uniaxial steel model), "Steel 01" (a uniaxial bilinear steel material object with kinematic hardening and optional isotropic hardening described by a non-linear evolution equation) or "Steel 02" (a uniaxial Giuffre-Menegotto-Pinto steel material object with isotropic strain hardening) (Filippou, et al. 1983), uniaxial bilinear steel material models, that are shown in Figure 5.5, Figure 5.6 and Figure 5.7, respectively. The material model was selected according to the sensitivity studies considering the convergence of the analyses.

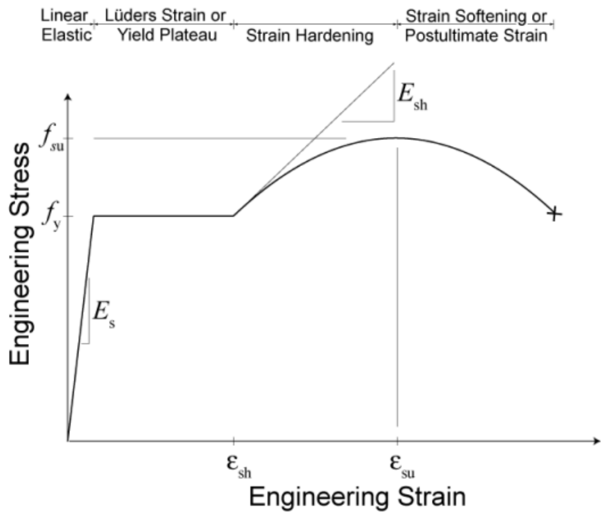

Figure 5.5 Reinforcing Steel material (Chang and Mander, 1994)

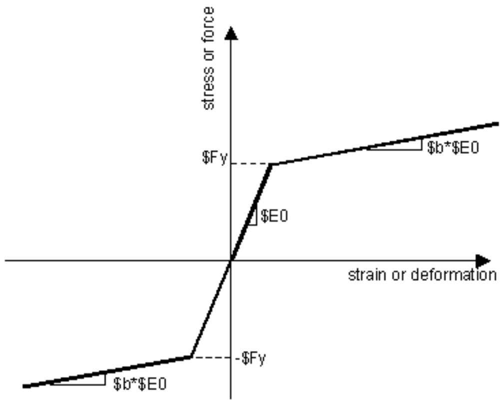

Figure 5.6 Steel 01 material

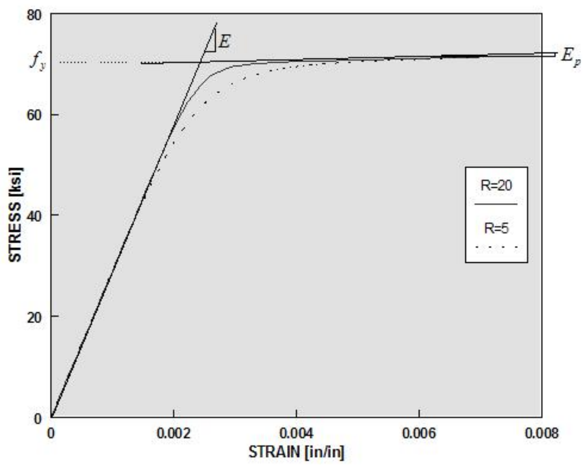

Figure 5.7 Steel 02 material (Filippou, et al. 1983)

5.3 ANALYTICAL MODELS

The modeling aspects and assumptions made for the analytical models of the buildings have been defined in this section.

5.3.1 Building Models

The 3D nonlinear models of the buildings were constructed using the geometric and material features presented in Section 4.2. In order to model the structural frame systems of the buildings, beam and column elements were used. Nonlinear stress–strain relationship for each of the material type was defined and assigned to beam–with–hinges elements (Section 5.2.1) in order to model the structural frame members.

3D views of the analytical models constructed for the buildings studied are presented in Appendix C.

In blue prints of the selected buildings, the concrete and reinforcing steel properties were given as C14 (BS14) and St-I (BÇ-I), respectively. The corresponding design compressive strength of concrete is given as 9.5 MPa, while the design tensile strength of reinforcing steel is 191 MPa, as presented in Table 4.1.

As explained in Section 3.5, since the post-earthquake survey teams used only rapid screening methods, there is lack of data about the actual strength values of structural materials of the buildings studied, e.g. cored concrete sample test results, technical reports, etc. However, some available technical reports about the buildings were discussed in Section 4.2. Considering limited information about the concrete strength, and other deficiencies for modeling and construction, as well as reliability of available data, the given design strength of the concrete was used as 9.5 MPa ($f_{cd} = f_{ck} / 1.5$) in this study.

According to ASCE/SEI-41, component load–deformation response is required to be represented by nonlinear load–deformation relations, where the nonlinear procedures are used (ASCE 2008, Section 6.3). Thus, the uncracked sections were used for the nonlinear analyses in this study. In the same document, component effective stiffness (cracked sections) corresponding to the secant value to the yield point of the component is required to be used for linear assessment procedures of the document. For the building models, nonlinear stress–strain relations of the materials were assigned to the structural components, via fiber modeling of the elements. With the fiber models, biaxial flexural behavior of beams and columns was simulated.

Due to convergence problems that occurred originating from the nonlinear modeling of the shear force–deformation relationship of the sections, structural elements' shear force–deformation relations were modeled based on their specified shear modulus and effective shear area and neglecting the plastic shear force–deformation capacity of the section.

It has been proven that flexural deformability may be reduced as coexisting shear forces increase. Since the shear capacity decreases with the increasing flexural ductility demands, shear failure may occur before theoretical flexural deformation capacities are reached (ASCE 2007). Shear capacity decreases due to the strength degradation of the concrete in plastic hinge zones, which occurs because of the crack openings due to the increasing flexural deformations. Hence, the shear (brittle) behavior may dominate the overall behavior of the element, if the shear strength decreases below the flexural strength.

Therefore, determination of the expected mode of failure of the columns is needed. For this purpose, the shear capacities associated with the shear-type and flexural-type failure were calculated for each of the column in the building according to TS-500 and TEC-2007. The assumption of flexural hinges at two end nodes of the columns was used for the flexural-type shear capacity (V_e) calculation, in order to be on the safe side (TEC-2007), using Equation (5.1).

$$\mathbf{V_e = (M_u + M_l) / l_n} \tag{5.1}$$

where M_u and M_l are the moment capacities at upper and lower ends of the column, and l_n is the length of the column.

The shear-type failure capacities (V_r) of the columns were calculated according to TS 500, as defined in Equation (5.2).

$$\mathbf{V_r = V_c + V_w = 0.8 * V_{cr} + A_{sw} / s * f_{ywd} * d} \tag{5.2}$$

where V_c is the capacity from concrete, V_w is the capacity from transverse reinforcement, A_{sw} is total area of transverse reinforcement within a distance of s, f_{ywd} is design yield strength of the transverse reinforcement, d is distance from extreme compression fiber to the centroid of longitudinal tension reinforcement, and V_{cr} is the cracking shear strength of the cross-section, which is defined in Equation (5.3).

$$\mathbf{V_{cr} = 0.65 * f_{ctd} * b_w * d (1 + \gamma * N_d / A_c)} \tag{5.3}$$

where f_{ctd} is design tensile strength of the concrete, b_w is the width of the cross-section, d is distance from extreme compression fiber to the centroid of longitudinal tension reinforcement, N_d is axial load and A_c the concrete area in cross-section. γ is taken as 0.07 considering the axial compression on columns.

The calculated shear capacity values, using Equations (5.1) and (5.2) were compared with each other by means of the V_r / V_e ratios, in order to determine the mode of failure of the columns. V_r / V_e ratios were calculated for columns for each of the orthogonal plan directions of the buildings, i.e. X and Y. The mode of failure for the columns having a V_r / V_e ratio which is lower than 1.0, is expected as brittle shear-type failure, which is an inadmissible situation for the seismic performance of the buildings. For these columns the shear capacity associated with shear type failure is lower than the shear capacity associated with flexure type failure. The comparison for the ground story columns is given in Figure 5.8 to Figure 5.17, for Buildings #1 to #10, respectively.

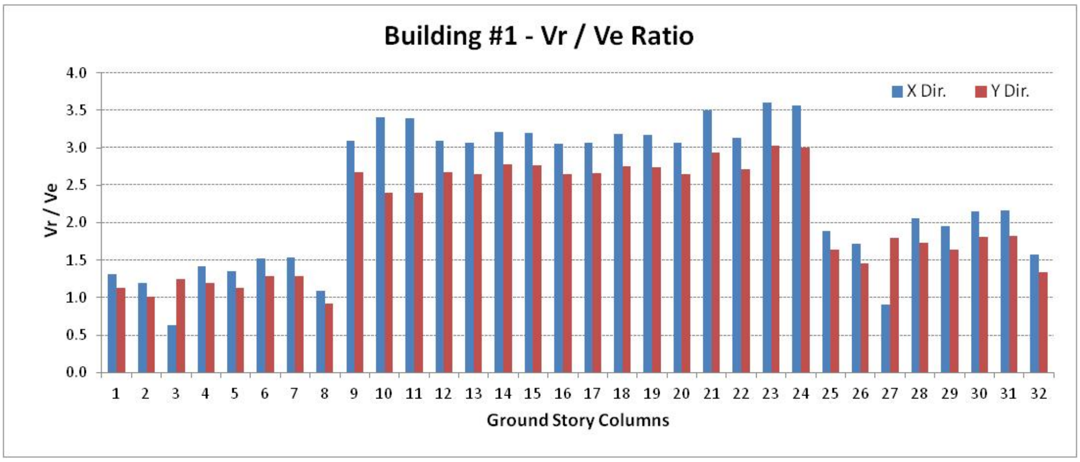

Figure 5.8 The *Vr / Ve* ratios for ground story columns of building #1

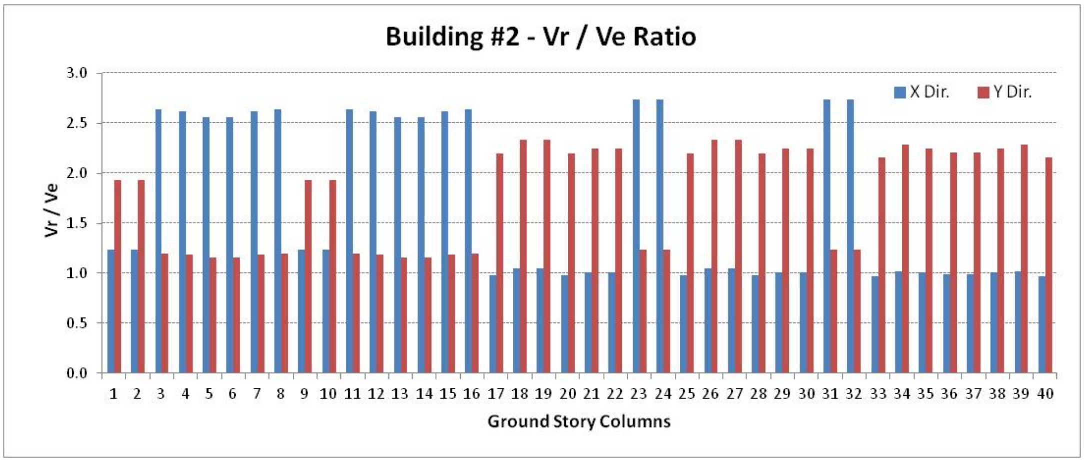

Figure 5.9 The *Vr / Ve* ratios for ground story columns of building #2

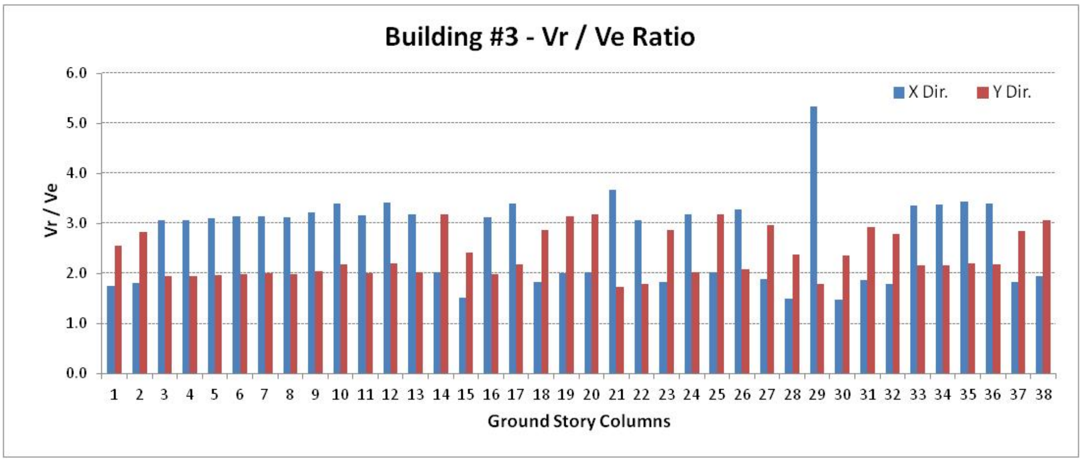

Figure 5.10 The *Vr / Ve* ratios for ground story columns of building #3

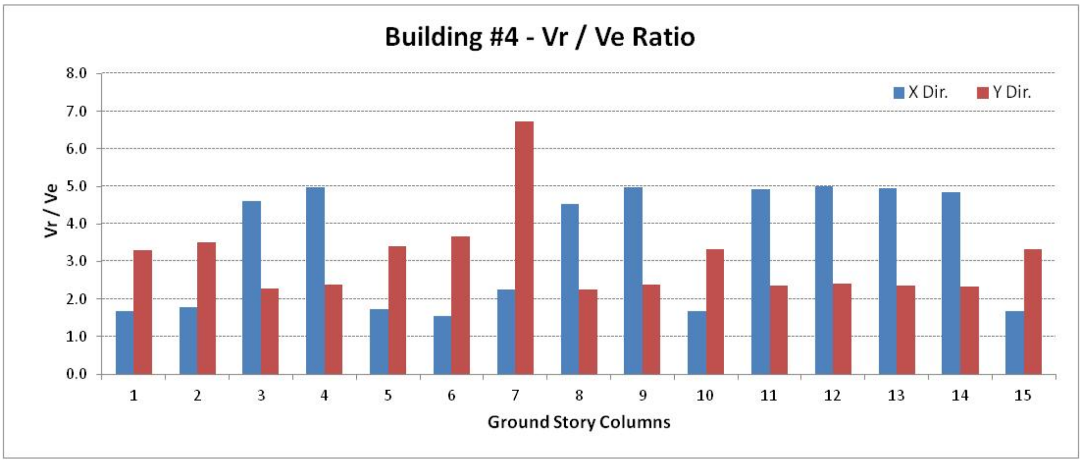

Figure 5.11 The *Vr / Ve* ratios for ground story columns of building #4

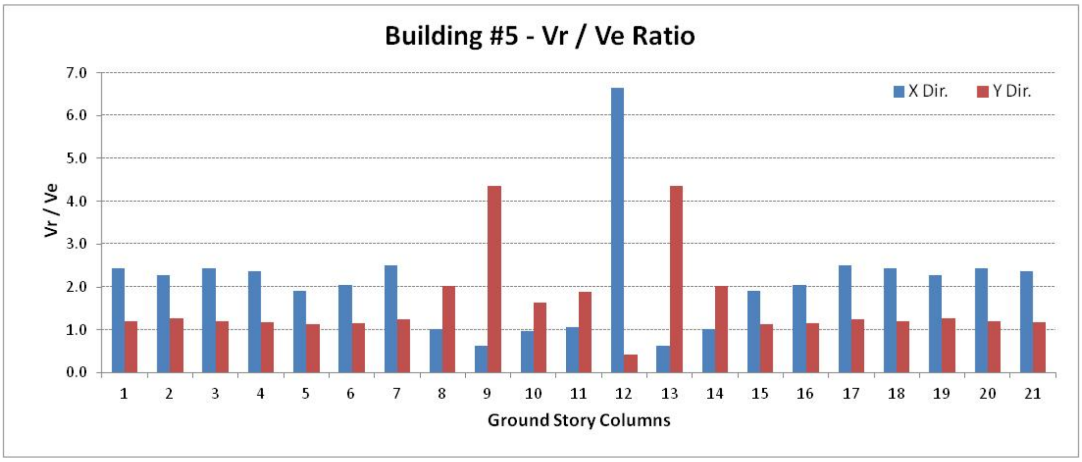

Figure 5.12 The *Vr / Ve* ratios for ground story columns of building #5

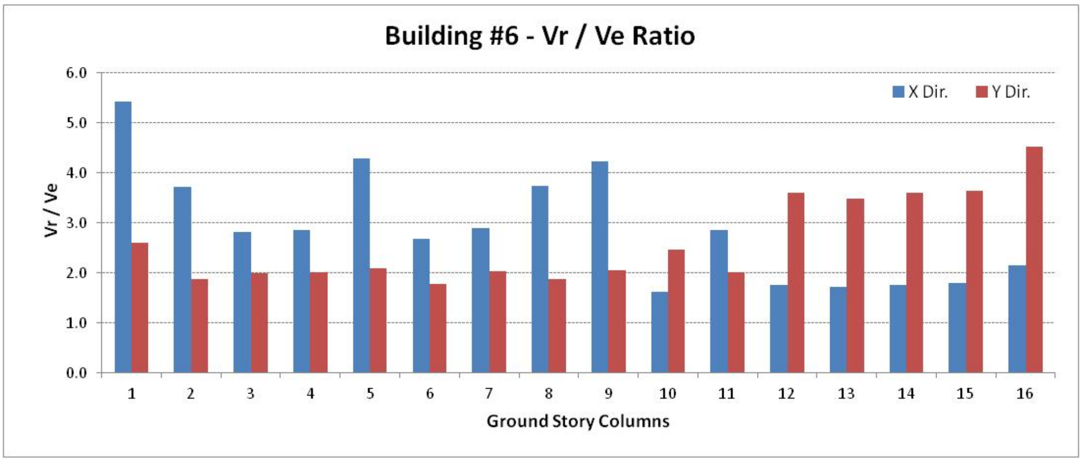

Figure 5.13 The *Vr / Ve* ratios for ground story columns of building #6

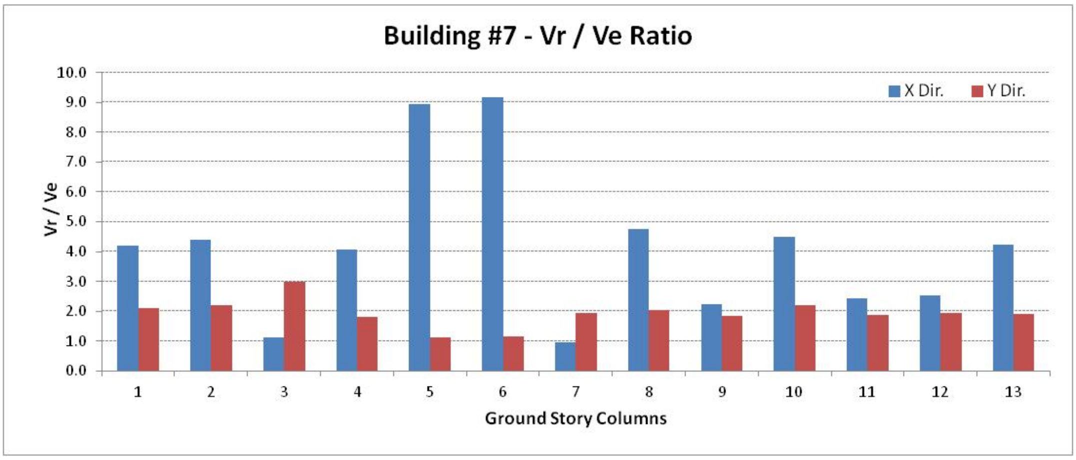

Figure 5.14 The *Vr / Ve* ratios for ground story columns of building #7

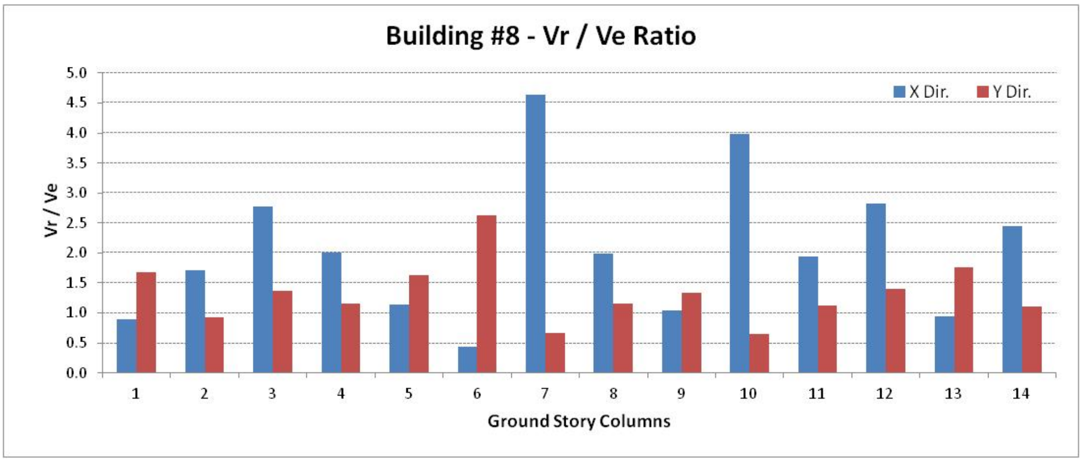

Figure 5.15 The *Vr / Ve* ratios for ground story columns of building #8

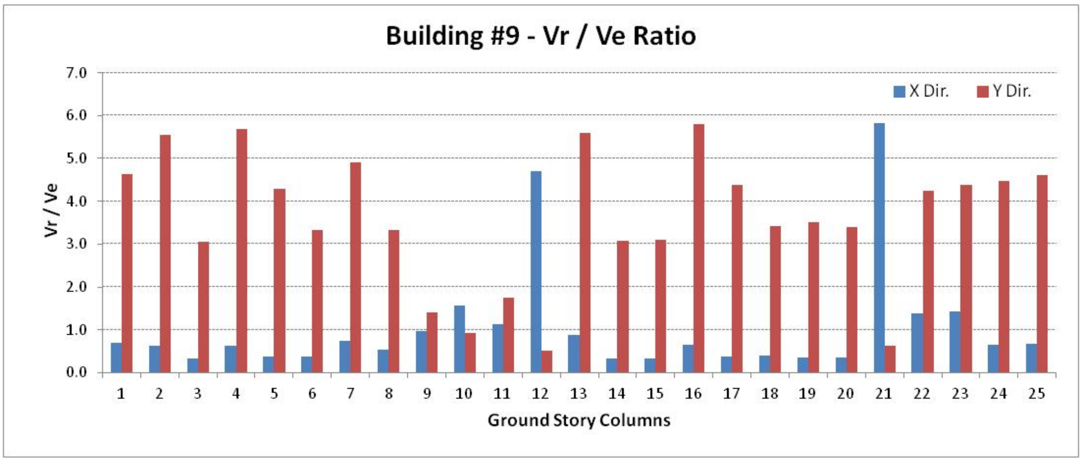

Figure 5.16 The *Vr / Ve* ratios for ground story columns of building #9

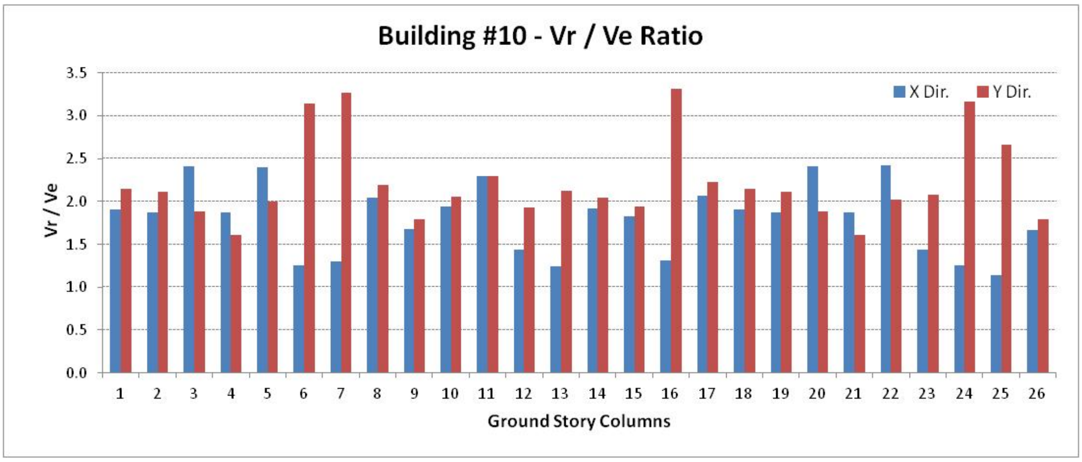

Figure 5.17 The *Vr / Ve* ratios for ground story columns of building #10

Building 1 has two shear-critical columns in the X direction and only one shear-critical column in the Y direction. Building 2 has seven shear-critical columns only in X direction with V_r / V_e ratios slightly lower than 1.0. Building 5 has three shear-critical columns in X direction and only one shear-critical column in Y direction of the building. Building 7 has only one shear-critical column in X direction with a V_r / V_e ratio slightly lower than 1.0. Building 8 has three shear-critical columns in X direction and three shear-critical columns in Y direction of the building.

In addition to these shear deficiency results on few of the columns of some buildings, Figure 5.16 shows that the X direction of Building 9 is highly vulnerable for shear failures. Especially due to the commercial concerns, the vertical structural members had been designed as structural walls that were stiff in X direction of the building. Thus, 20 of totally 25 ground story columns are shear-critical members in the X direction.

In general, the V_r / V_e ratio comparison results presented in Figure 5.8 – Figure 5.17 indicate that the shear capacities associated with shear-type failure are higher than those associated with flexural-type failure for most of the columns, except a few shear-critical cases. Therefore, ductile flexural failure of the columns is expected to develop before brittle shear failure occurs. However, the shear-critical cases where brittle failure is also probable (i.e. Buildings #9, #1, #2, #5, #7, #8) were also examined.

In 3D models of the buildings, infill walls were neglected, considering the small amount of regular, continuous walls without any window or door openings in buildings (Yakut 2004). The contribution of the infill walls in buildings to the overall initial stiffness and the initial fundamental period was investigated according to Yakut (2004) and shown in Table 5.1. According to the empirical Equations (5.4) and (5.5), the ratios of K_d/K_c and T_d/T_c can be estimated by α and β coefficients, respectively; where K_d is the initial stiffness of the frame system with infill walls, K_c is the initial stiffness of the bare frame system, T_d is the initial period of the frame system with infill walls, T_c is the initial period of the bare frame system, *IWR* is the ratio of infill wall area at critical floor to total area of the floor as percents and *n* is total number of the floors.

$$\mathbf{K_d = \alpha * K_c \quad ; \quad \alpha = 1 + 1.5\,(IWR) / n} \tag{5.4}$$

$$\mathbf{T_d = \beta * T_c \quad ; \quad \beta = 1 - 0.365\,(IWR) / n} \tag{5.5}$$

When the α and β coefficients examined in Table 5.1, the contribution of infill walls on initial period and initial stiffness of the buildings is very limited. The effect on initial stiffness is less than 2 percent, where the effect on initial period is less than 1 percent. For these calculations, the regular, continuous infill walls without any openings were considered, by definition (Yakut 2004). Due to insignificant contribution of infill walls, they were not included in building models.

Table 5.1 Contribution of infill walls to initial stiffness and initial fundamental period

Building ID No	Direc.	Number of Stories	Total Floor Area, m^2	Masonry Wall Length at Base, m	Masonry Wall Area at Base, m^2	$\alpha = K_d / K_ç$	T difference calculated by α	$\beta = T_d / T_ç$
# 1	X Dir.	4+1M	1265.34	40	8	1.009	0.995	0.998
	Y Dir.		1265.34	75	15	1.018	0.991	0.996
# 2	X Dir.	5	2108	144	28.8	1.020	0.990	0.995
	Y Dir.		2108	85	17	1.012	0.994	0.997
# 3	X Dir.	4	1365	80	16	1.018	0.991	0.996
	Y Dir.		1365	72	14.4	1.016	0.992	0.996
# 4	X Dir.	4	485	26	5.2	1.016	0.992	0.996
	Y Dir.		485	20	4	1.012	0.994	0.997
# 5	X Dir.	5	910.2	55	11	1.018	0.991	0.996
	Y Dir.		910.2	65.6	13.12	1.022	0.989	0.995
# 6	X Dir.	5	550.05	22.8	4.56	1.012	0.994	0.997
	Y Dir.		550.05	28.95	5.79	1.016	0.992	0.996
# 7	X Dir.	6	1144.5	43.6	8.72	1.011	0.994	0.997
	Y Dir.		1144.5	68	13.6	1.018	0.991	0.996
# 8	X Dir.	5	585.2	36	7.2	1.018	0.991	0.996
	Y Dir.		585.2	33	6.6	1.017	0.992	0.996
# 9	X Dir.	5+1M	1285.1	100	20	1.023	0.989	0.994
	Y Dir.		1285.1	40.5	8.1	1.009	0.995	0.998
# 10	X Dir.	5	1487.5	61.5	12.3	1.012	0.994	0.997
	Y Dir.		1487.5	45	9	1.009	0.995	0.998

The mass of each story was calculated and assigned evenly to the column end nodes at the story, assuming that the tributary areas of each column were approximately the same. Hence, any additional mass moment of inertia was not assigned to story mass centers. On the other hand, the assumption of the same tributary area was verified by small calculations on building plans. Total gravity load of each floor was calculated, considering 100 percent of dead loads (DL) plus 30 percent of live loads (LL), i.e. *DL + 0.3*LL*. The calculated gravity load was used as seismic dead load for mass calculation.

5.3.2 Modeling Assumptions

In addition to the general information given in Section 5.3.1 about modeling the buildings, some other assumptions made related to these models are summarized in this section.

First of all, the rigid diaphragm assumption was applied for floor levels of each building. The rigid diaphragm constraint is physically valid for the type of buildings selected for the study, i.e. 4-6 floor RC frames. Second, for beam models, the effective flange width was not taken into consideration, in order to be on the safe side. Third, $P - \Delta$ effects were not considered. Finally, during the NRHA of all buildings, Rayleigh damping was used and assumed to be 5 percent.

5.4 EIGENVALUE ANALYSIS AND MODAL PROPERTIES

In order to obtain the modal properties and corresponding periods of the 3D analytical models of the buildings, Eigenvalue analyses were carried out. The fundamental mode periods of each building are given in Table 5.2, for both orthogonal directions and torsion.

Table 5.2 Fundamental mode periods in orthogonal directions and torsion

	Period (sec)		
Building ID	**X Dir.**	**Y Dir.**	**Torsion**
1	0.92	0.79	0.74
2	0.54	0.62	0.62
3	0.60	0.56	0.62
4	0.50	0.59	0.53
5	0.60	0.44	0.63
6	0.64	0.56	0.53
7	0.97	0.66	0.89
8	0.53	0.43	0.51
9	0.34	0.61	0.47
10	0.72	0.78	0.77

The fundamental periods were obtained within the range of 0.5-1.0 seconds. Due to the irregularities, especially in plan, torsion is effective for all buildings. The torsion is the fundamental mode for Buildings #3 and #5. For other buildings, one of the orthogonal direction modes is followed by the torsional mode.

5.5 NONLINEAR RESPONSE HISTORY ANALYSIS OF THE BUILDINGS

The buildings were analyzed using the 3D nonlinear models, which are described in detail above. For each building, NRHA was performed in each of the orthogonal plan direction of the buildings separately, because only one component (east-west component) of the strong ground motion is available (Section 3.3).

5.5.1 Results of Nonlinear Response History Analysis (NRHA)

The normalized roof drift response history results for moderately damaged buildings and severely damaged buildings are given in Figure 5.18 and Figure 5.19, respectively. The corresponding normalized total base shear response history results (by total weight of the building) are shown in Figure 5.20 and Figure 5.21.

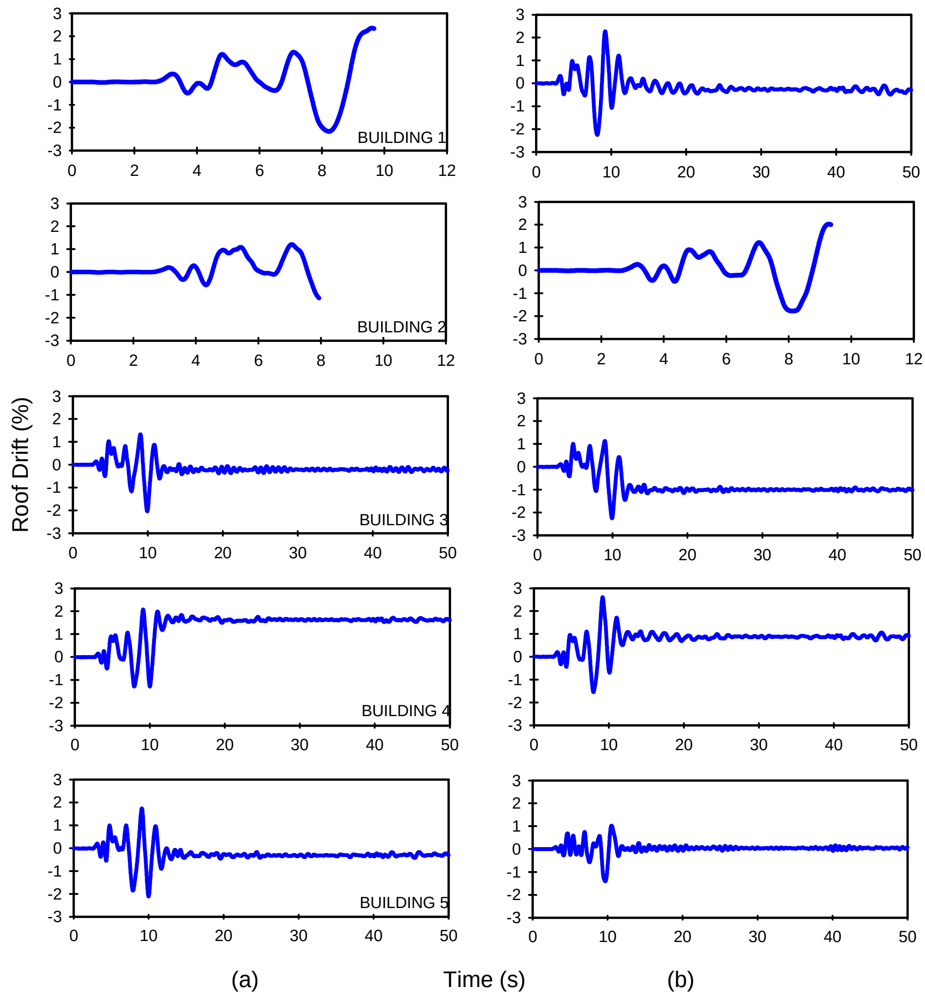

Figure 5.18 Normalized roof drift response history of moderately damaged buildings, (a) X direction and (b) Y direction

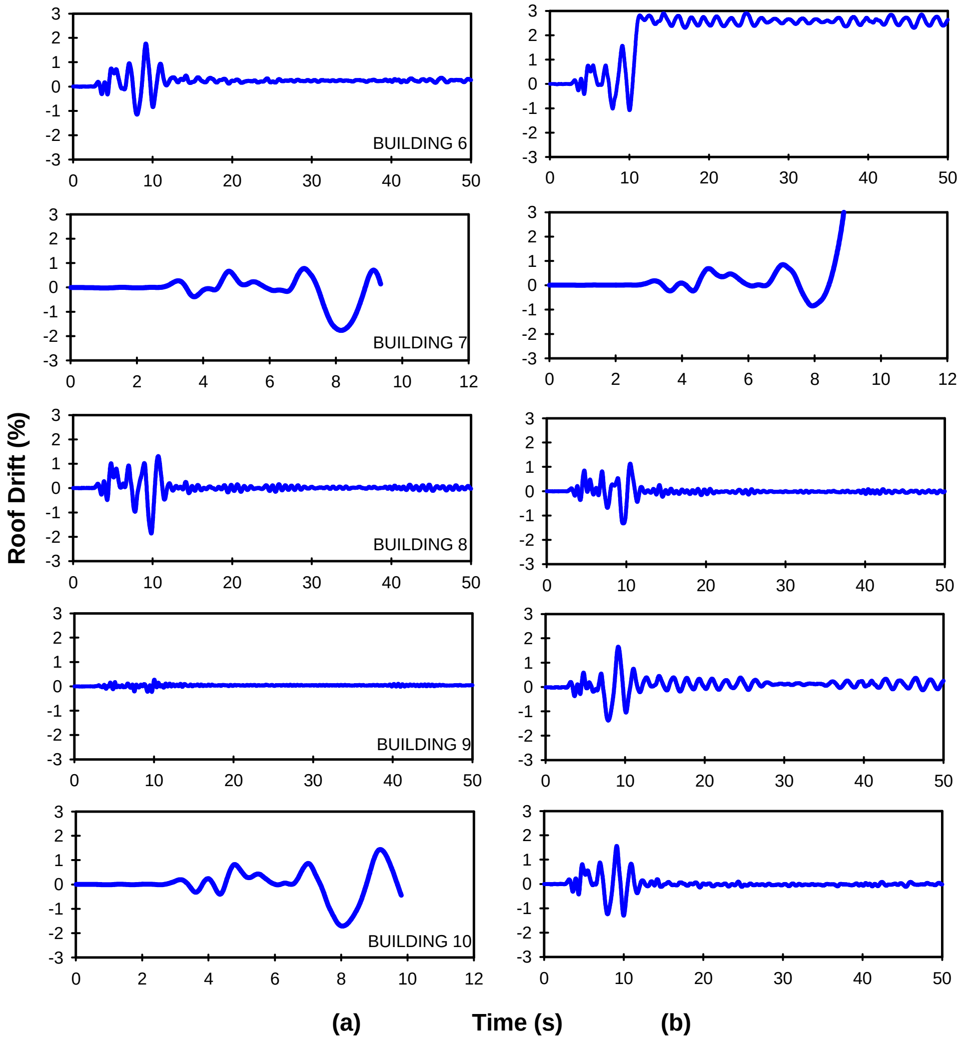

Figure 5.19 Normalized roof drift response history of severely damaged buildings, (a) X direction and (b) Y direction

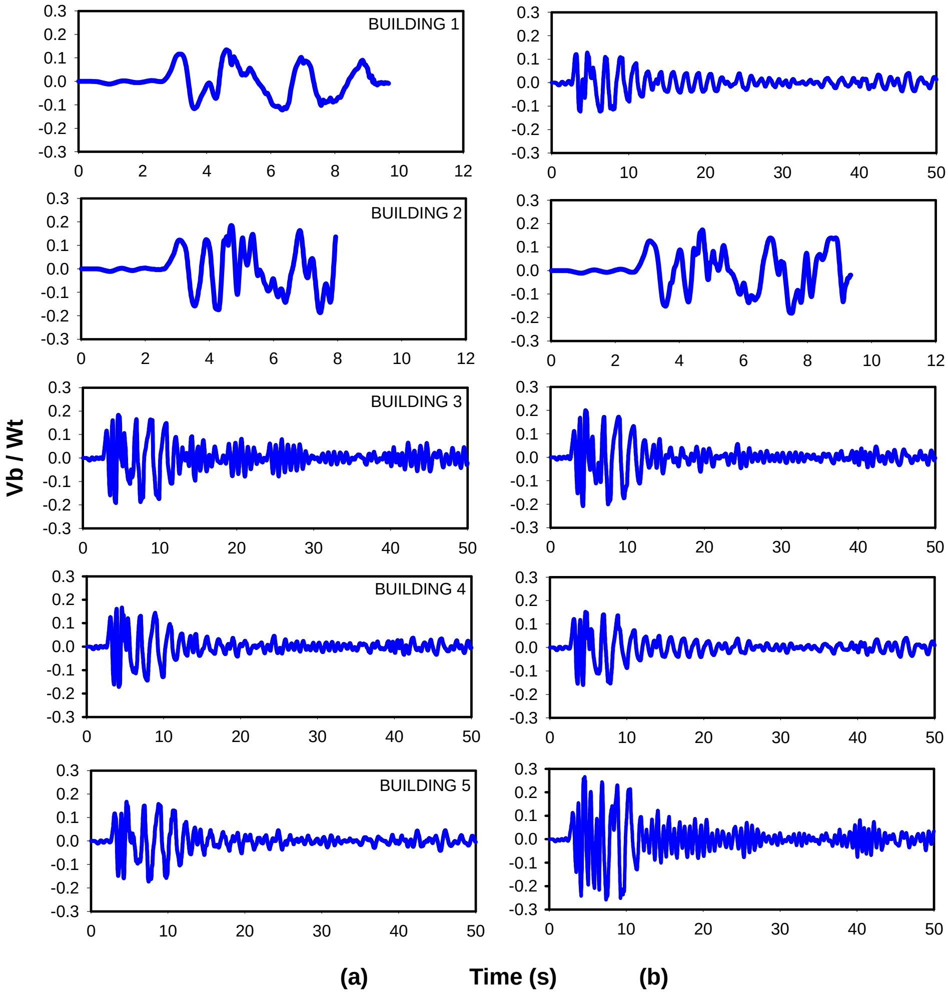

Figure 5.20 Normalized total base shear response history of moderately damaged buildings, (a) X direction and (b) Y direction

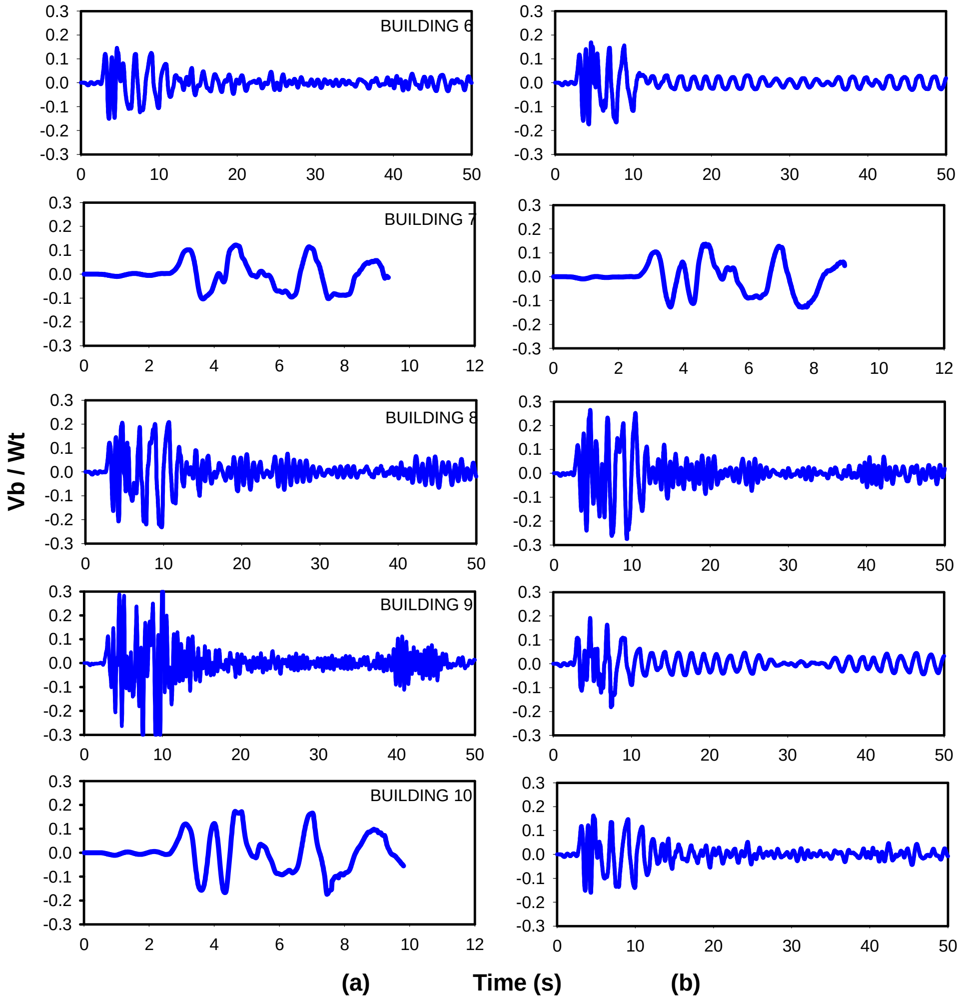

Figure 5.21 Normalized total base shear response history of severely damaged buildings, (a) X direction and (b) Y direction

The force–deformation hysteresis (by means of normalized base shear vs. roof drift) plots of the Nonlinear Response History Analyses are shown in Figure 5.22 and Figure 5.23 for moderately damaged buildings and severely damaged buildings, respectively. In the figures, the normalized roof drift is used as the deformation parameter where the normalized total base shear value is used as the force parameter during the analysis.

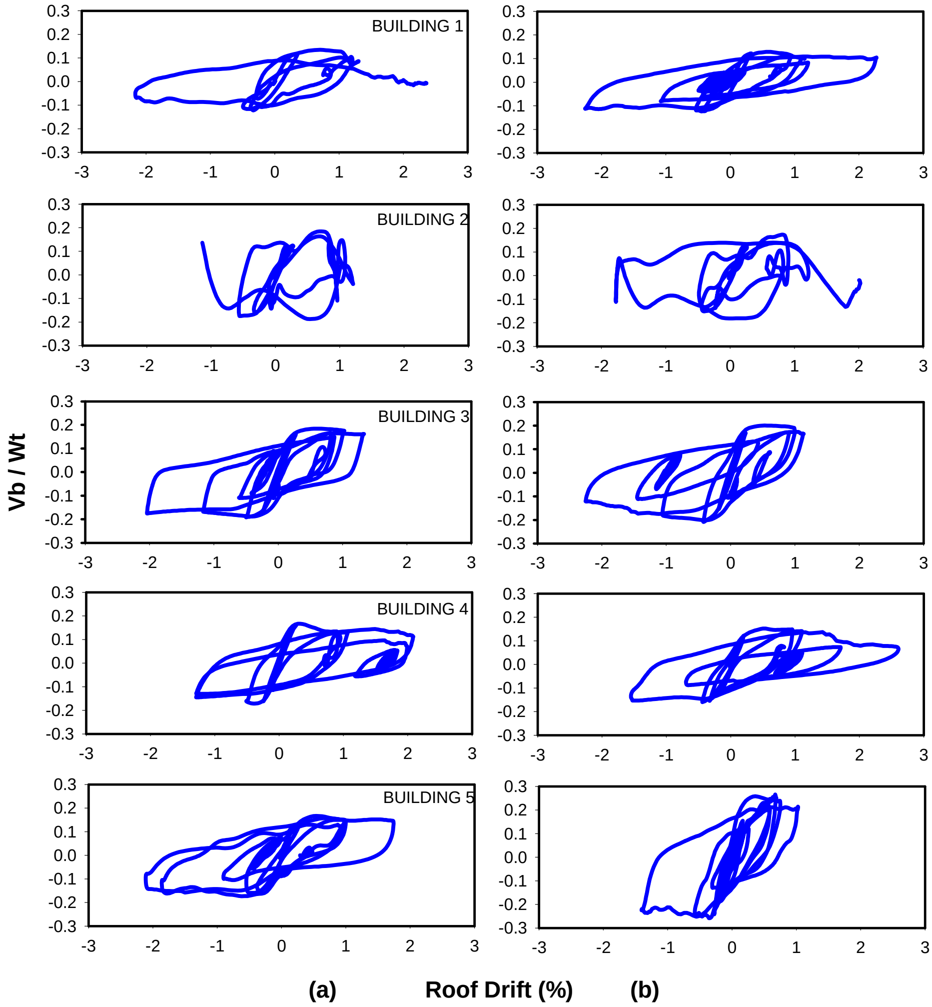

Figure 5.22 The normalized base shear–roof drift hysteresis plots of the NRHA for moderately damaged buildings, (a) X direction and (b) Y direction

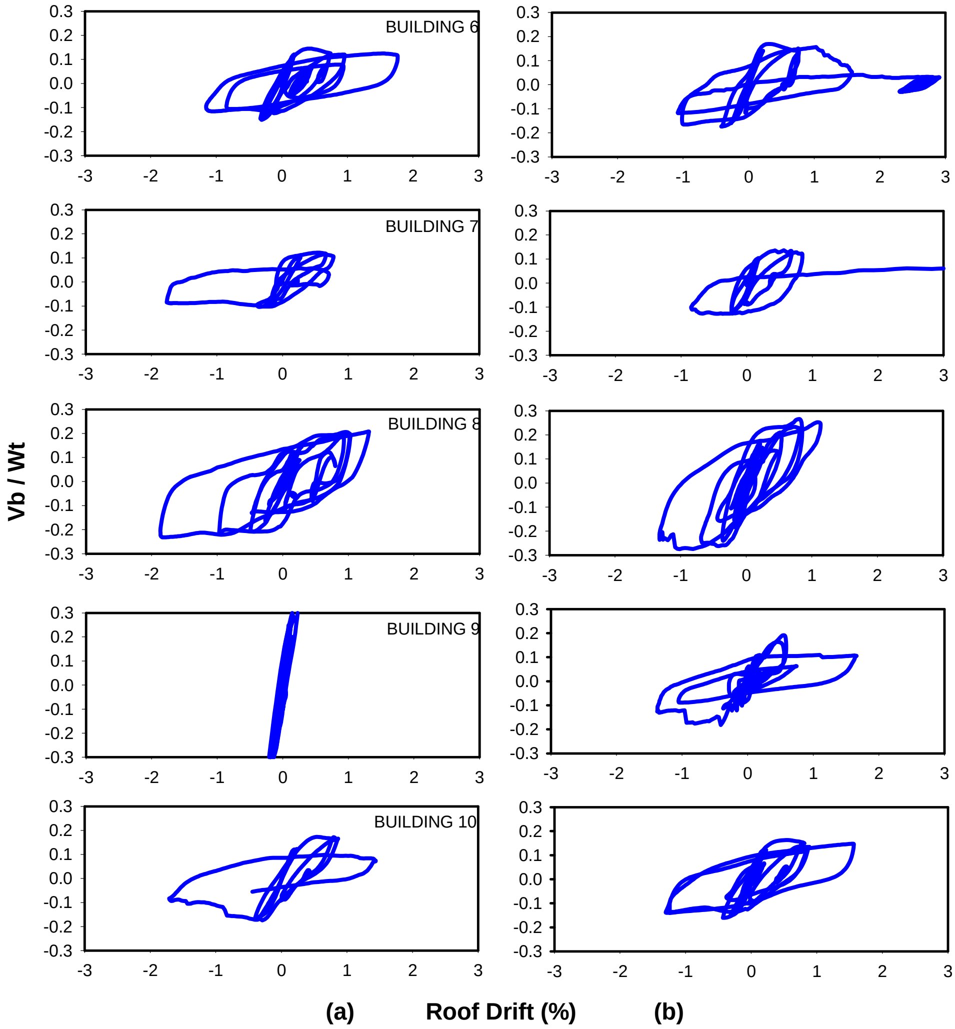

Figure 5.23 The normalized base shear–roof drift hysteresis plots of the NRHA for severely damaged buildings, (a) X direction and (b) Y direction

The calculated maximum values of roof displacement and total base shear response during NRHA for each building are given in Table 5.3 for all buildings. In Table 5.3, the global drift ratios (max roof displacement normalized with total height of the building) and normalized base shear values (max base shear divided by total weight of the building) are also given. The total weight values of the buildings, W_T, have been calculated at the initial step of the NRHA, considering the gravity load combination given in Equation (5.6).

$$W_T = 1.0 * DL + 0.3 * LL \tag{5.6}$$

Table 5.3 Calculated and normalized NRHA results for the buildings studied

					NRHA Results			
	Building No	Direction	H_T (m)	W_T (kN)	Δr (m)	Vb (kN)	Drift %	Vb / W_T
Moderately Damaged Buildings	1	X	13.1	14140	0.2626	1188.2	2.005	0.084
		Y			0.2979	1472.2	2.274	0.104
	2	X	13.2	22235	0.1130	2909.4	0.856	0.131
		Y			0.1352	2593.0	1.024	0.117
	3	X	12.4	16566	0.2531	2903.3	2.041	0.175
		Y			0.2040	2452.4	1.645	0.148
	4	X	12.4	6401	0.2586	720.4	2.085	0.113
		Y			0.1923	866.1	1.551	0.135
	5	X	13.6	11775	0.2848	1608.8	2.094	0.137
		Y			0.1912	2645.1	1.406	0.225
Severely Damaged Buildings	6	X	15.4	7511	0.2723	830.8	1.768	0.111
		Y			0.1780	912.7	1.156	0.122
	7	X	17.5	8480	0.3089	713.6	1.765	0.084
		Y			0.1482	860.0	0.847	0.101
	8	X	13.5	7082	0.2519	1455.0	1.866	0.205
		Y			0.1782	1600.5	1.320	0.226
	9	X	17.5	15862	0.0484	6462.7	0.277	0.407
		Y			0.2902	1679.9	1.658	0.106
	10	X	15.6	18180	0.1293	2800.5	0.865	0.166
		Y			0.2441	2648.4	1.570	0.105

The maximum roof drift ratio results were obtained for Building 1, as 2.01 percent and 2.27 percent for X and Y directions of the building, respectively. In general, larger lateral roof drift values were obtained for moderately damaged buildings. Buildings having larger roof drift capacities performed better and experienced less damage during the earthquake.

The corresponding inter-story drift ratios (ISDRs) were also examined for each of the buildings. The distributions of lateral drift over the height of the building were presented in Figure 5.24 and Figure 5.25 for moderately damaged buildings and severely damaged buildings, respectively. The maximum ISDRs were obtained for the ground story of Building 9, as 8.46 percent in Y direction, while the max ISDR in X direction was the lowest as 0.31 percent. As it was emphasized in Section 5.3.1, most of the vertical structural members of Building 9 had been designed as structural walls with strong axis parallel to X direction of the building. Thus, the building was extremely stiff in X direction, while it was so soft in Y direction. Therefore, the elastic behavior in X direction can be clearly observed in Figure 5.23.

Moreover, high ISDR values were also obtained for other buildings. For instance, Buildings #3, #4, #6 in X direction, and Building #1 in Y direction had max ISDR values higher than 5 percent. In general, “soft story behavior” was observed on the buildings analyzed, according to the results of max ISDR values, which are presented in Figure 5.24 and Figure 5.25. Unlike the other buildings, for Building 2 the max ISDR values were obtained in 2nd story of the building as 2.82 percent and 3.97 percent in X and Y directions, respectively. The reason for this unexpected behavior is that all columns of the story have reduced dimensions, due to the decreasing vertical loads in upper stories.

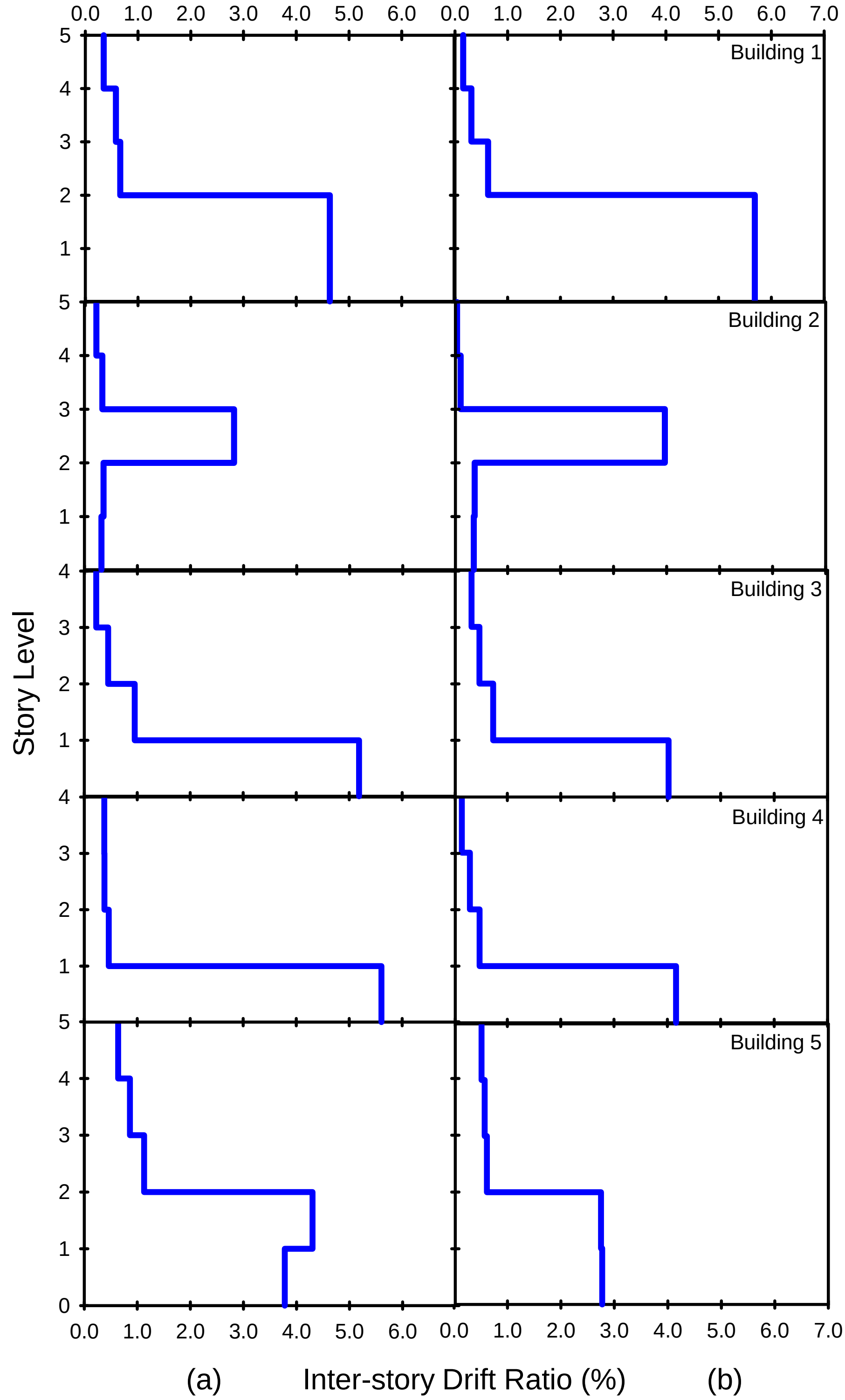

Figure 5.24 ISDRs for moderately damaged buildings according to NRHA, (a) X direction and (b) Y direction

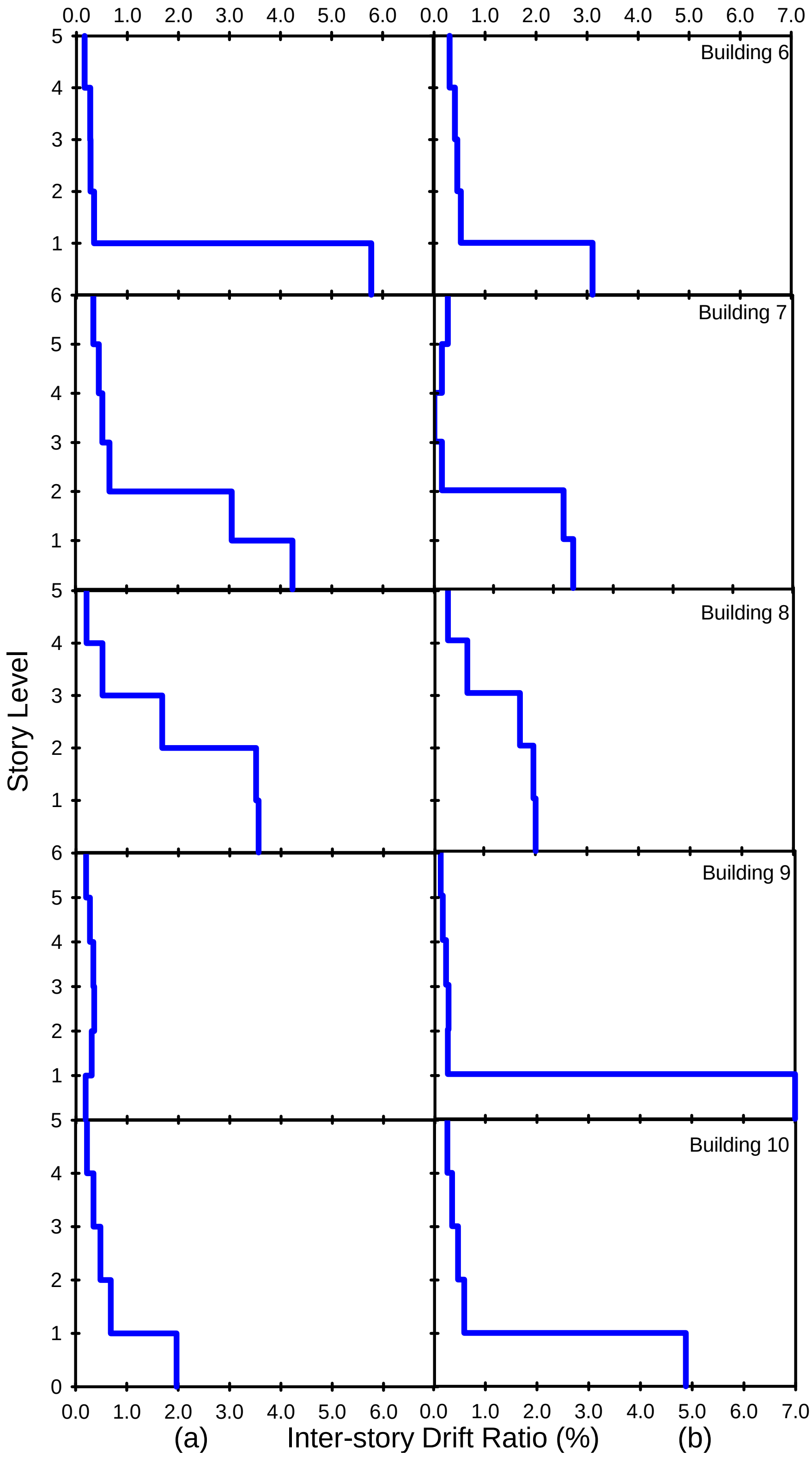

Figure 5.25 ISDRs for severely damaged buildings according to NRHA, (a) X direction and (b) Y direction

The global roof drift ratios that are given in Table 5.3 and max ISDR results presented in Figure 5.24 and Figure 5.25 can be compared with the global acceptability limits of ATC-40 (ATC 1996) and TEC-2007 (Section 2.4). The max ISDR is specified as 2 percent in ATC-40 for Life Safety (LS) performance level and 3 percent in TEC-2007. The limits for Collapse Prevention (CP), on the other hand, is defined as $0.33*V_i/P_i$ in ATC-40 and 4 percent in TEC-2007.

For moderately damaged buildings, considering the global roof drift ratios obtained from NRHA, the acceptability limits of ATC-40 for Life Safety (LS) performance level were exceeded either in X or Y direction of the building. This outcome is inconsistent with the observed damage state of the buildings. The LS limit of TEC-2007, however, was not exceeded.

For severely damaged buildings, on the contrary, none of the buildings had a roof drift ratio exceeding 2 percent (Table 5.3). From the global roof drift ratio point of view, moderately damaged buildings would have experienced more serious damages than severely damaged buildings, which is not consistent with the observed global damage.

On the other hand, the ISDRs can also be compared with these global acceptability limits for LS and CP performance levels. In general, most of the buildings have significantly high ISDRs, especially for the ground stories. The comparison of these ISDRs with given acceptability limits of both ATC-40 and TEC-2007, would result inconsistent outcomes considering the observed damages. According to such a comparison, the expected global damage state of moderately damaged buildings would also have been severe damage. Thus, it might be concluded that the damage is not strictly correlated with max ISDRs obtained from the NRHA.

5.5.2 Examination of Incomplete NRHA Results

The NRHA was conducted up to 50 seconds with the 3D nonlinear models of the buildings. The NRHA results were presented in Section 5.5.1. As it can be seen there, the NRHA were not completed until 50 s, for Buildings #2 and #7 in both X and Y directions and for Buildings #1 and #10 in only X direction. Therefore, the analyses results were examined in order to explain this incompleteness, whether it is in consequence of numerical or structural failure of the model.

For this purpose, first energy content of the strong ground motion was investigated by means of the Arias Intensity (IA) measure. Second, hinging of the columns was checked, using the moment demand values obtained from NRHA.

The Arias Intensity (percent) of the site-specific ground motion (Section 3.3) is shown in Figure 5.26. Significant amount of energy (which is defined as 5 – 95 percent of total energy) was discharged between 4.2s and 15.75s. The IA percentages at 8s, 9s and 10s are 50 percent, 70 percent and 85 percent, respectively.

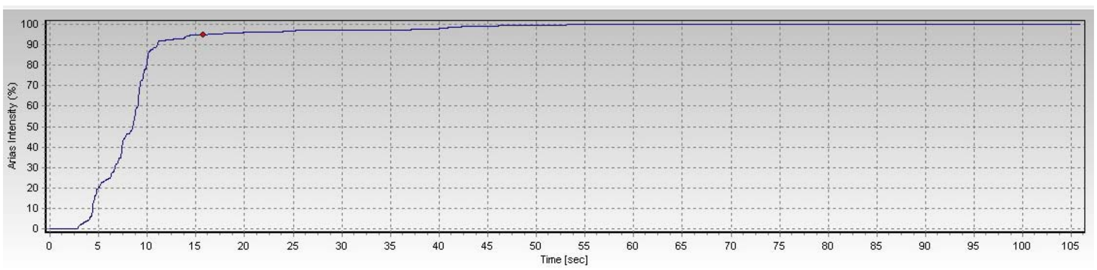

Figure 5.26 Arias Intensity (percent) of Sakarya site-specific ground motion

Only the NRHA of Building 2 in X direction was stopped at 8s, while other incomplete results were ended up later than 9s. Thus, the reason of the incompleteness is expected as structural failure rather than any numerical convergence failure.

At this stage, the moment demand (M_d) values obtained from NRHA were compared with the moment capacities (M_r) of the columns, in order to determine whether hinging (yielding) occur in the columns. The structural failure mechanism situations were examined due to yielding in columns of the critical stories. The comparison of moment demands with the moment capacities of critical story columns of the Buildings #1, #2, #7, and #10 are given in Table 5.4 to Table 5.7, respectively. In these tables, M_d / M_r ratios that are greater than 1.0 show the yielding of that structural member.

Table 5.4 Comparison of moment demands with the capacities of Building #1 columns (mezzanine and 1st stories), for NRHA in the X direction of the building

Story	Column ID	M_r (kN.m)	M_d (kN.m)	$(M_d / M_r)_X$
mez	33	135	144.35	1.07
mez	35	153	157.32	1.03
mez	37	385	415.42	1.08
mez	39	122	119.66	0.98
mez	41	122	128.53	1.05
mez	43	122	131.28	1.08
mez	45	122	138.52	1.14
mez	47	153	156.49	1.02
1	1	135	134.82	1.00
1	2	151	158.82	1.05
1	3	151	156.77	1.04
1	4	135	135.66	1.00
1	5	135	131.86	0.98
1	6	135	143.17	1.06
1	7	135	142.68	1.06
1	15	135	132.00	0.98
1	17	135	131.07	0.97
1	19	135	143.18	1.06
1	21	135	145.73	1.08
1	23	135	130.98	0.97
1	25	122	124.21	1.02
1	27	135	138.33	1.02
1	29	122	132.51	1.09
1	31	122	134.75	1.10
1	34	135	144.08	1.07
1	36	153	158.24	1.03
1	38	385	418.23	1.09
1	40	122	132.69	1.09
1	42	122	120.68	0.99
1	44	122	132.26	1.08
1	46	122	129.54	1.06
1	48	153	136.48	0.89

Table 5.5 Comparison of moment demands with the capacities of Building #2 columns (ground story), for NRHA in X and Y directions of the building

Story	Column ID	M_{rX} (kN.m)	M_{rY} (kN.m)	M_{dX} (kN.m)	M_{dY} (kN.m)	$(M_d / M_r)_X$	$(M_d / M_r)_Y$
1	1	193	123	238.84	173.19	1.24	1.41
1	2	193	123	238.72	173.19	1.24	1.41
1	3	86	190	95.98	240.81	1.12	1.27
1	4	86	190	94.64	240.50	1.10	1.27
1	5	86	190	92.94	240.81	1.08	1.27
1	6	86	190	92.23	240.81	1.07	1.27
1	7	86	190	94.55	240.50	1.10	1.27
1	8	86	190	95.95	240.81	1.12	1.27
1	9	193	123	238.84	171.21	1.24	1.39
1	10	193	123	238.72	171.21	1.24	1.39
1	11	86	190	95.98	241.76	1.12	1.27
1	12	86	190	94.64	242.31	1.10	1.28
1	13	86	190	92.94	239.23	1.08	1.26
1	14	86	190	92.23	239.23	1.07	1.26
1	15	86	190	94.55	242.31	1.10	1.28
1	16	86	190	95.95	241.76	1.12	1.27
1	17	194	87	208.73	109.03	1.08	1.25
1	18	194	87	215.54	111.00	1.11	1.28
1	19	194	87	214.68	111.00	1.11	1.28
1	20	194	87	209.42	109.03	1.08	1.25
1	21	194	87	209.10	110.23	1.08	1.27
1	22	194	87	209.64	110.23	1.08	1.27
1	23	86	190	98.03	241.54	1.14	1.27
1	24	86	190	98.31	241.54	1.14	1.27
1	25	194	87	208.73	109.78	1.08	1.26
1	26	194	87	215.54	111.23	1.11	1.28
1	27	194	87	214.68	111.23	1.11	1.28
1	28	194	87	209.42	109.78	1.08	1.26
1	29	194	87	209.10	110.90	1.08	1.27
1	30	194	87	209.64	110.90	1.08	1.27
1	31	86	190	98.03	244.55	1.14	1.29
1	32	86	190	98.31	244.55	1.14	1.29
1	33	194	87	209.30	107.43	1.08	1.23
1	34	194	87	212.99	111.02	1.10	1.28
1	35	194	87	211.88	110.94	1.09	1.28
1	36	194	87	207.68	109.63	1.07	1.26
1	37	194	87	207.70	109.63	1.07	1.26
1	38	194	87	209.71	110.94	1.08	1.28
1	39	194	87	213.60	111.02	1.10	1.28
1	40	194	87	209.67	107.43	1.08	1.23

Table 5.6 Comparison of moment demands with the capacities of Building #7 columns (ground and 2nd stories), for NRHA in X and Y directions of the building

Story	Column ID	M_{rX} (kN.m)	M_{rY} (kN.m)	M_{dX} (kN.m)	M_{dY} (kN.m)	$(M_d / M_r)_X$	$(M_d / M_r)_Y$
1	1	82	164	96.50	180.36	1.18	1.10
1	2	82	164	93.16	186.18	1.14	1.14
1	3	348	129	363.09	118.59	1.04	0.92
1	4	87	193	80.34	194.96	0.92	1.01
1	5	81	649	75.28	661.99	0.93	1.02
1	6	81	649	65.01	718.79	0.80	1.11
1	7	550	275	584.04	243.56	1.06	0.89
1	8	80	186	72.64	197.25	0.91	1.06
1	9	232	280	288.88	326.78	1.25	1.17
1	10	77	157	88.46	179.72	1.15	1.14
1	11	180	232	189.67	259.42	1.05	1.12
1	12	180	232	166.20	219.62	0.92	0.95
1	13	87	193	84.60	201.27	0.97	1.04
2	59	82	164	93.18	68.74	1.14	0.42
2	60	82	164	92.02	98.66	1.12	0.60
2	61	268	99	292.48	77.09	1.09	0.78
2	62	86	171	94.85	97.64	1.10	0.57
2	63	48	421	71.13	361.65	1.48	0.86
2	64	48	421	75.38	401.71	1.57	0.95
2	65	300	103	310.66	109.71	1.04	1.07
2	66	85	176	86.07	181.34	1.01	1.03
2	67	134	197	159.83	173.33	1.19	0.88
2	68	46	101	64.10	58.40	1.39	0.58
2	69	99	206	111.87	155.27	1.13	0.75
2	71	90	180	94.17	115.71	1.05	0.64
2	120	112	199	99.72	151.77	0.89	0.76

In Table 5.4 to Table 5.7, yielding of the columns can be seen clearly. The columns of mezzanine and 1st stories of Building 1 yielded under the excitation in the X direction of the building. Similarly, all columns in ground story of the Building 2 yielded under the excitations in both X and Y directions. In Building 7, all 2nd story columns yielded in addition to the half of the ground story columns, in the X direction. In the Y direction of Building 7, significant part of the ground story columns yielded with some of the upper story columns. Lastly, also for Building 10, structural failure mechanism occurred due to yielding of all ground story columns, during the NRHA in the X direction.

Table 5.7 Comparison of moment demands with the capacities of Building #10 columns (ground story), for NRHA in the X direction of the building

Story	Column ID	M_r (kN.m)	M_d (kN.m)	$(M_d / M_r)_X$
1	1	256	314.93	1.23
1	2	256	289.28	1.13
1	3	197	196.14	1.00
1	4	275	273.17	0.99
1	5	210	219.98	1.05
1	6	365	420.69	1.15
1	7	365	464.34	1.27
1	8	217	219.42	1.01
1	9	310	315.47	1.02
1	10	265	270.40	1.02
1	11	178	193.85	1.09
1	12	407	460.17	1.13
1	13	414	474.00	1.14
1	14	313	333.62	1.07
1	15	313	326.38	1.04
1	19	365	451.73	1.24
1	20	217	219.57	1.01
1	21	256	314.46	1.23
1	22	256	289.63	1.13
1	23	197	195.41	0.99
1	24	275	273.31	0.99
1	25	210	225.16	1.07
1	27	365	439.98	1.21
1	48	310	315.06	1.02
1	49	265	270.10	1.02
1	50	178	195.39	1.10

As a result of the examination of incomplete Nonlinear Response History Analyses, which is discussed in this section, it is concluded that the incompleteness of the analyses is in consequence of structural failure of the models during NRHA, rather than any numerical convergence failure.

5.6 NONLINEAR STATIC ANALYSIS OF THE BUILDINGS

Nonlinear static (pushover) analyses were carried out on the 3D nonlinear models of the buildings studied. Pushover (capacity) curves were obtained as the outcomes of these analyses for each of the buildings studied. During the pushover analyses, lateral loads were applied to the analytical models in each of the orthogonal plan directions of the building, which were proportional to the fundamental mode shape of corresponding direction.

As explained in Section 4.2, the detailed damage distribution information could not be obtained for the buildings assessed, the study was concentrated on the global damage states only, not prediction of the damage distribution. In order to estimate the global seismic response of the buildings, the roof displacement demand parameter was used. The deformation demand of each structural element differs by different roof displacements. Thus, the roof displacement is used as a global parameter for estimation of the probable damage of the building. If the demand is within tight limits, the performance estimations can be consistent.

The pushover curves obtained from the nonlinear analyses were idealized and bilinearized capacity curves were obtained. The approximate NSPs were applied on the bilinearized curves, in order to obtain the global seismic response of the buildings studied. The performance points (or target displacements) of the buildings were calculated using the NSPs of several methods: i. Nonlinear Dynamic Analysis of Equivalent SDOF Systems (Eq. SDOF), ii. Displacement Coefficient Method (DCM) of FEMA 356 (FEMA 2000), iii. Capacity Spectrum Method (CSM) of ATC-40 (ATC 1996), iv. DCM of FEMA 440 (ATC 2005), v. CSM of FEMA 440 (ATC 2005), and vi. Modified Modal Pushover Analysis (MMPA) procedure (Chopra et al. 2004). The details of the NSPs used in this study and bilinearization procedure were given in Section 2.2. The response predictions of the buildings obtained from these approximate nonlinear static procedures (NSPs) were compared with one another.

For each of the building, the capacity curves that were obtained as the results of pushover analyses and the performance estimations of NSPs are presented in the following sections. The results of NRHA (which were summarized in Table 5.3) are also plotted for the corresponding figures. Sections from 5.6.1 to 5.6.5 comprise of moderately damaged buildings during the earthquake, while the severely damaged buildings are given in sections from 5.6.6 to 5.6.10. The performance predictions of the procedures that are not shown in the figures are beyond the figure borders.

The site specific ground motion that is given in Section 3.3 was used as the ground motion for the NSPs.

5.6.1 Building #1

The 4-story building has a mezzanine in the ground floor, and the ground floor has been commercially used. The total height is 13.1 m and the total weight of the building is estimated as 14140 kN. The pushover curve with performance estimations are shown in Figure 5.27.

As it can be seen in the Figure 5.27, most of the performance estimations obtained from approximate procedures are far beyond the capacity (pushover) curves for each direction of the building. For the Y direction of the building only, the expected performance point by DCM of both FEMA356 and FEMA440 are on the pushover curve. Although these estimations mean that the building would be severely damaged or collapse, the building experienced moderate damage during the earthquake. On the other hand, NRHA results for X and Y directions are also close to the ultimate drift values indicated by pushover curves.

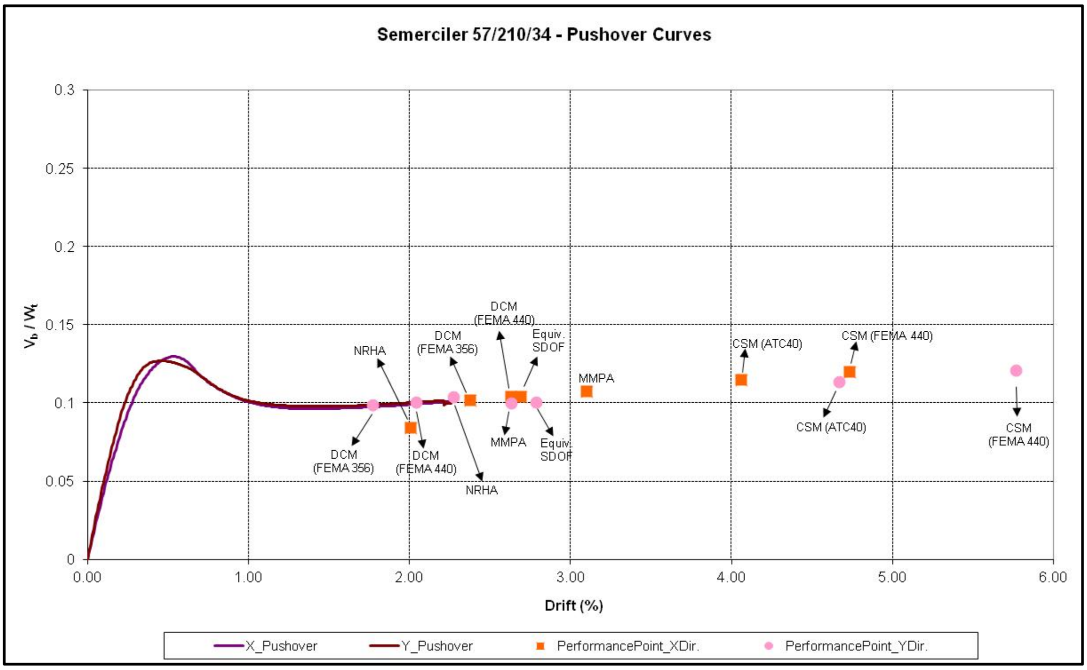

Figure 5.27 Pushover curves and the performance estimations for building #1

5.6.2 Building #2

The total height of the 5-story building is 13.2 m and the total weight of the building was calculated as 22200 kN. The building is located in a building site having 7 similar apartment blocks. The Block C was investigated in this study. The pushover curve with performance estimations are shown in Figure 5.28.

The pushover analysis results show that the building has a limited ductility capacity. Performance estimations of NSP's are far beyond the capacity (pushover) curves for each direction of the building. According to the estimations mean that the building would have been severely damaged / collapse, the building experienced moderate damage during the earthquake. On the other hand, the result of the NRHA simulation also may cause misunderstanding about the actual global seismic response of the building. Inconsistently to the damage observed during the earthquake, the NRHA results also indicate severe damage, in both X and Y directions of the building.

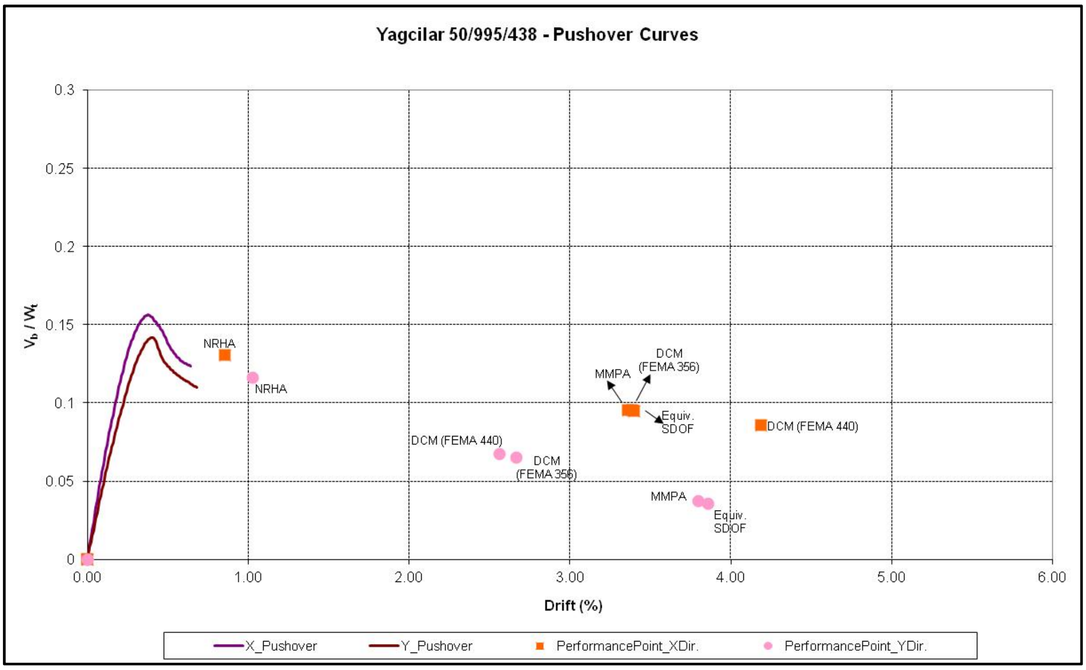

Figure 5.28 Pushover curves and the performance estimations for building #2

5.6.3 Building #3

The ground floor of the 4-story building has been commercially used on the street side, while the back side has a residential use. The total height is 12.4 m and the total weight of the building is 16500 kN. The pushover curve with performance estimations are shown in Figure 5.29.

According to the analyses along the X axis of the building, the estimations of DCM, Equiv. SDOF, and MMPA fit with the moderate damage of the building. The estimations of CSM imply that the building would be severely damaged during the earthquake. In the Y direction, however, just the estimations of DCM are consistent with the actual response level of the building. The results of the NRHA are consistent with the global damage state of the building for both X and Y directions.

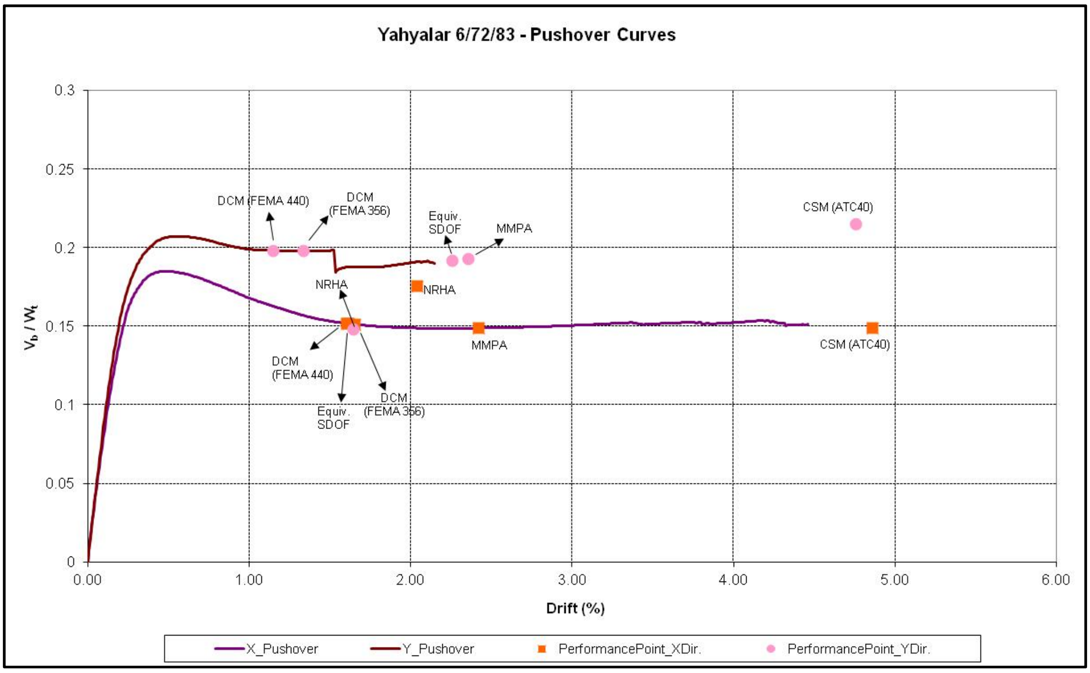

Figure 5.29 Pushover curves and the performance estimations for building #3

5.6.4 Building #4

The ground floor of the 4-story building has been commercially used. The total height is 12.4 m and the total weight of the building is 6400 kN. The pushover curve with performance estimations are shown in Figure 5.30.

While the target displacement expectations of DCM's for the X direction of the building are consistent with the moderate damage of the building, for the Y direction the expected target displacements are so close to the ultimate roof displacement capacity of the building according to the pushover analysis. The expected roof displacement results of other NSPs imply that the building would experience severe damage or collapse. The NRHA result in the Y direction is also beyond the ultimate drift ratio obtained from the pushover analyses.

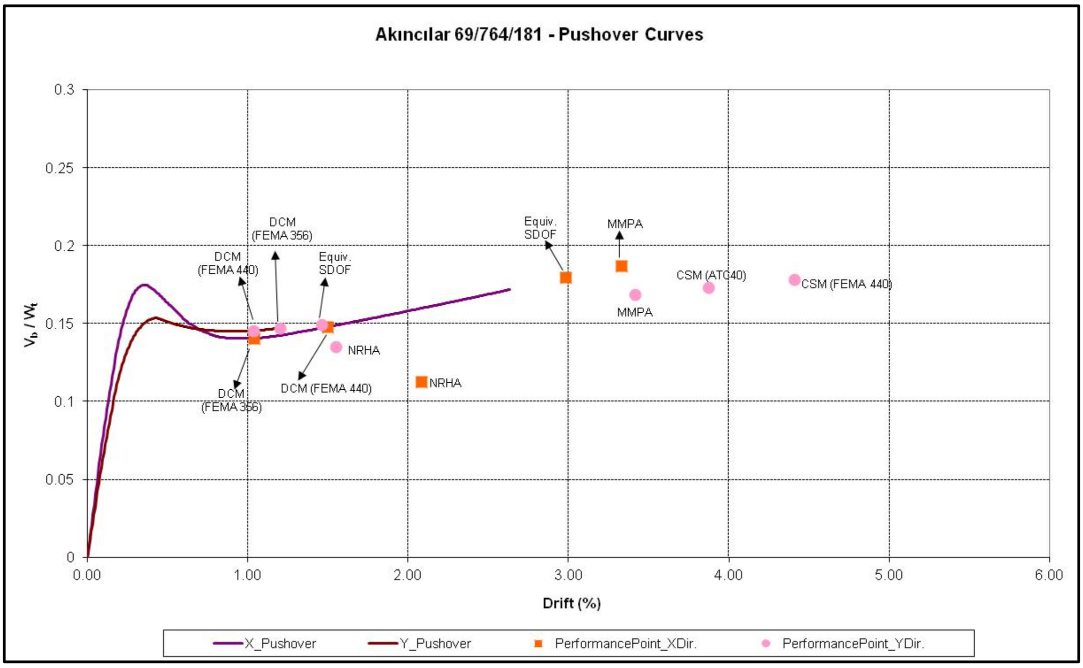

Figure 5.30 Pushover curves and the performance estimations for building #4

5.6.5 Building #5

The total height of the 5-story building is 13.6 m and the total weight of the building is 11800 kN. The pushover curve with performance estimations are shown in Figure 5.31.

Especially for the Y direction of the building has a limited ultimate ductility capacity, and the ultimate drift ratio is 0.84 percent. According to the assessment only the estimations of DCM in both X and Y directions fit with the moderate damage of the building. The other estimations imply that the building would be severely damaged during the earthquake. On the other hand, the results of the NRHA are also beyond the lateral drift capacity of the building for each of the orthogonal directions.

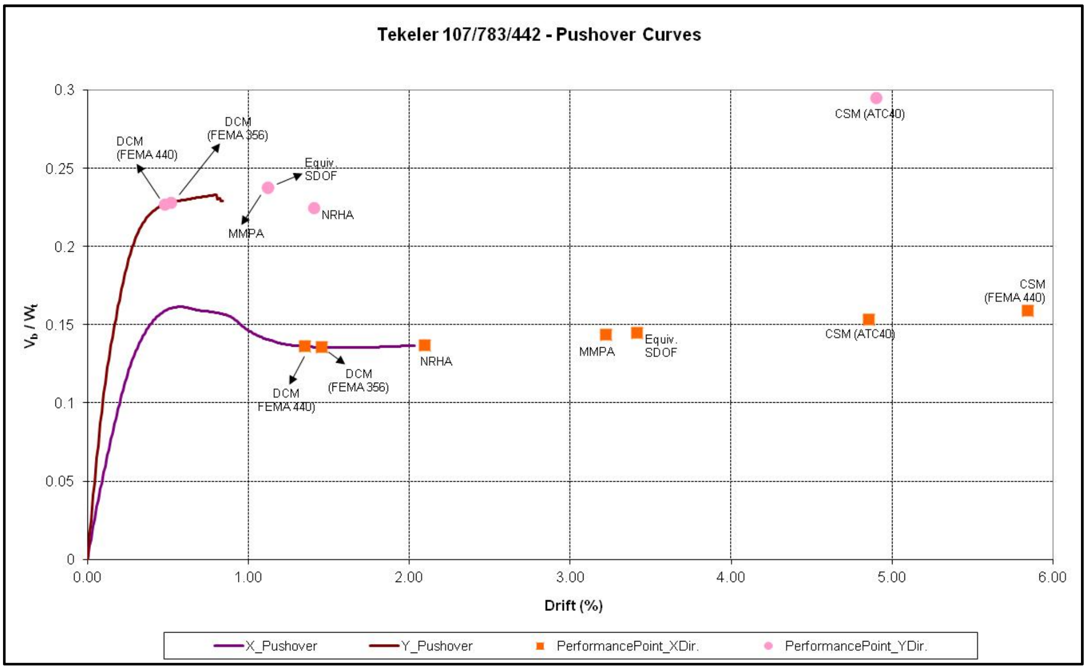

Figure 5.31 Pushover curves and the performance estimations for building #5

5.6.6 Building #6

The building had 5 stories and ground floor had been commercially used. The total height was 15.4 m, and the total weight was calculated as 7500 kN. The pushover curves with performance estimations are shown in Figure 5.32.

The target displacement values determined by DCM's of FEMA 356 and FEMA 440 for the X direction are very close to Life Safety (LS) performance level, considering the 75 percent of ultimate drift ratio. For the Y direction, the performance expectations of the DCM's imply moderate damage, where the building experienced severe damage. The expected performance roof drifts of NSP's of Equivalent SDOF, MMPA and CSM's are beyond the capacity curve. The NRHA results show the actual severe damage.

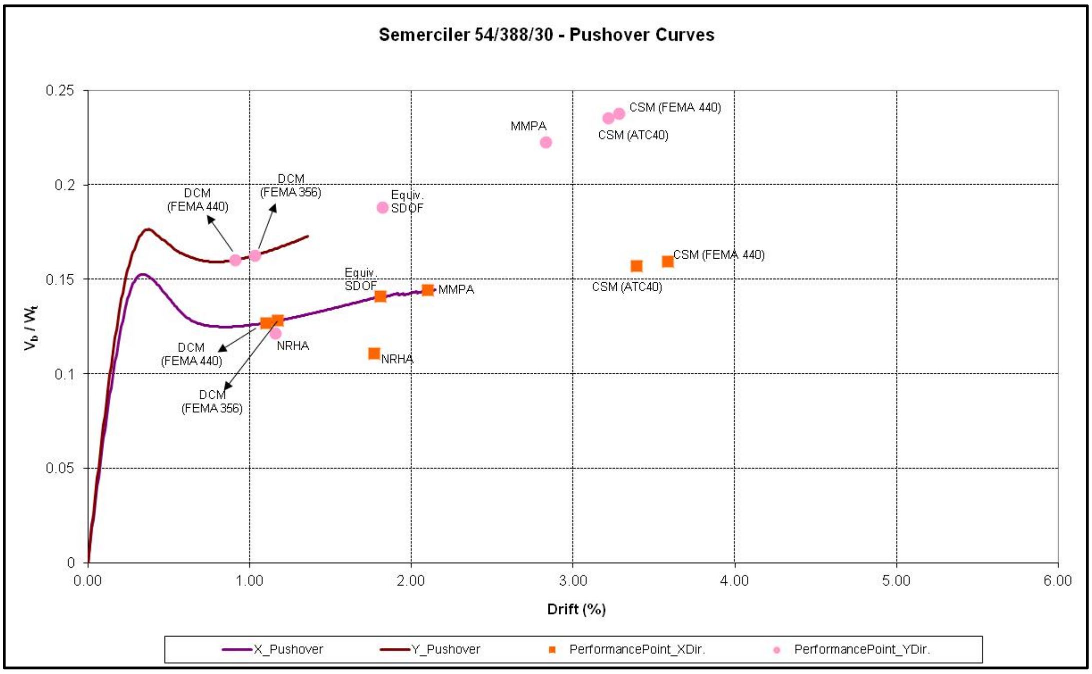

Figure 5.32 Pushover curves and the performance estimations for building #6

5.6.7 Building #7

The ground floor of the 6-story building had been commercially used. The total height was 17.5 m, and the total weight was 8500 kN. This building experienced severe damage during 1999 Earthquake. The pushover curves with performance estimations are shown in Figure 5.33.

All of the performance point estimations of assessment procedures are beyond the building capacity. The NRHA results are close to the ultimate points of the pushover curves, which imply the actual severe damage during the earthquake. However, as it can be seen from Figure 5.33 the NSP results for the target displacement are not close to neither the NRHA results, nor each other.

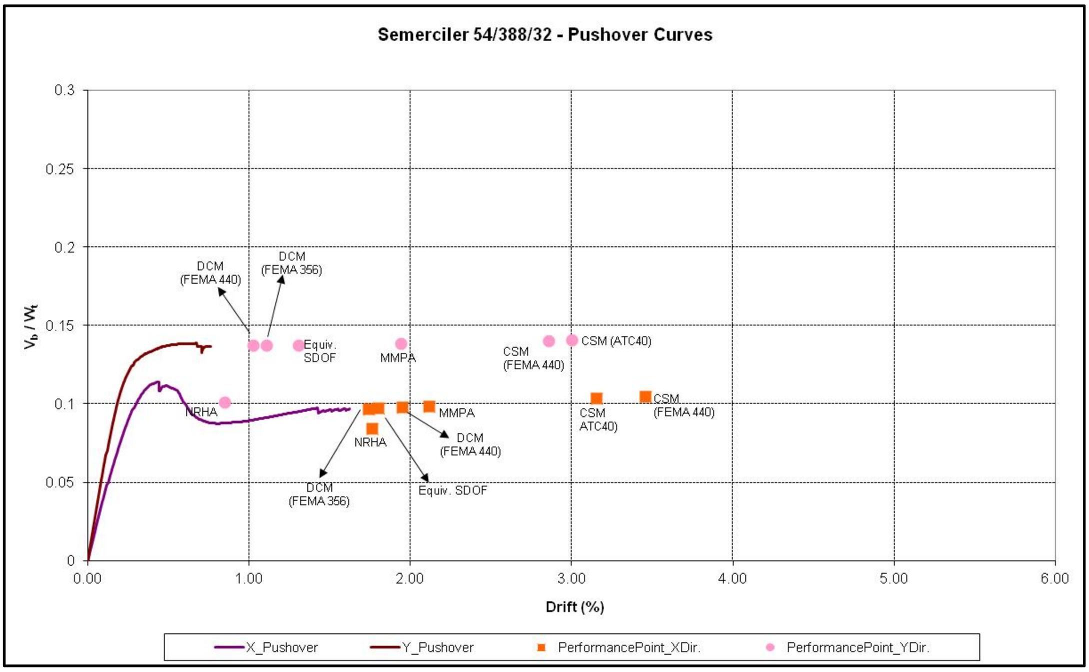

Figure 5.33 Pushover curves and the performance estimations for building #7

5.6.8 Building #8

The building had 5 stories with the total roof height of 13.5 m, and the total weight was calculated as 7100 kN. The pushover curves with corresponding performance estimations are shown in Figure 5.34.

The consistency of the NSP results with NRHA and actual damage state of the building is quite different for both directions of the analysis. In the X direction, the NSP's of DCM's, Equivalent SDOF, and MMPA determine the performance level within the Life Safety (LS) region. Even according to the NRHA in this direction the expected damage would be moderate in the X direction. In the Y direction, on the other hand, only Equivalent SDOF determines the target point within the LS region. All other performance point estimations of assessment procedures are beyond the building capacity curve implying the actual severe damage during the earthquake.

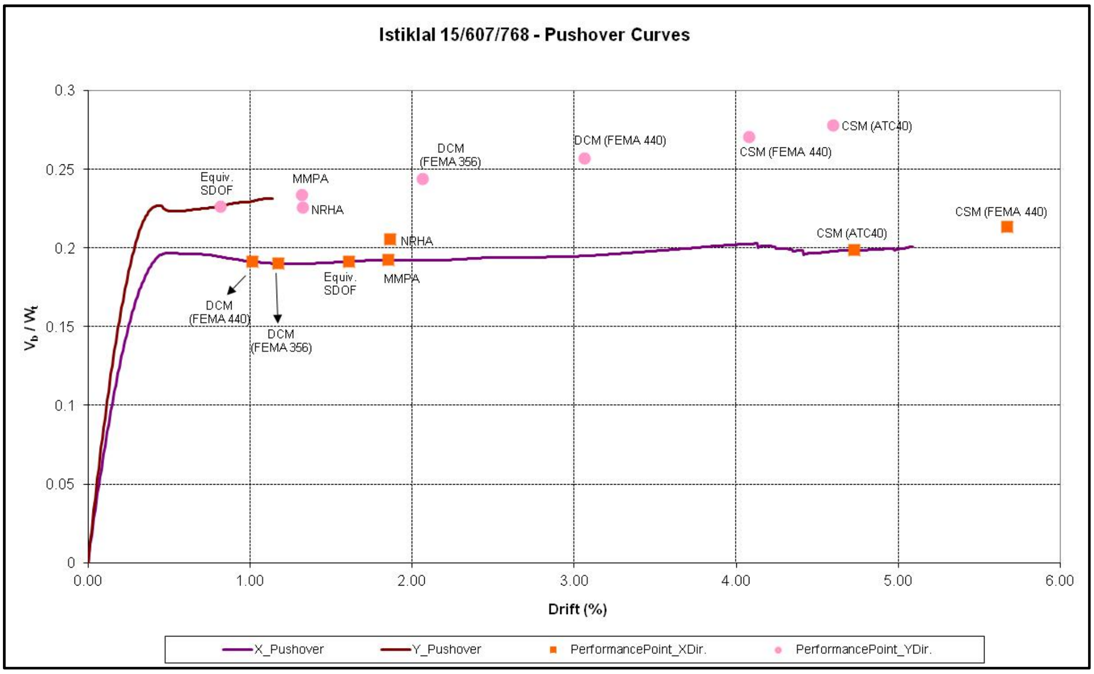

Figure 5.34 Pushover curves and the performance estimations for building #8

5.6.9 Building #9

The total height of the 6-story building was 17.5 m and its estimated total weight was 15850 kN. The pushover curve with performance estimations are shown in Figure 5.35. The lowest two stories of the building had been commercially used. As it has been emphasized in Section 5.3.1, most of the vertical structural members of Building 9 had been designed as structural walls with strong axis parallel to X direction of the building. Thus, the building is extremely strong in the X direction.

The pushover analysis results show that the building has limited ductility capacity, especially in the X direction. Performance estimations of DCM method, according to both FEMA356 and FEMA 440, are parallel to NRHA result; as elastic behavior. In addition, the Equiv. SDOF and MMPA expectations are seem to be very close to the LS damage limits. In the Y direction, on the other hand, the NSP results are far beyond the capacity (pushover) curve, except DCMs that are within the LS limit.

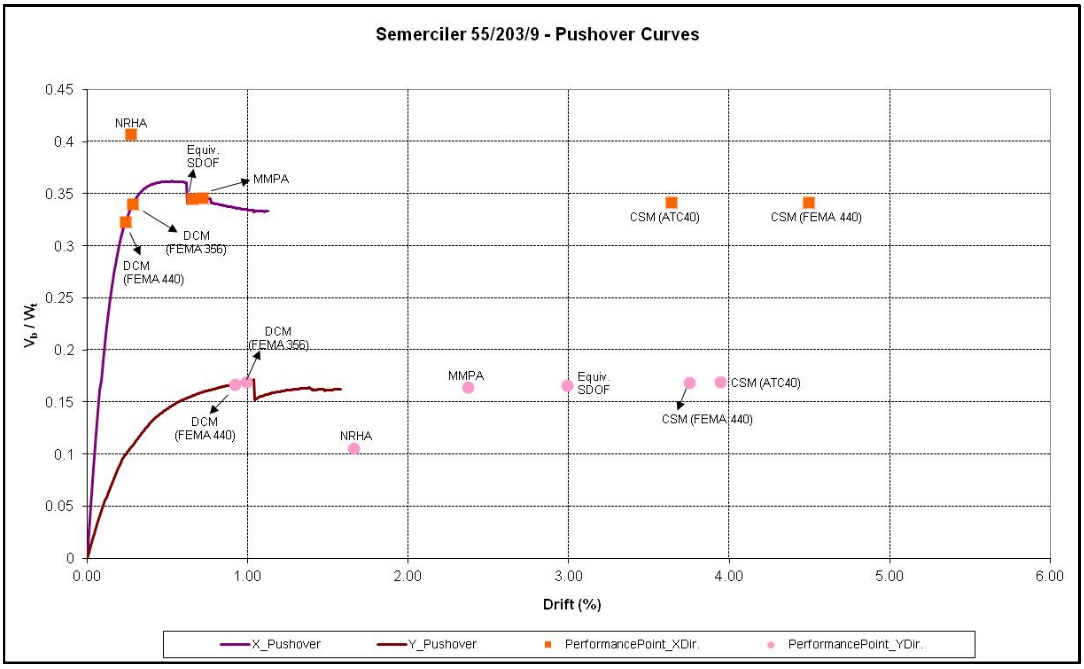

Figure 5.35 Pushover curves and the performance estimations for building #9

5.6.10 Building #10

The total height of the 5-story building was 15.6 m and estimated total weight was 18200 kN. The pushover curve with performance estimations are shown in Figure 5.36.

As it can be seen in the Figure 5.36, performance estimations obtained from approximate procedures are far beyond the capacity (pushover) curves for each direction of the building. These estimations imply that the building would experience severe damage / collapse. The building experienced severe damage during the earthquake. The results of the NRHA in both directions are consistent with the real damage.

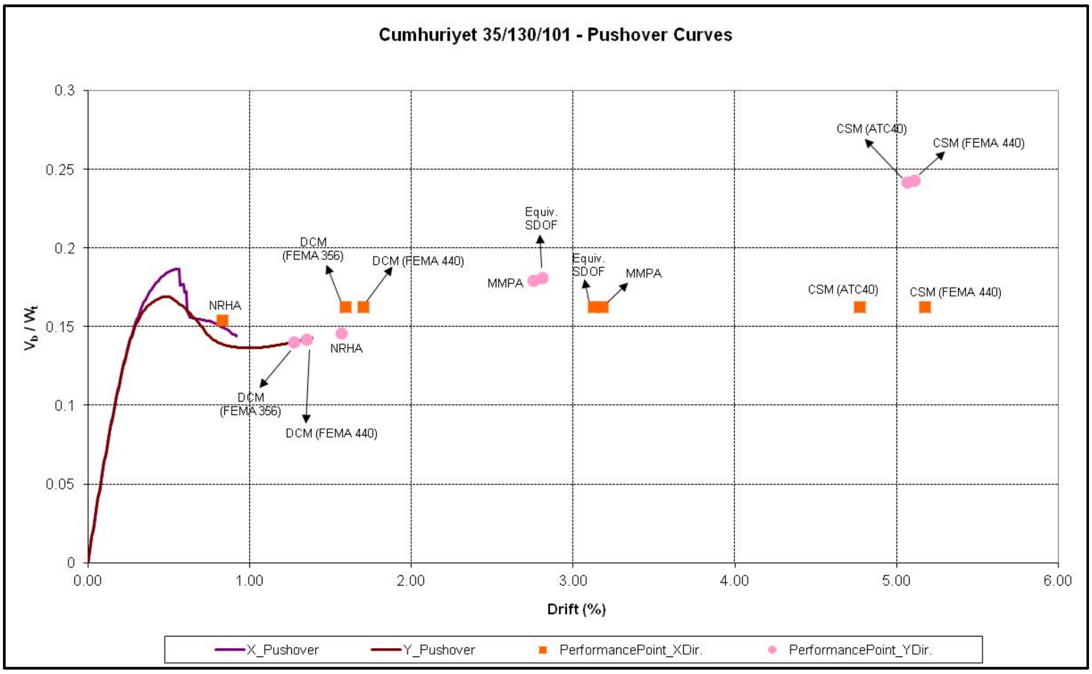

Figure 5.36 Pushover curves and the performance estimations for building #10

5.6.11 Discussion of the NSP Results

Since it is known that the first five buildings (given in sections from 5.6.1 to 5.6.5) were moderately damaged and the latter five buildings (given in sections from 5.6.6 to 5.6.10) severely damaged during the earthquake, it is possible to validate the predictions of nonlinear static procedures. This is possible, at least in global scales, since only global damage states of the buildings were recorded in the databases constituted after the 1999 Earthquake.

The expected limit states according to each of the analysis procedures differ from each other. According to the results given above, there is no clear and compelling evidence that any of the procedures used can identify the performance point suitably well for each condition. The results of the NSPs, on the other hand, do not comply with the results of the NRHA most of the time. However, the results of the NRHA are more accurate while determining the global damage state than the NSPs. Especially considering the moderately damaged buildings, the DCM's of both

FEMA 356 and FEMA 440 are the best performing approximate procedures for the performance point assessment. The CSM of both ATC-40 and FEMA 440 overestimate the performance point by means of the global roof drift parameter.

The studied buildings experienced altered damage during the earthquake. However, most of the analyses results could not predict the level of damage accurately. Using these results it is not possible to determine the seismic performance point and the corresponding damage state of the buildings before the occurrence of earthquake.

Thus, detailed assessment of the seismic response is needed in structural elements level. The results of such a detailed assessment are given and discussed in Chapter 6.

CHAPTER 6

PERFORMANCE ASSESSMENT OF THE BUILDINGS

6.1 INTRODUCTION

According to the objectives of this study, the results of current widely used nonlinear static (pushover) analysis procedures (NSPs) are compared with the observations (real building performance during the earthquake). In this manner, selected buildings were examined using nonlinear static analysis (pushover) and nonlinear response history analysis (NRHA) (Sections 5.5 and 5.6).

These global comparisons were conducted in two ways, generally, as discussed in previous chapter. First, the results of the pushover procedures were compared with each other and with the results of NRHA. Second, all analytical results obtained from the pushover procedures and NRHA were compared with the sample building site observations after the 1999 Marmara Earthquake.

After the global perspective previously given in Sections 5.5 and 5.6, the buildings were also examined using the detailed evaluation procedures of ASCE/SEI-41/06 (ASCE 2007), and its Supplement-1 (ASCE 2008), Turkish Earthquake Code (TEC 2007) and EuroCode-8-3 (EC 2005) thoroughly in this chapter. Each of these codes proposes detailed Nonlinear Static (NSA) and Nonlinear Dynamic (NDP) Assessment Procedures, and these examinations were done using both NSA and

NDP (The linear assessment procedures proposed by the codes were not considered in this study). The nonlinear assessment procedures are classified as NSA (Nonlinear Static Assessment Procedure) and NDP (Nonlinear Dynamic Assessment Procedure), according to the method used for inelastic response prediction of the building. The assessment procedure is named as NSA when the performance point is predicted using pushover (nonlinear static) based methods. If the NRHA is conducted, then the assessment procedure is called as NDP. This detailed assessment of the seismic response in structural elements level is necessary especially after the unclear results of the global evaluation.

In this chapter, first, structural member based ductility checks were done by comparing the shear demands obtained from nonlinear analyses with the shear capacity of the sections. Then, selected buildings were investigated by applying the detailed assessment procedures of ASCE/SEI-41 and its Supplement-1 (ASCE 2007, ASCE 2008), Turkish Earthquake Code (TEC 2007) and EuroCode-8-3 (EC 2005), and the results were presented. Nonlinear Dynamic Procedure (NDP) and Nonlinear Static Assessment Procedure (NSA) of these codes were applied based on the results of Nonlinear Response History Analysis (NRHA) and Pushover Analysis (Sections 5.5 and 5.6), respectively. Finally, all detailed assessment results were discussed, comparatively.

6.2 SHEAR CHECK (DEMAND / CAPACITY)

In addition to the shear capacity investigation and comparison considering the failure modes (i.e. shear-type failure and flexure-type failure) in Section 5.3.1, those capacity values of the columns were investigated in comparison with the shear demand values obtained from the nonlinear analyses. Although, any brittle/shear failure was not reported for most of the columns of the buildings by owners and engineers met in Adapazarı, such a comparison is needed because of the lack of detailed damage information about the buildings. This detailed shear comparison of demand vs. capacity will be presented and discussed here.

In the following tables, the maximum shear force demand values (V_d) are given with the shear-type capacity (V_r) and flexural-type capacity (V_e), together (Section 5.3). The demand values were obtained from the NRHA (Section 5.5). These demand shear forces of critical story columns, i.e. generally the ground story columns, were compared with the corresponding shear capacities, and the calculated ratios of V_d/V_r are given in the last two columns of the tables for X and Y directions of the buildings. Table 6.1 through Table 6.10, present these comparisons for the 10 buildings studied, respectively.

Table 6.1 Comparison of shear force capacities with corresponding demands for the ground story (incl. mezzanine) columns of Building #1

Story	Column ID	V_r (kN)	V_{eX} (kN)	V_{eY} (kN)	V_{dX} (kN)	V_{dY} (kN)	V_{dX} / V_r	V_{dY} / V_r
mez	33	187	142	164	103	144	0.55	0.77
mez	35	193	161	191	166	80	0.86	0.41
mez	37	254	405	204	327	130	**1.28**	0.51
mez	39	182	128	153	103	122	0.56	0.67
mez	41	173	128	153	60	132	0.34	0.76
mez	43	196	128	153	135	131	0.69	0.67
mez	45	197	128	153	129	107	0.65	0.54
mez	47	176	161	191	137	147	0.78	0.83
1	1	178	57	66	56	59	0.32	0.33
1	2	219	64	91	66	75	0.30	0.34
1	3	218	64	91	66	77	0.30	0.35
1	4	178	57	66	55	59	0.31	0.33
1	5	176	57	66	56	64	0.32	0.36
1	6	184	57	66	60	61	0.33	0.33
1	7	184	57	66	61	61	0.33	0.33
1	15	176	57	66	54	64	0.31	0.36
1	17	177	57	66	56	65	0.32	0.37
1	19	183	57	66	60	62	0.33	0.34
1	21	182	57	66	61	61	0.34	0.34
1	23	176	57	66	54	65	0.31	0.37
1	25	181	52	62	53	64	0.29	0.35
1	27	180	57	66	56	67	0.31	0.37
1	29	187	52	62	56	65	0.30	0.35
1	31	185	52	62	56	65	0.30	0.35
1	34	182	96	111	98	109	0.54	0.60
1	36	188	109	129	113	121	0.60	0.64
1	38	249	275	139	293	122	**1.18**	0.49
1	40	179	87	104	92	100	0.52	0.56
1	42	171	87	104	85	94	0.50	0.55
1	44	188	87	104	88	108	0.47	0.58
1	46	189	87	104	89	104	0.47	0.55
1	48	173	109	129	97	117	0.56	0.68

In X direction of Building 1, the shear demand value was exceeded the corresponding capacity, only for 2 of the story columns.

Table 6.2 Comparison of shear force capacities with corresponding demands for the ground story columns of building #2

Story	Column ID	V_r (kN)	V_{eX} (kN)	V_{eY} (kN)	V_{dX} (kN)	V_{dY} (kN)	V_{dX} / V_r	V_{dY} / V_r
1	1	190	154	98	134	110	0.70	0.58
1	2	190	154	98	136	110	0.71	0.58
1	3	182	69	152	71	118	0.39	0.65
1	4	180	69	152	74	119	0.41	0.66
1	5	176	69	152	68	112	0.39	0.63
1	6	176	69	152	67	112	0.38	0.63
1	7	180	69	152	74	119	0.41	0.66
1	8	182	69	152	71	118	0.39	0.65
1	9	190	154	98	134	130	0.70	0.68
1	10	190	154	98	136	132	0.71	0.69
1	11	182	69	152	71	134	0.39	0.74
1	12	180	69	152	74	147	0.41	0.82
1	13	176	69	152	68	132	0.39	0.75
1	14	176	69	152	67	132	0.38	0.75
1	15	180	69	152	74	162	0.41	0.90
1	16	182	69	152	71	137	0.39	0.75
1	17	153	155	70	122	86	0.80	0.56
1	18	163	155	70	133	86	0.82	0.53
1	19	163	155	70	137	86	0.84	0.53
1	20	153	155	70	114	86	0.75	0.56
1	21	156	155	70	138	85	0.88	0.54
1	22	156	155	70	133	85	0.85	0.54
1	23	188	69	152	73	147	0.39	0.78
1	24	188	69	152	74	147	0.40	0.78
1	25	153	155	70	122	86	0.80	0.56
1	26	163	155	70	133	85	0.82	0.52
1	27	163	155	70	137	85	0.84	0.52
1	28	153	155	70	114	86	0.75	0.56
1	29	156	155	70	138	84	0.88	0.54
1	30	156	155	70	133	84	0.85	0.54
1	31	188	69	152	73	144	0.39	0.76
1	32	188	69	152	74	144	0.40	0.76
1	33	150	155	70	115	84	0.77	0.56
1	34	159	155	70	134	87	0.84	0.55
1	35	157	155	70	147	88	0.94	0.56
1	36	153	155	70	148	87	0.96	0.57
1	37	153	155	70	145	87	0.95	0.57
1	38	157	155	70	148	88	0.95	0.56
1	39	159	155	70	141	87	0.89	0.55
1	40	150	155	70	113	84	0.75	0.56

Table 6.3 Comparison of shear force capacities with corresponding demands for the ground story columns of building #3

Story	Column ID	V_r (kN)	V_{eX} (kN)	V_{eY} (kN)	V_{dX} (kN)	V_{dY} (kN)	V_{dX} / V_r	V_{dY} / V_r
1	1	188	107	74	121	90	0.65	0.48
1	2	187	104	66	106	71	0.57	0.38
1	3	203	67	105	70	99	0.34	0.49
1	4	204	67	105	70	100	0.34	0.49
1	5	206	67	105	70	102	0.34	0.50
1	6	208	67	105	73	102	0.35	0.49
1	7	209	67	105	75	103	0.36	0.49
1	8	208	67	105	70	110	0.33	0.53
1	9	214	67	105	76	114	0.35	0.53
1	10	210	62	97	70	102	0.33	0.49
1	11	210	67	105	73	111	0.35	0.53
1	12	212	62	97	69	104	0.33	0.49
1	13	213	67	105	74	126	0.35	0.59
1	14	192	95	61	100	67	0.52	0.35
1	15	195	129	81	131	106	0.67	0.54
1	16	208	67	105	73	110	0.35	0.53
1	17	210	62	97	69	101	0.33	0.48
1	18	189	104	66	114	75	0.60	0.40
1	19	190	95	61	98	66	0.52	0.35
1	20	193	95	61	95	71	0.49	0.37
1	21	226	62	131	69	131	0.30	0.58
1	22	207	68	116	81	145	0.39	0.70
1	23	190	104	66	115	72	0.61	0.38
1	24	212	67	105	80	111	0.38	0.53
1	25	193	95	61	99	70	0.52	0.37
1	26	218	67	105	79	102	0.36	0.47
1	27	195	104	66	116	77	0.59	0.40
1	28	193	129	81	131	104	0.68	0.54
1	29	323	61	180	76	259	0.24	0.80
1	30	191	129	81	139	97	0.73	0.51
1	31	193	104	66	111	77	0.58	0.40
1	32	184	104	66	104	70	0.57	0.38
1	33	208	62	97	68	98	0.33	0.47
1	34	209	62	97	67	95	0.32	0.46
1	35	213	62	97	70	91	0.33	0.43
1	36	211	62	97	73	90	0.35	0.43
1	37	189	104	66	110	74	0.59	0.39
1	38	185	95	61	101	60	0.55	0.32

Table 6.4 Comparison of shear force capacities with corresponding demands for the ground story columns of building #4

Story	Column ID	V_r (kN)	V_{eX} (kN)	V_{eY} (kN)	V_{dX} (kN)	V_{dY} (kN)	V_{dX} / V_r	V_{dY} / V_r
1	1	145	87	44	100	49	0.69	0.34
1	2	154	87	44	107	50	0.69	0.32
1	3	177	39	78	45	105	0.25	0.59
1	4	171	35	72	42	85	0.25	0.50
1	5	150	87	44	104	53	0.70	0.35
1	6	171	110	47	133	54	0.78	0.32
1	7	360	159	54	177	66	0.49	0.18
1	8	174	39	78	46	107	0.26	0.61
1	9	171	35	72	40	88	0.23	0.51
1	10	146	87	44	105	49	0.72	0.34
1	11	170	35	72	41	93	0.24	0.55
1	12	173	35	72	40	96	0.23	0.56
1	13	171	35	72	37	97	0.22	0.57
1	14	167	35	72	41	98	0.24	0.58
1	15	146	87	44	101	50	0.70	0.34

Table 6.5 Comparison of shear force capacities with corresponding demands for the ground story columns of building #5

Story	Column ID	V_r (kN)	V_{eX} (kN)	V_{eY} (kN)	V_{dX} (kN)	V_{dY} (kN)	V_{dX} / V_r	V_{dY} / V_r
1	1	179	73	148	71	125	0.39	0.70
1	2	184	81	144	88	132	0.48	0.72
1	3	179	73	148	79	133	0.44	0.75
1	4	174	73	148	76	132	0.43	0.76
1	5	184	97	162	102	174	0.56	0.94
1	6	185	90	162	95	165	0.51	0.89
1	7	184	73	148	73	147	0.40	0.80
1	8	151	148	74	109	84	0.72	0.56
1	9	174	274	40	307	58	**1.76**	0.33
1	12	155	160	95	176	105	**1.14**	0.68
1	13	158	149	84	124	93	0.78	0.59
1	14	631	95	1463	142	1214	0.23	**1.92**
1	15	174	274	40	307	58	**1.76**	0.33
1	18	151	148	74	109	82	0.72	0.55
1	19	184	97	162	102	173	0.56	0.94
1	20	185	90	162	95	165	0.51	0.89
1	21	184	73	148	73	142	0.40	0.77
1	22	179	73	148	71	122	0.39	0.68
1	23	184	81	144	88	127	0.48	0.69
1	24	179	73	148	79	125	0.44	0.70
1	25	174	73	148	76	140	0.43	0.81

In Building 5, few of vertical structural members were designed as structural walls. These members have V_r/V_e ratio less than 1.0, and they are shear-critical members (Section 5.3.1). According to the NRHA results, the shear demand value exceeded the corresponding capacity, for these shear-critical columns, both in X and Y directions. Shear failure was observed also for the same columns in upper stories of Building 5.

Table 6.6 Comparison of shear force capacities with corresponding demands for the ground story columns of building #6

Story	Column ID	V_r (kN)	V_{eX} (kN)	V_{eY} (kN)	V_{dX} (kN)	V_{dY} (kN)	V_{dX} / V_r	V_{dY} / V_r
1	1	173	32	67	37	81	0.21	0.47
1	2	177	48	95	48	114	0.27	0.64
1	3	212	75	107	72	100	0.34	0.47
1	4	215	75	107	74	99	0.34	0.46
1	8	178	41	85	41	95	0.23	0.54
1	10	220	82	124	90	157	0.41	0.71
1	11	218	75	107	76	112	0.35	0.51
1	12	178	48	95	44	119	0.25	0.66
1	13	176	41	85	41	99	0.23	0.56
1	14	198	121	80	137	105	0.69	0.53
1	15	215	75	107	76	110	0.35	0.51
1	16	144	81	40	93	48	0.65	0.33
1	17	140	81	40	92	44	0.66	0.32
1	18	144	81	40	96	47	0.67	0.32
1	19	146	81	40	95	48	0.65	0.33
1	20	142	66	31	86	49	0.61	0.35

Table 6.7 Comparison of shear force capacities with corresponding demands for the ground story and 2nd story columns of building #7

Story	Column ID	V_r (kN)	V_{eX} (kN)	V_{eY} (kN)	V_{dX} (kN)	V_{dY} (kN)	V_{dX} / V_r	V_{dY} / V_r
1	1	173	41	82	46	69	0.26	0.40
1	2	180	41	82	47	73	0.26	0.41
1	3	193	174	65	171	58	0.89	0.30
1	4	176	44	97	41	77	0.23	0.44
1	5	362	41	325	39	262	0.11	0.72
1	6	371	41	325	39	234	0.10	0.63
1	7	268	275	138	258	111	0.96	0.42
1	8	190	40	93	38	83	0.20	0.44
1	9	259	116	140	136	129	0.53	0.50
1	10	173	39	79	44	64	0.25	0.37
1	11	218	90	116	91	99	0.42	0.46
1	12	227	90	116	82	100	0.36	0.44
1	13	184	44	97	43	68	0.23	0.37
2	59	170	59	117	67	80	0.39	0.47
2	60	176	59	117	66	90	0.38	0.51
2	61	188	191	71	208	66	**1.10**	0.35
2	62	173	61	122	66	72	0.38	0.42
2	63	335	34	301	50	254	0.15	0.76
2	64	343	34	301	54	172	0.16	0.50
2	65	204	214	74	211	70	**1.04**	0.34
2	66	184	61	126	59	129	0.32	0.70
2	67	219	96	141	104	122	0.47	0.56
2	68	169	33	72	45	66	0.27	0.39
2	69	179	71	147	68	117	0.38	0.65
2	71	180	64	129	59	72	0.33	0.40
2	120	187	80	142	68	94	0.37	0.50

In Building 7, there is no shear failure in columns in ground story. However, shear demand of 2 columns were exceeded the capacity in second story. These columns had a cross-section of 80 cm * 30 cm, making the member shear-critical by increasing moment capacity and dependent flexural-type shear capacity (V_e), in long direction of the member.

Table 6.8 Comparison of shear force capacities with corresponding demands for the first, second and third story columns of building #8

Story	Column ID	V_r (kN)	V_{eX} (kN)	V_{eY} (kN)	V_{dX} (kN)	V_{dY} (kN)	V_{dX} / V_r	V_{dY} / V_r
1	1	149	166	89	152	81	**1.02**	0.54
1	2	187	110	203	104	216	0.56	**1.16**
1	3	173	62	126	63	94	0.36	0.54
1	4	178	89	153	70	191	0.39	**1.08**
1	5	177	155	109	127	129	0.72	0.72
1	6	154	358	58	491	67	**3.19**	0.44
1	7	267	58	398	70	425	0.26	**1.59**
1	8	176	89	153	72	192	0.41	**1.09**
1	9	172	166	128	155	110	0.90	0.64
1	10	227	57	350	65	380	0.29	**1.68**
1	11	172	89	153	76	163	0.44	0.95
1	12	176	62	126	59	90	0.33	0.51
1	13	157	166	89	193	67	**1.23**	0.43
1	14	172	70	156	76	120	0.44	0.69
2	49	146	151	81	124	71	0.85	0.49
2	50	182	100	185	95	104	0.52	0.57
2	51	171	57	115	54	82	0.32	0.48
2	52	174	81	139	63	163	0.36	0.94
2	53	172	141	99	130	122	0.75	0.71
2	54	149	325	53	425	54	**2.85**	0.36
2	55	264	52	361	65	445	0.25	**1.69**
2	56	172	81	139	67	154	0.39	0.89
2	57	168	151	116	126	91	0.75	0.54
2	58	223	52	319	57	233	0.26	**1.04**
2	59	169	81	139	71	148	0.42	0.88
2	60	173	57	115	57	76	0.33	0.44
2	61	152	151	81	158	57	**1.04**	0.37
2	62	170	64	142	63	89	0.37	0.53
3	147	142	116	62	98	58	0.69	0.41
3	148	176	81	154	81	133	0.46	0.76
3	149	168	48	101	53	71	0.32	0.42
3	150	170	57	122	66	128	0.39	0.75
3	151	167	113	79	116	104	0.70	0.62
3	152	145	255	41	340	49	**2.35**	0.34
3	153	260	41	289	56	259	0.22	0.99
3	154	169	57	122	68	131	0.40	0.77
3	155	163	119	92	118	83	0.72	0.51
3	156	219	40	247	48	169	0.22	0.77
3	157	166	57	122	50	133	0.30	0.80
3	158	170	48	101	50	74	0.29	0.43
3	159	146	127	63	142	60	0.97	0.41
3	160	167	51	112	58	83	0.35	0.50

In Building 8, shear failure occurred in 3 columns in the X direction and 5 columns in the Y direction, in ground story. Unlike Buildings #5 and #7, some of the shear-critical columns of Building 8 had cross-section of 30 cm * 60 cm, which is one of the typical cross-section dimensions used for design of these buildings. However, 1 column having a cross-section of 100 cm * 20 cm in the X direction, and 2 columns with cross-sections of 20 cm * 100 cm and 20 cm * 120 cm in the Y direction, experienced shear failure during NRHA in corresponding orthogonal directions of the building.

Table 6.9 Comparison of shear force capacities with corresponding demands for the ground story columns of building #9

Story	Column ID	V_r (kN)	V_{eX} (kN)	V_{eY} (kN)	V_{dX} (kN)	V_{dY} (kN)	V_{dX} / V_r	V_{dY} / V_r
1	103	136	195	30	239	39	**1.75**	0.28
1	104	211	340	38	311	56	**1.48**	0.26
1	105	216	645	71	423	81	**1.96**	0.37
1	106	216	340	38	285	58	**1.32**	0.27
1	108	316	843	73	509	96	**1.61**	0.30
1	109	214	554	64	340	71	**1.59**	0.33
1	110	145	195	30	211	44	**1.46**	0.30
1	111	164	304	49	284	59	**1.73**	0.36
1	112	232	237	165	134	143	0.58	0.62
1	113	258	164	278	79	344	0.31	**1.33**
1	114	244	216	139	92	187	0.38	0.77
1	115	463	98	918	38	1434	0.08	**3.10**
1	116	140	157	25	239	35	**1.71**	0.25
1	117	218	645	71	449	80	**2.06**	0.37
1	118	219	645	71	441	78	**2.01**	0.36
1	119	221	340	38	326	57	**1.48**	0.26
1	120	321	843	73	534	96	**1.66**	0.30
1	121	219	554	64	299	70	**1.36**	0.32
1	122	266	741	76	526	78	**1.97**	0.29
1	123	258	741	76	507	90	**1.97**	0.35
1	124	358	62	577	11	824	0.03	**2.30**
1	125	84	60	20	28	23	0.34	0.27
1	126	86	60	20	26	22	0.30	0.26
1	127	179	271	40	221	54	**1.23**	0.30
1	128	175	264	38	235	51	**1.34**	0.29

As discussed in Section 5.3.1, Building 9 was extremely vulnerable for shear in the X direction. According to the NRHA results in this direction, 18 out of 20 shear-critical (out of 25 total) columns of ground story experienced shear failure. Complete shear failure mechanism was occurred in the X direction, as expected. The shear failure was observed also for second and third stories. On the other hand, 3 structural walls were damaged due to shear failure, in the Y direction.

Table 6.10 Comparison of shear force capacities with corresponding demands for the ground story columns of building #10

Story	Column ID	V_r (kN)	V_{eX} (kN)	V_{eY} (kN)	V_{dX} (kN)	V_{dY} (kN)	V_{dX} / V_r	V_{dY} / V_r
1	1	244	128	114	132	124	0.54	0.51
1	2	240	128	114	139	128	0.58	0.54
1	3	237	99	126	96	133	0.40	0.56
1	4	257	138	160	132	179	0.51	0.70
1	5	252	105	126	106	127	0.42	0.50
1	6	228	183	73	202	77	0.88	0.34
1	7	237	183	73	202	77	0.85	0.33
1	8	222	109	101	100	107	0.45	0.48
1	9	260	155	145	133	174	0.51	0.67
1	10	257	133	125	131	132	0.51	0.52
1	11	204	89	89	93	95	0.45	0.46
1	12	294	204	153	194	156	0.66	0.53
1	13	257	207	121	221	110	0.86	0.43
1	14	301	157	147	156	159	0.52	0.53
1	15	286	157	147	150	156	0.52	0.55
1	19	240	183	73	189	79	0.79	0.33
1	20	225	109	101	99	108	0.44	0.48
1	21	243	128	114	133	128	0.55	0.53
1	22	240	128	114	138	130	0.58	0.54
1	23	237	99	126	97	136	0.41	0.57
1	24	257	138	160	132	184	0.51	0.71
1	25	254	105	126	107	127	0.42	0.50
1	27	230	183	73	190	76	0.83	0.33
1	48	259	155	145	133	173	0.51	0.67
1	49	258	133	125	131	136	0.51	0.53
1	50	204	89	89	93	93	0.46	0.46

In Building 10, none of the columns demanded shear force over than its capacity, according to the NRHA.

As discussed in Section 5.3.1, the expected failure mode for all of these buildings was flexure-type failure, in general. There, shear-type failure risk emphasized only for Buildings #9, #1, #2, #5, #8, according to the comparison of shear capacities V_r and V_e, among those 10 buildings. There was no shear failure in Building 2, although it was included in the “risky” group.

According to the ductile behavior check carried out and summarized in this section, Buildings #2, #3, #4, #6, and #10 experienced no shear failure during the NRHA, neither in the X nor in the Y direction.

The complete shear failure for Building 9 is so clear according to the NRHA in the X direction, as expected (Table 6.9). The reason of the failure was discussed previously (Section 5.3.1).

Building 8 is the another building which experienced significant shear failure among those 10 buildings, i.e. shear failure in 7 columns within first 3 stories in the X direction and 7 columns within first 2 stories in the Y direction (Table 6.8). The reason for the distinct ductility capacity (obtained over pushover curves) of the building in X and Y directions (Section 5.6.8) is thought to be from the shear failure experienced, because, in the X direction only 3 out of 7 failed columns located in ground story, while 5 out of 7 columns located in ground story in the Y direction.

Few columns of Buildings #1, #5 and #7, which were noted as shear-critical, were failed under shear forces during the NRHA. These failures were not thought to be so significant for overall behavior of these buildings.

According to these results, shear check investigation can be concluded that the shear-type brittle failure was occurred for limited number of cases, except for Building 9 (in the X direction) and Building 8 (in the Y direction), as presented. Therefore, since, the shear capacities were not exceeded, the assumption of neglecting nonlinear shear behavior of the sections in analytical models of these buildings (discussed in Section 5.3.1) is satisfactory.

6.3 DETAILED ASSESSMENT ACCORDING TO ASCE/SEI-41

In detailed nonlinear assessment procedure of ASCE/SEI-41 (ASCE 2007), the ultimate plastic hinge rotation limits have been defined for RC structural members, for each limit state (Section 2.4.2). The damage state of the structural member is determined by the most critical section, having the most severe damage state, using these acceptance criteria. The overall structural performance is then obtained by judgement of damage level and their distribution over the building.

All columns of the buildings studied were evaluated according to the NSA (Nonlinear Static Assessment) and NDP (Nonlinear Dynamic Procedure) assessment procedures of ASCE/SEI-41 (Section 2.2). The NSA procedure was applied to the buildings at the performance points estimated by NSPs (which are discussed in Section 5.6). However, if these performance estimations are beyond the capacity (pushover) curves, the NSA procedure was applied considering the ultimate roof displacement points on the pushover curve as the performance point.

The columns of the buildings studied were classified as "Condition ii", according to the transverse reinforcement and shear demand of the columns (as discussed in Section 2.4.2). Thus, for the detailed assessment of the buildings studied, the acceptance criteria defined for Condition ii were used.

In the following sections, for each of the buildings studied, the detailed assessment results are given according to ASCE/SEI-41. The results are given for the most critical story which was decided by the examination of detailed assessment results. The plastic hinge rotation (θ_{pl}) demands of the columns of critical story are shown in figures in comparison with the damage state limits of Immediate Occupancy (θ_{pl} *IO*), Life Safety (θ_{pl} *LS*) and Collapse Prevention (θ_{pl} *CP*). The different damage state limits for each of the structural member, according to the axial force and shear force levels on the member, as well as transverse reinforcement ratio are shown in the figures. The columns were accepted as "collapsed", if the computed θ_{pl} value was beyond the θ_{pl} given for *CP* limit. Besides the plastic hinge rotation demand comparison for the critical story columns, these demand values are also plotted against the normalized shear ($v = V / b_w d \sqrt{f_c}$) values in the figures for each building.

The plastic hinge rotation (θ_{pl}) demands of the structural members were calculated by Equation (6.1).

$$\theta_{pl} = (\phi_u - \phi_y) * l_p \qquad \textbf{(6.1)}$$

Where;

ϕ_u = ultimate curvature (calculated by the analysis and recorded by OpenSees software),

ϕ_y = yield curvature $= M / EI$,

l_p = plastic hinge length = $0.5 * h$ (TEC 2007),

h = depth of the column in the direction of analysis.

6.3.1 Building #1

The critical story of the 4-story building, including a mezzanine in the ground floor, was selected as the ground story. This story has 32 columns. The maximum plastic hinge rotation demands obtained by NRHA, in both X and Y directions of the building are shown in Figure 6.1.

It is obvious that the damage state of the building was overestimated by the NDP of ASCE/SEI-41. Although the building experienced moderate damage during the earthquake, the results presented in Figure 6.1, indicate that most of the columns would collapse, which implies the collapse of whole building. For NRHA in X direction, lower mezzanine columns of the critical story were slightly over the IO damage state limit (moderately damaged), where all others were collapsed (17 columns) or severely damaged (7 columns).

In addition to the severe damage at critical story of the building, the damage state of most of the upper story columns were estimated as “moderately damaged” by NDP in the X direction of the building.

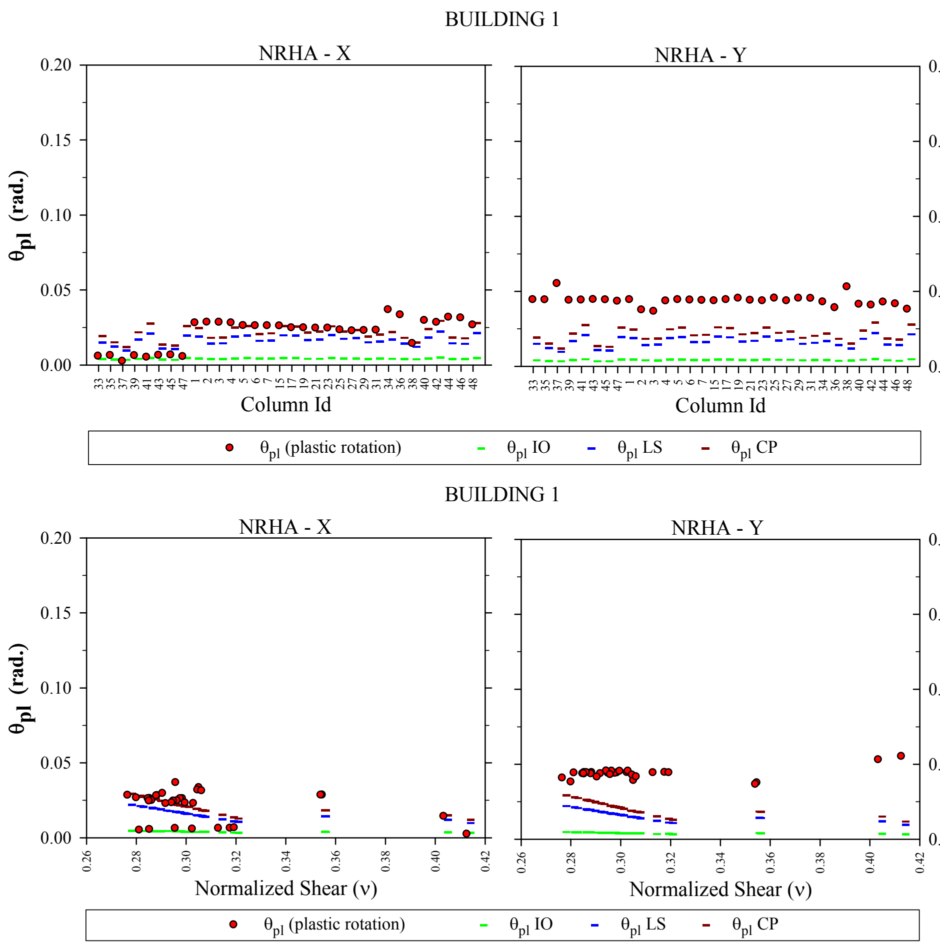

Figure 6.1 Plastic Hinge Rotation, θ_{pl}, results for Building 1 columns, computed by NRHA in X and Y directions

When the plastic hinge rotation demands for the columns are plotted against the normalized shear (ν), no obvious trend line was observed within the range.

The NSA of ASCE/SEI-41 was applied at ultimate roof displacement of the pushover curve in X direction (since, there is no performance expectation of NSPs falling on the pushover curve) and at the performance points estimated by approximate procedures (NSPs) in Y direction. The results in X and Y directions are shown in Figure 6.2 and Figure 6.3, respectively.

It can be clearly stated that the damage states computed by the NSA of ASCE/SEI-41 at the performance points obtained by the NSPs were overestimated. In X direction, at ultimate roof displacement of the pushover curve, only 8 of the columns (which are the lower mezzanine columns) did not reach the IO limit according to the NSA of ASCE/SEI-41. In the Y direction, on the other hand, all the critical story columns were expected to collapse, even at the performance point of FEMA356 which is 62 percent of the ultimate roof displacement. Thus, the damage state of the building was also overestimated according to NSA, similar to the NDP.

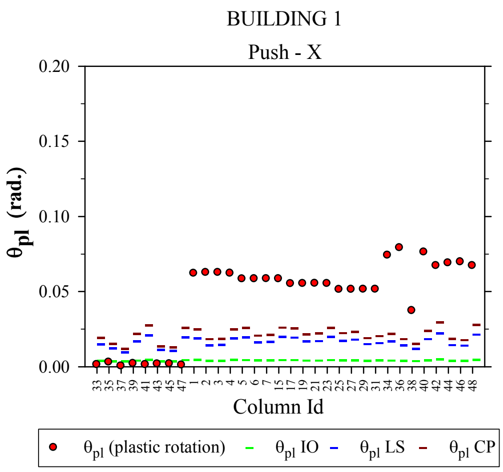

Figure 6.2 Plastic Hinge Rotation, θ_{pl}, results for Building 1 columns, computed at ultimate roof displacement of the pushover curve in the X direction

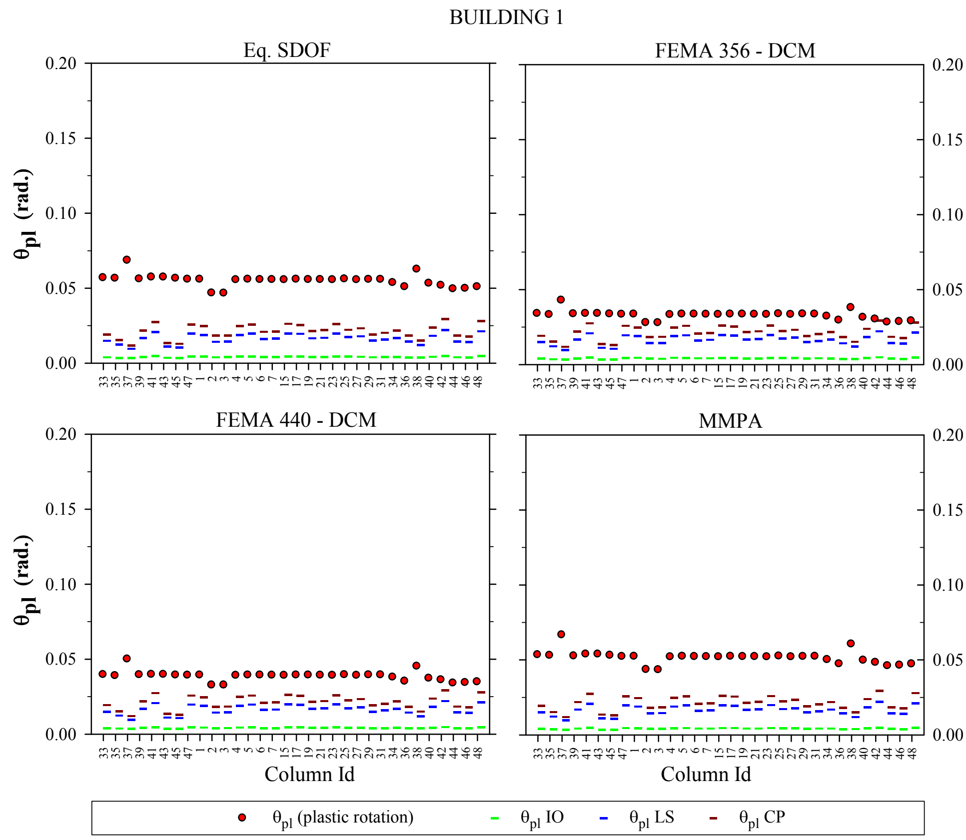

Figure 6.3 Plastic Hinge Rotation, θ_{pl}, results for Building 1 columns, computed by Eq.SDOF, FEMA356-DCM, FEMA440-DCM and MMPA in the Y direction

6.3.2 Building #2

The critical story of the building was selected as its third story where the max ISDR demands computed as discussed in Section 5.5.1. This story has 40 columns. The max plastic hinge rotation demands obtained by NRHA, in both X and Y directions of the building are shown in Figure 6.4.

The assessment results of the critical story columns, using the NDP of ASCE/SEI-41 in both X and Y directions indicate that all columns would fail; despite the real damage state was moderate. Moreover, in both X and Y directions, severe damage was not expected for the other story columns, but approximately half of those columns would be in between IO-LS limits (Damage Control Range).

As seen in Section 5.6.2, all performance estimations of NSP's are far beyond the capacity (pushover) curves for each direction of the building. Thus, the NSA procedure of ASCE/SEI-41 was applied only for the ultimate roof drift value of the capacity curve, and the results are shown in Figure 6.5.

According to the assessment results using the NSA in X direction, 20 of critical story columns reached to the LS limit, where the rest of the columns are so close to this limit, by means of plastic hinge rotation. In X direction, the building seems to be on the verge of Damage Control and Limited Safety Ranges. In Y direction analysis, 16 of the columns were expected to collapse, where the rest were in Damage Control Range (between IO and LS limits).

In general, it can be concluded that the assessment results of both NDP and NSA of ASCE/SEI-41 overestimated the damage state of the building as severe damage/collapsed.

When the plastic hinge rotation demands for the columns are plotted against the normalized shear (ν), it is observed that the plastic hinge rotation demands have been increased by the normalized shear. This trend, however, is observed only for Y direction analysis, not in the X direction.

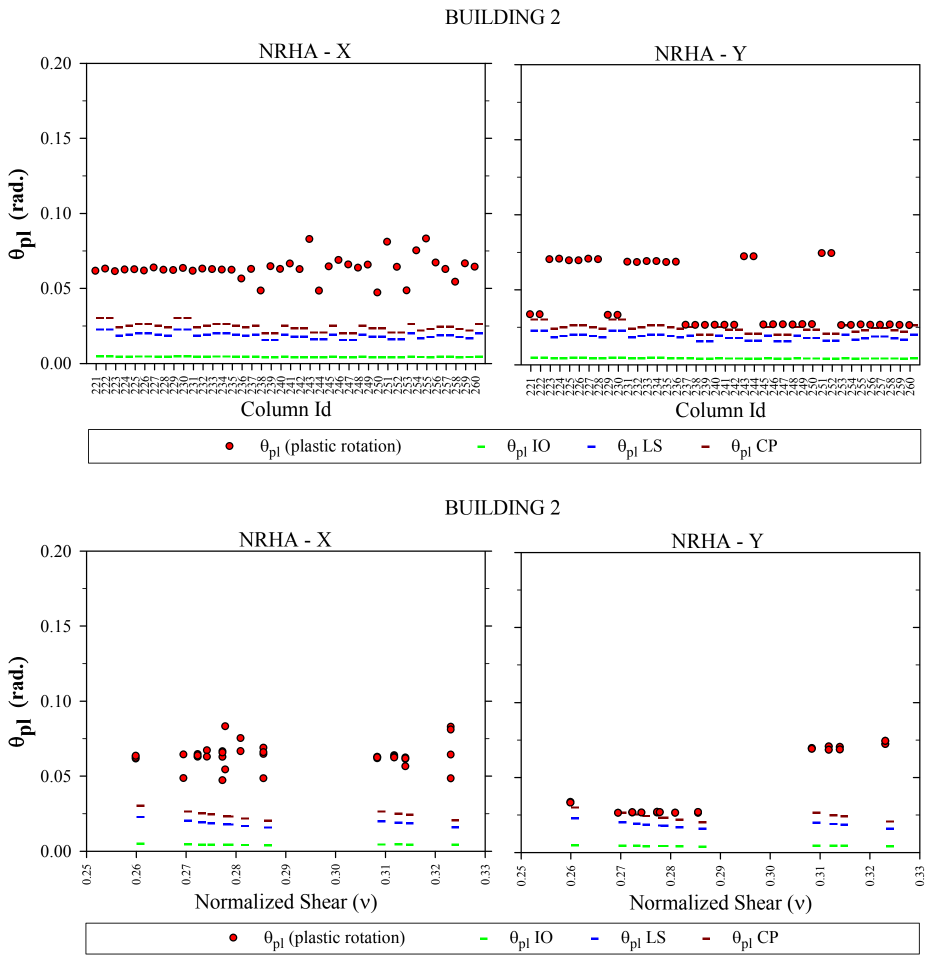

Figure 6.4 Plastic Hinge Rotation, θ_{pl}, results for Building 2 columns, computed by NRHA in X and Y directions

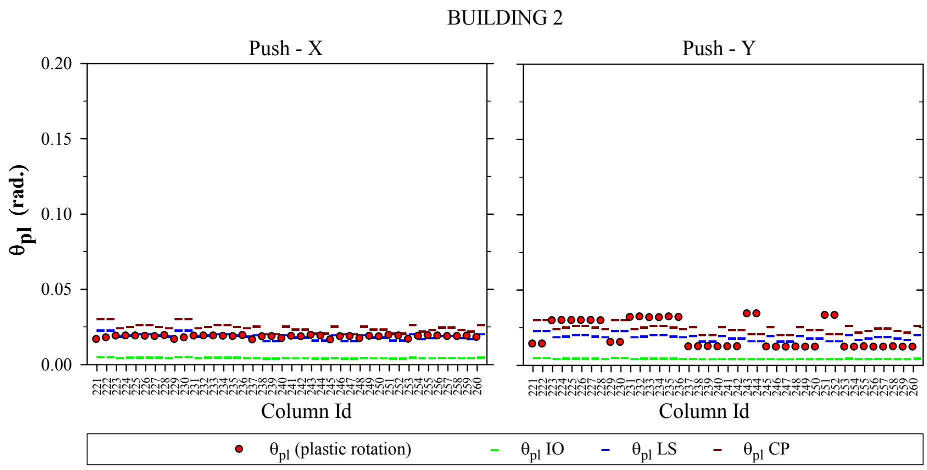

Figure 6.5 Plastic Hinge Rotation, θ_{pl}, results for Building 2 columns, computed at ultimate roof displacement of the pushover curve in X and Y directions

6.3.3 Building #3

The critical story of the 4-story building was selected as the ground story. This story has 38 columns. The max plastic hinge rotation demands obtained by NRHA, in both X and Y directions of the building are shown in Figure 6.6.

It is obvious that the damage state of Building 3 was overestimated by the NDP of ASCE/SEI-41. While all the columns were collapsed in the X direction analyses, 1 column was experienced severe damage rather than collapse in the Y direction. Nevertheless, the overall damage state of the building was determined as collapsed, despite the building experienced moderate damage during the earthquake.

In addition to the severe damage at critical story of the building, the damage state of all second story columns were estimated to collapse by NSA in the X direction of the building. At ultimate roof displacement of capacity curve in the Y direction, half of the second story columns were also estimated to collapse or severely damaged.

When the plastic hinge rotation demands for the columns are plotted against the normalized shear (v), it is observed that the plastic hinge rotation demands have been increased by the normalized shear. This trend, however, is observed only for Y direction analysis, not in the X direction.

At the performance points estimated by approximate procedures (NSPs), the NSA of ASCE/SEI-41 applied. The assessment results for these performance points, in X and Y directions are shown in Figure 6.7 and Figure 6.8, respectively.

As shown in Figure 6.7, at performance point of Equiv. SDOF, 20 of columns would collapse and 18 of them would be severely damaged. For these severely damaged columns, the max plastic hinge rotation demands were slightly below the CP limit. According to DCMs of both FEMA356 and FEMA440, 22 columns would fail, while 16 columns would be moderately damaged. And, according to MMPA, 32 columns would collapse and 6 columns would be severely damaged. Therefore, at performance points obtained by all 4 NSPs, the performance of the building was computed as collapsed. In the Y direction (Figure 6.8), on the other hand, at performance point of FEMA356, 20 columns would collapse, where 16 of them would be moderately and 2 of them would be severely damaged. At performance point of FEMA440 in this direction, 10 columns would collapse, where 16 of them would be moderately and 12 of them would be severely damaged. Thus, either in X or Y direction, the damage state of the building was overestimated by detailed assessment procedure of ASCE/SEI-41 at all performance points obtained by the NSPs.

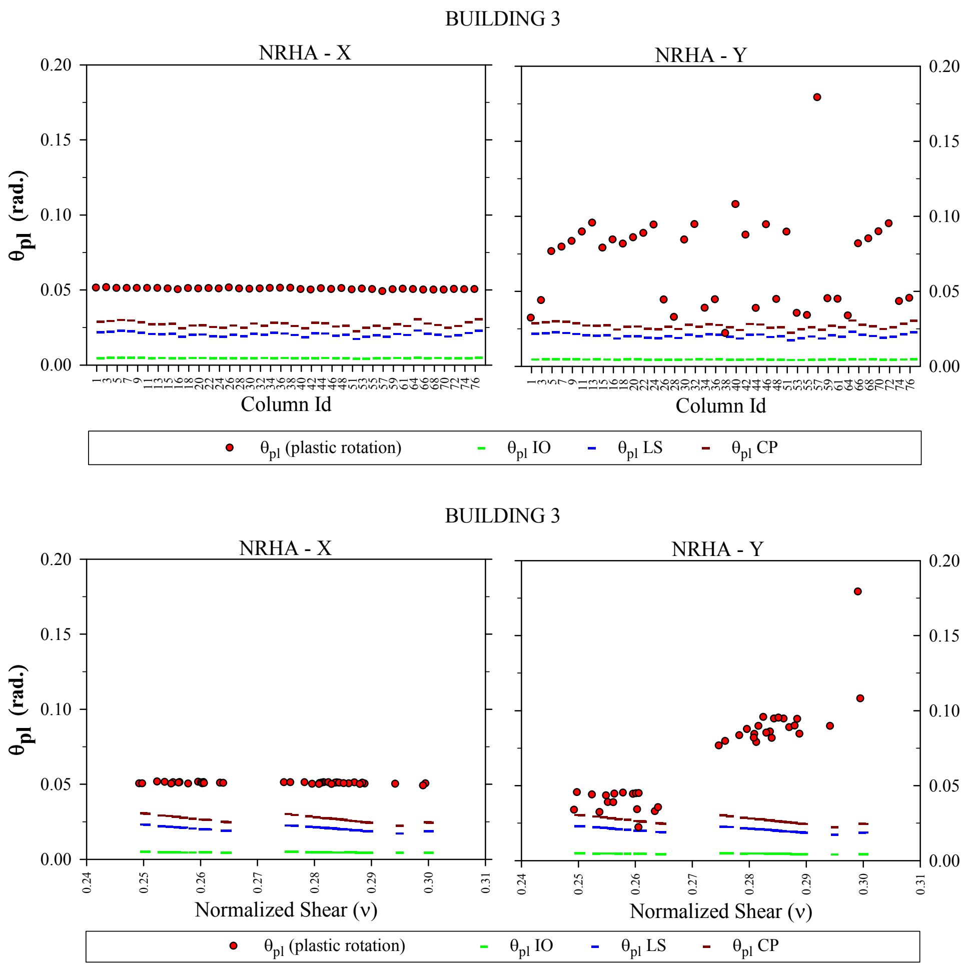

Figure 6.6 Plastic Hinge Rotation, θ_{pl}, results for Building 3 columns, computed by NRHA in X and Y directions

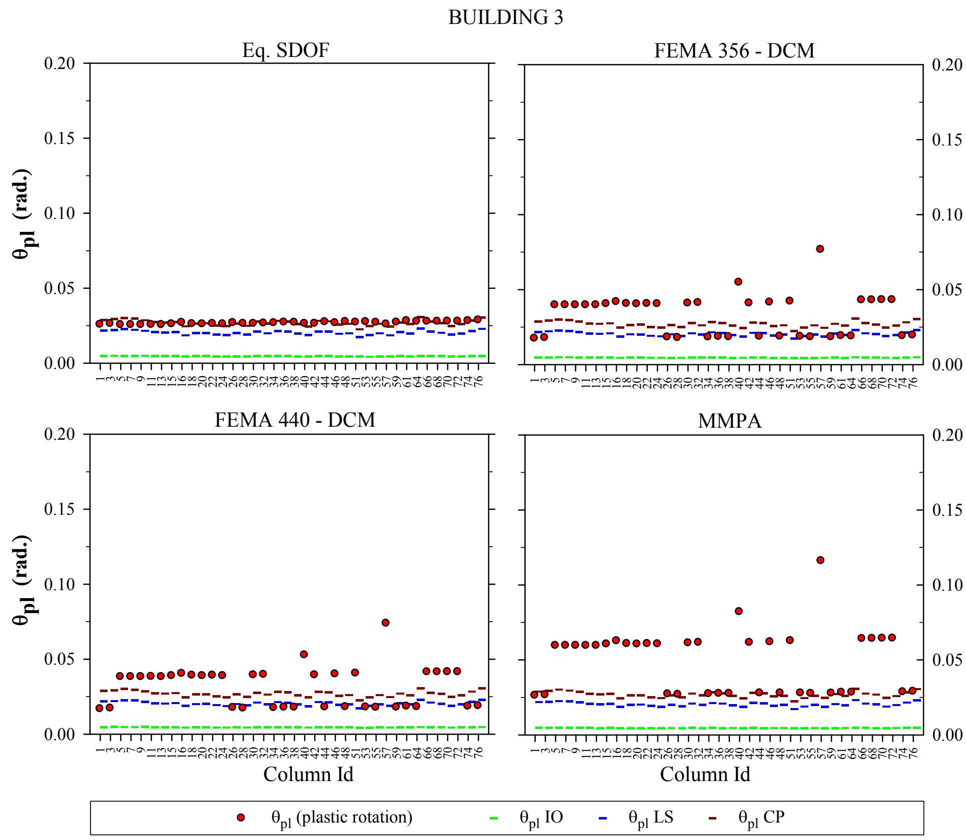

Figure 6.7 Plastic Hinge Rotation, θ_{pl}, results for Building 3 columns, computed by Eq.SDOF, FEMA356-DCM, FEMA440-DCM and MMPA in the X direction

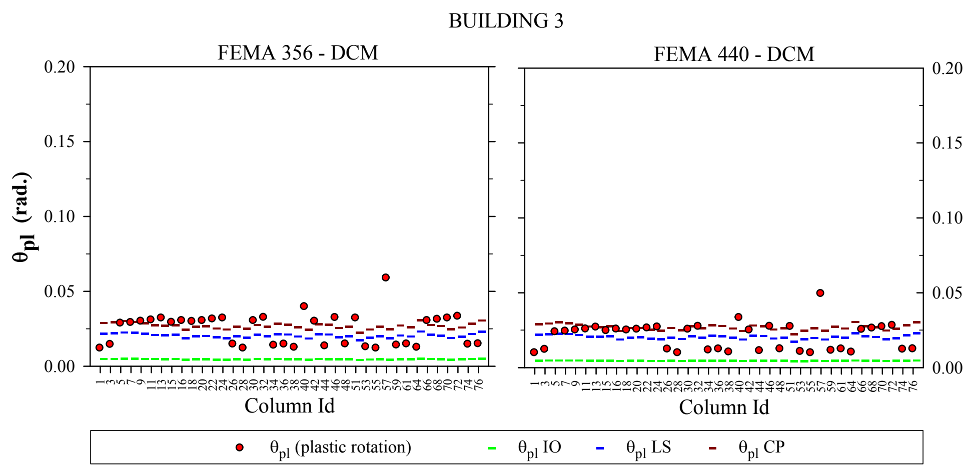

Figure 6.8 Plastic Hinge Rotation, θ_{pl}, results for Building 3 columns, computed by FEMA356-DCM, and FEMA440-DCM in the Y direction

6.3.4 Building #4

The critical story of the 4-story building was selected as the ground story. This story has 15 columns. The max plastic hinge rotation demands obtained by NRHA, in both X and Y directions of the building are shown in Figure 6.9.

Again, for Building 4, the damage state was overestimated by all nonlinear procedures of ASCE/SEI-41. All columns were expected to collapse, according to NDP, in both X and Y directions of the building. Unduly, the overall damage state of the building was determined as collapsed, despite the building experienced moderate damage during the earthquake.

In upper stories, no moderate or severe damage were expected according to the max plastic hinge rotation demands that were computed by NDP of ASCE/SEI-41.

When the plastic hinge rotation demands for the columns are plotted against the normalized shear (ν), it is observed that the plastic hinge rotation demands have been increased by the normalized shear. This trend, however, is observed only for Y direction analysis, not in the X direction. The only exception for this observation is the column having the max normalized shear value of 0.486, with the cross-sectional dimensions of 80 * 30 (cm * cm) (strong in X direction of the building), did not have a high θ_{pl} value, inconsistent with the increasing trend observed.

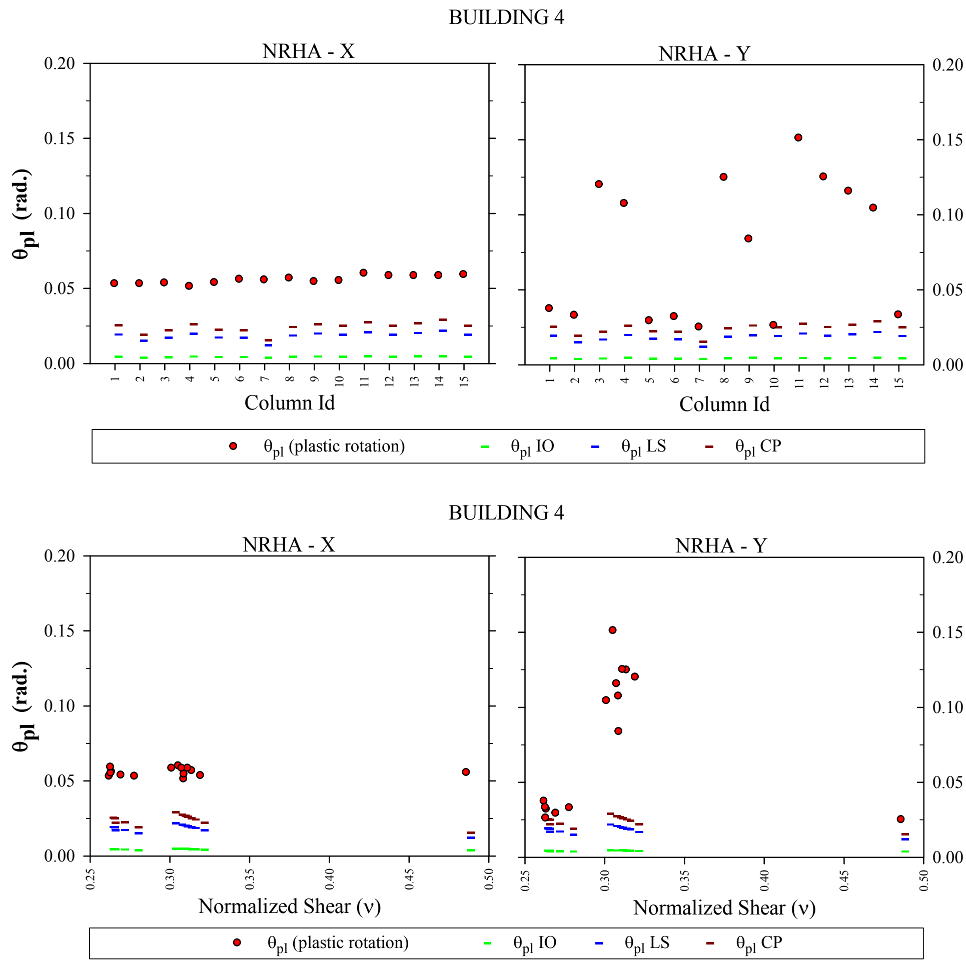

Figure 6.9 Plastic Hinge Rotation, θ_{pl}, results for Building 4 columns, computed by NRHA in X and Y directions

At the performance points estimated by approximate procedures (NSPs), the NSA of ASCE/SEI-41 applied. The assessment results for these performance points, in X and Y directions are shown in Figure 6.10 and Figure 6.11, respectively.

In X direction (Figure 6.10), at the performance point estimation of FEMA440, all columns of the critical story were expected to collapse. At the FEMA356 estimation, 9 columns were expected to collapse while the 6 columns would be severely damaged. In Y direction (Figure 6.11), at the performance point estimation of FEMA440, 7 columns were expected to be moderately damaged, and 1 column was expected to be severely damaged, while the remaining 7 columns would collapse. Again, in both directions of the building, the overall damage state of the building was overestimated by NSA of ASCE/SEI-41, at all performance points estimated by NSPs.

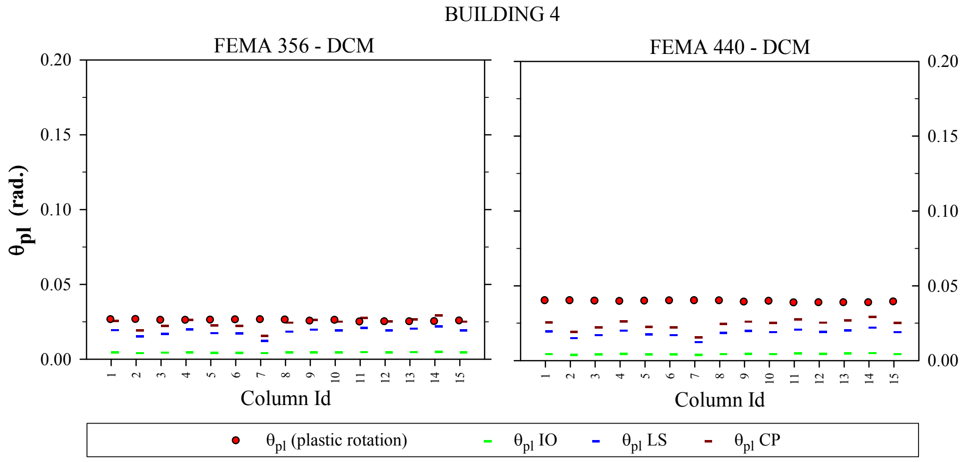

Figure 6.10 Plastic Hinge Rotation, θ_{pl}, results for Building 4 columns, computed by FEMA356-DCM, and FEMA440-DCM in the X direction

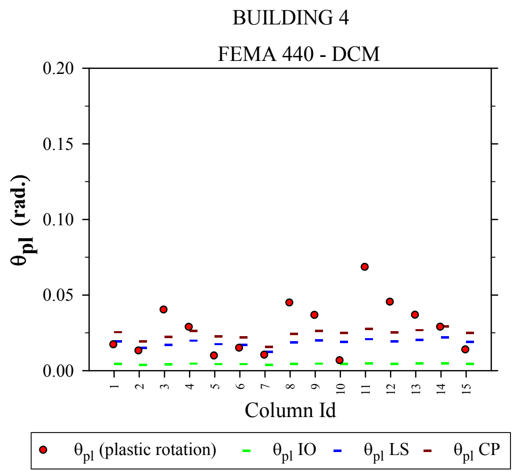

Figure 6.11 Plastic Hinge Rotation, θ_{pl}, results for Building 4 columns, computed by FEMA440-DCM in the Y direction

6.3.5 Building #5

The critical story of the 5-story building was selected as the ground story. This story has 21 columns. The max plastic hinge rotation demands obtained by NRHA, in both X and Y directions of the building are shown in Figure 6.12.

The overall damage state of Building 5 was determined as collapsed, despite the building experienced moderate damage during the earthquake, by the NDP of ASCE/SEI-41. All columns were expected to collapse in X direction of the building. In the Y direction, the max plastic hinge rotation value was obtained for the mid-column (column #14) with the cross-sectional dimensions of 20 * 280 (cm * cm) (strong in the Y direction), as 0.39. So, this structural member which is detailed as a structural wall was evaluated as collapsed. Consequently, totally 6 columns located in the same mid-frame and close to this collapsed column, experienced relatively less damage; i.e. 5 of them with moderate damage and 1 of them with negligible damage.

Similar to the critical ground story, in second story, significant damage was expected according to NDP of ASCE/SEI-41.

When the plastic hinge rotation demands for the columns are plotted against the normalized shear (ν), it is observed that the plastic hinge rotation demands have been increased by the normalized shear. This trend, however, is observed only for Y direction analysis, not in the X direction.

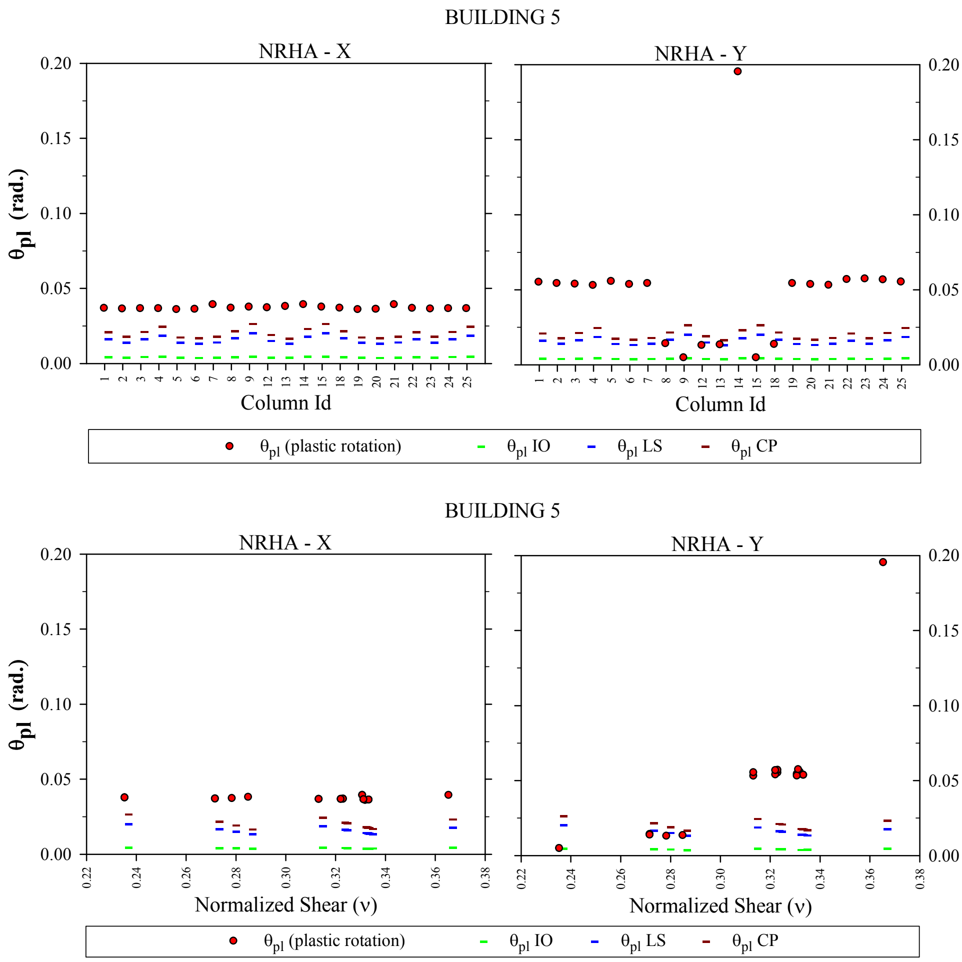

Figure 6.12 Plastic Hinge Rotation, θ_{pl}, results for Building 5 columns, computed by NRHA in X and Y directions

At the performance points estimated by approximate procedures (NSPs), the NSA of ASCE/SEI-41 applied. The assessment results for these performance points, in X and Y directions are shown in Figure 6.13 and Figure 6.14, respectively.

At the performance point estimations of both FEMA356 and FEMA440 in X direction (Figure 6.13), the columns of the critical story were evaluated as either collapsed or severely damaged by NSA of ASCE/SEI-41. 2 columns for the former and 4 columns for the latter would be severely damaged, while all other columns would collapse. In the Y direction (Figure 6.14), on the other hand, at the performance point estimation of both FEMA356 and FEMA440, only the column

#14, which is discussed in the paragraphs above, was expected to collapse. 14 of critical story columns would be moderately damaged, for each of the assessment, while the other 6 columns remained in IO damage state. Although, the damage state in X direction was overestimated again, according to these results, the evaluation results in the Y direction seem to be consistent with the actual damage observed during the earthquake (moderate damage).

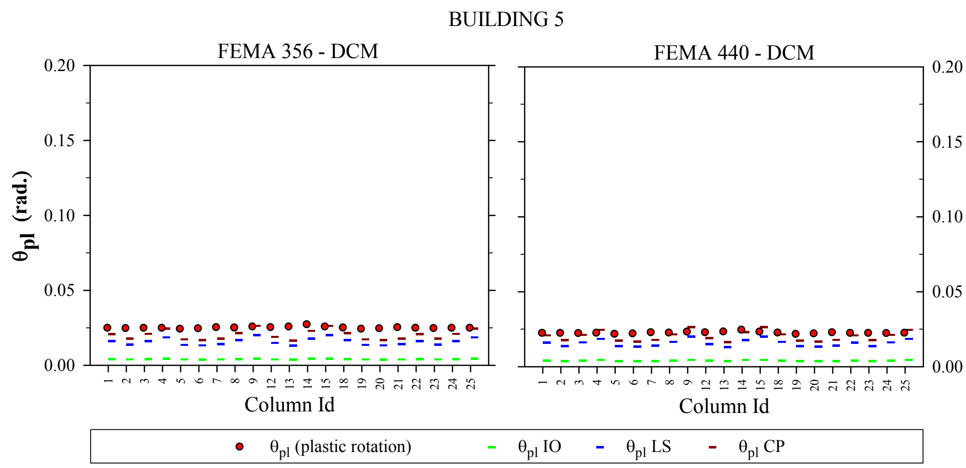

Figure 6.13 Plastic Hinge Rotation, θ_{pl}, results for Building 5 columns, computed by FEMA356-DCM, and FEMA440-DCM in the X direction

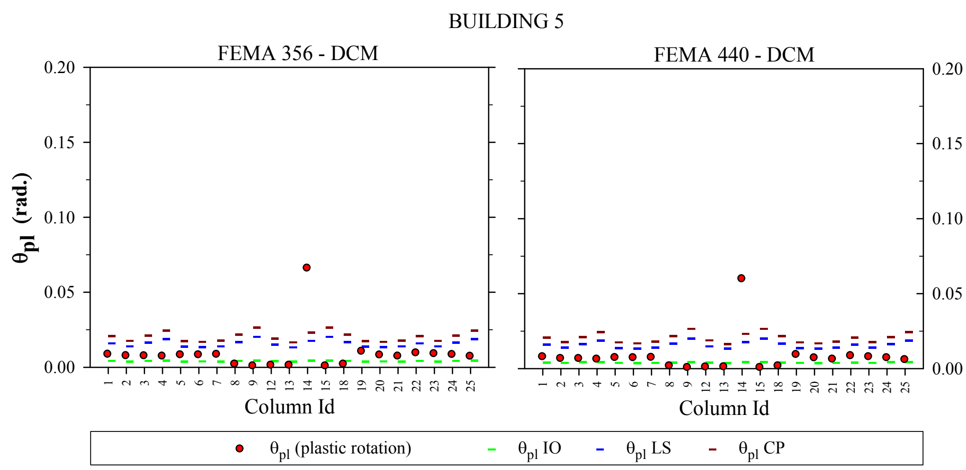

Figure 6.14 Plastic Hinge Rotation, θ_{pl}, results for Building 5 columns, computed by FEMA356-DCM, and FEMA440-DCM in the Y direction

6.3.6 Building #6

The critical story of the 5-story building was selected as the ground story. This story has 16 columns. The max plastic hinge rotation demands obtained by NRHA, in both X and Y directions of the building are shown in Figure 6.15.

Building 6 was marked as collapsed by all nonlinear procedures of ASCE/SEI-41. In the X direction, all columns of the critical story were expected to collapse, according to NDP. The max hinge rotation demands for all columns computed by NDP in the Y direction also imply that all of them would collapse.

In upper stories, no significant damage was expected according to the max plastic hinge rotation demands that were computed by NDP and NSA of ASCE/SEI-41. Thus, the soft story behavior of the building is very likely to be the reason of severe damage / collapse of the building during the earthquake.

When the plastic hinge rotation demands for the columns are plotted against the normalized shear (ν), it is observed that the plastic hinge rotation demands have been increased by the normalized shear. This trend, however, is observed only for Y direction analysis, not in the X direction.

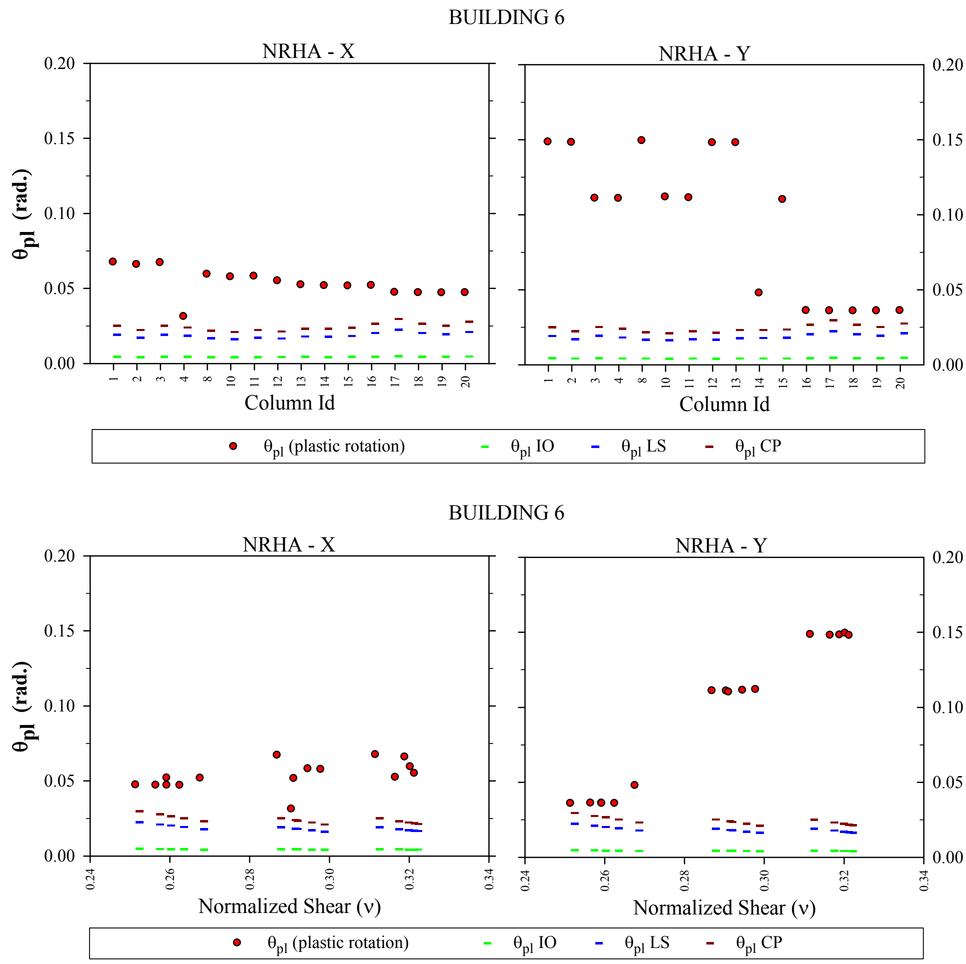

Figure 6.15 Plastic Hinge Rotation, θ_{pl}, results for Building 6 columns, computed by NRHA in X and Y directions

At the performance points estimated by approximate procedures (NSPs), the NSA of ASCE/SEI-41 was applied. The assessment results for these performance points, in X and Y directions are shown in Figure 6.16 and Figure 6.17, respectively.

As shown in Figure 6.16, at all performance points estimated by NSPs, all of the critical story columns were expected to collapse in X direction, according to NSA of ASCE/SEI-41. In the Y direction assessments, at performance point obtained by FEMA356, the columns were expected to experience damage of various degrees, as 5 moderately and 1 severely damaged columns, while the remaining 10 columns would fail. In case of FEMA440, there were 6 moderately damaged columns with 10 collapsed columns (Figure 6.17). Thus, the expected damage state of the building was determined as collapsed, using the procedures of ASCE/SEI-41.

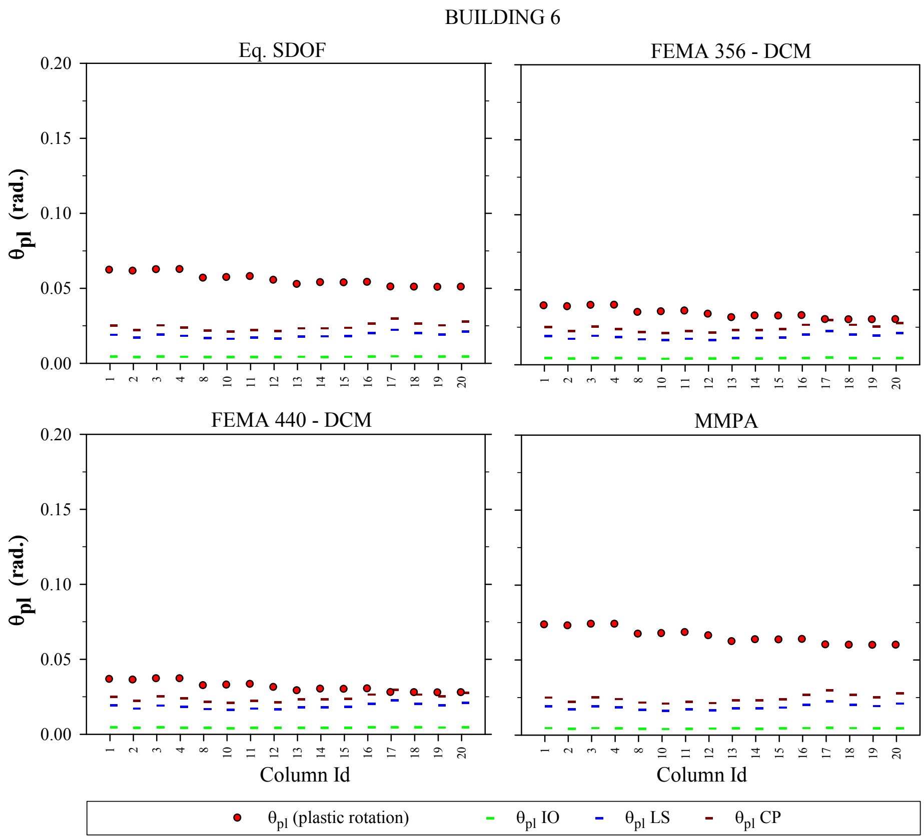

Figure 6.16 Plastic Hinge Rotation, θ_{pl}, results for Building 6 columns, computed by Eq. SDOF, FEMA356-DCM, FEMA440-DCM and MMPA in the X direction

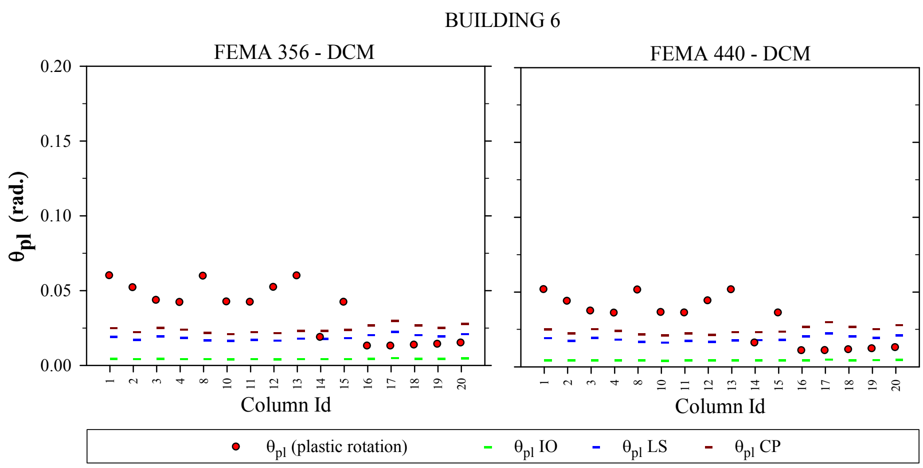

Figure 6.17 Plastic Hinge Rotation, θ_{pl}, results for Building 6 columns, computed by FEMA356-DCM and FEMA440-DCM in the Y direction

6.3.7 Building #7

The critical story of the 6-story building was selected as the ground story. This story has 13 columns. The max plastic hinge rotation demands obtained by NRHA, in both X and Y directions of the building are shown in Figure 6.18.

For Building 7, the final assessment decision was "collapsed" according to nonlinear dynamic procedure of ASCE/SEI-41. In the X direction, all columns of the critical story were expected to collapse. On the other hand, in the Y direction, 2 columns would be moderately damaged, while 11 of them would collapse. However, the overall damage state of the building was determined as collapsed.

In addition to the severe damage of critical story, upper stories were also expected to be severely damaged, according to the max plastic hinge rotation demands that were computed by NDP.

When the plastic hinge rotation demands for the columns are plotted against the normalized shear (ν), it is observed that the plastic hinge rotation demands have been increased by the normalized shear. This trend, however, is observed only for Y direction analysis, not in the X direction.

As seen in Section 5.6.7, all performance estimations of NSP's were beyond the capacity (pushover) curves for each direction of the building. Thus, the NSA procedure of ASCE/SEI-41 was applied only for the ultimate roof drift value of the capacity curve, and the results are shown in Figure 6.19.

According to these NSA results, all columns of the critical story would collapse in the X direction. In the Y direction, on the other hand, 6 columns were expected to be moderately damaged while the remaining 7 columns would be severely damaged / collapsed.

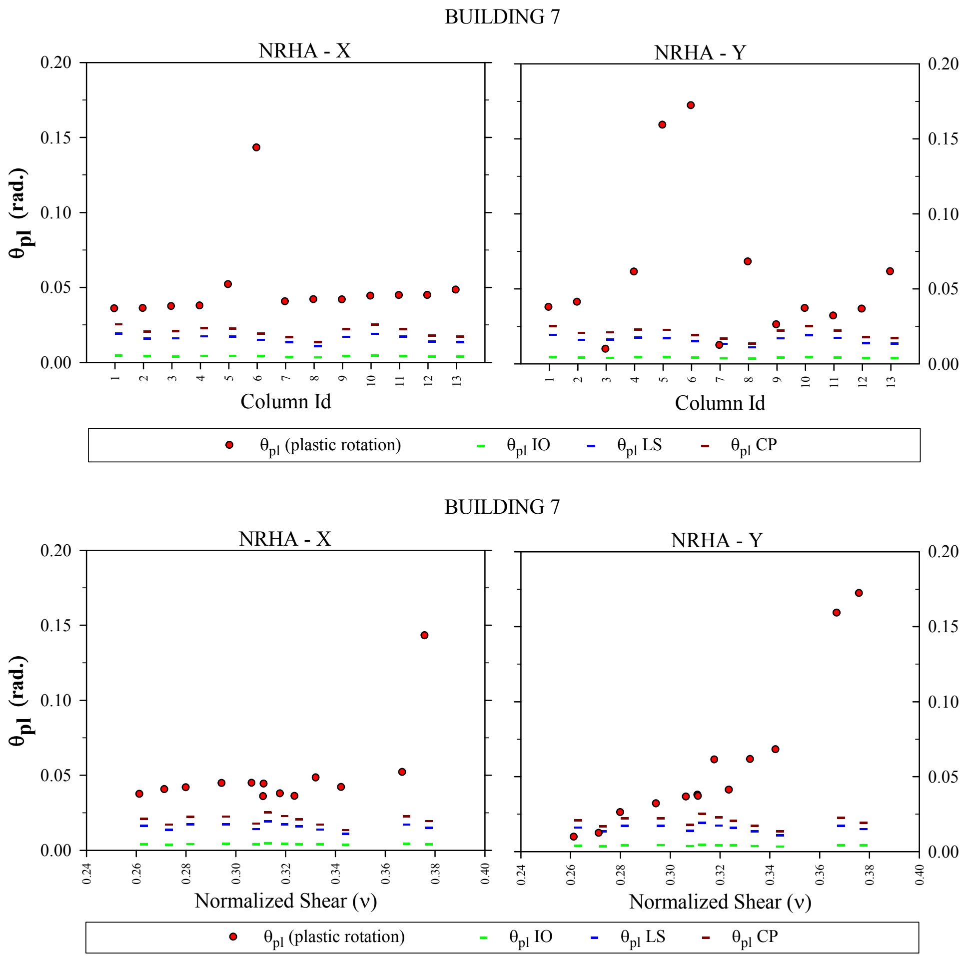

Figure 6.18 Plastic Hinge Rotation, θ_{pl}, results for Building 7 columns, computed by NRHA in X and Y directions

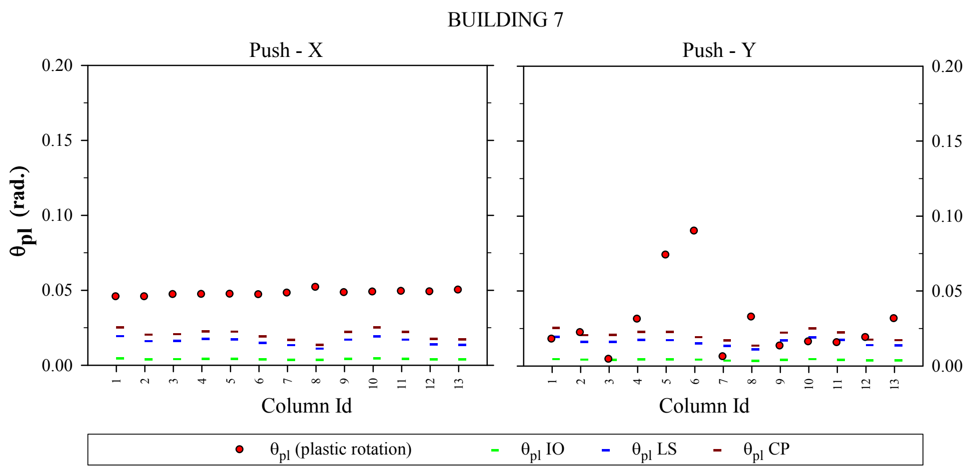

Figure 6.19 Plastic Hinge Rotation, θ_{pl}, results for Building 7 columns, computed at ultimate roof displacement of the pushover curve in X and Y directions

6.3.8 Building #8

The critical story of the 5-story building was selected as the ground story. This story has 14 columns. The max plastic hinge rotation demands obtained by NRHA, in both X and Y directions of the building are shown in Figure 6.20.

For Building 8, the final assessment decision was "collapsed" according to nonlinear dynamic procedure (NDP) of ASCE/SEI-41. In the X direction, all columns of the critical story were expected to collapse, and in the Y direction, 4 columns were expected to be moderately damaged and 1 column was expected to be severely damaged, while 9 of them would collapse. Nevertheless, the overall damage state of the building was determined as collapsed for both assessment procedures.

In addition to the severe damage of critical story, upper stories were also expected to be significantly damaged. According to the analyses computed in X direction, upper stories would be severely damaged where they would be moderately damaged in Y direction of the building.

When the plastic hinge rotation demands for the columns are plotted against the normalized shear (ν), it is observed that the plastic hinge rotation demands have been increased by the normalized shear. This trend, however, is observed only for Y direction analysis, not in the X direction.

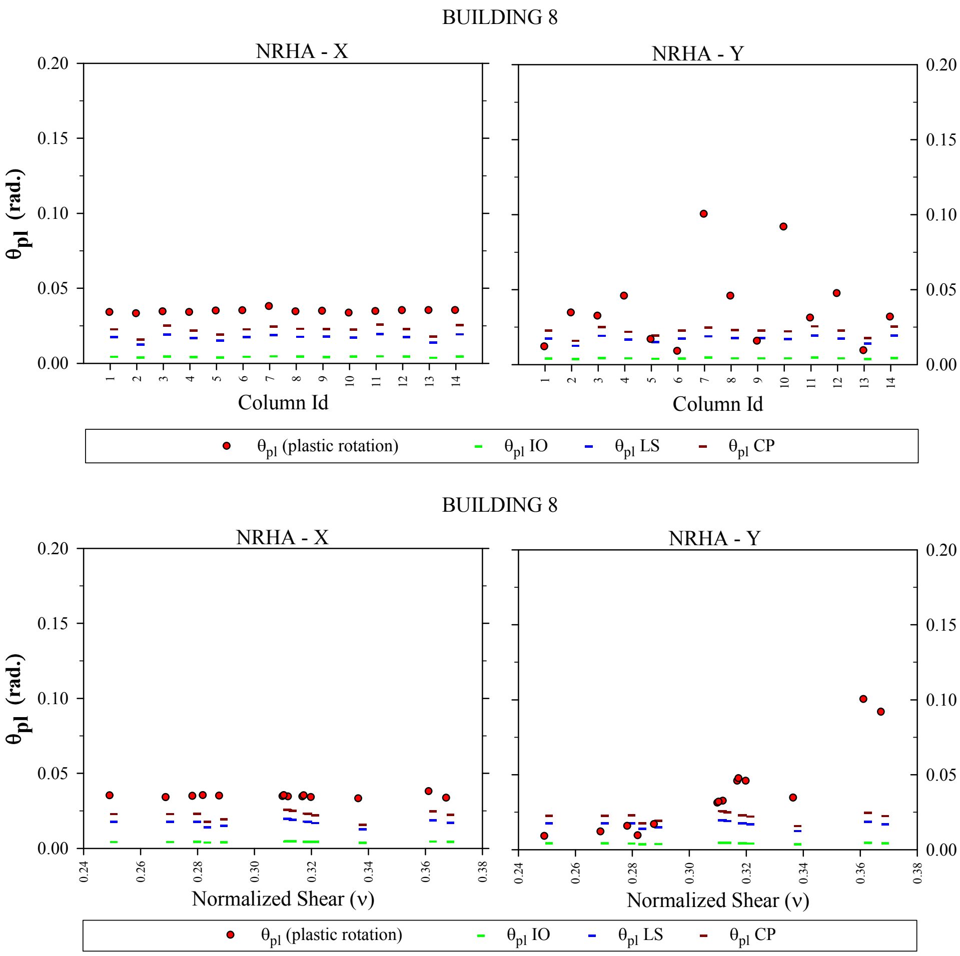

Figure 6.20 Plastic Hinge Rotation, θ_{pl}, results for Building 8 columns, computed by NRHA in X and Y directions

At the performance points estimated by approximate procedures (NSPs), the NSA of ASCE/SEI-41 applied. The assessment results for these performance points, in X and Y directions are shown in Figure 6.21 and Figure 6.22, respectively.

As shown in Figure 6.21, the assessment results in X direction, at the performance points obtained by NSPs imply various degrees of damage. According to the results at FEMA440 performance point, all columns of the critical story remained within the LS damage state. At FEMA356 performance point, only 3 of these columns were expected to be severely damaged, while the others would be moderately damaged. Since, the damage state observed was severe damage, these 2 assessment results were underestimated the damage state. In addition to these assessment results at relatively low performance points, all the critical story columns were expected to collapse at the performance points of MMPA and CSM, which are relatively high than the others. Lastly, 6 severely damaged and 8 collapsed columns were expected at Eq. SDOF performance point.

In Y direction (Figure 6.22), at Eq. SDOF performance point, 7 moderately damaged, 1 severely damaged and 5 collapsed columns were expected, while the remaining 1 column experienced negligible damage. In this direction, the columns having strong directions parallel to the direction of analysis were experienced more severe damage than the others. One important note should be reminded that these critical ground story columns with severe damage were the ones that brittle shear failure was expected (Section 6.2).

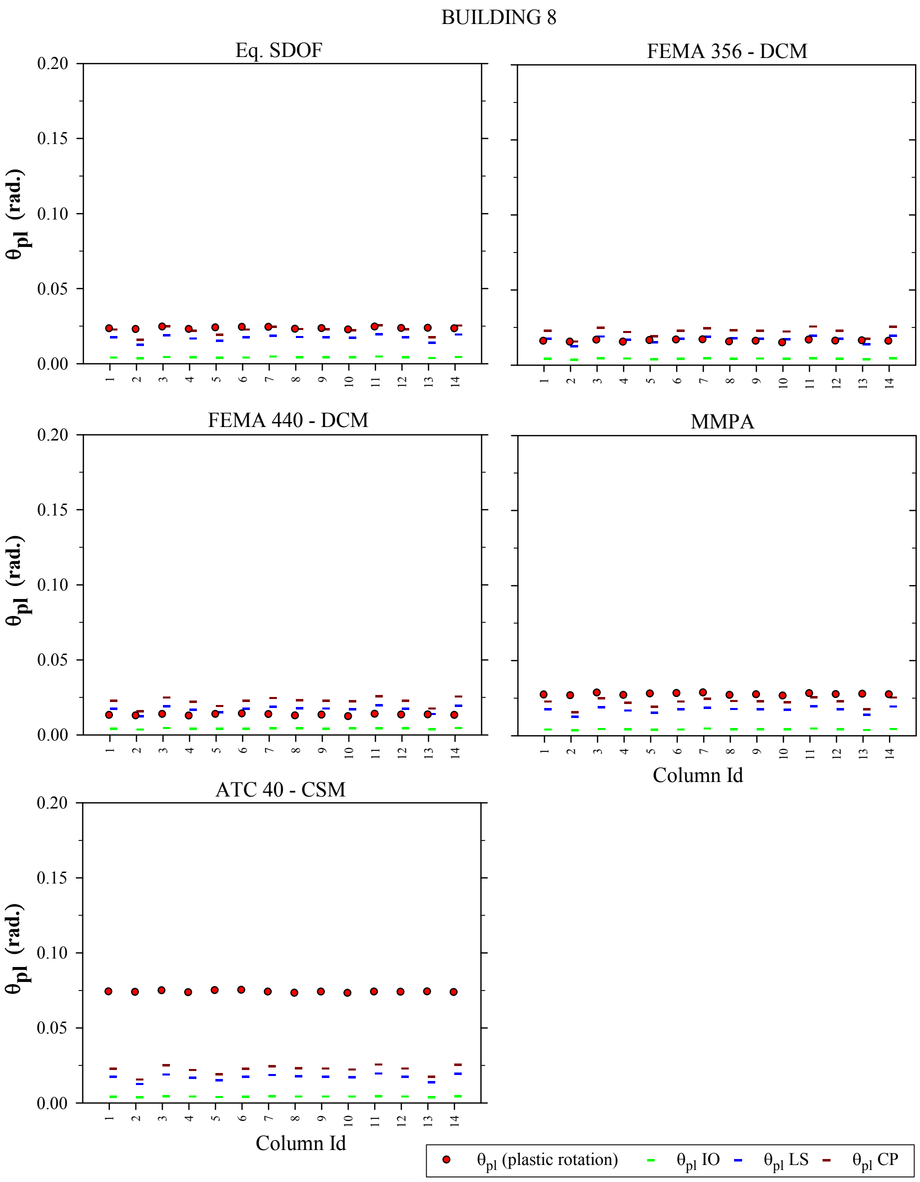

Figure 6.21 Plastic Hinge Rotation, θ_{pl}, results for Building 8 columns, computed by Eq. SDOF, FEMA356-DCM, FEMA440-DCM, MMPA and CSM of ATC-40 in the X direction

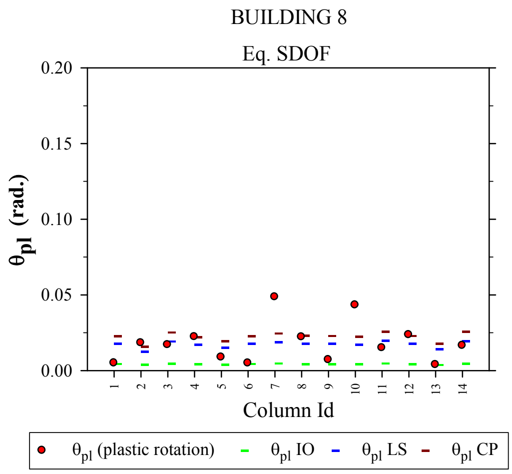

Figure 6.22 Plastic Hinge Rotation, θ_{pl}, results for Building 8 columns, computed by Eq. SDOF in the Y direction

6.3.9 Building #9

Although the failure mode of the building was expected to be "shear" as discussed in Section 6.2, detailed nonlinear assessment procedures of ASCE/SEI-41 were also applied to Building 9, and the results of the assessment were given in this section. The critical story of the 6-story building was selected as the ground story. This story has 25 columns. The max plastic hinge rotation demands obtained by NRHA, in both X and Y directions of the building are shown in Figure 6.23.

In X direction, since the building is strong enough in this direction with the structural walls, the building remained in immediate occupancy range according to NDP of ASCE/SEI-41. In the Y direction, 8 columns were expected to collapse while the other columns were expected to be moderately damaged. Thus, the overall damage state of the building was determined as collapsed in Y direction.

In addition to the severe damage of critical story, no significant damage was determined for upper stories, generally.

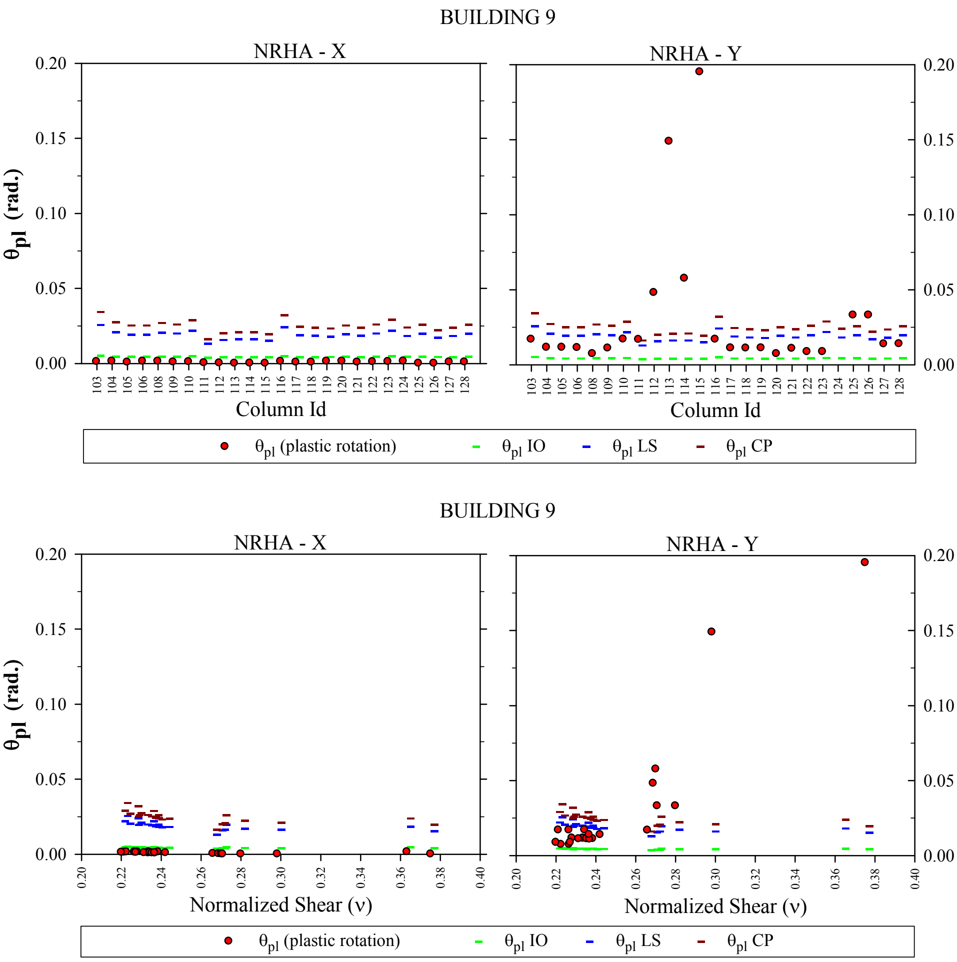

Figure 6.23 Plastic Hinge Rotation, θ_{pl}, results for Building 9 columns, computed by NRHA in X and Y directions

When the plastic hinge rotation demands for the columns are plotted against the normalized shear (ν), it is observed that the plastic hinge rotation demands have been increased by the normalized shear. This trend, however, is observed only for Y direction analysis, not in the X direction.

At the performance points estimated by approximate procedures (NSPs), the NSA of ASCE/SEI-41 applied. The assessment results for these performance points, in X and Y directions are shown in Figure 6.24 and Figure 6.25, respectively.

In X direction of the building (Figure 6.24), the assessment results at performance points obtained by NSPs imply that the overall damage state of the building was either IO or slightly over the IO. All critical story columns remained elastic at performance points of DCMs of both FEMA356 and FEMA440. 15 columns and 21 columns would be moderately damaged at performance points of Eq. SDOF, and MMPA, respectively, while the rest of columns remained elastic for each case. However, the failure mode of the building in this direction was brittle shear failure (Section 6.2).

In Y direction (Figure 6.25), according to the assessment results at performance points of both FEMA356 and FEMA 440, 2 strongest columns in Y direction were expected to collapse. Actually, these columns were the same of those were expected to fail because of shear. Few of the other columns were also experienced moderate damage for these cases.

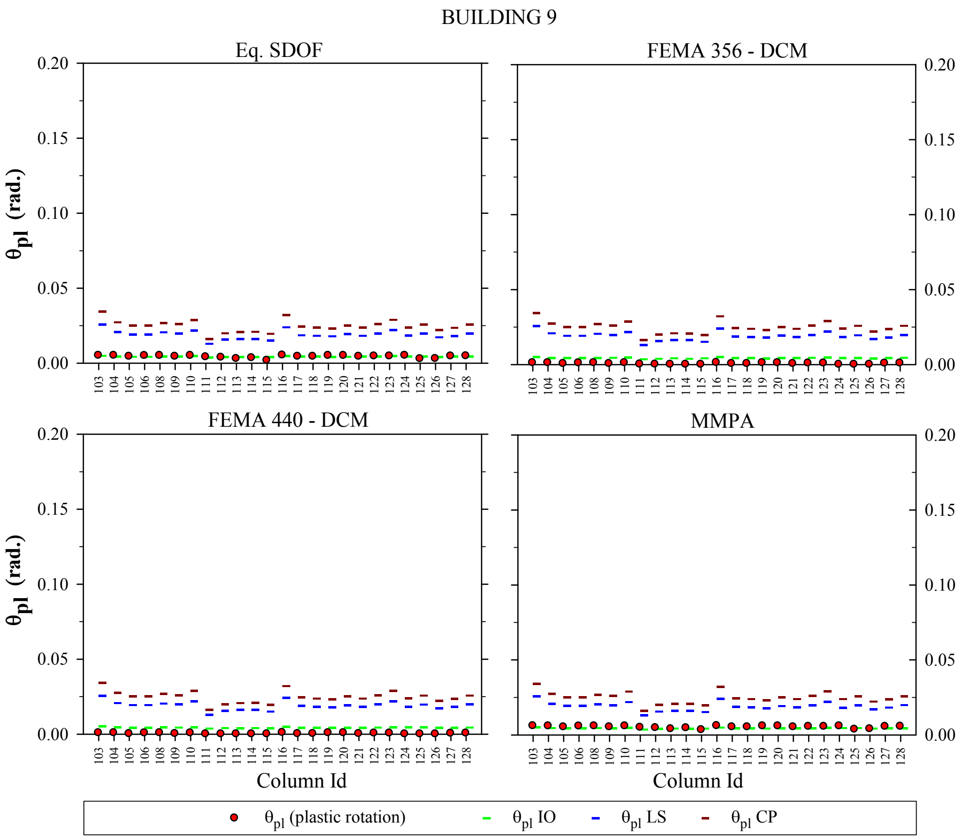

Figure 6.24 Plastic Hinge Rotation, θ_{pl}, results for Building 9 columns, computed by Eq. SDOF, FEMA356-DCM, FEMA440-DCM and MMPA in the X direction

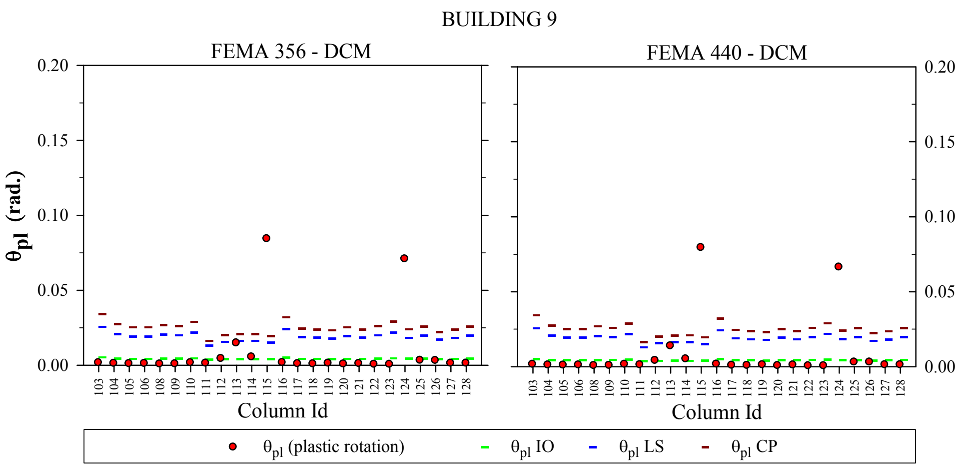

Figure 6.25 Plastic Hinge Rotation, θ_{pl}, results for Building 9 columns, computed by FEMA356-DCM and FEMA440-DCM in the Y direction

6.3.10 Building #10

The critical story of the 5-story building was selected as the ground story. This story has 26 columns. The max plastic hinge rotation demands obtained by NRHA, in both X and Y directions of the building are shown in Figure 6.26.

In X direction of the building, 5 columns of the critical story were expected to collapse and 4 columns would be severely damaged while the remaining 17 columns experienced moderate damage (damage control range) according to NDP assessment. In the Y direction, on the other hand, all columns of the critical story were expected to collapse. Therefore, the overall damage state of the building was determined as collapsed for both directions.

In addition to the severe damage of critical story, upper stories would be moderately damaged, according to the NDP in X direction. In the Y direction however, no significant damage was computed.

When the plastic hinge rotation demands for the columns are plotted against the normalized shear (v), no obvious trend line was observed within the range.

The NSA of ASCE/SEI-41 was applied at ultimate roof displacement of the pushover curve in X direction (since, there is no performance expectation of NSPs falling on the pushover curve) and at the performance points estimated by approximate procedures (NSPs) in Y direction. The results in X and Y directions are shown in Figure 6.27 and Figure 6.28, respectively.

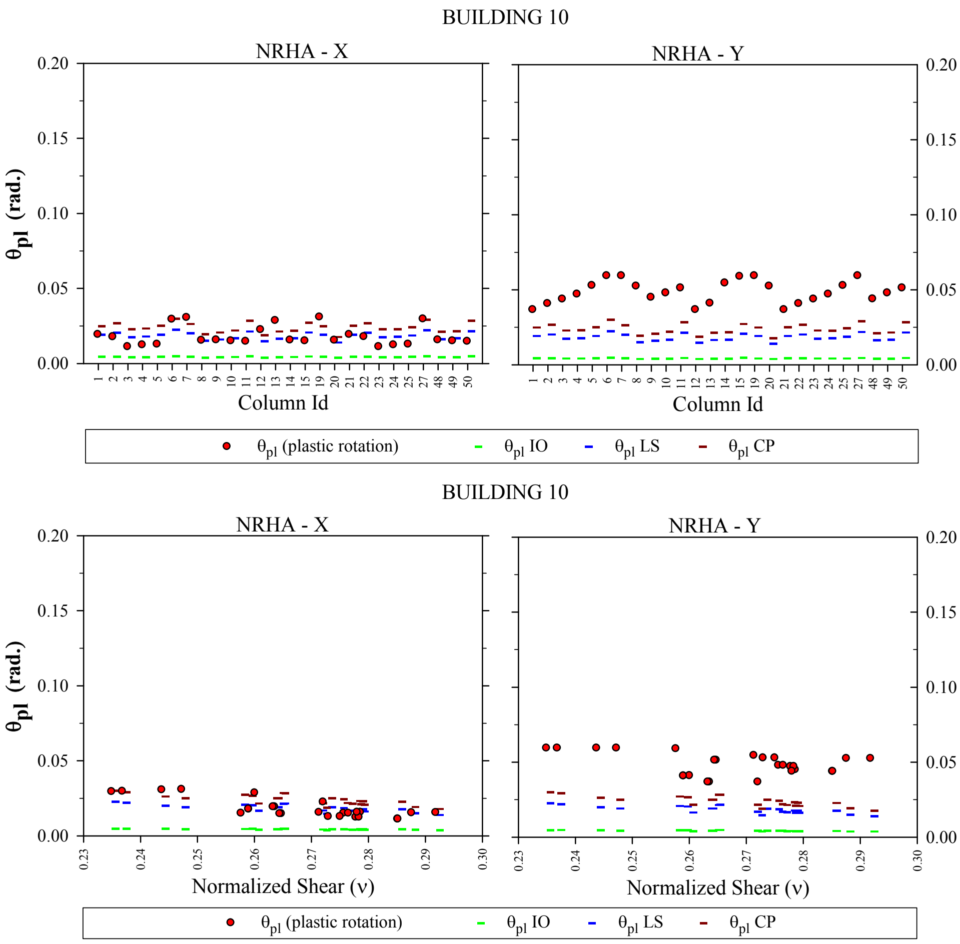

Figure 6.26 Plastic Hinge Rotation, θ_{pl}, results for Building 10 columns, computed by NRHA in X and Y directions

In X direction, there were 7 moderately damaged columns and 11 severely damaged columns where the remaining 8 columns were expected to collapse. Therefore, the overall damage state was evaluated as collapsed by NSA.

In Y direction, on the other hand, at both performance points, all the critical story columns were expected to collapse, according to NSA of ASCE/SEI-41.

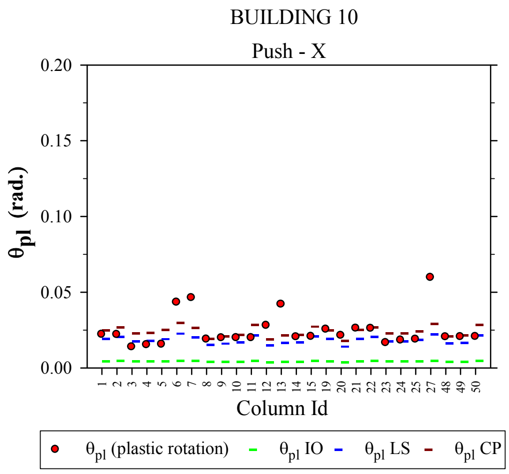

Figure 6.27 Plastic Hinge Rotation, θ_{pl}, results for Building 10 columns, computed at ultimate roof displacement of the pushover curve in the X direction

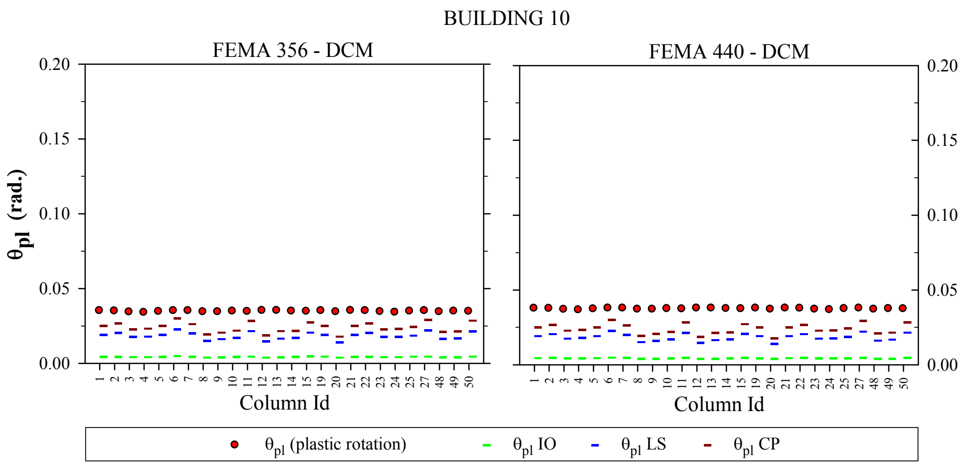

Figure 6.28 Plastic Hinge Rotation, θ_{pl}, results for Building 10 columns, computed by FEMA356-DCM and FEMA440-DCM in the Y direction

6.4 DETAILED ASSESSMENT ACCORDING TO TEC-2007

The buildings studied here are all residential buildings. Thus, the limit state for all these buildings would be Life Safety (LS), under an expected earthquake with a probability of exceedance of 10 percent in 50 years, according to Turkish Earthquake Code (TEC-2007). On the other hand, the damage states observed of the buildings studied here during the earthquake were tried to reach using the detailed nonlinear assessment procedure of current seismic code of Turkey.

In detailed assessment procedure of TEC-2007, the ultimate strain limits have been defined for concrete and reinforcing steel fibers of the sections of RC structural members, for each limit state, as explained in Section 2.4.3.

The transverse reinforcement of the structural members, however, should be designed and built according to the rules given by the Code, i.e. closed stirrups with an angle of 135° rather than 90°, adequate amount of stirrups within confinement zone of the member, etc. Nonconforming transverse reinforcement shall be neglected in assessment process (TEC-2007).

The RC members of the buildings investigated in this study assumed to be "nonconforming", considering the transverse reinforcement information derived from the built-in design projects of the buildings. According to the blue prints of these buildings, the stirrups of RC sections have a closing angle of 90° instead of 135° which is obliged by the Code. On the other hand, for significant majority of the elements the confinement zone design is not adequate, by means of total amount of transverse confinement. Moreover, the transverse reinforcement within the beam–column joints has never been applied.

The damage state of any structural member is determined by the most critical fiber section, having the most severe damage state, using the acceptance criteria. Concrete and steel strain limits at the fibers of a cross section for minimum damage limit (MN), safety limit (SF) and collapse limit (CL) were given in the Equations (2.26) to (2.28).

The overall structural performance is then obtained by accounting for the distribution of member damages over the building, using the rules for each of the performance level designated as follows;

Immediate Occupancy

Up to 10 percent of the beams in the direction of the earthquake loads at any story, are in the significant damage state, beyond the MN limit. All other structural members shall be in the minimum damage state.

Life Safety

Up to 20 percent of the beams and some of the columns are in the extreme damage state, beyond the SF limit. All other structural members should be in the minimum or significant damage states. Total shear, however, carried by the columns that are in the extreme damage state shall not exceed 20 percent of the story shear at each story.

Collapse Prevention

At any story, in the direction of the applied earthquake loads, up to 20 percent of beams are in the collapse state, beyond the CL limit. All other structural members are in the minimum, significant or extreme damage states. However, total shear carried by the columns, whose both the top and bottom sections are beyond the MN limit, shall not exceed 30 percent of the story shear at each story. In other words, such columns should not lead to a stability loss.

Collapse

If the building fails to satisfy the CP performance level above, it is decided to be in the collapse state.

In the following sections, for each of the buildings studied, the detailed assessment results were given according to TEC-2007. The results were given for the same critical story, used for ASCE/SEI-41 in Section 6.3, which was decided by the examination of detailed assessment results. The concrete and steel strain (ε_c , ε_s) demands of the columns of critical story were shown in figures in comparison with the damage state limits. The concrete strain limits, ε_c *MN*, ε_c *SF* and ε_c *CL*, were calculated as 0.0035, 0.0035 and 0.004, respectively, for the buildings studied. The steel strain limits ε_s *MN*, ε_s *SF* and ε_s *CL*, were used as 0.01, 0.04 and 0.06, respectively.

These demand values are also plotted against the normalized shear ($\nu = V / b_w d \sqrt{f_c}$) values in the figures for each building.

6.4.1 Building #1

The critical story of the building was selected as the ground story, having 32 columns. The maximum strain demands obtained by NRHA, in both X and Y directions of the building are shown in Figure 6.29.

Although the building experienced moderate damage during the earthquake, the damage state of Building 1 was overestimated by the NDP of TEC-2007, similar to the assessment results of ASCE/SEI-41. The results presented in the Figure 6.29, indicate that all columns would collapse, in both directions of the building. It can be seen that the state of the steel material differs, while the concrete reaches its ultimate strain. Thus, in general, the overall damage states of the columns were defined by concrete. Actually, this situation was expected, due to the low material strength of the concrete.

In addition to the severe damage at critical story of the building, the damage state of all upper story columns were estimated as "collapsed" by NDP, but more significant in X direction rather than in Y direction of the building.

When the strain demands for the columns are plotted against the normalized shear (ν), no obvious trend line was observed within the range.

The NSA of TEC-2007 was applied at ultimate roof displacement of the pushover curve in X direction and at the performance points estimated by approximate procedures (NSPs) in Y direction. The assessment results for these performance points, in X and Y directions are shown in Figure 6.30 and Figure 6.31, respectively.

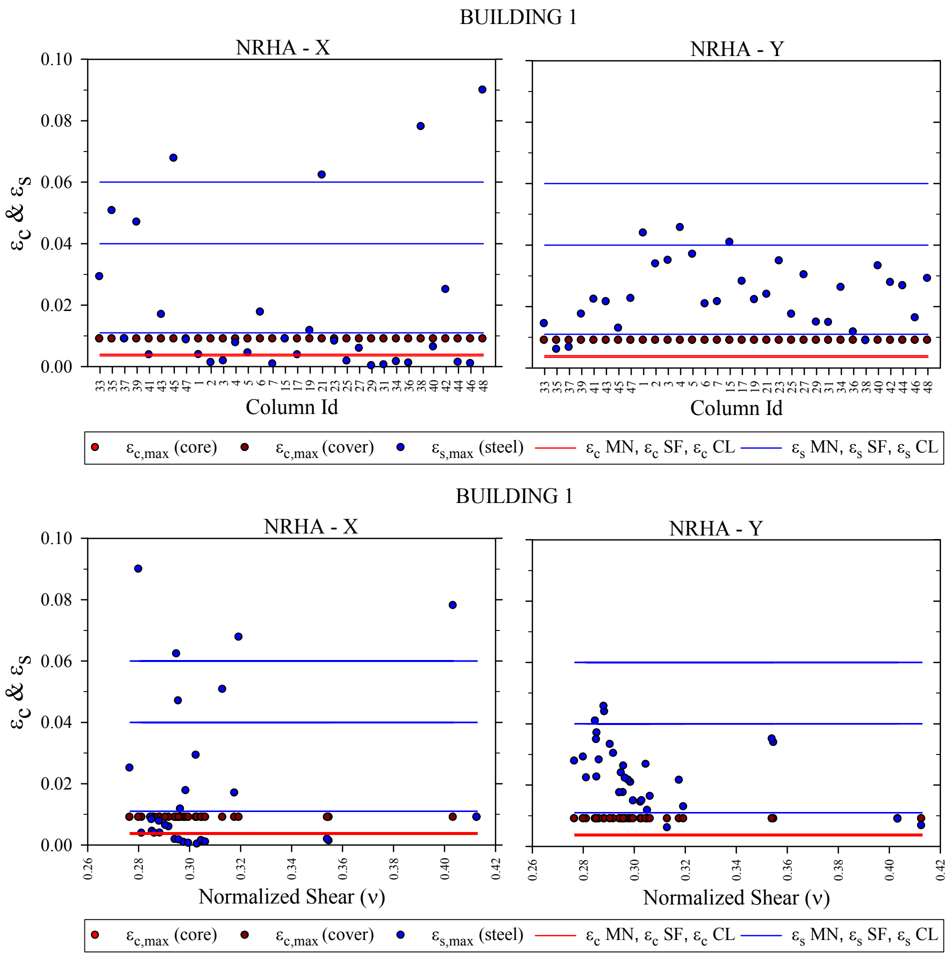

Figure 6.29 Max Strain, $\varepsilon_{c,max}$ and $\varepsilon_{s,max}$ results for Building 1 columns, computed by NRHA in X and Y directions

In the X direction, 8 of the columns (which are the lower mezzanine columns) did not reach the MN limit, while the remaining columns would collapse due to the concrete strain demands, according to the NSA of TEC-2007.

Similar to the results of the ASCE/SEI-41, all columns would collapse according to NSA of TEC-2007 at the performance points obtained by the NSPs in Y direction, especially because of the concrete material reaches its ultimate strain capacity. Thus, the overall damage state of the building was overestimated.

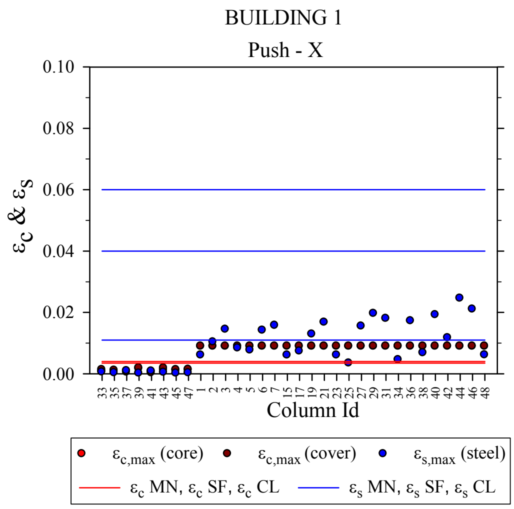

Figure 6.30 Max Strain, $\varepsilon_{c,max}$ and $\varepsilon_{s,max}$ results for Building 1 columns, computed at ultimate roof displacement of the pushover curve in the X direction

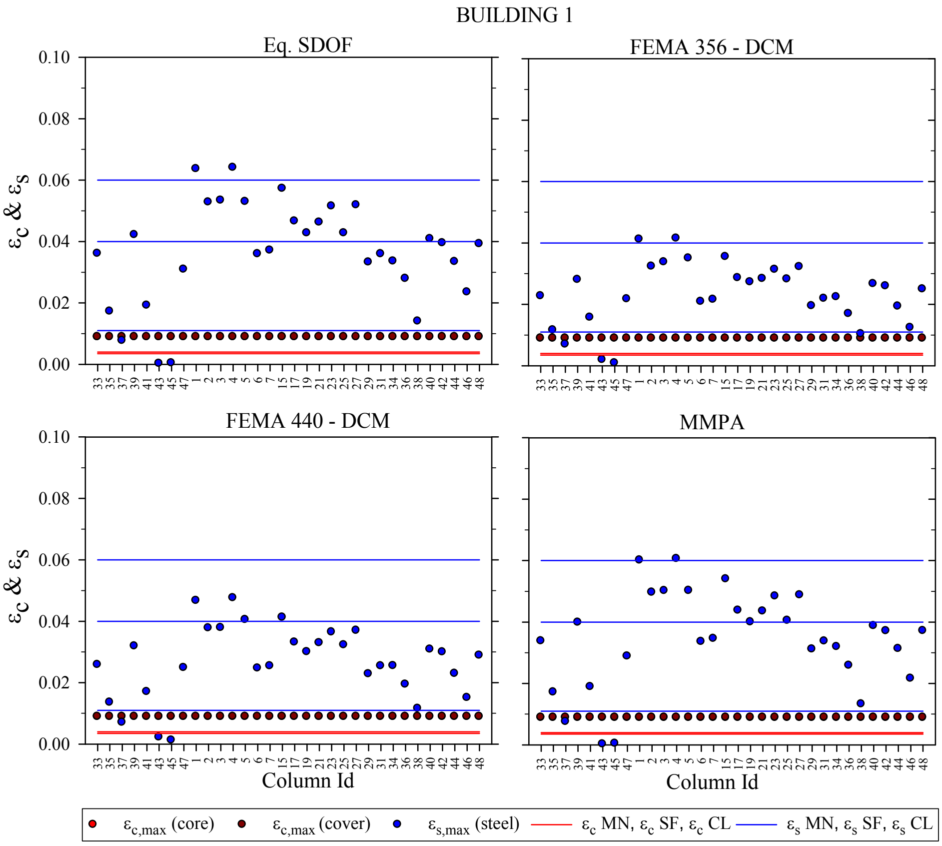

Figure 6.31 Max Strain, $\varepsilon_{c,max}$ and $\varepsilon_{s,max}$, results for Building 1 columns, computed by Eq. SDOF, FEMA356-DCM, FEMA440-DCM and MMPA in the Y direction

6.4.2 Building #2

The critical story was selected as third story where the max ISDR demands computed, having 40 columns. The maximum strain demands obtained by NRHA, in both X and Y directions of the building are shown in Figure 6.32.

The assessment results of the critical story columns, using NDP and TEC-2007 in both X and Y directions indicate that all columns would collapse; despite the real damage state was moderate. The columns would collapse according to the concrete strain demands, however, the steel strain demands were scattered in different damage states.

When the strain demands for the columns are plotted against the normalized shear (ν), no obvious trend line was observed within the range.

As seen in Section 5.6.2, all performance estimations of NSP's are far beyond the capacity (pushover) curves for each direction of the building. Thus, the NSA procedure of TEC-2007 was applied only for the ultimate roof drift value of the capacity curve, and the results are shown in Figure 6.33. In both directions, all columns were expected to collapse.

In general, it can be concluded that the assessment results of both NDP and NSA of TEC-2007, similar to the results of ASCE/SEI-41, overestimated the damage state of the building as collapsed.

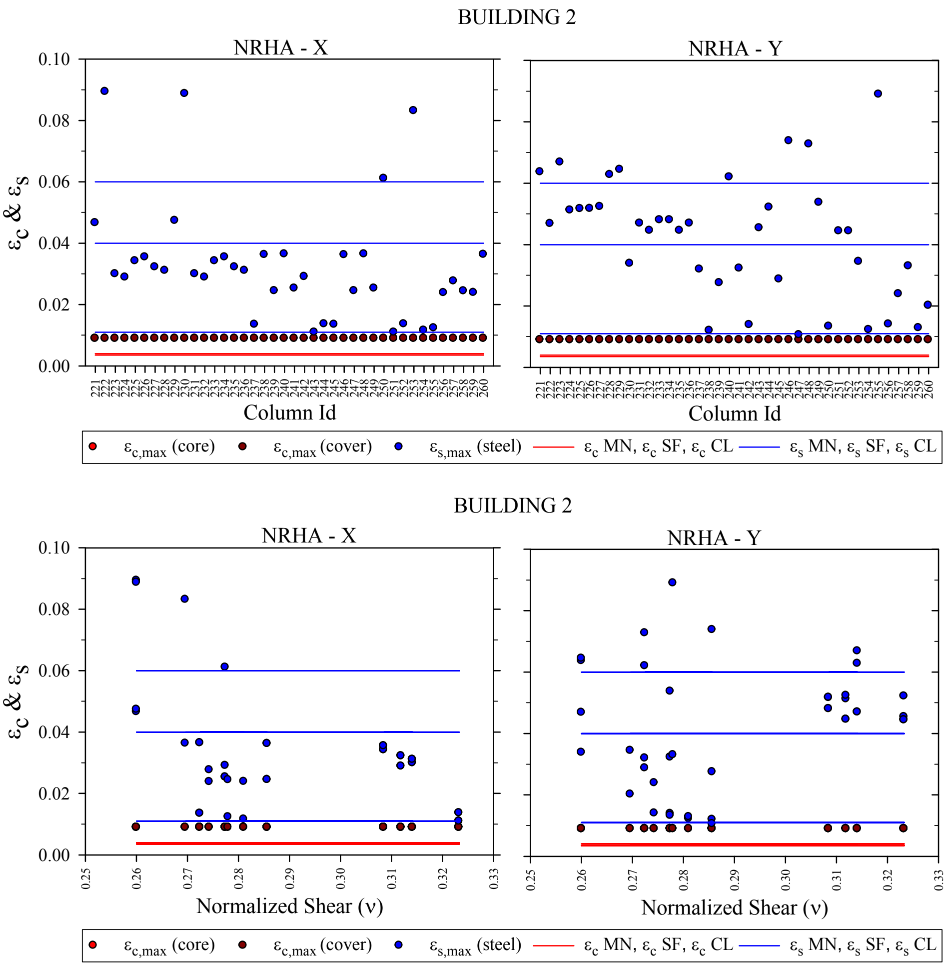

Figure 6.32 Max Strain, $\varepsilon_{c,max}$ and $\varepsilon_{s,max}$ results for Building 2 columns, computed by NRHA in X and Y directions

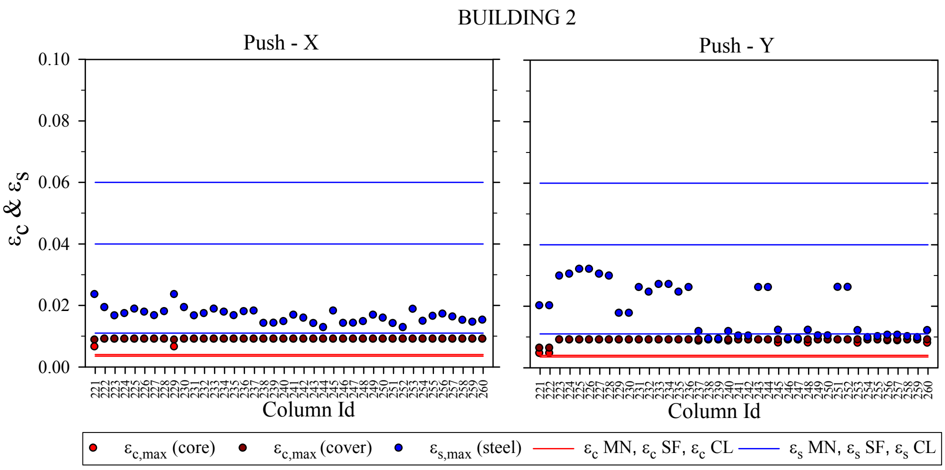

Figure 6.33 Max Strain, $\varepsilon_{c,max}$ and $\varepsilon_{s,max}$ results for Building 2 columns, computed at ultimate roof displacement of the pushover curve in X and Y directions

6.4.3 Building #3

The critical story of the building was selected as the ground story, with 38 columns. The maximum strain demands obtained by NRHA, in both X and Y directions of the building are shown in Figure 6.34.

The damage state of Building 3 was obviously overestimated by both the NDP of TEC-2007, similar to the assessment using ASCE/SEI-41. Despite the building experienced moderate damage during the earthquake, all the columns were evaluated as failed indicating that the overall damage state of the building was determined as collapsed.

In addition to the severe damage at critical story of the building, significant damage was expected in upper stories. Especially, the damage states of most of the second story columns were estimated as collapsed by NDP.

When the strain demands for the columns are plotted against the normalized shear (ν), no obvious trend line was observed within the range.

At the performance points estimated by approximate procedures (NSPs), the NSA of TEC-2007 applied. The assessment results for these performance points, in X and Y directions are shown in Figure 6.35 and Figure 6.36, respectively.

The assessment results of TEC-2007 were similar to the decision derived from ASCE/SEI-41. Although, the steel strain demands scattered within different damage states, all critical story columns were expected to collapse according to the concrete strain demands, at all 4 performance points obtained by NSPs, in X direction (Figure 6.35). In the Y direction, on the other hand, the overall damage state of the building also was expected as collapsed, at both performance points obtained by NSPs (Figure 6.36). In this case, however, 5 columns located in same axis that is perpendicular to the direction of loading, experienced less damage (MN) according to the core concrete strain demands. However, these columns were tagged as "severely damaged", due to corresponding steel strain demands.

Thus, similar to the ASCE/SEI-41 assessments, either in X or Y direction, the damage state of the building was overestimated by detailed assessment procedure of TEC-2007, at all performance points obtained by the NSPs.

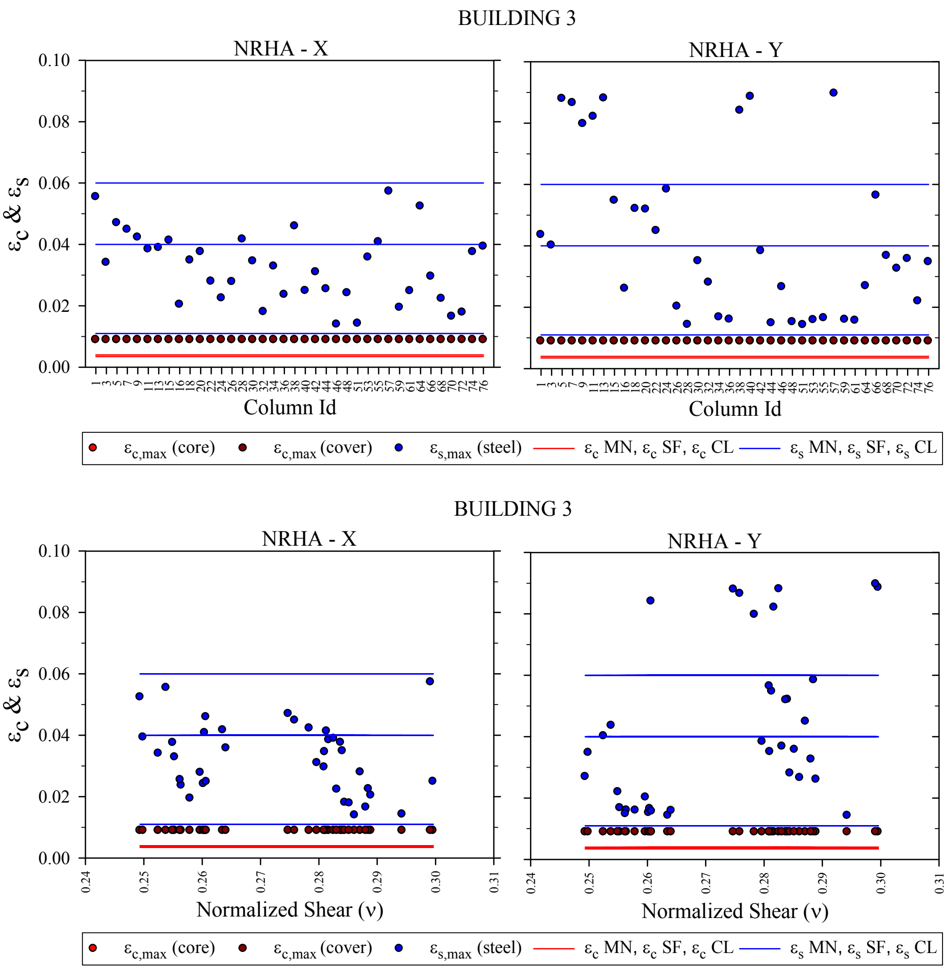

Figure 6.34 Max Strain, $\varepsilon_{c,max}$ and $\varepsilon_{s,max}$ results for Building 3 columns, computed by NRHA in X and Y directions

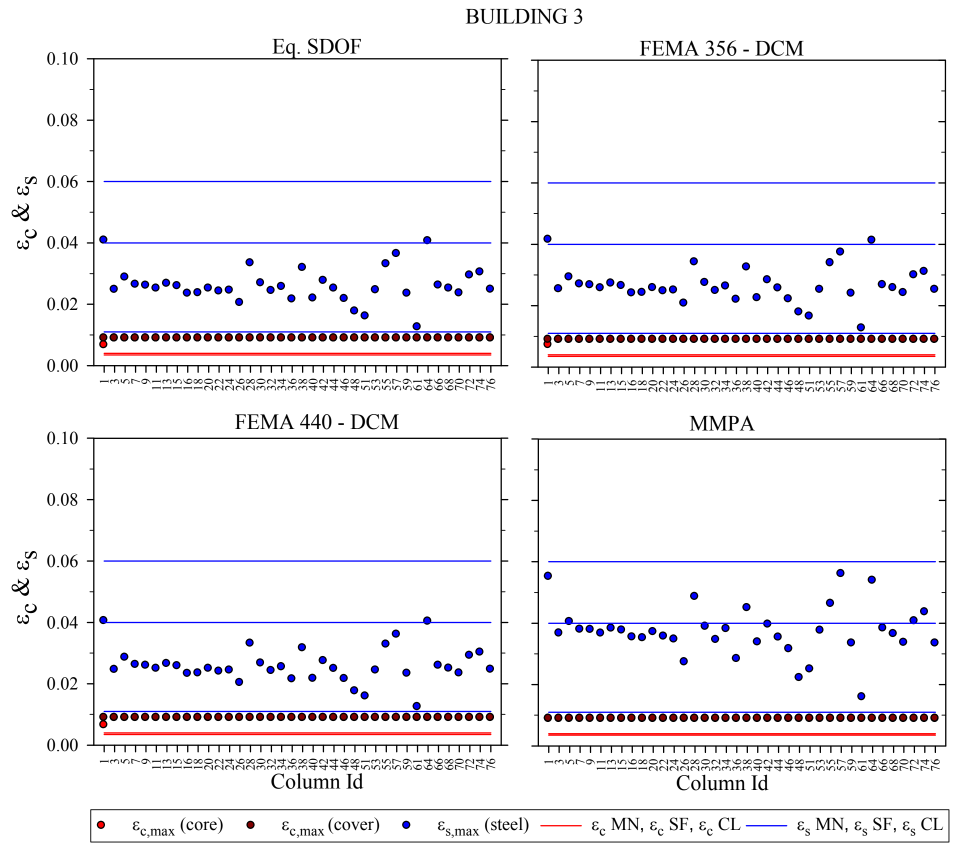

Figure 6.35 Max Strain, $\varepsilon_{c,max}$ and $\varepsilon_{s,max}$, results for Building 3 columns, computed by Eq. SDOF, FEMA356-DCM, FEMA440-DCM and MMPA in the X direction

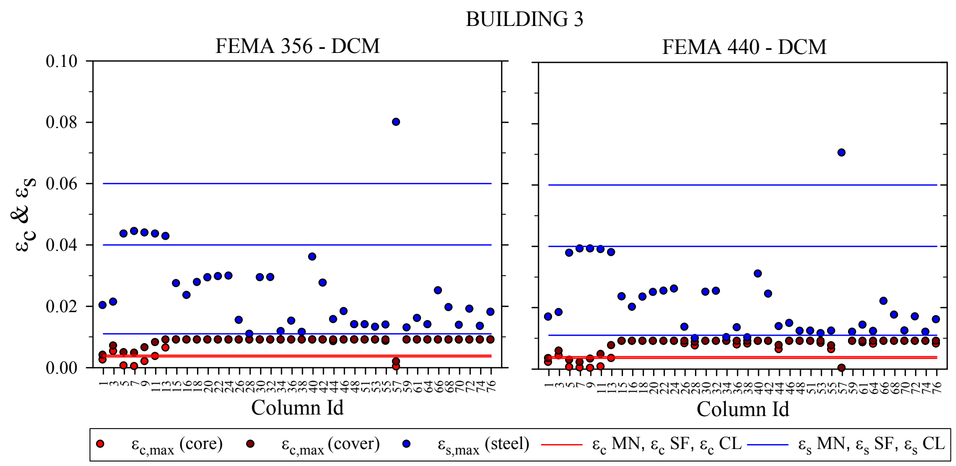

Figure 6.36 Max Strain, $\varepsilon_{c,max}$ and $\varepsilon_{s,max}$, results for Building 3 columns, computed by FEMA356-DCM and FEMA440-DCM in the Y direction

6.4.4 Building #4

The critical story of the building was selected as the ground story, with 15 columns. The maximum strain demands obtained by NRHA, in both X and Y directions of the building are shown in Figure 6.37.

Similar to the assessment results of ASCE/SEI-41, the damage state of Building 4 was overestimated by nonlinear dynamic procedure of TEC-2007. All columns were expected to collapse, according to NDP, in both X and Y directions of the building. Therefore, the overall damage state of the building was determined as collapsed, despite the building experienced moderate damage during the earthquake. Again, the damage states of the columns were graded by the characteristic deformation of concrete material.

In upper stories, no moderate or severe damage were expected according to the max strain demands, with a few number of column exceptions in the Y direction.

When the strain demands for the columns are plotted against the normalized shear (ν), no obvious trend line was observed within the range.

At the performance points estimated by approximate procedures (NSPs), the NSA of TEC-2007 applied. The assessment results for these performance points, in X and Y directions are shown in Figure 6.38 and Figure 6.39, respectively.

In both X and Y directions, at all performance points estimated by NSPs, all columns of the critical story were expected to collapse, according to the NSA of TEC-2007. Although, the steel strain demands scattered within different damage states, this evaluation was governed by the concrete strain demands. Similar to ASCE/SEI-41, the overall damage state of the building was overestimated by NSA of TEC-2007 at all performance points estimated by NSPs, in both directions of the building.

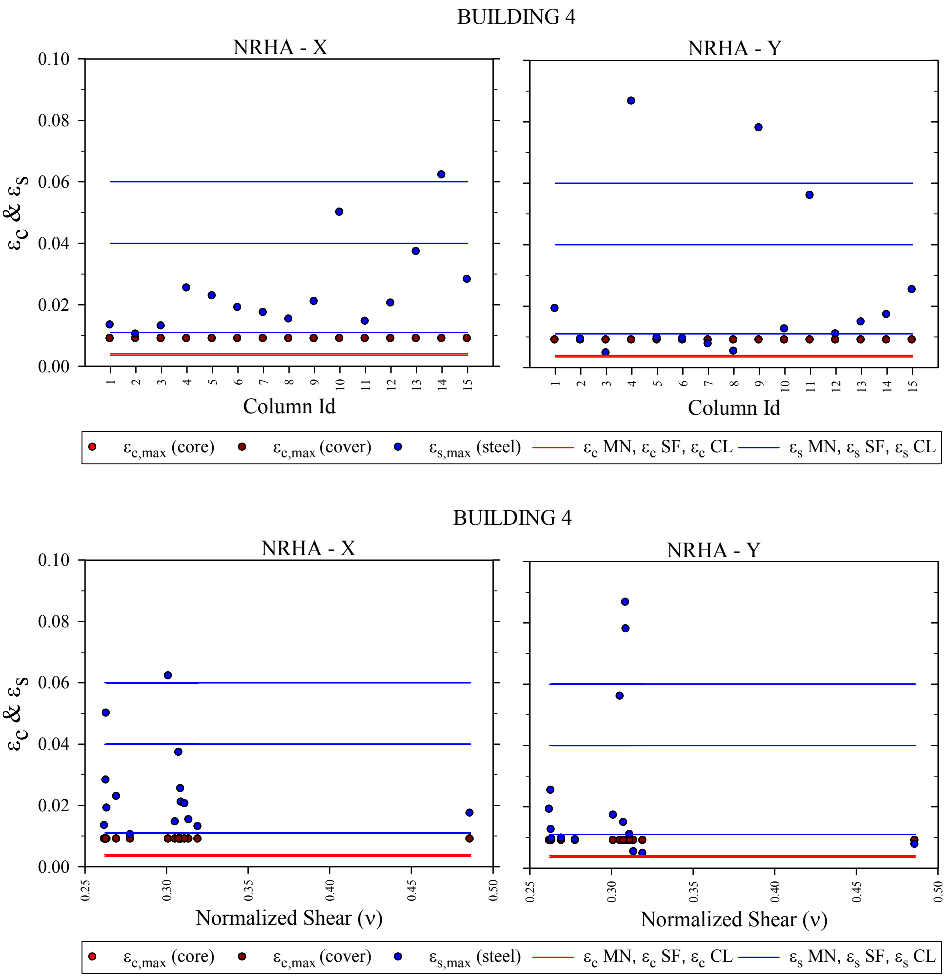

Figure 6.37 Max Strain, $\varepsilon_{c,max}$ and $\varepsilon_{s,max}$ results for Building 4 columns, computed by NRHA in X and Y directions

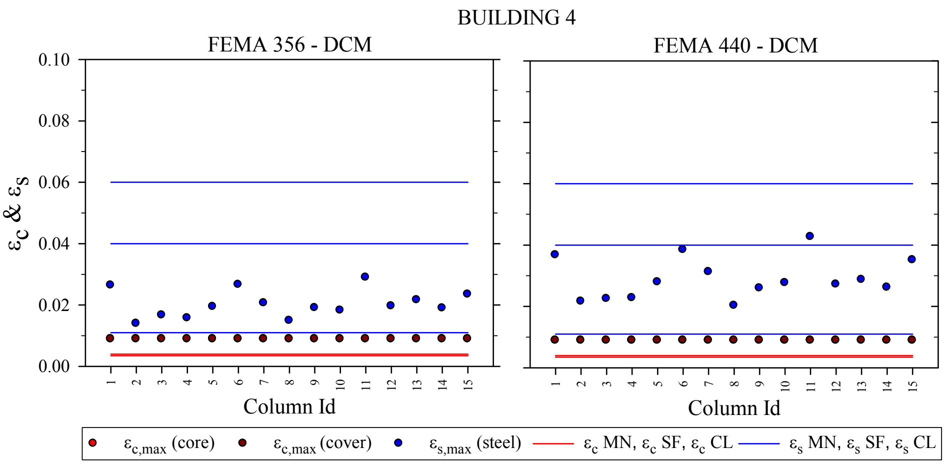

Figure 6.38 Max Strain, $\varepsilon_{c,max}$ and $\varepsilon_{s,max}$, results for Building 4 columns, computed by FEMA356-DCM and FEMA440-DCM in the X direction

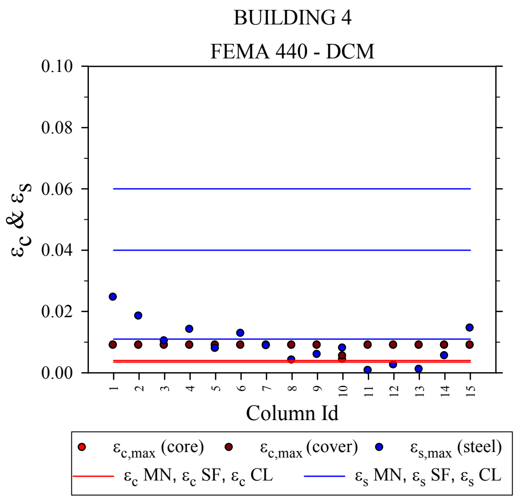

Figure 6.39 Max Strain, $\varepsilon_{c,max}$ and $\varepsilon_{s,max}$, results for Building 4 columns, computed by FEMA440-DCM in the Y direction

6.4.5 Building #5

The critical story of the building was selected as the ground story having 21 columns. The maximum strain demands obtained by NRHA, in both X and Y directions of the building are shown in Figure 6.40.

Despite the building experienced moderate damage during the earthquake, the overall damage state of building was determined as collapsed by the NDP of TEC-2007. These assessment results were again similar to those from ASCE/SEI-41. All columns were expected to collapse, according to NDP.

In the Y direction, the assessment results of the mid-frame columns by TEC-2007 were not as explicit as for ASCE/SEI-41which was discussed in Section 6.3.5, is also similar to the assessment. This result is thought to be in consequence of the strain limits designated by TEC-2007 which cause the code to be more conservative than ASCE/SEI-41.

Similar to the critical ground story, in upper stories, significant damage was expected according to both NDP and NSA results of TEC-2007.

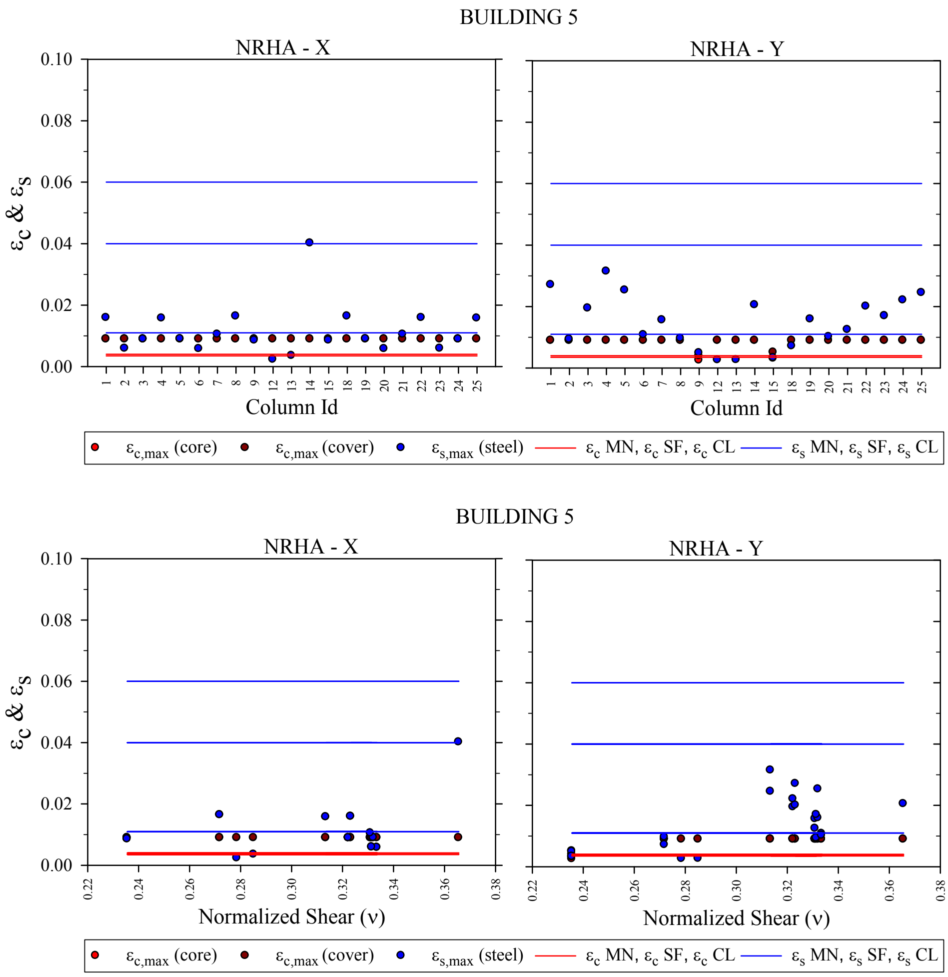

Figure 6.40 Max Strain, $\varepsilon_{c,max}$ and $\varepsilon_{s,max}$ results for Building 5 columns, computed by NRHA in X and Y directions

When the strain demands for the columns are plotted against the normalized shear (ν), it is observed that the steel strain demands have been increased by the normalized shear. This trend, however, is observed only for Y direction analysis, not in the X direction.

At the performance points estimated by approximate procedures (NSPs), the NSA of TEC-2007 applied. The assessment results for these performance points, in X and Y directions are shown in Figure 6.41 and Figure 6.42, respectively.

In X direction (Figure 6.41), at both performance points of FEMA356 and FEMA440, the concrete strain demands of 4 columns remained within the Minimum Damage State, however, according to the corresponding steel strain demands the columns were evaluated as moderately damaged. The remaining 17 columns were evaluated as collapsed. Therefore, the overall damage state of critical story was evaluated as collapsed by NSA. In Y direction (Figure 6.42), at both performance points of FEMA356 and FEMA440, the column #14, which is discussed in the paragraphs above, was expected to collapse, while the other columns located in same frame remained in Minimum Damage State. Similar to the results of ASCE/SEI-41, the damage state in X direction was overestimated by TEC-2007. In Y direction, however, in contrary with the results of ASCE/SEI-41, the overall damage state was also overestimated.

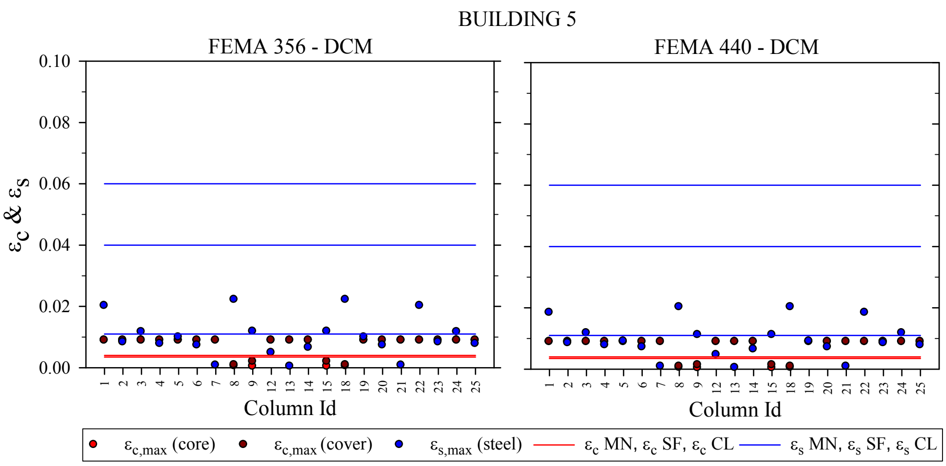

Figure 6.41 Max Strain, $\varepsilon_{c,max}$ and $\varepsilon_{s,max}$, results for Building 5 columns, computed by FEMA356-DCM and FEMA440-DCM in the X direction

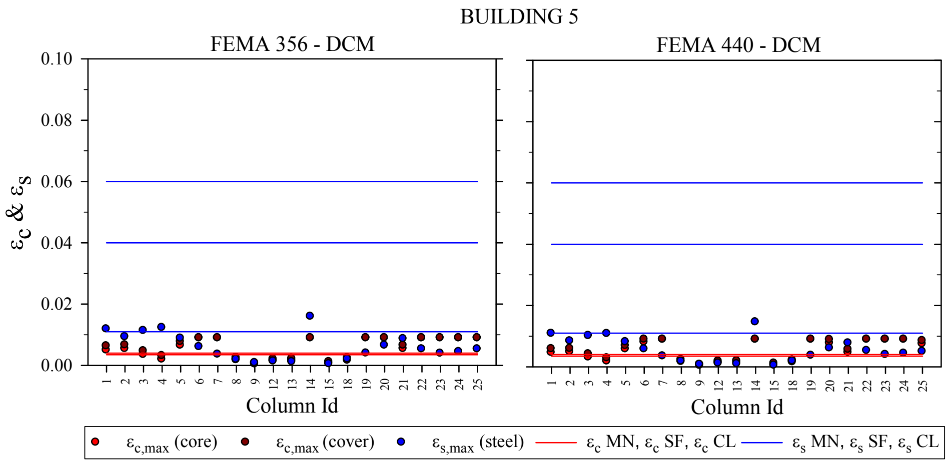

Figure 6.42 Max Strain, $\varepsilon_{c,max}$ and $\varepsilon_{s,max}$, results for Building 5 columns, computed by FEMA356-DCM and FEMA440-DCM in the Y direction

6.4.6 Building #6

The critical story of the building was selected as the ground story, with 16 columns. The maximum strain demands obtained by NRHA, in both X and Y directions of the building are shown in Figure 6.43.

Similar to the ASCE/SEI-41, Building 6 was marked as collapsed by NDP of TEC-2007. All columns of the critical story were expected to collapse, according to nonlinear dynamic procedure in both directions of the building. Therefore, the overall damage state of the building was determined as collapsed.

In upper stories, no significant damage was expected according to the maximum strain demands that were computed by NDP and NSA of TEC-2007. Thus, the soft story behavior of the building is very likely to be the reason of severe damage / collapse of the building during the earthquake.

When the strain demands for the columns are plotted against the normalized shear (ν), it is observed that the steel strain demands have been increased by the normalized shear. This trend, however, is observed only for NSA in Y direction, not in other cases.

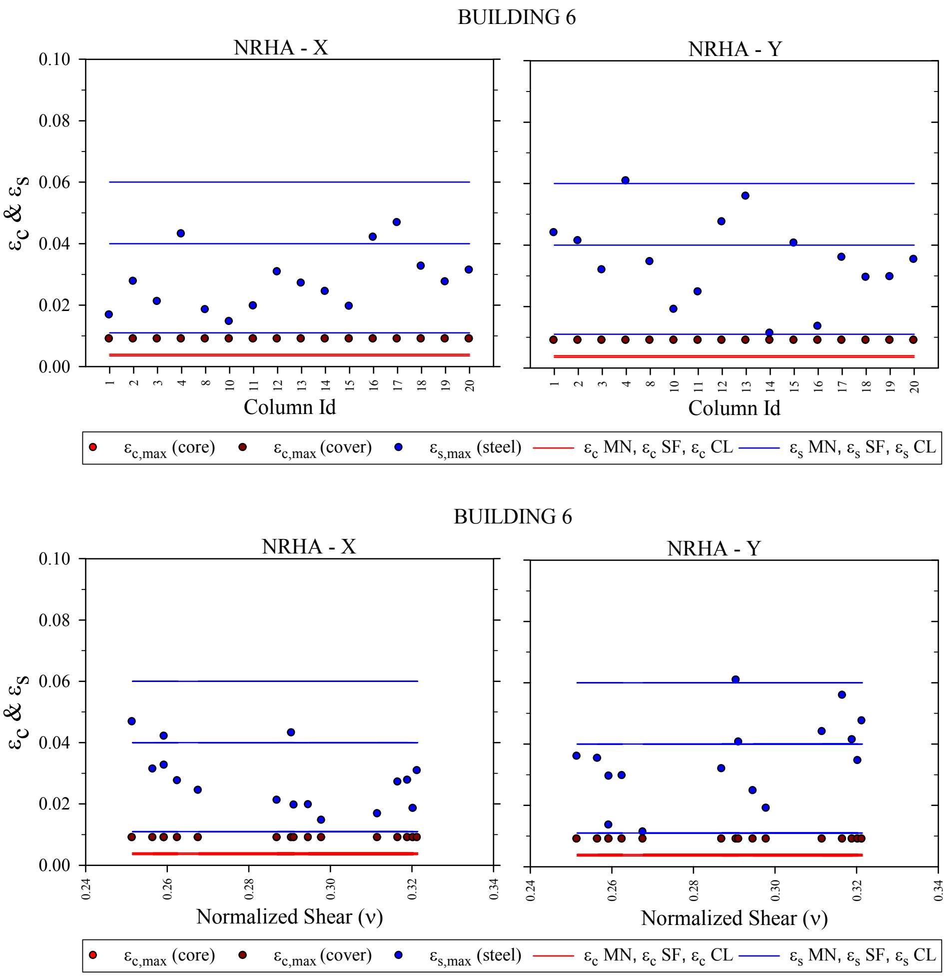

Figure 6.43 Max Strain, $\varepsilon_{c,max}$ and $\varepsilon_{s,max}$ results for Building 6 columns, computed by NRHA in X and Y directions

At the performance points estimated by approximate procedures (NSPs), the NSA of TEC-2007 applied. The assessment results for these performance points, in X and Y directions are shown in Figure 6.44 and Figure 6.45, respectively.

Even though, the steel strain demands were scattered within different damage states, governing by the concrete strain demands, the building was evaluated as collapsed, at all performance points of X and Y directions, by NSA of TEC-2007.

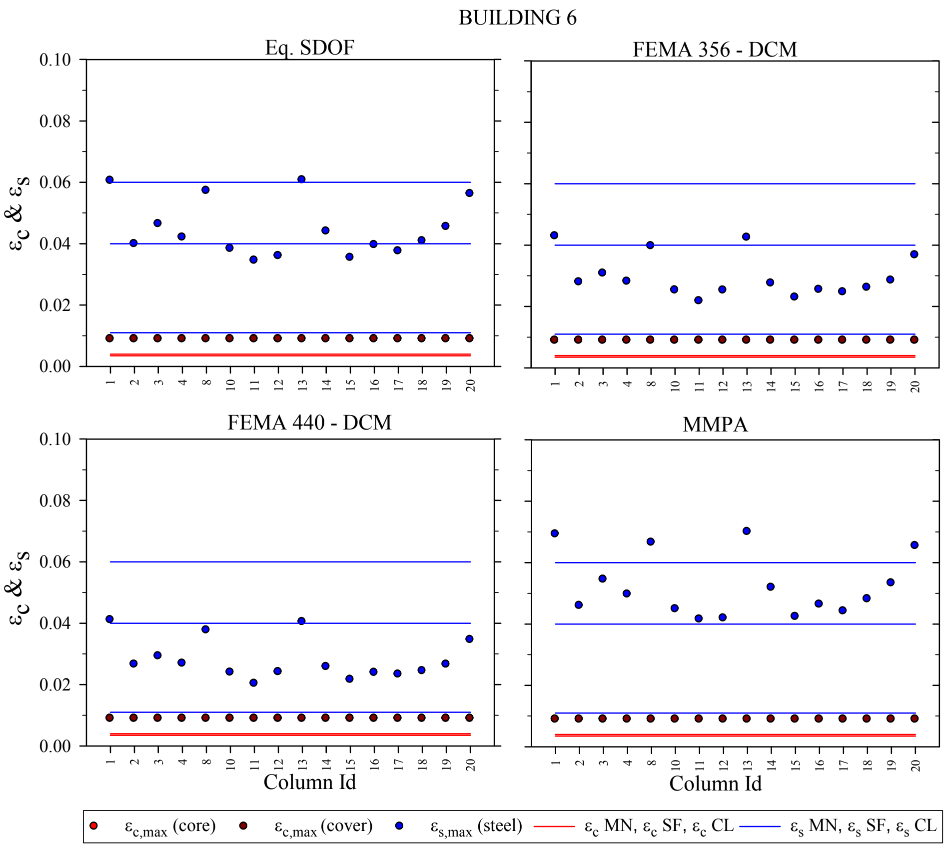

Figure 6.44 Max Strain, $\varepsilon_{c,max}$ and $\varepsilon_{s,max}$, results for Building 6 columns, computed by Eq. SDOF, FEMA356-DCM, FEMA440-DCM and MMPA in the X direction

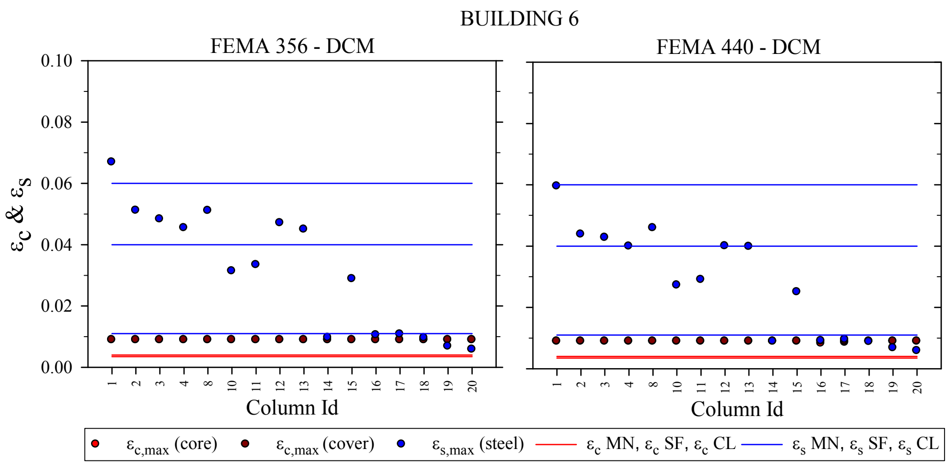

Figure 6.45 Max Strain, $\varepsilon_{c,max}$ and $\varepsilon_{s,max}$, results for Building 6 columns, computed by FEMA356-DCM and FEMA440-DCM in the Y direction

6.4.7 Building #7

The critical story of the building was selected as the ground story having 13 columns. The maximum strain demands obtained by NRHA, in both X and Y directions of the building are shown in Figure 6.46.

The final assessment decision for Building 7 was "collapsed" in both orthogonal directions according to nonlinear dynamic procedure of TEC-2007. In X and Y directions, all columns of the critical story were expected to collapse.

In addition to the severe damage of critical story, upper stories were also expected to be severely damaged, according to the maximum strain demands that were computed by NDP of TEC-2007.

When the strain demands for the columns are plotted against the normalized shear (ν), no obvious trend line was observed within the range.

As seen in Section 5.6.7, all performance estimations of NSP's were beyond the capacity (pushover) curves for each direction of the building. Thus, the NSA procedure of TEC-2007 was applied only for the ultimate roof drift value of the capacity curve, and the results of NSA are shown in Figure 6.47. Similar to the results of NDP of TEC-2007 and ASCE/SEI-41, all columns were evaluated as collapsed.

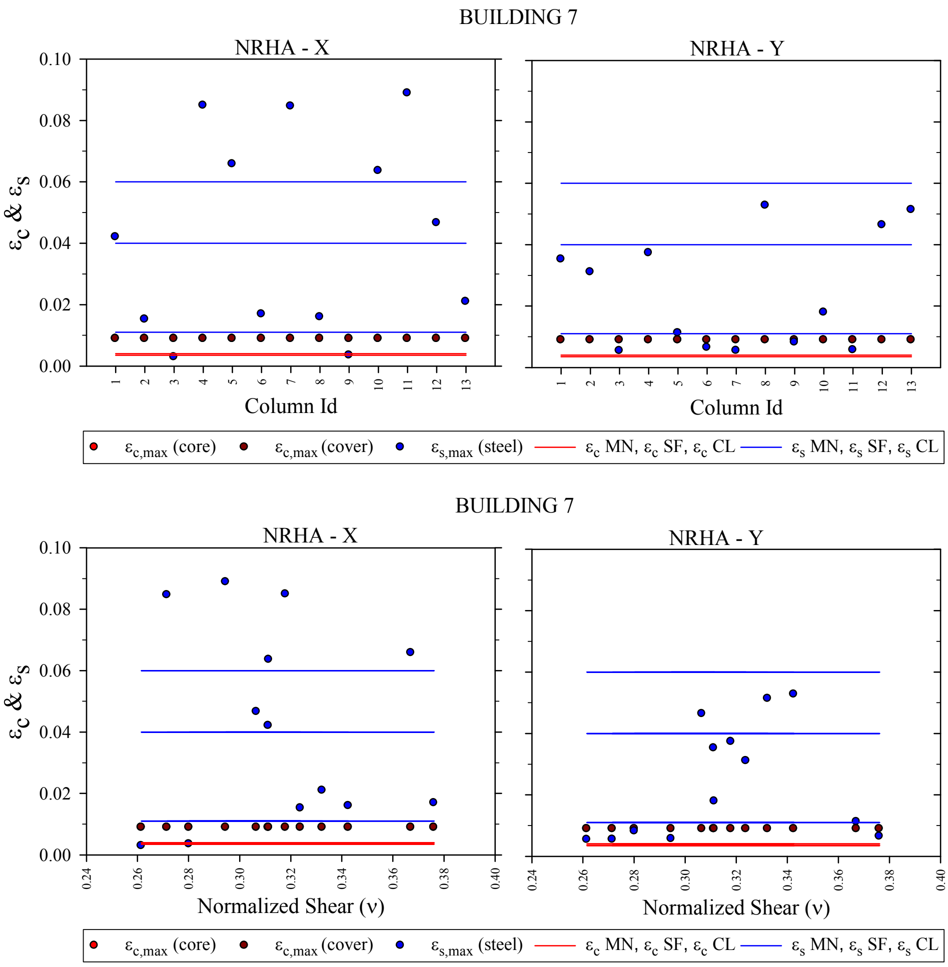

Figure 6.46 Max Strain, $\varepsilon_{c,max}$ and $\varepsilon_{s,max}$ results for Building 7 columns, computed by NRHA in X and Y directions

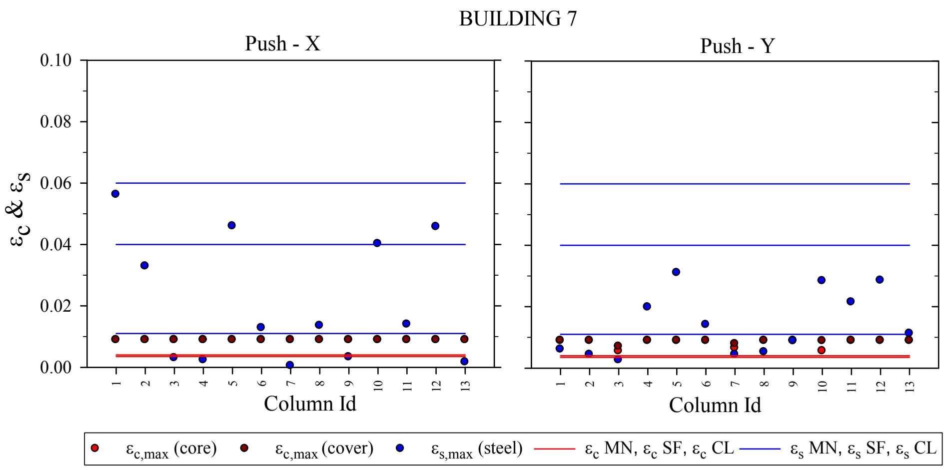

Figure 6.47 Max Strain, $\varepsilon_{c,max}$ and $\varepsilon_{s,max}$ results for Building 7 columns, computed at ultimate roof displacement of the pushover curve in X and Y directions

6.4.8 Building #8

The critical story of the building was selected as the ground story with 14 columns. The maximum strain demands obtained by NRHA, in both X and Y directions of the building are shown in Figure 6.48.

For Building 8, the final assessment decision was "collapsed" according to NDP of TEC-2007. In the X direction, all columns of the critical story were expected to collapse, while in the Y direction, all columns were expected to collapse, but only column #6 would be moderately damaged. This column was located close to column #7 that was 20*120 (cm) and strong in Y direction. The column #6 would experience less damage, while the column #7 would collapse, according to the assessment results. However, the overall damage state of the building was determined as collapsed for the assessment procedure.

In addition to the severe damage of critical story, upper stories were also expected to be significantly damaged. According to the analyses computed in X and Y directions, upper stories would be severely damaged.

When the strain demands for the columns are plotted against the normalized shear (ν), it is observed that the steel strain demands have been increased by the normalized shear. This trend, however, is clear only for NDP in Y direction, not in other cases.

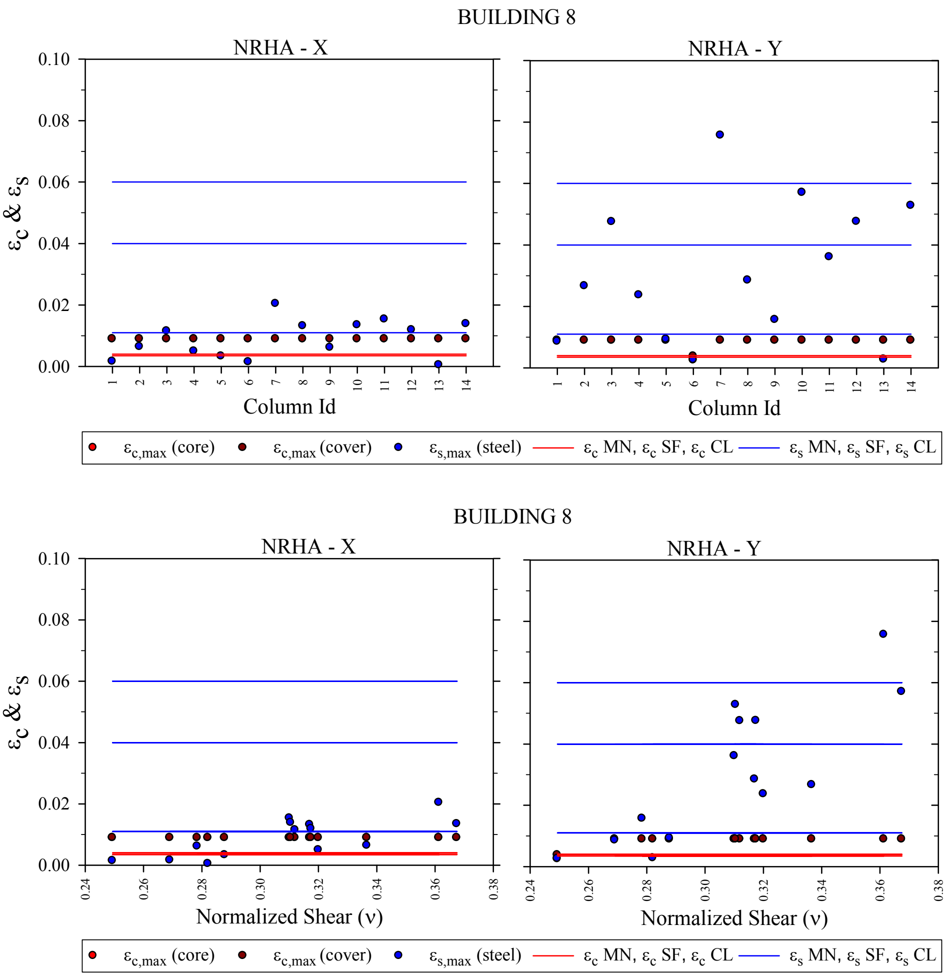

Figure 6.48 Max Strain, $\varepsilon_{c,max}$ and $\varepsilon_{s,max}$ results for Building 8 columns, computed by NRHA in X and Y directions

At the performance points estimated by approximate procedures (NSPs), the NSA of TEC-2007 applied. The assessment results for these performance points, in X and Y directions are shown in Figure 6.49 and Figure 6.50, respectively.

In general, the critical story columns were expected to collapse in both X and Y directions. Although, very limited number of columns were expected to be moderately or severely damaged rather than collapse especially for the cases of low performance point expectations, i.e. DCMs of FEMA356 and FEMA440, the overall damage state of the building was evaluated as “collapsed”, at all performance points.

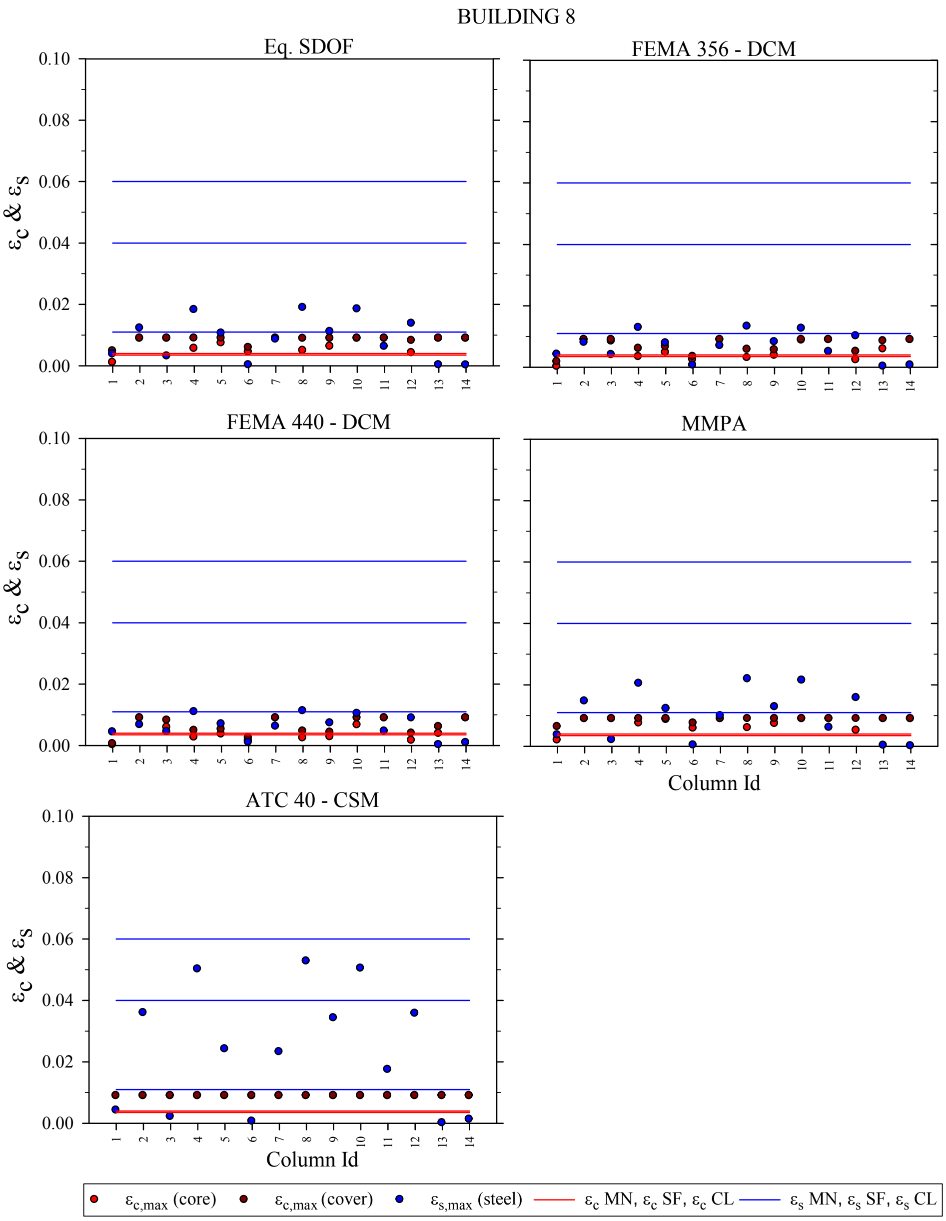

Figure 6.49 Max Strain, $\varepsilon_{c,max}$ and $\varepsilon_{s,max}$, results for Building 8 columns, computed by Eq. SDOF, FEMA356-DCM, FEMA440-DCM, MMPA and ATC40-CSM in the X direction

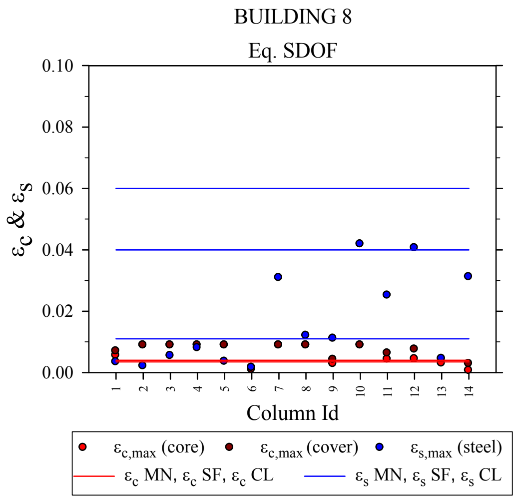

Figure 6.50 Max Strain, $\varepsilon_{c,max}$ and $\varepsilon_{s,max}$, results for Building 8 columns, computed by Eq. SDOF in the Y direction

6.4.9 Building #9

The expected failure mode of the building was "shear" (Section 6.2). However, detailed nonlinear assessment procedures of TEC-2007 were also applied to building, and the results of the assessment were given in this section. The critical story of the building was selected as the ground story with 25 columns. The maximum strain demands obtained by NRHA, in both X and Y directions of the building are shown in Figure 6.51.

In X direction of building, the building remained in minimum damage state according to NDP of TEC-2007, similar to the assessment of ASCE/SEI-41. On the other hand, in Y direction, all columns were expected to collapse.

In addition to the severe damage of critical story, no significant damage was determined for upper stories, generally.

When the strain demands for the columns are plotted against the normalized shear (ν), it is observed that the steel strain demands have been increased by the normalized shear. This trend, however, is observed only for Y direction analysis, not in the X direction.

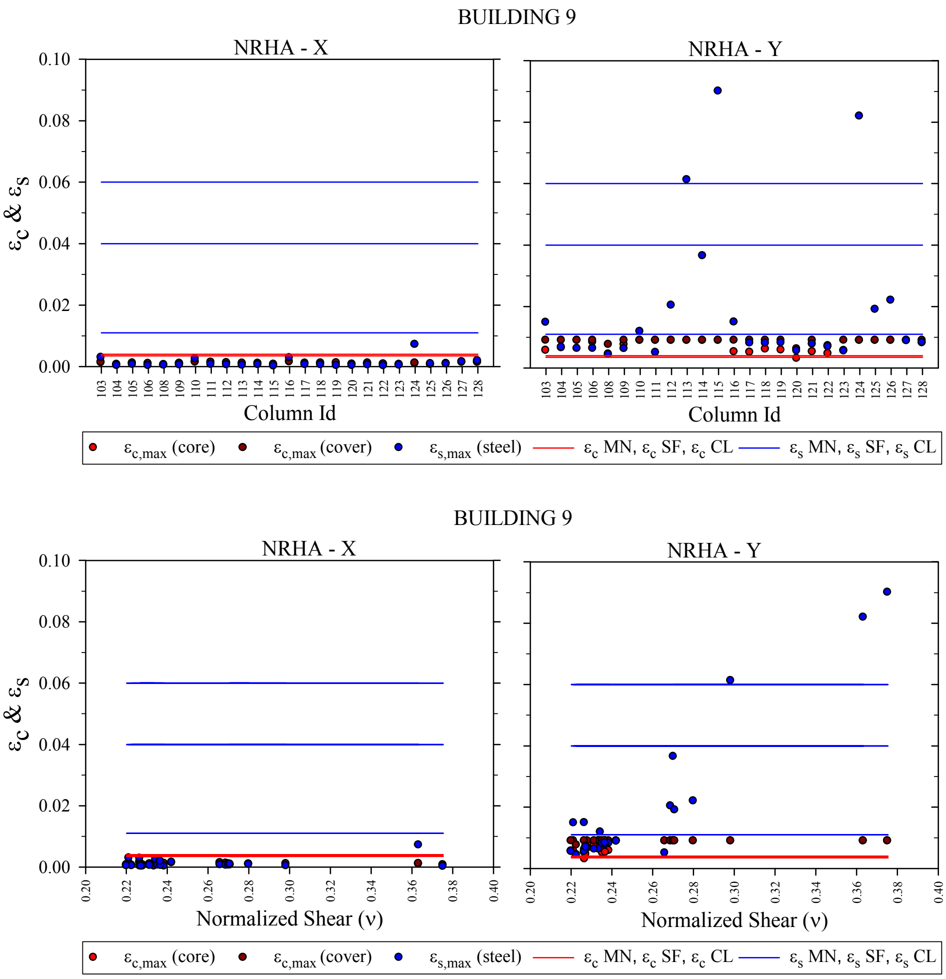

Figure 6.51 Max Strain, $\varepsilon_{c,max}$ and $\varepsilon_{s,max}$ results for Building 9 columns, computed by NRHA in X and Y directions

At the performance points estimated by approximate procedures (NSPs), the NSA of TEC-2007 applied. The assessment results for these performance points, in X and Y directions are shown in Figure 6.52 and Figure 6.53, respectively.

Parallel to the NDP results, at performance points estimated by DCMs of both FEMA-356 and FEMA-440, all critical story columns were remained in Minimum Damage State, in the X direction. At performance points of Eq. SDOF and MMPA, 4 and 7 columns were expected to collapse or be severely damaged, respectively, where the other columns were remained within MN. In Y direction of the building, similar to the assessments according to ASCE/SEI-41, 5 and 4 columns were expected to collapse or be severely damaged at performance points of FEMA-356 and FEMA-440, respectively. In this assessment results, the strongest column indicated in Section 6.3.9, was also expected to collapse, where the second strongest column would remain in MN.

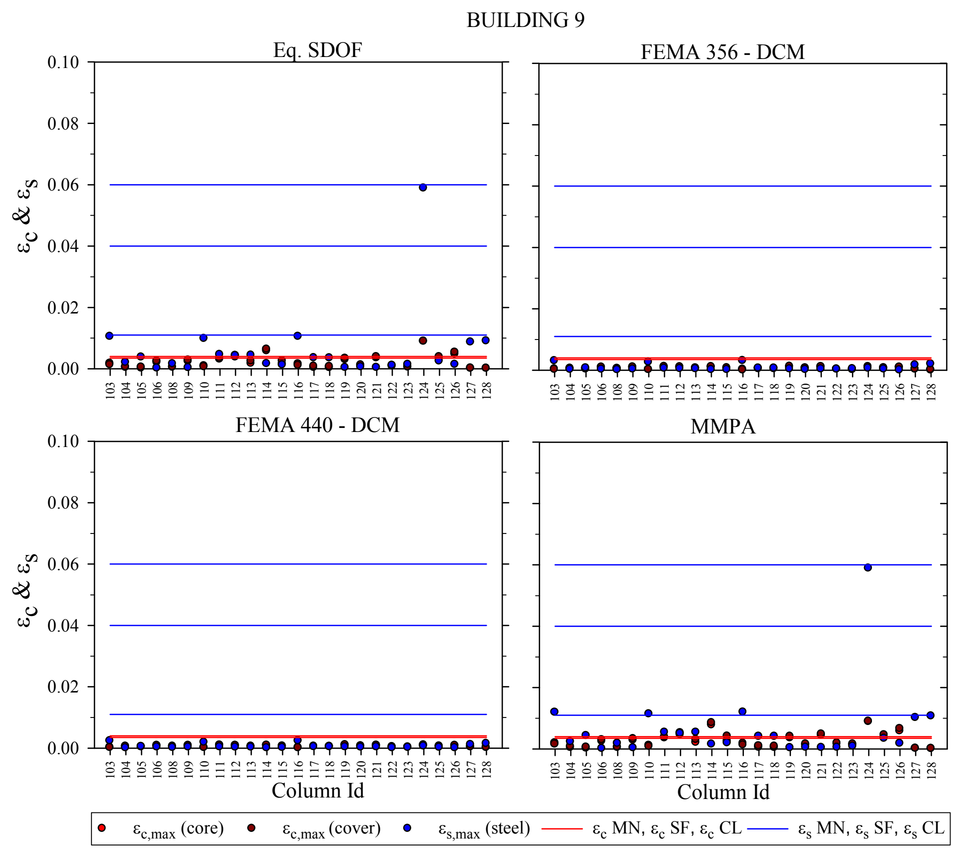

Figure 6.52 Max Strain, $\varepsilon_{c,max}$ and $\varepsilon_{s,max}$, results for Building 9 columns, computed by Eq. SDOF, FEMA356-DCM, FEMA440-DCM and MMPA in the X direction

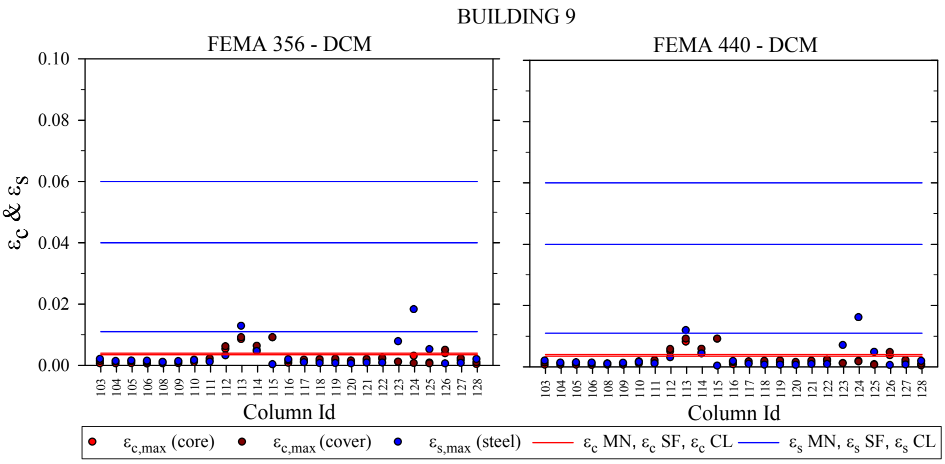

Figure 6.53 Max Strain, $\varepsilon_{c,max}$ and $\varepsilon_{s,max}$, results for Building 9 columns, computed by FEMA356-DCM and FEMA440-DCM in the Y direction

6.4.10 Building #10

The critical story of the building was selected as the ground story with 26 columns. The maximum strain demands obtained by NRHA, in both X and Y directions of the building are shown in Figure 6.54.

All columns of the critical story were expected to collapse, according to NDP, in both X and Y directions of the building. Therefore, the overall damage state of the building was determined as collapsed.

In addition to the severe damage of critical story, upper stories were also expected to be significantly damaged, according to the NDP in X direction. In Y direction, however, severe damage was computed for few columns.

When the strain demands for the columns are plotted against the normalized shear (ν), no obvious trend line was observed within the range.

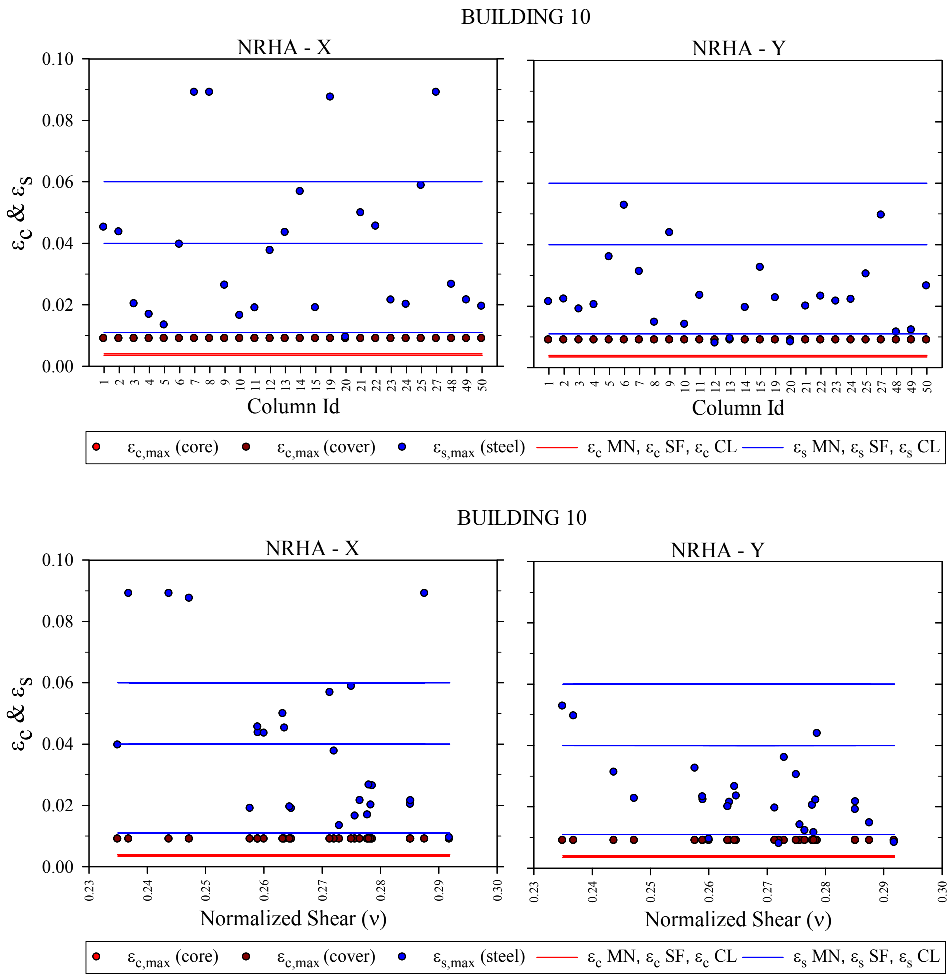

Figure 6.54 Max Strain, $\varepsilon_{c,max}$ and $\varepsilon_{s,max}$ results for Building 10 columns, computed by NRHA in X and Y directions

The NSA of TEC-2007 was applied at ultimate roof displacement of the pushover curve in X direction and at the performance points estimated by approximate procedures (NSPs) in Y direction. The results in X and Y directions are shown in Figure 6.55 and Figure 6.56, respectively.

In the X direction, all critical story columns were expected to collapse at ultimate roof drift computed by the pushover analysis. On the other hand, in the Y direction, at both performance points of FEMA-356 and FEMA-440, all the critical story columns were expected to collapse, according to NSA of TEC-2007.

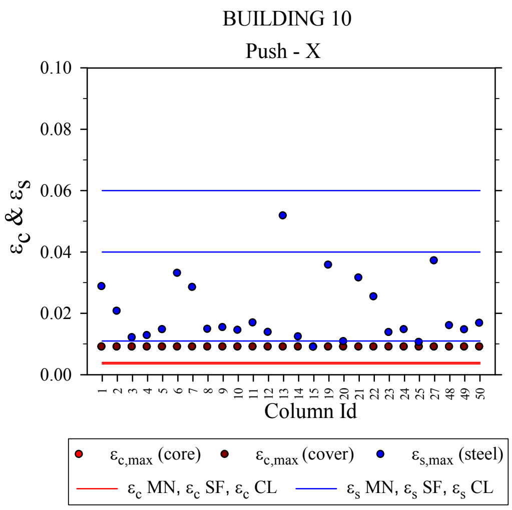

Figure 6.55 Max Strain, $\varepsilon_{c,max}$ and $\varepsilon_{s,max}$ results for Building 10 columns, computed at ultimate roof displacement of the pushover curve in the X direction

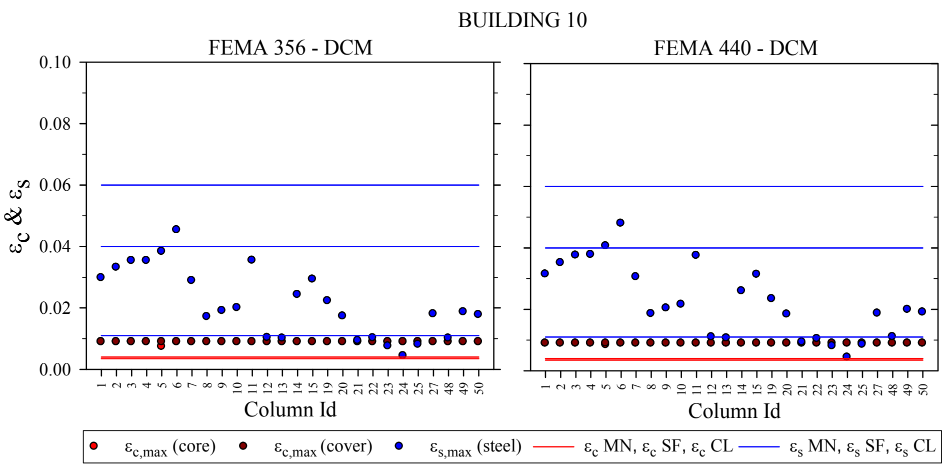

Figure 6.56 Max Strain, $\varepsilon_{c,max}$ and $\varepsilon_{s,max}$, results for Building 10 columns, computed by FEMA356-DCM and FEMA440-DCM in the Y direction

6.5 DETAILED ASSESSMENT ACCORDING TO EC8-3

The seismic performance definitions of each damage state and corresponding acceptance criteria of EuroCode 8-3 (EC 2005) have been given in Section 2.3.3 and 2.4.4, respectively. In addition to the designation of limit states by means of the chord rotation parameter, the shear limits are seperately defined corresponding to each damage state by EC8-3. However, in this study, since the shear behavior of the buildings were modeled as elastic and the shear demand values of columns were compared with the capacity as discussed in Sections 5.3.1 and 6.2, the shear limitations of EC8-3 were not taken into consideration.

Although, the transverse reinforcement detailing of the buildings studied were not conforming to the earthquake resistant design requirements, the ultimate chord rotation capacity (Equation (2.30)) of the structural members were not reduced deviding by the factor of 1.2. The α, however, in the same equation, was taken as "zero", since the stirrups were not closed with 135° hoops.

In the following sections, for each of the buildings studied, the detailed assessment results were given according to EC8-3. Similar to the Sections 6.3 and 6.4, the results were given for the critical story which was decided by the examination of detailed assessment results. The chord rotation (θ) demands of the columns of critical story were shown in the figures in comparison with the damage state limits. Indeed, the damage state limits are different for each of the structural member, since the limits are functions of the axial force level, shear force level of the member and reinforcement ratio as well as plastic hinge length and moment capacity. In this study, all the columns were evaluated using the corresponding damage limit state. The damage state limits (Damage Limitation, Significant Damage, and Near Collapse) calculated for the critical story members are plotted on the figures as θ_{DL}, θ_{SD}, and θ_{NC}, respectively, in comparison with the demand values. The columns were accepted as "collapsed", if the computed θ value was beyond the θ_{NC} limit. These demand values are also plotted against the normalized shear ($v = V / b_w d \sqrt{f_c}$) values in the figures for each building.

6.5.1 Building #1

The critical story of the building, including a mezzanine in the ground floor, was selected as the ground story. This story has 32 columns. The maximum chord rotation demands obtained by NRHA, in both X and Y directions of the building are shown in Figure 6.57.

Similar to the assessment results of ASCE/SEI-41 and TEC-2007, the damage state of the building was overestimated by the NDP of EC8-3. Although the building experienced moderate damage during the earthquake, the results presented in Figure 6.57, indicate that all the columns would collapse, which means the collapse of whole building.

In addition to the severe damage at critical story of the building, for significant part of the upper story columns moderate to severe damage were estimated by NDP of EC8-3.

When the chord rotation demands for the columns are plotted against the normalized shear (ν), no obvious trend line was observed within the range.

The NSA of EC8-3 was applied at ultimate roof displacement of the pushover curve in X direction and at the performance points estimated by approximate procedures (NSPs) in Y direction. The assessment results for these performance points, in X and Y directions are shown in Figure 6.58 and Figure 6.59, respectively.

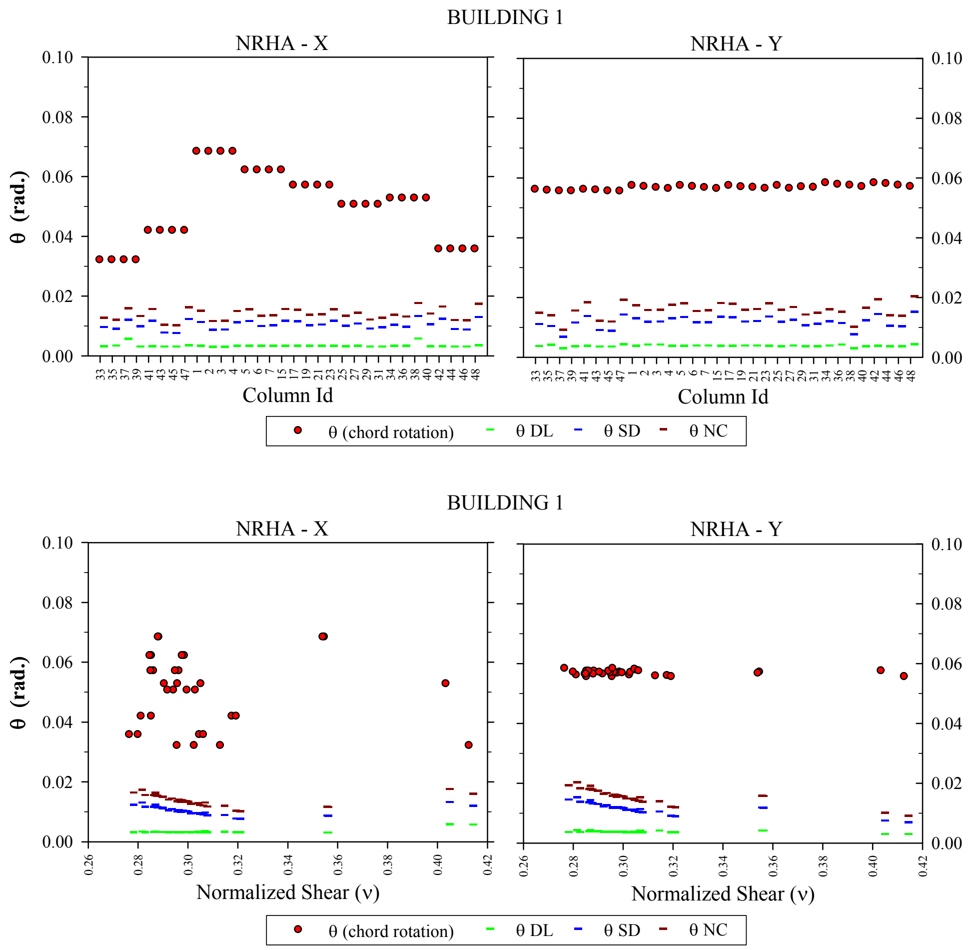

Figure 6.57 Chord Rotation, θ, results for Building 1 columns, computed by NRHA in X and Y directions

In X direction, at ultimate roof displacement of the pushover curve, the 8 lower mezzanine columns did not reach the DL limit according to the NSA of EC8-3, where the other columns were expected to collapse, similar to the results of ASCE/SEI-41 and TEC-2007. All columns of the critical story were expected to collapse according to NSA at the performance points obtained by the NSPs in Y direction. Thus, the overall damage state of the building was overestimated.

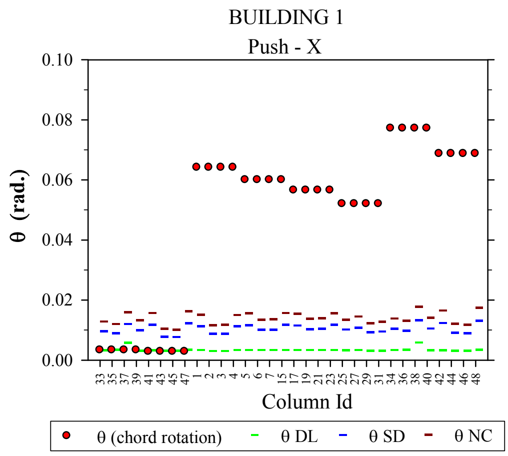

Figure 6.58 Chord Rotation, θ, results for Building 1 columns, computed at ultimate roof displacement of the pushover curve in the X direction

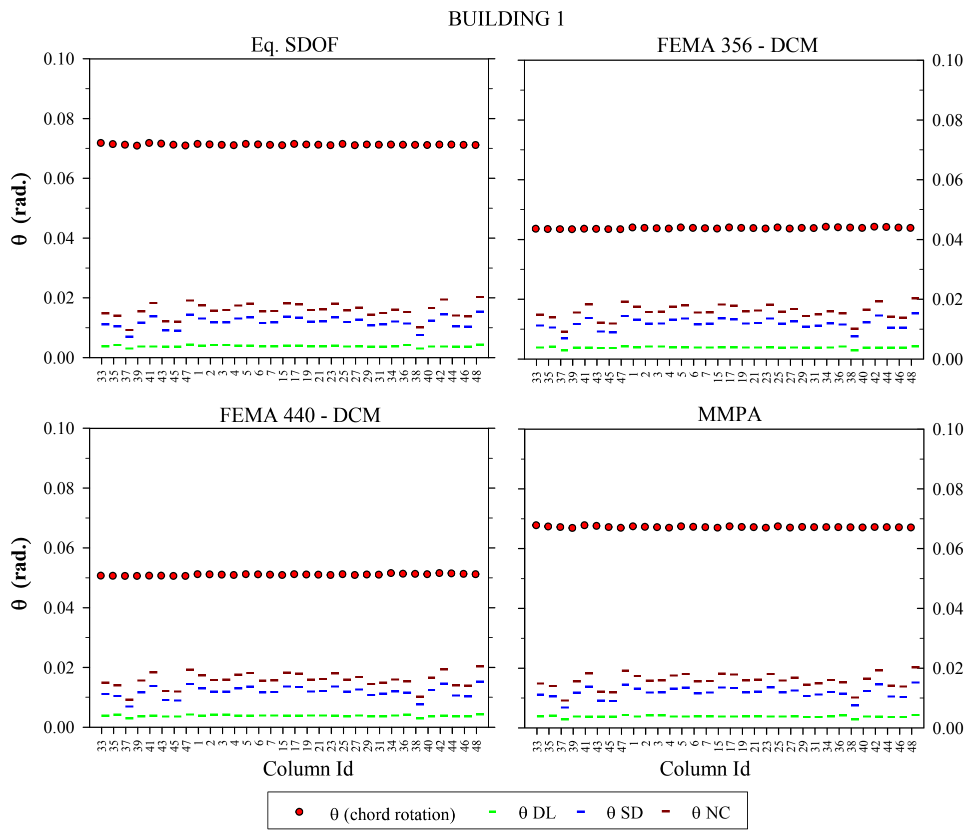

Figure 6.59 Chord Rotation, θ, results for Building 1 columns, computed by Eq. SDOF, FEMA356-DCM, FEMA440-DCM and MMPA in the Y direction

6.5.2 Building #2

The critical story of the building was selected as third story. This story has 40 columns. The maximum chord rotation demands obtained by NRHA, in both X and Y directions of the building are shown in Figure 6.60.

The assessment results of the critical story columns, using NDP of EC8-3 in both X and Y directions indicate that all columns would collapse; despite the real damage state was moderate. Moreover, by NDP, especially in X direction but also in Y direction of the building, the other story columns were evaluated as significantly damaged (moderate, severe or collapse).

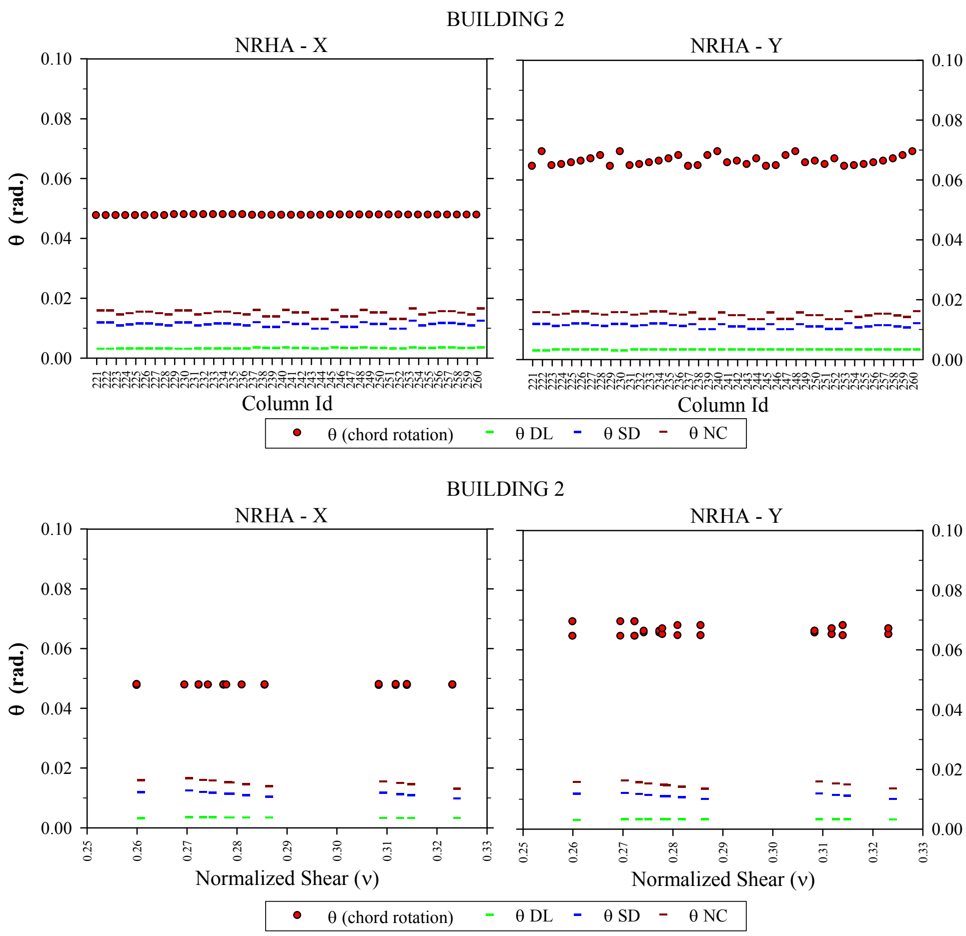

Figure 6.60 Chord Rotation, θ, results for Building 2 columns, computed by NRHA in X and Y directions

When the chord rotation demands for the columns are plotted against the normalized shear (ν), no obvious trend line was observed within the range.

As seen in Section 5.6.2, all performance estimations of NSP's are far beyond the capacity (pushover) curves for each direction of the building. Thus, the NSA procedure of EC8-3 was applied only for the ultimate roof drift value of the capacity curve, and the results are shown in Figure 6.61. In both directions, all columns were expected to collapse.

In general, it can be concluded that the assessment results of both NDP and NSA of EC8-3 were overestimated the damage state of the building as severe damage/collapsed, similar to the results of ASCE/SEI-41 and TEC-2007.

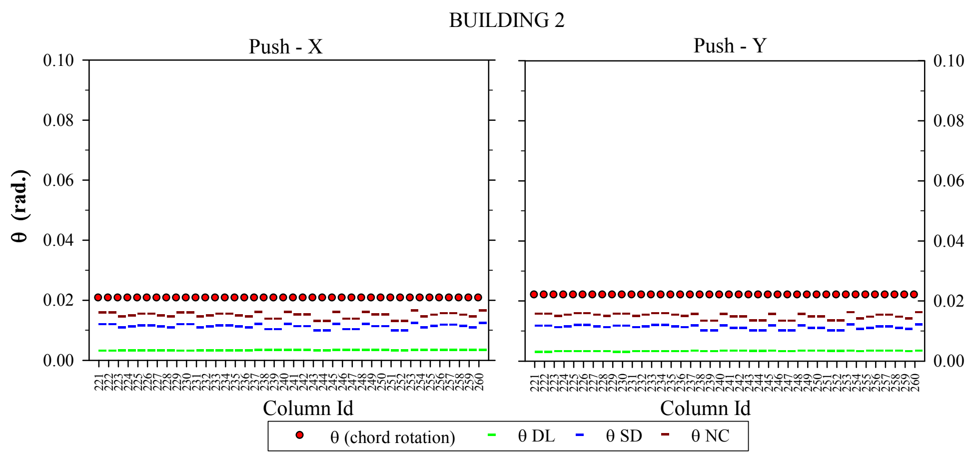

Figure 6.61 Chord Rotation, θ, results for Building 2 columns, computed at ultimate roof displacement of the pushover curve in X and Y directions

6.5.3 Building #3

The critical story of the building was selected as the ground story. This story has 38 columns. The maximum chord rotation demands obtained by NRHA, in both X and Y directions of the building are shown in Figure 6.62.

The results of the assessment procedures according to EC8-3 were similar to the results of ASCE/SEI-41 and TEC-2007. Again, the damage state of building was overestimated by the NDP of EC8-3. All the columns of the critical story were expected to collapse, despite the building experienced moderate damage during the earthquake.

In addition to the severe damage at critical story of the building, the upper story columns were estimated as moderately damaged by NDP in both X and Y direction of the building.

When the chord rotation demands for the columns are plotted against the normalized shear (ν), no obvious trend line was observed within the range.

At the performance points estimated by approximate procedures (NSPs), the NSA of EC8-3 applied. The assessment results for these performance points, in X and Y directions are shown in Figure 6.63 and Figure 6.64, respectively.

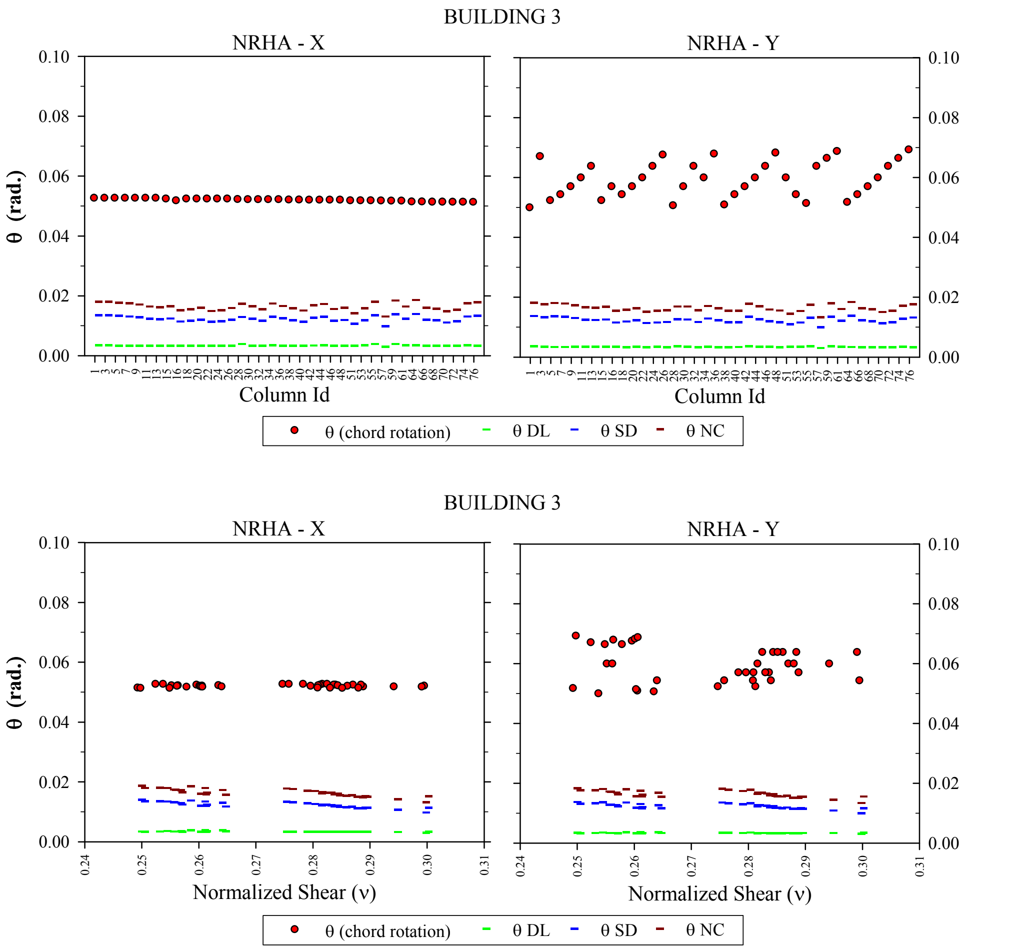

Figure 6.62 Chord Rotation, θ, results for Building 3 columns, computed by NRHA in X and Y directions

As it can be seen in figures, all critical story columns were expected to collapse. The only exception is for NSA at FEMA-440 performance point in Y direction, where 6 of the columns within the limited safety range (severely damaged), with very close chord rotation demands to the collapse limit, designated by EC8-3. Similar to the ASCE/SEI-41 and TEC-2007 assessment results either in X or Y direction, the damage state of the building was overestimated as “collapsed”, by detailed assessment procedure of EC8-3, at all performance points obtained by the NSPs.

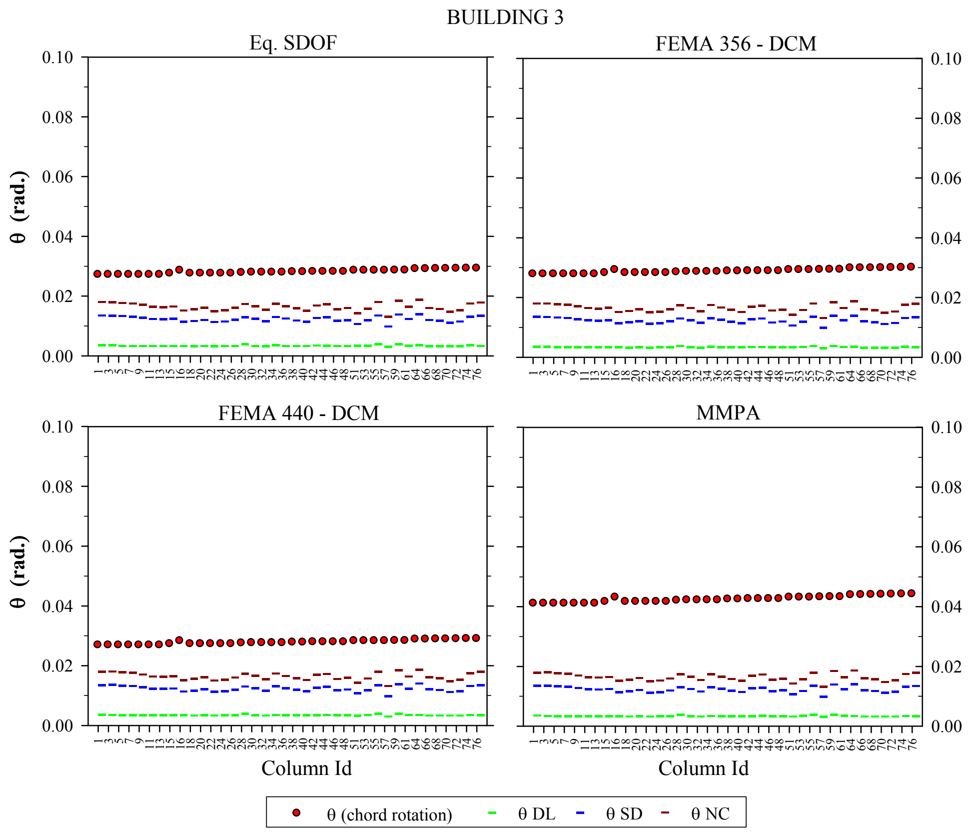

Figure 6.63 Chord Rotation, θ, results for Building 3 columns, computed by Eq. SDOF, FEMA356-DCM, FEMA440-DCM and MMPA in the X direction

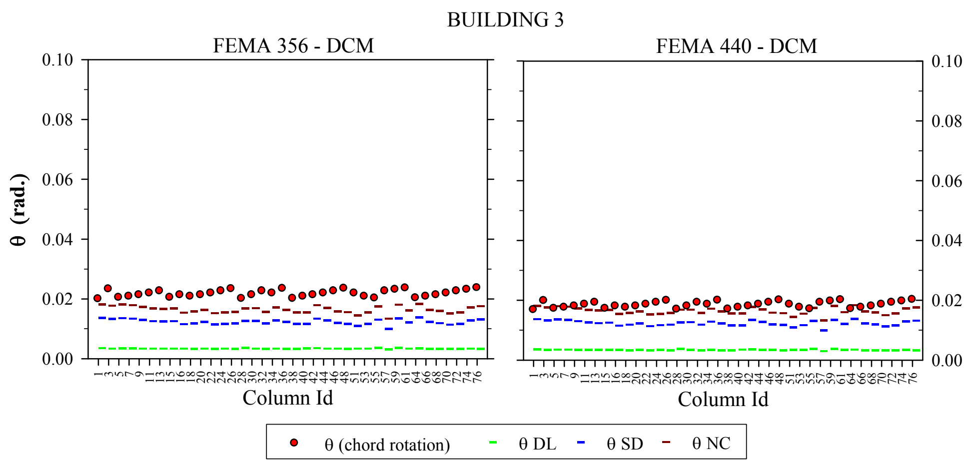

Figure 6.64 Chord Rotation, θ, results for Building 3 columns, computed by FEMA356-DCM, and FEMA440-DCM in the Y direction

6.5.4 Building #4

The critical story of the building was selected as the ground story. This story has 15 columns. The maximum chord rotation demands obtained by NRHA, in both X and Y directions of the building are shown in Figure 6.65.

All columns of the critical story were expected to collapse, according to NDP, in both X and Y directions of the building. Thus, the damage state of the building was overestimated by EC8-3, since it was moderately damaged during the earthquake. The results of the EC8-3 assessment were parallel to those obtained from ASCE/SEI-41 and TEC-2007.

All upper story columns were also expected to be moderately damaged according to NDP in both directions of the building.

When the chord rotation demands for the columns are plotted against the normalized shear (ν), no obvious trend line was observed within the range.

At the performance points estimated by approximate procedures (NSPs), the NSA of EC8-3 applied. The assessment results for these performance points, in X and Y directions are shown in Figure 6.66 and Figure 6.67, respectively.

All of the columns of critical story were expected to collapse in X direction analyses, and only 2 of the columns would be severely damaged with a chord rotation demand close to the collapse limit, while the others would collapse. Thus, the overall damage state of building was evaluated as collapsed in both X and Y directions. These results of the NSA of EC8-3 were parallel to the results of ASCE/SEI-41 and TEC-2007.

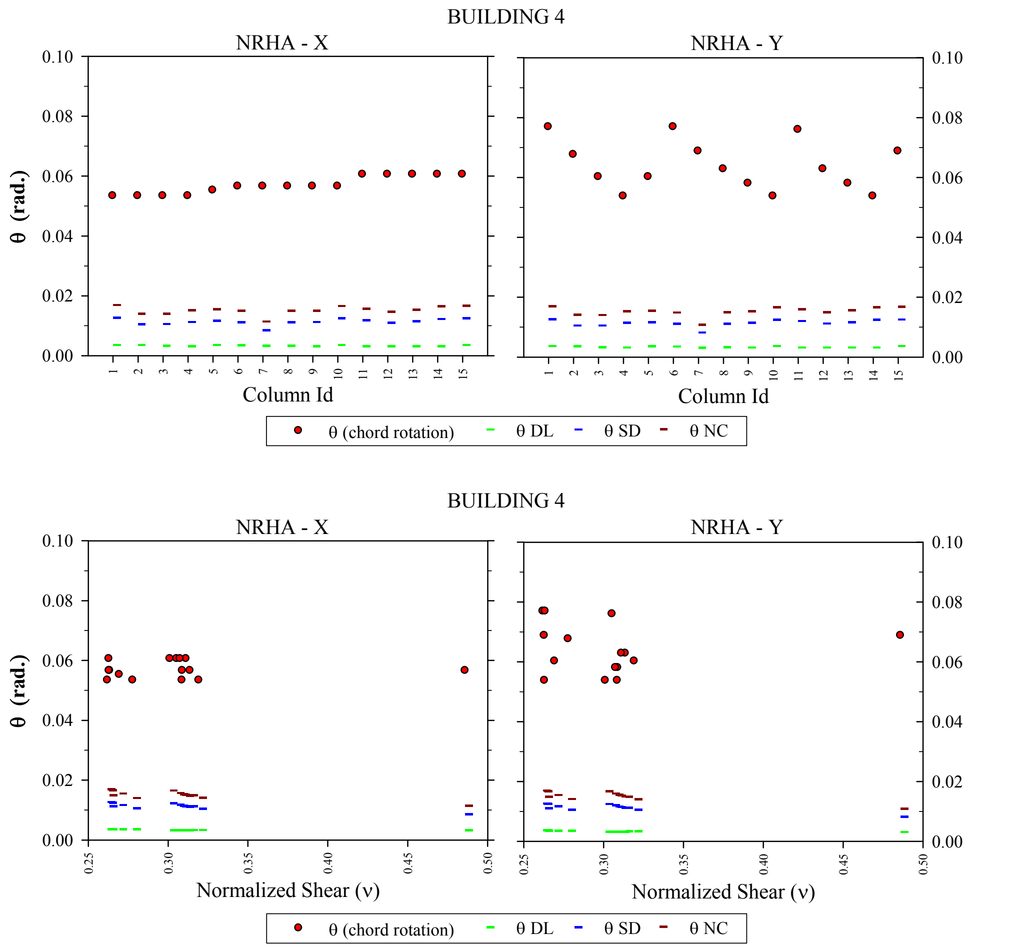

Figure 6.65 Chord Rotation, θ, results for Building 4 columns, computed by NRHA in X and Y directions

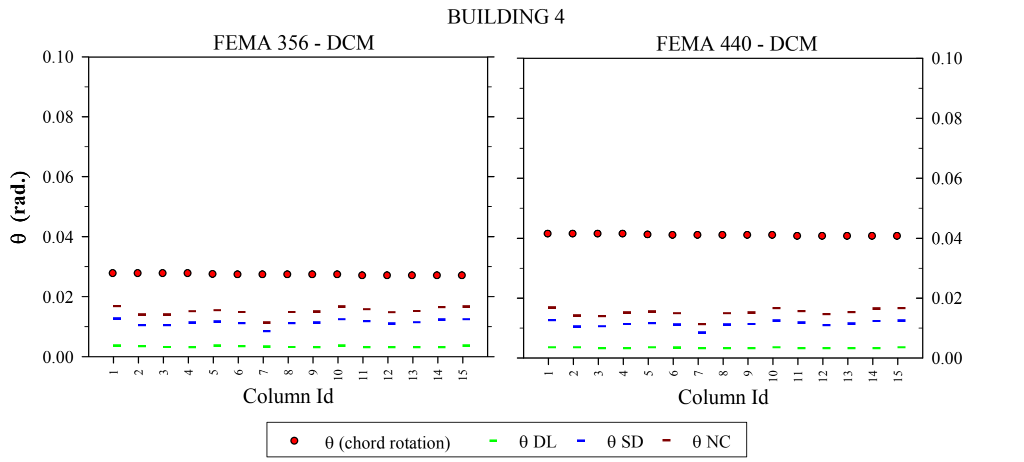

Figure 6.66 Chord Rotation, θ, results for Building 4 columns, computed by FEMA356-DCM, and FEMA440-DCM in the X direction

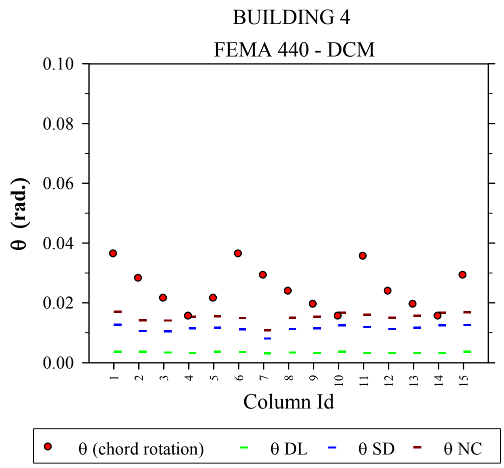

Figure 6.67 Chord Rotation, θ, results for Building 4 columns, computed by FEMA440-DCM in the Y direction

6.5.5 Building #5

The critical story of the building was selected as the ground story. This story has 21 columns. The maximum chord rotation demands obtained by NRHA, in both X and Y directions of the building are shown in Figure 6.68.

The overall damage state of Building 5 was determined as collapsed, despite the building experienced moderate damage during the earthquake, by the NDP of EC8-3, similar to the results of ASCE/SEI-41 and TEC-2007. All critical story columns were expected to collapse, according to NDP in both X and Y directions.

The distinct behavior and relatively less damage of mid-frame, due to the mid-column (column #14) behavior, in Y direction, which was discussed in Sections 6.3.5 and 6.4.5, was not observed when the assessment procedures of EC8-3 applied. In consequence of the damage parameter used, chord rotation, the damage states of the columns in any story (given that the story height is constant) are more or less the same, especially if the torsional irregularity does not affect, since the rigid diaphragm constraint applied, as in this case.

In addition to the critical ground story, all the second story columns were expected to collapse by NDP in both directions. Moreover, the upper stories were evaluated as moderately damaged.

When the chord rotation demands for the columns are plotted against the normalized shear (ν), no obvious trend line was observed within the range.

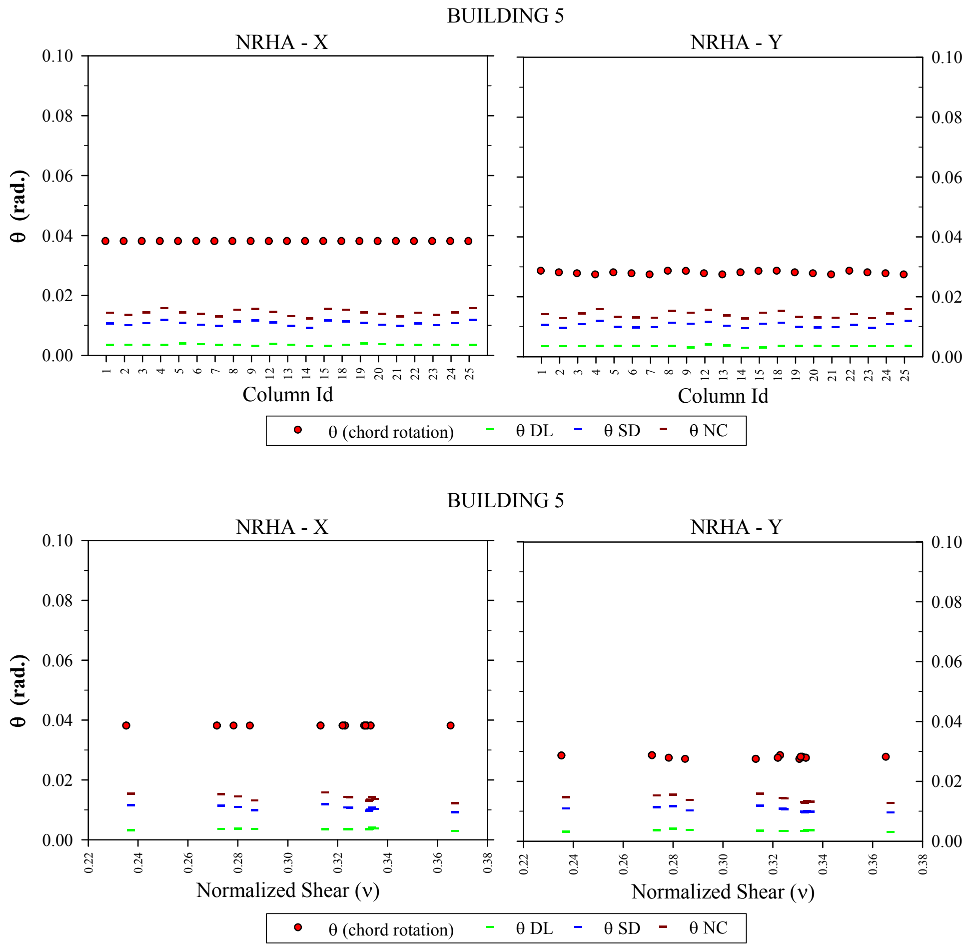

Figure 6.68 Chord Rotation, θ, results for Building 5 columns, computed by NRHA in X and Y directions

At the performance points estimated by approximate procedures (NSPs), the NSA of EC8-3 applied. The assessment results for these performance points, in X and Y directions are shown in Figure 6.69 and Figure 6.70, respectively.

In X direction, all critical story columns were expected to collapse, where in Y direction these columns were expected to remain within damage control range (moderately damaged). These results were similar to those obtained from ASCE/SEI-41. In this sense, only the assessment results of EC8-3 in Y direction were consistent with the actual damage state observed during the earthquake.

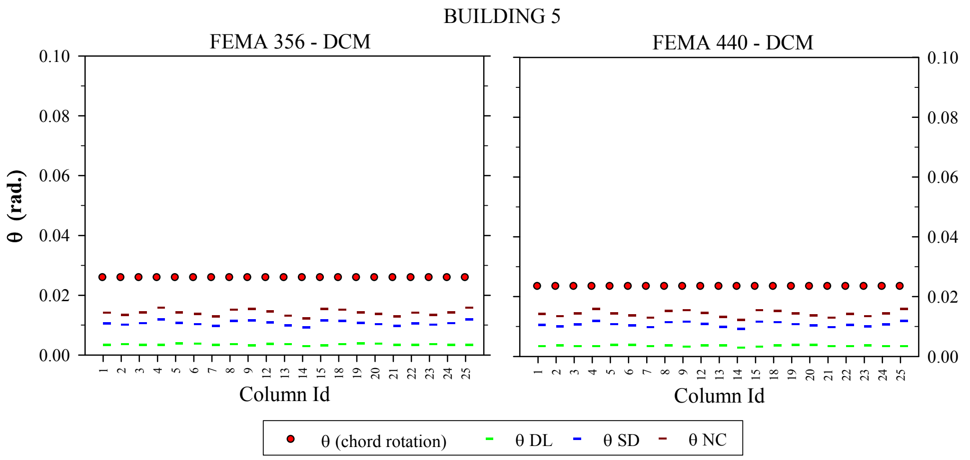

Figure 6.69 Chord Rotation, θ, results for Building 5 columns, computed by FEMA356-DCM, and FEMA440-DCM in the X direction

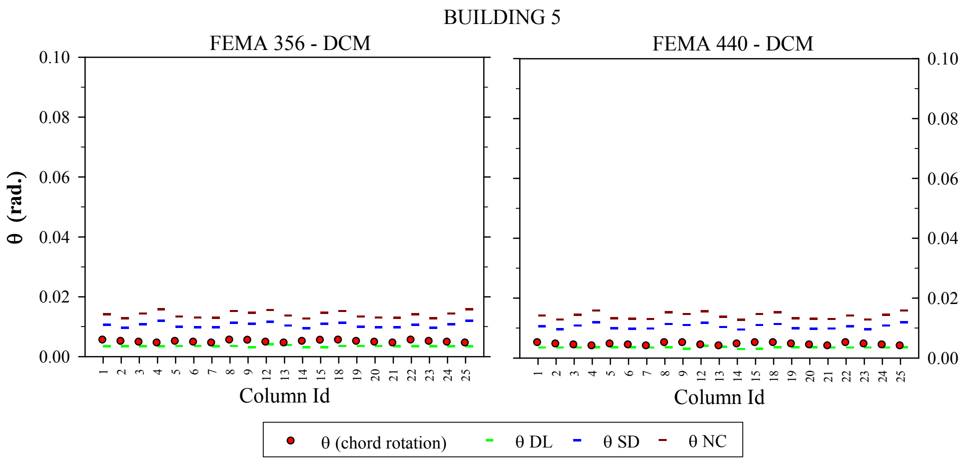

Figure 6.70 Chord Rotation, θ, results for Building 5 columns, computed by FEMA356-DCM, and FEMA440-DCM in the Y direction

6.5.6 Building #6

The critical story of the building was selected as the ground story. This story has 16 columns. The maximum chord rotation demands obtained by NRHA, in both X and Y directions of the building are shown in Figure 6.71.

All columns of the critical story of Building 6 was marked as collapsed by NDP of EC8-3, in both X and Y directions. These results are parallel to those obtained from ASCE/SEI-41 and TEC-2007.

The upper stories were expected to be severely damaged in Y direction by NDP of EC8-3, while they were expected to be moderately damaged in X direction. These results given for the upper stories are distinct from those obtained from assessment procedures of ASCE/SEI-41 and TEC-2007 which were implying the soft story behavior as the reason of severe damage / collapse of the building during the earthquake (Sections 6.3.6 and 6.4.6).

When the chord rotation demands for the columns are plotted against the normalized shear (ν), no obvious trend line was observed within the range.

At the performance points estimated by approximate procedures (NSPs), the NSA of EC8-3 applied. The assessment results for these performance points, in X and Y directions are shown in Figure 6.72 and Figure 6.73, respectively.

Similar to the assessment results of ASCE/SEI-41 and TEC-2007, EC8-3 evaluated the overall damage state as "collapsed" at all performance points obtained by NSPs, in both X and Y directions of the building.

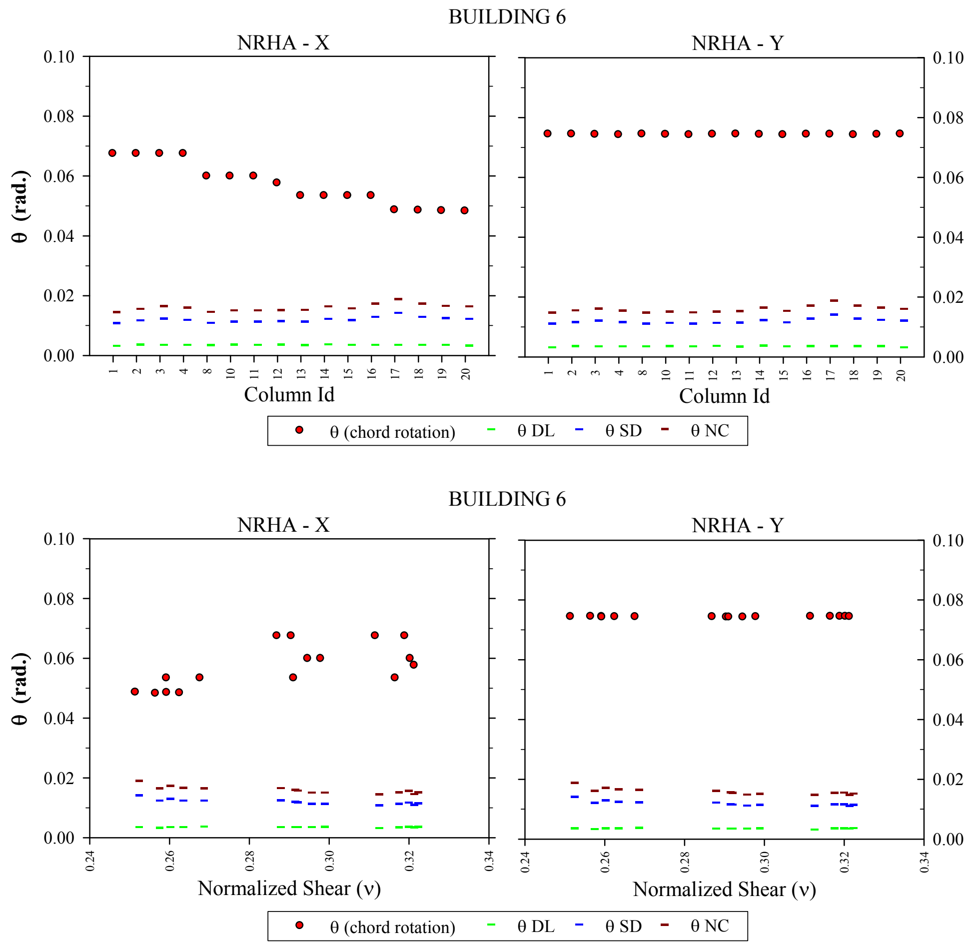

Figure 6.71 Chord Rotation, θ, results for Building 6 columns, computed by NRHA in X and Y directions

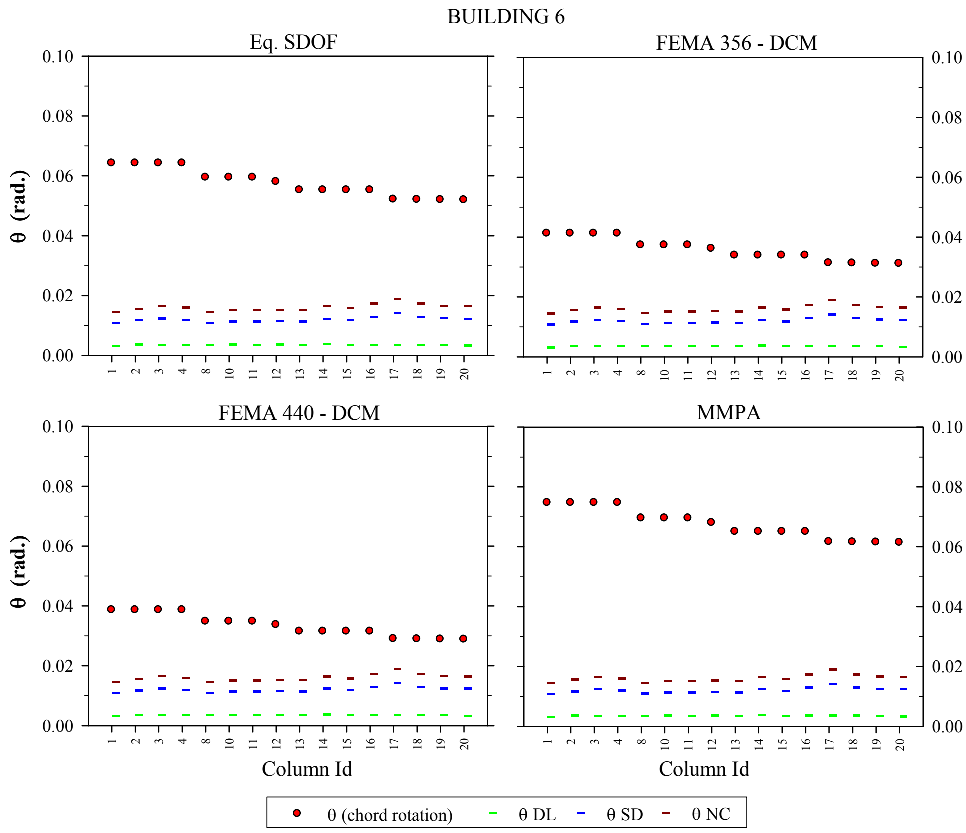

Figure 6.72 Chord Rotation, θ, results for Building 6 columns, computed by Eq. SDOF, FEMA356-DCM, FEMA440-DCM and MMPA in the X direction

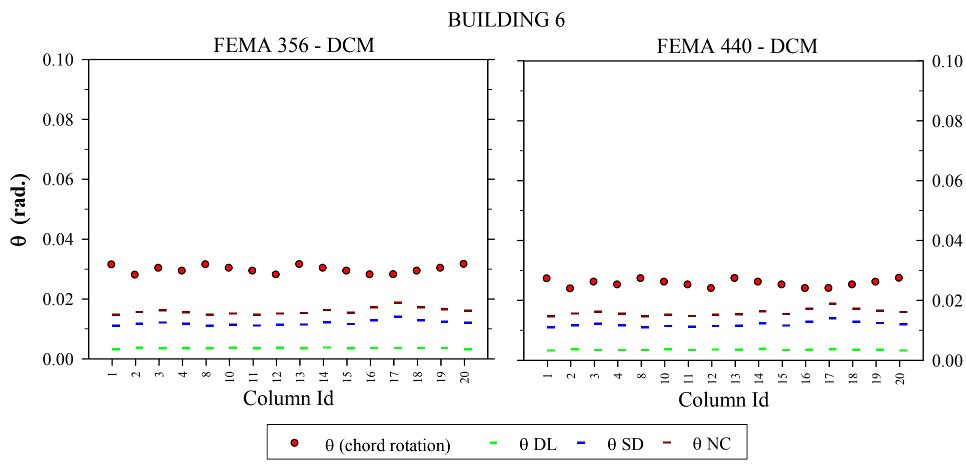

Figure 6.73 Chord Rotation, θ, results for Building 6 columns, computed by FEMA356-DCM and FEMA440-DCM in the Y direction

6.5.7 Building #7

The critical story of the building was selected as the ground story. This story has 13 columns. The maximum chord rotation demands obtained by NRHA, in both X and Y directions of the building are shown in Figure 6.74.

For Building 7, all columns of the critical story were expected to collapse, according to NDP of EC8-3. Thus, the overall damage state of the building was determined as collapsed, similar to those by ASCE/SEI-41 and TEC-2007.

In addition to the severe damage of critical story, upper stories were also expected to be severely damaged due to moderate to severely damaged columns.

When the chord rotation demands for the columns are plotted against the normalized shear (ν), no obvious trend line was observed within the range.

As seen in Section 5.6.7, all performance estimations of NSP's were beyond the capacity (pushover) curves for each direction of the building. Thus, the NSA procedure of EC8-3 was applied only for the ultimate roof drift value of the capacity curve, and the results are shown in Figure 6.75.

In both directions of the building, all columns were expected to collapse, where the only exception was two columns in Y direction were expected to be severely damaged (near collapse) according to NSA.

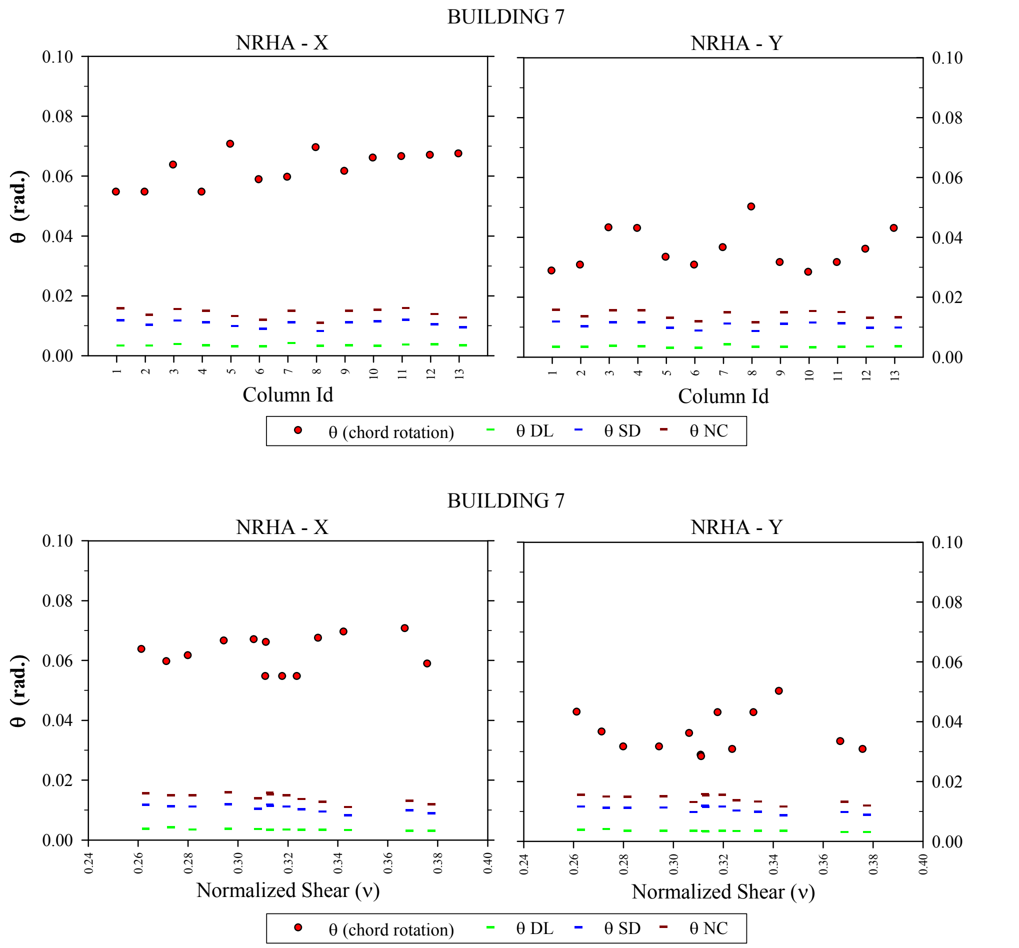

Figure 6.74 Chord Rotation, θ, results for Building 7 columns, computed by NRHA in X and Y directions

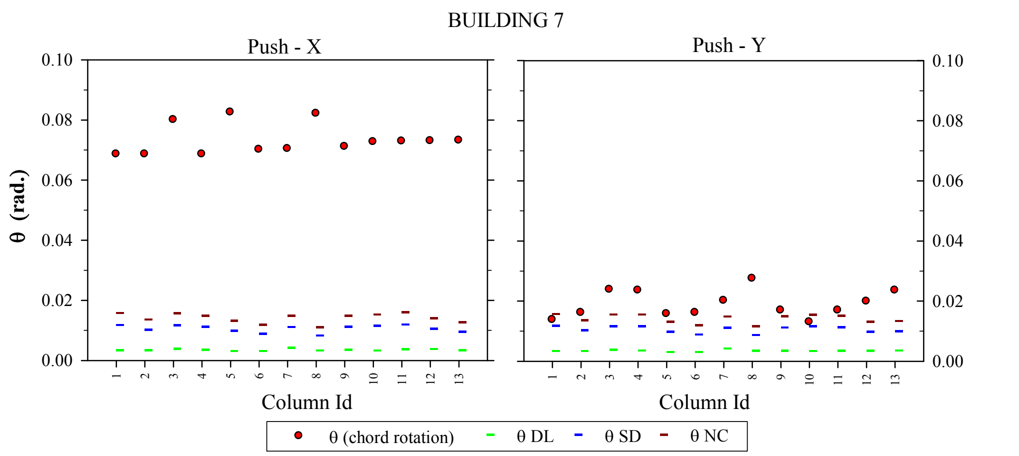

Figure 6.75 Chord Rotation, θ, results for Building 7 columns, computed at ultimate roof displacement of the pushover curve in X and Y directions

6.5.8 Building #8

The critical story of the building was selected as the ground story. This story has 14 columns. The maximum chord rotation demands obtained by NRHA, in both X and Y directions of the building are shown in Figure 6.76.

All columns of the critical story were expected to collapse, according to NDP in both X and Y directions. So, the overall damage state of the building was determined as collapsed for nonlinear dynamic assessment procedure of EC8-3. The final assessment decision was same as those from ASCE/SEI-41 and TEC-2007.

In addition to the severe damage of critical story, upper stories were also expected to be significantly damaged in both directions, due to moderate to severe damage of the columns, as well as collapse of them.

When the chord rotation demands for the columns are plotted against the normalized shear (ν), no obvious trend line was observed within the range.

At the performance points estimated by approximate procedures (NSPs), the NSA of EC8-3 applied. The assessment results for these performance points, in X and Y directions are shown in Figure 6.77 and Figure 6.78, respectively.

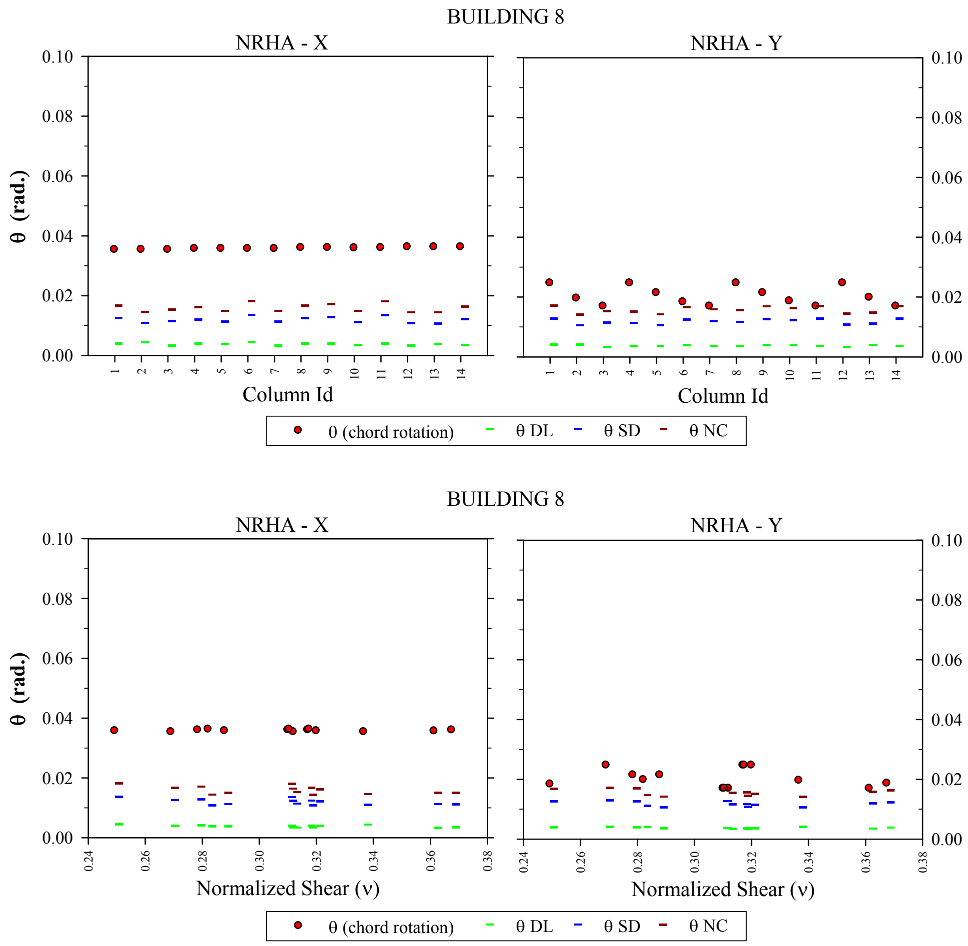

Figure 6.76 Chord Rotation, θ, results for Building 8 columns, computed by NRHA in X and Y directions

In the X direction, at performance points of Eq. SDOF, MMPA and CSM of ATC40, all critical story columns were evaluated as collapsed by NSA of EC8-3. At performance points of FEMA356 and FEMA440, on the other hand, columns were evaluated either as collapsed or severely damaged (within limited safety range). For FEMA 356 and FEMA 440, 2 and 10 of the columns were expected to be severely damaged, respectively, while the remaining columns would collapse. Thus, the overall damage state of the building was pointed out as "collapsed" in X direction.

In the Y direction, the building overall damage state was seemed to be on the edge of Significant Damage (SD) limit. At performance point of Eq. SDOF, 4 columns were expected to be within limited safety range while 10 columns would be significantly damaged (within damage control range), with high chord rotation demands close to SD limit. The final decision in this direction was severe damage. It should be reminded that this direction of the building was shear critical according to the analyses which were discussed in Section 6.2.

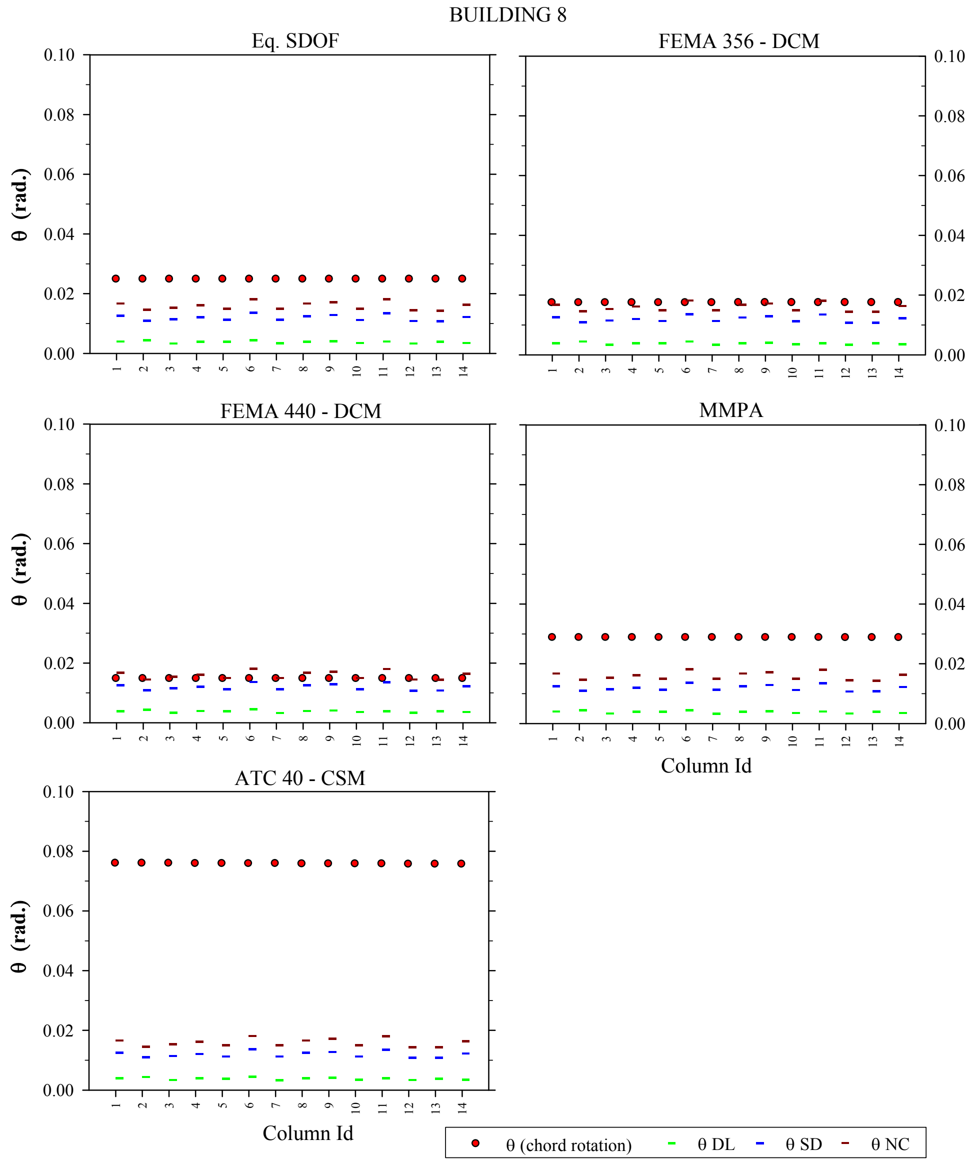

Figure 6.77 Chord Rotation, θ, results for Building 8 columns, computed by Eq. SDOF, FEMA356-DCM, FEMA440-DCM, MMPA and ATC40-CSM in the X direction

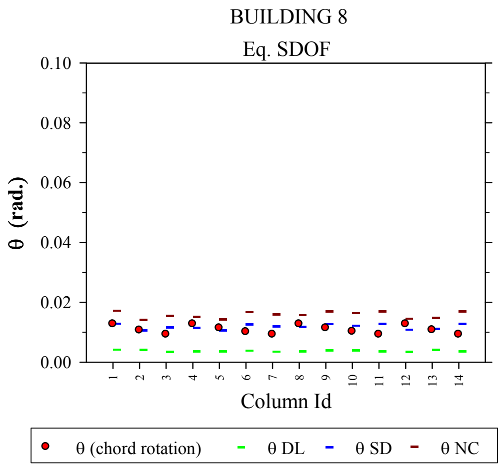

Figure 6.78 Chord Rotation, θ, results for Building 8 columns, computed by Eq. SDOF in the Y direction

6.5.9 Building #9

Although, the failure mode of the building was expected to be "shear" as discussed in Section 6.2, detailed nonlinear assessment procedures of EC8-3 were also applied to Building 9, and the results of the assessment were given in this section. The critical story of the building was selected as the ground story with 25 columns. The maximum chord rotation demands obtained by NRHA, in both X and Y directions of the building are shown in Figure 6.79.

In the X direction, since the building is strong in this direction with the structural walls, the building remained in damage limitation range according to NDP of EC8-3. In the Y direction, on the other hand, all columns were expected to collapse according to the assessment results.

In addition to the severe damage of critical story, no significant damage was determined for upper stories, according to NDP.

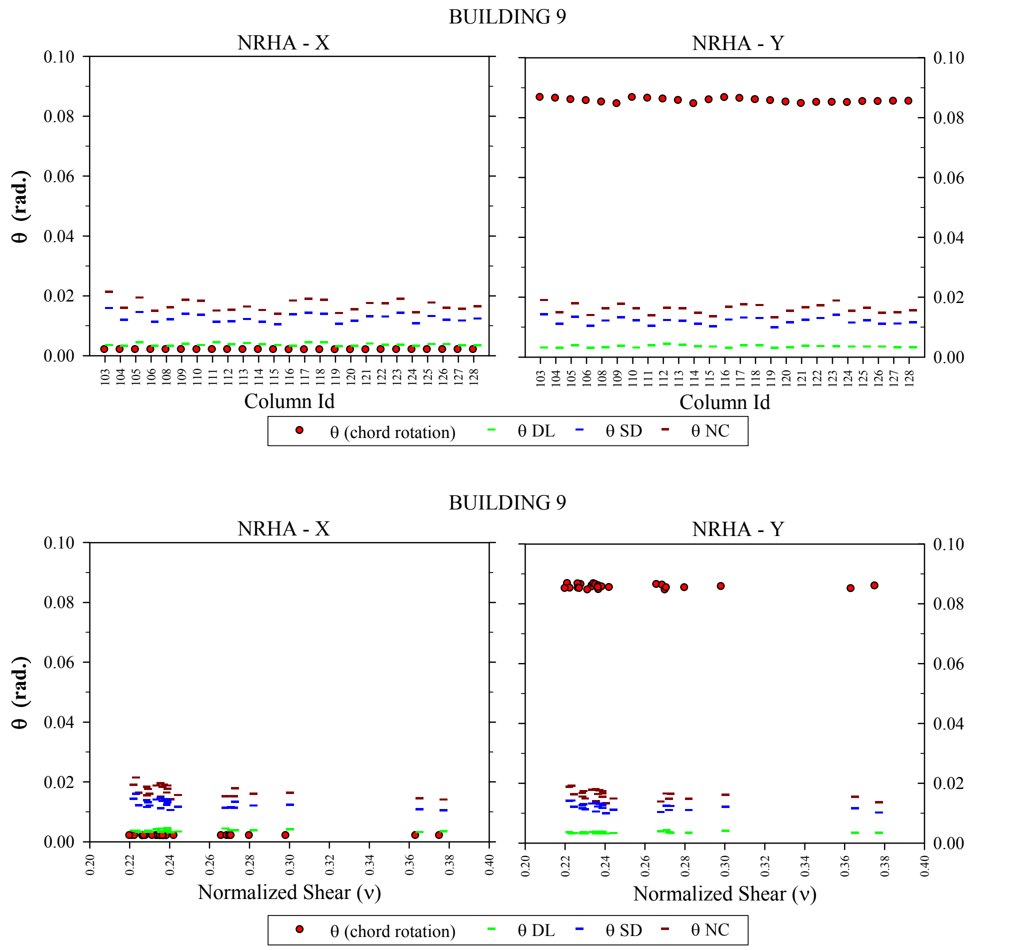

Figure 6.79 Chord Rotation, θ, results for Building 9 columns, computed by NRHA in X and Y directions

When the chord rotation demands for the columns are plotted against the normalized shear (ν), no obvious trend line was observed within the range.

At the performance points estimated by approximate procedures (NSPs), the NSA of EC8-3 applied. The assessment results for these performance points, in X and Y directions are shown in Figure 6.80 and Figure 6.81, respectively.

Although, the building was evaluated as moderately damaged (damage control range) at performance points of Eq. SDOF and MMPA, and within damage limitation (DL) damage state at performance points of DCMs of both FEMA-356 and FEMA-440, the failure mode of the building in X direction was brittle shear failure.

In the Y direction, the building was evaluated as moderately damaged (within damage control range) according to the chord rotation demands of critical story columns at performance points of DCMs of both FEMA-356 and FEMA-440. This assessment result of EC8-3 was inconsistent with the severe damage observed during the earthquake.

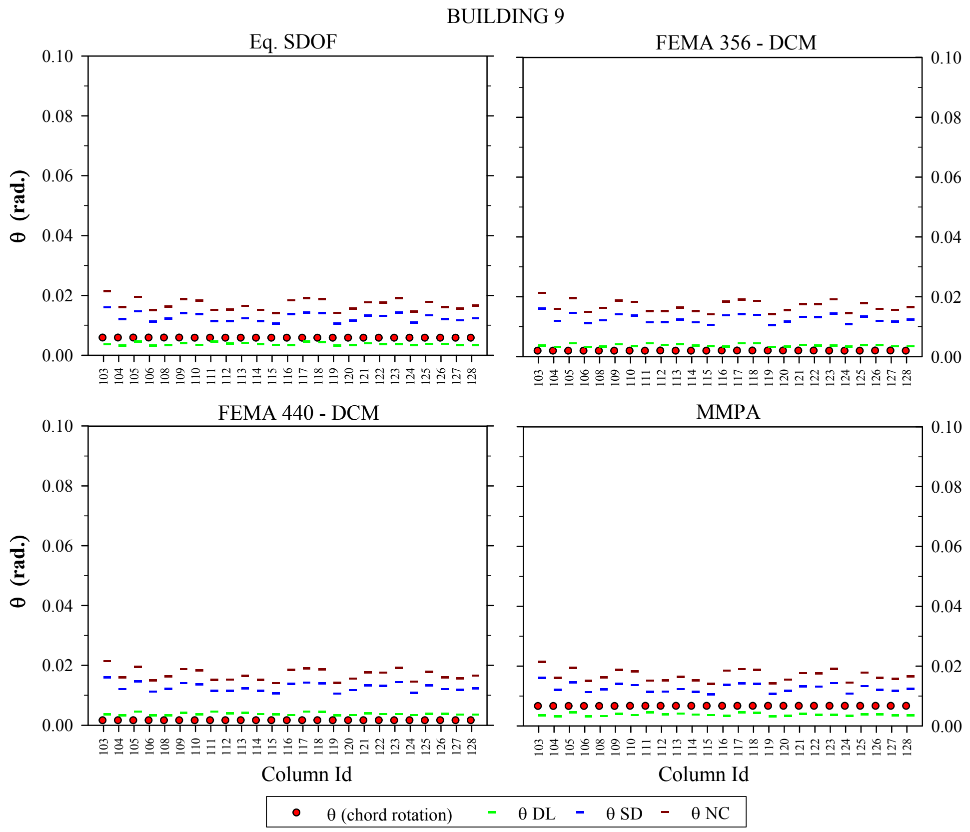

Figure 6.80 Chord Rotation, θ, results for Building 9 columns, computed by Eq. SDOF, FEMA356-DCM, FEMA440-DCM and MMPA in the X direction

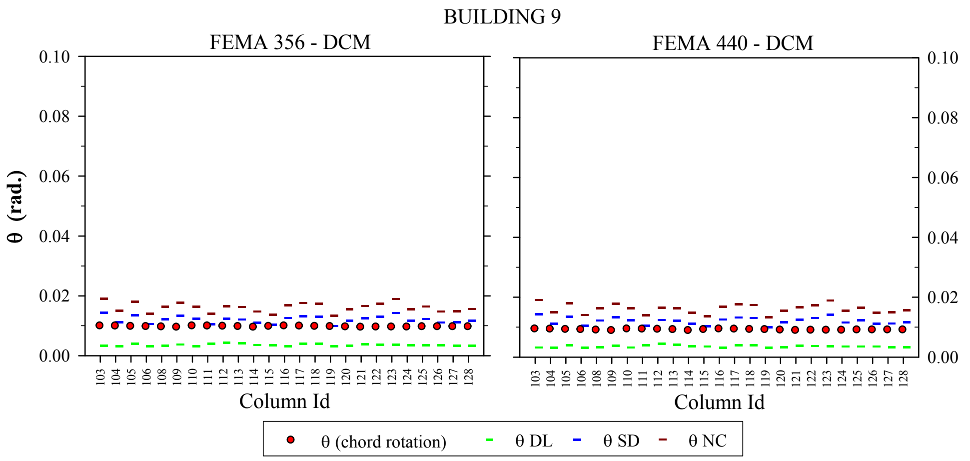

Figure 6.81 Chord Rotation, θ, results for Building 9 columns, computed by FEMA356-DCM and FEMA440-DCM in the Y direction

6.5.10 Building #10

The critical story of the building was selected as the ground story. This story has 26 columns. The maximum chord rotation demands obtained by NRHA, in both X and Y directions of the building are shown in Figure 6.82.

All columns of the critical story were expected to collapse by NDP of EC8-3, in both X and Y directions of the building. Therefore, the overall damage state of the building was determined as collapsed. This evaluation is parallel to the assessments by ASCE/SEI-41 and TEC-2007.

In addition to the severe damage of critical story, upper stories were also expected to be moderately damaged, for all cases.

When the chord rotation demands for the columns are plotted against the normalized shear (ν), no obvious trend line was observed within the range.

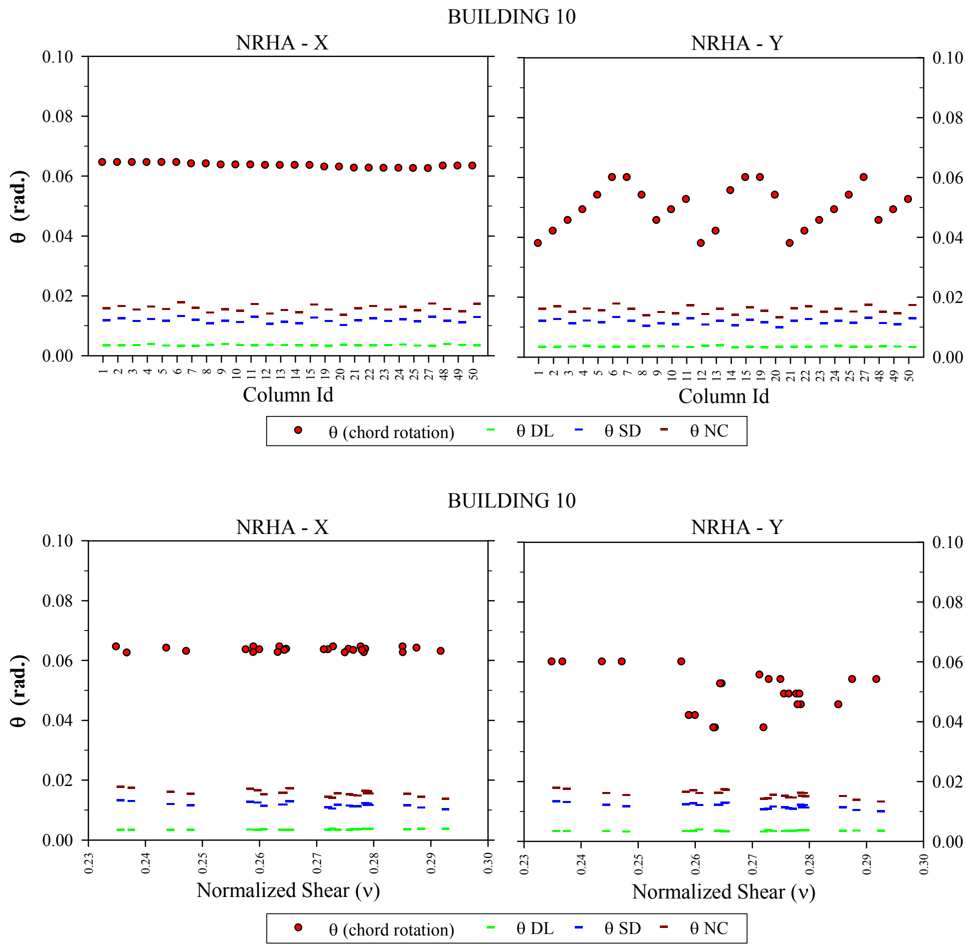

Figure 6.82 Chord Rotation, θ, results for Building 10 columns, computed by NRHA in X and Y directions

The NSA of EC8-3 was applied at ultimate roof displacement of the pushover curve in the X direction and at the performance points estimated by approximate procedures (NSPs) in the Y direction. The assessment results for these performance points, in X and Y directions are shown in Figure 6.83 and Figure 6.84, respectively.

At ultimate roof drift computed by pushover analysis, in the X direction, all columns were expected to collapse according to the NSA of EC8-3. Furthermore, in the Y direction, at both performance points of FEMA-356 and FEMA-440, all the critical story columns were expected to collapse, according to NSA of EC8-3, similar to the results of both ASCE/SEI-41 and TEC-2007.

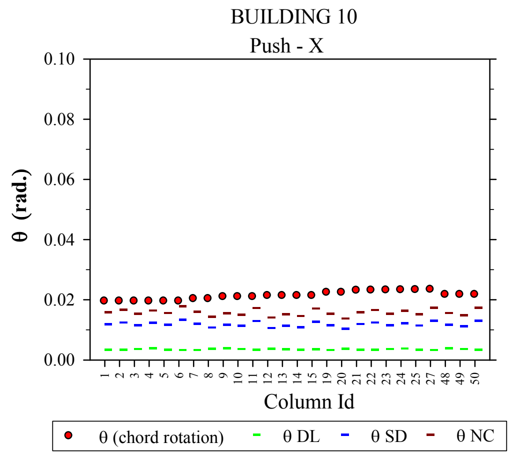

Figure 6.83 Chord Rotation, θ, results for Building 10 columns, computed at ultimate roof displacement of the pushover curve in the X direction

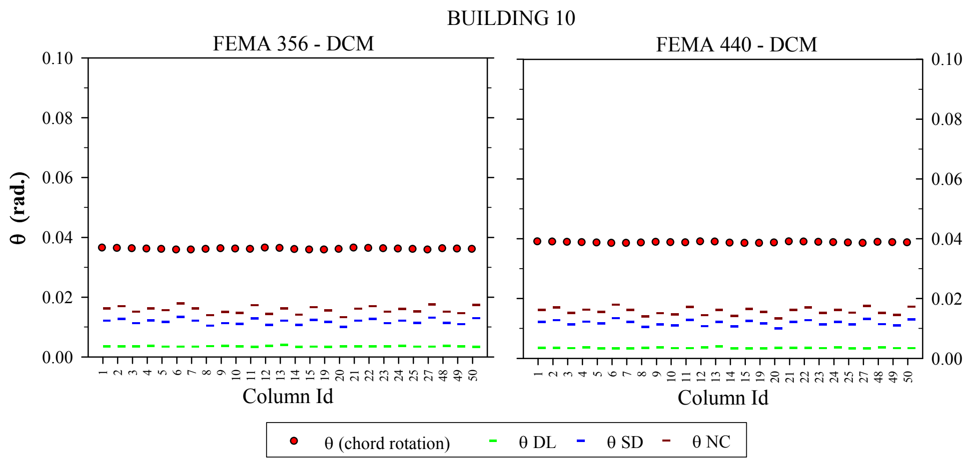

Figure 6.84 Chord Rotation, θ, results for Building 10 columns, computed by FEMA356-DCM and FEMA440-DCM in the Y direction

6.6 DISCUSSION OF THE ASSESSMENT RESULTS AND COMPARISONS

Ten selected buildings were investigated by applying the detailed assessment procedures of current three important codes of ASCE/SEI-41 and its Supplement-1 (ASCE 2007, ASCE 2008), TEC-2007, and EC8-3 (EC 2005). Nonlinear Dynamic Procedure (NDP) and Nonlinear Static Assessment Procedure (NSA) were applied based on the results of Nonlinear Response History Analysis (NRHA) and Pushover Analysis, which were discussed in Sections 5.5 and 5.6, respectively.

Since there was no detailed damage report of the buildings in hand, the detailed assessment results on columns could not be compared with the actual member damages. However, this comparison was focused on corresponding overall damage.

As a summary, although, the detailed assessments resulted with varying degrees of damage levels for the columns, all buildings examined were evaluated as “severely damaged” or “collapsed” by all detailed assessment procedures of all codes considered, regardless of their actual damage state observed during the earthquake. In this sense, the damage states of the moderately damaged buildings (Buildings #1 to #5) were also estimated as “severe damage” or “collapsed”, similar to the severely damaged buildings. Therefore, actual damage states could not be replicated, and the buildings could not be qualified, using any of these detailed assessment procedures.

The calculated performance levels of the buildings overestimated the observed damage levels (especially for the moderately damaged buildings). From this point of view, when all assessment results are examined for all buildings (not only for critical stories), it can be concluded that while TEC-2007 is the least accurate, on the basis of the estimated damage on columns of these 10 buildings.

Since it was thought that the acceptance criteria of the ASCE/SEI-41 (ASCE 2007) were conservative; they were liberalized by its Supplement-1 (ASCE 2008), as discussed in Section 2.4.2. According to the detailed assessments of the moderately damaged buildings (Buildings #1 to #5), the current criteria can still be decided as "conservative", compared to the damage states observed.

Similar conservative assessment results are thought to be related with the high safety margin of the codes, especially for the nonconforming transverse reinforcement condition. This high safety margin is a natural result of limited research on the seismic behavior of similarly constructed RC buildings because laboratory specimen details are not deliberately made poor in the interest of replicating particular construction practices. On the other hand, the definitions of the acceptance criteria and the corresponding deformation parameters are different for each of the detailed assessment procedure.

According to TEC-2007 assessment results, in general, the concrete material was reached to its ultimate strain value before the steel material, due to low material strength. Thus, the overall member damage state was controlled by concrete.

In consequence of the damage parameter used (chord rotation) by EC8-3, the damage states of the columns in any story (given that the story height is constant) are more or less the same, especially if the torsional irregularity does not affect, since the rigid diaphragm constraint applied in building models.

However, it can be concluded that the detailed assessment results of all documents investigated, i.e. ASCE/SEI-41, TEC-2007 and EC8-3, are consistent with the global damage indicator of ISDR, which was discussed in Section 5.5.1. Even though the global acceptability limits proposed by only TEC-2007 and ATC-40, high interstory drift demands are correlated with the structural member deformations. Thus, all the buildings studied were evaluated as severely damaged, due to high deformation demands. Furthermore, in general, the structural mechanism of “soft story” was very likely for the buildings studied.

The assessment results may be precise enough for the test structures in laboratories. However, the consistency of the damage expectations by the assessment procedures with the field observations is much less, due to the variability of actual properties of the existing buildings, as well as the ground motion at the site. The valuable information about the seismic behavior of reinforced concrete buildings obtained from the tests should be supported with more data obtained from the field. This strikes a pessimistic tone because if the inconsistencies between field data and assessment procedures described in guidelines on account of fluctuations of material properties, geometries, ground motion variations and many other parameters considered then a clear need exists to be sanguine about the predictive powers of these methods.

To conclude, this study revealed that the actual damage states of the buildings studied after the earthquake were not consistent with the assessment results of both global and local scales, especially for the moderately damaged buildings.

CHAPTER 7

EVALUATION USING PRELIMINARY ASSESSMENT PROCEDURES

7.1 INTRODUCTION

The actual damage states of the buildings were estimated using detailed assessment procedures at the performance points obtained from NSPs, as discussed in previous chapters. However, actual damage states could not be obtained and the buildings could not be accurately qualified, using none of these detailed assessment procedures (Section 6.6). Therefore, considering the high effort given for the computation and post-process of the analyses results regardless of reliable evaluation results, global seismic performance of the buildings were also assessed by preliminary assessment procedures.

While, the detailed assessment procedures examine the buildings using detailed information about the building and the force-resisting frame system; the preliminary assessment procedures are more quick methods in order to determine the priority of detailed assessment for the building inventories using the limited data of general properties and/or irregularities of the buildings. Actually, the main objective of the preliminary assessment procedures proposed is to identify the buildings that are highly vulnerable to damage.

The subject buildings of this study were evaluated to determine their likely performance under the given ground motion effects, by preliminary assessment procedures proposed by Hassan and Sözen (1997), Yakut (2004) and Özcebe et al. (2004), that are one level below of the accuracy of the detailed assessment procedures.

In this chapter, the general features of the preliminary assessment procedures, their applications on the buildings studied and corresponding assessment results are presented, and these assessment results are compared with the results of both detailed assessment results and the real damage states observed during the earthquake.

7.2 PRELIMINARY ASSESSMENT PROCEDURES

7.2.1 Hassan and Sözen (1997) Procedure

This procedure is proposed for reinforced concrete, low rise, and monolithic buildings as a simplified method of ranking according to their vulnerability to seismic damage. In order to apply the procedure, only the lateral load resisting member dimensions and the total floor area are required. The procedure does not take material properties, quality, architectural features, and regional seismicity into consideration. Actually, the material quality and type of construction are assumed to be reasonably uniform, as well as the earthquake demand. Although, the database for the procedure was taken from Erzincan, Turkey, this is a drawback for the procedure. However, the objective is to qualify the vulnerable low rise RC buildings by simple calculations.

To rank the buildings, each building is represented by a point in a two-coordinate representation. In this representation, the x-axis represents the "column index (*CI*)", while the y-axis represents the "wall index (*WI*)". These indices are computed by the Equations (7.1) and (7.2).

$$CI = \frac{A_{ce}}{A_{ft}} * 100 \tag{7.1}$$

$$WI = \frac{A_{wt}}{A_{ft}} * 100 \tag{7.2}$$

where,

$A_{ce} = \frac{A_{col}}{2} =$ the effective cross-sectional area of columns at base,

$A_{wt} = A_{cw} + \frac{A_{mw}}{10} =$ the effective cross-sectional area of walls in a given horizontal direction,

A_{col} is the total cross-sectional area of columns above base,

A_{cw} is the total cross-sectional area of the RC walls in one horizontal direction at base,

A_{mw} is the cross-sectional area of the unreinforced masonry infill walls in one horizontal direction at base,

A_{ft} is the total floor are above base in a building.

The application of the Hassan and Sözen (1997) procedure is shown in Table 7.1. The preliminary assessment procedure was applied in both X and Y directions, separately. For the buildings studied, the infill wall thicknesses were assumed to be constant and equal to 20 cm and members with a dimension of 1.0 m and above have been assumed as structural walls. The evaluation results are shown in Figure 7.1 in graphical format.

Table 7.1 Hassan and Sözen (1997) preliminary assessment on the buildings studied

Building ID No	Dir.	Number of Stories	Total Floor Area, m^2	Column Area at Base, m^2	RC Wall Area at Base, m^2	Masonry Wall Length at Base, m	Column Index, %	Wall Index, %	Damage State
1	X	5	1265.34	5.00	0	40	0.20	0.08	Moderate
	Y		1265.34	5.00	0	75	0.20	0.15	
2	X	5	2108	7.44	0	144	0.18	0.17	Moderate
	Y		2108	7.44	0	85	0.18	0.10	
3	X	4	1365	9.17	0	80	0.34	0.15	Moderate
	Y		1365	9.17	0	72	0.34	0.13	
4	X	4	485	2.73	0	26	0.28	0.13	Moderate
	Y		485	2.73	0	20	0.28	0.10	
5	X	5	910.2	3.24	0.48	55	0.18	0.20	Moderate
	Y		910.2	3.24	0.24	65.6	0.18	0.21	
6	X	5	550.05	3.24	0	22.8	0.29	0.10	Moderate
	Y		550.05	3.24	0	28.95	0.29	0.13	
7	X	6	1144.5	2.42	0	43.6	0.11	0.10	Severe
	Y		1144.5	2.42	0.64	68	0.11	0.20	
8	X	5	585.2	2.02	0.44	36	0.17	0.23	Moderate
	Y		585.2	2.02	0.2	33	0.17	0.18	
9	X	6	1285.1	1.02	5.46	100	0.04	0.62	Severe
	Y		1285.1	1.02	0.72	40.5	0.04	0.13	
10	X	5	1487.5	7.80	0	61.5	0.26	0.10	Moderate
	Y		1487.5	7.80	0	45	0.26	0.08	

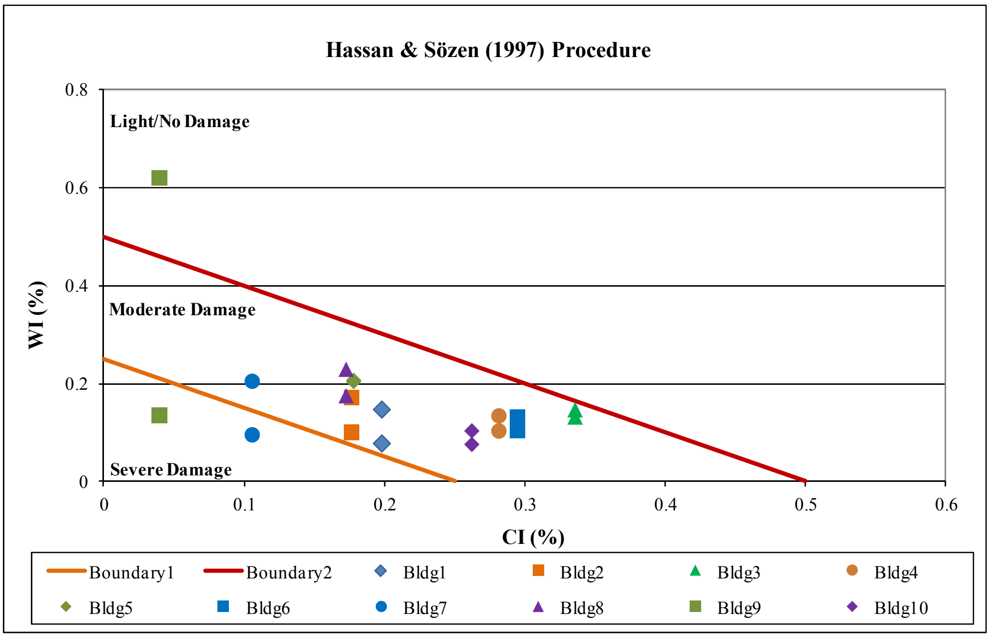

Figure 7.1 Preliminary assessment results of Hassan and Sözen (1997) procedure

The boundaries for the damage regions that are shown in Figure 7.1 are taken from the proposed study, considering that the buildings evaluated in this study were selected from another first-degree earthquake zone as Erzincan. However, in the proposed procedure, it is emphasized that there is no absolute basis for locating the boundaries, and the graphical scheme is simply to evaluate the relative vulnerability of the buildings in a given region.

The results of preliminary assessments according to Hassan & Sözen Procedure imply that the expected damage states were accurate for the moderately damaged buildings during the earthquake, either in X and Y directions of the buildings, in contrary with the detailed assessment results that were discussed in Chapter 6. For severely damaged buildings, on the other hand, the evaluation results generally underestimated the damage states. Only for building 7 and building 9, the results were accurate in one direction of the building. The remaining 3 severely damaged buildings (building 6, building 8 and building 10) were expected to be moderately damaged according to this preliminary assessment.

This procedure is effective for the selection of buildings with higher seismic vulnerability. The method requires only the dimensions of the structure as input. But the procedure does not account for strength (quality) of concrete, quality of construction, as-built properties (detailing), regional seismicity, type of underlying soil, the negative effect of architectural features and the quality of construction. In addition, the effect of well-accepted secondary factors such as soft story, short column, and vertical irregularity are not taken into account. These are the drawbacks for this procedure. Further detailed assessment is required for the building.

7.2.2 Yakut (2004) Procedure

The proposed preliminary assessment procedure is prepared based on the information of major damages occurred in recent earthquakes. The main reasons of structural damage indicated by post-earthquake observations can be classified as;

- improper configuration of architectural and structural system,
- poor and inadequate detailing and proportioning,
- substandard construction quality due to lack of technical control and supervision.

Since these reasons were underlying of the significant earthquake damage observed, they should be considered in any assessment procedure for adequate evaluation. Yakut (2004) procedure is an improved preliminary vulnerability assessment technique trying to minimize the drawbacks of preliminary procedures and result in more adequate predictions.

Yakut (2004) procedure computes a "Capacity Index (*CPI*)" for ranking the RC buildings, according to their vulnerability to seismic damage. This index considers the orientation, size and material properties of the components that consists lateral load resisting structural system. The advantageous side of this procedure is that, it takes quality of workmanship and materials, and architectural features into account, modifying Capacity Index (*CPI*) with some coefficients related especially to the secondary factors such as soft story, short column, and vertical irregularity.

Using the ground floor dimensions, size, orientation and concrete strength of the components comprising the lateral load resisting system, the base shear capacity of the building is calculated. Base shear capacity (V_c) of the ground floor is computed by summing the shear capacities of the individual columns (V_{ci}). The base shear capacity is approximated based on the concrete contribution as given in Equation (7.3).

$$V_c = \sum V_{ci} = c * \alpha * f_{ctk} * b_w * h \quad \textbf{(7.3)}$$

In this equation, the coefficient, c, is taken as 2/3 when the capacity in the longitudinal direction of the member is calculated, and 1/3 in the transverse direction, in order to consider the column orientation. The coefficient, c, is used as 1.0 for longitudinal direction of the shear walls. The coefficient, α, is taken as 0.65 depending on Turkish Design Code (2000) and it represents the combined effect of strength reduction factor and the empirical coefficient that relates shear strength to the tensile strength. The concrete tensile strength, f_{ctk}, is computed as 1.08 MPa (TS500) for the buildings studied and b_w and h represent the dimensions of the member.

An empirical relation is proposed for the yield base shear capacity calculation (V_y), as a function of the computed base shear capacity (V_c) and number of stories (n), as given in Equation (7.4), that is only applicable for the buildings without infill walls.

$$V_y = \frac{V_c}{0.95e^{0.125n}} \quad \textbf{(7.4)}$$

Considering the influence of infill walls on the lateral load resistance of the building, the yield base shear capacity with infill walls (V_{yw}) is computed using the empirical relation given in Equation (7.5), where A_w is the total area of the infill walls and A_{tf} is the total floor area of the building.

$$V_{yw} = V_y\left(46\frac{A_w}{A_{tf}} + 1\right) \quad \textbf{(7.5)}$$

The Basic Capacity Index (BCPI), which is also called as yield over-strength ratio in literature, is computed by Equation (7.6), where V_{code} is the code required design base shear. For the buildings studied here, V_{code} values were obtained dividing the total weight of the building by the reduction factor, R. The R factor was used as 4, assuming the ductility capacity of the buildings as normal.

$$BCPI = \frac{V_{yw}}{V_{code}} \quad \textbf{(7.6)}$$

It should be noted that the seismic zone and the soil condition are implicitly considered by the computation of code required base shear (V_{code}), since V_{code} is based on the regional seismicity and soil type of the site.

In order to reflect the architectural features and construction quality, *BCPI* is attempted to improve by introducing the coefficients, C_A and C_M, respectively, and Capacity Index (*CPI*) is computed by Equation (7.7). For the preliminary assessments of the buildings studied here, C_A is taken as 0.85 which is given as a reasonable alternative by Yakut (2004). This coefficient of C_A accounts for the soft story behavior, presence of short column, plan irregularity and significance of overhangs. The buildings studied are considered as 'average' in terms of quality and construction workmanship. For the average construction quality, the C_M is calculated by Equation (7.8), assuming the Q_r value as 0.55 as recommended for Turkey by Yakut (2004).

$$CPI = C_A * C_M * BCPI \quad \textbf{(7.7)}$$

$$C_M = 1.0 - Q_r(1 - C_A)/3 \quad \textbf{(7.8)}$$

The computed *CPI* value for an existing building is compared against a benchmark *CPI* value of 1.2, which is provided by Yakut (2004), according to the studies on databases comprised of Turkish building inventory. The values higher than the benchmark value imply that the building is "safe".

The application of the Yakut (2004) procedure is given in Table 7.2, for X and Y directions, separately. In consistent with the Hassan and Sözen procedure, the infill wall thicknesses were assumed to be constant and equal to 20 cm and members with a dimension of 1.0 m and above have been assumed as structural walls. The total infill wall length of the ground story and corresponding wall area values for each building are given in the table. The base shear capacity values are also shown and the indices of *BCPI* and *CPI* are computed. The computed capacity indices are compared with the benchmark *CPI* value of 1.2, as shown in Figure 7.2.

Table 7.2 Yakut (2004) preliminary assessment on the buildings studied

Building ID No	Dir.	L_w (m)	A_w (m^2)	A_{tf} (m^2)	V_y (kN)	V_{yw} (kN)	V_{code} (kN)	BCPI	CPI
1	X	40	8.0	1265	794	1025	3535	0.29	0.24
	Y	75	15.0	1265	1445	2232	3535	0.63	0.52
2	X	144	28.8	2108	1580	2573	5559	0.46	0.38
	Y	85	17.0	2108	1359	1863	5559	0.34	0.28
3	X	80	16.0	1365	1951	3003	4141	0.73	0.60
	Y	72	14.4	1365	2235	3320	4141	0.80	0.66
4	X	26	5.2	485	689	1029	1600	0.64	0.53
	Y	20	4.0	485	667	920	1600	0.57	0.48
5	X	55	11.0	910	785	1221	2944	0.41	0.34
	Y	66	13.1	910	1043	1735	2944	0.59	0.49
6	X	23	4.6	550	577	797	1878	0.42	0.35
	Y	29	5.8	550	703	1044	1878	0.56	0.46
7	X	44	8.7	1145	421	568	2120	0.27	0.22
	Y	68	13.6	1145	721	1114	2120	0.53	0.43
8	X	36	7.2	585	503	788	1771	0.44	0.37
	Y	33	6.6	585	632	960	1771	0.54	0.45
9	X	100	20.0	1285	2165	3714	3966	0.94	0.77
	Y	41	8.1	1285	1029	1327	3966	0.33	0.28
10	X	62	12.3	1488	1550	2140	4545	0.47	0.39
	Y	45	9.0	1488	1312	1677	4545	0.37	0.30

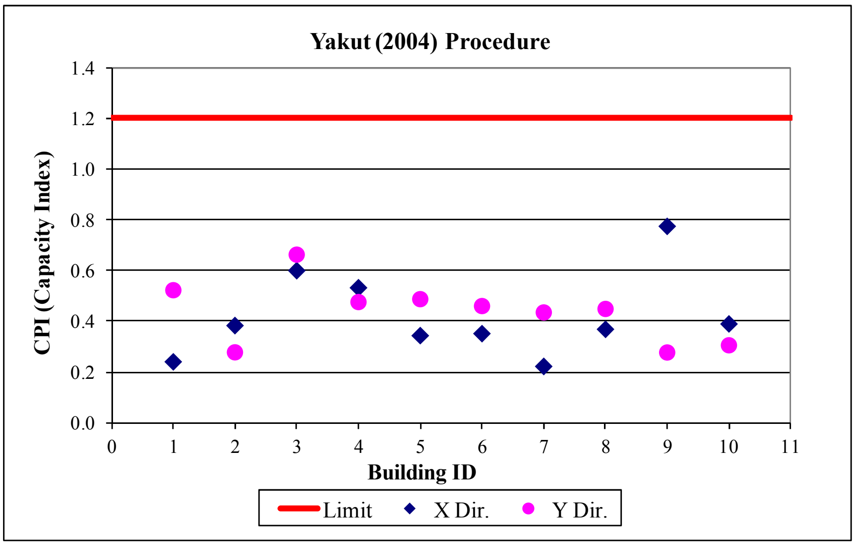

Figure 7.2 Preliminary assessment results of Yakut (2004) procedure

According to Yakut (2004) procedure, all the buildings assessed were expected to be unsafe, since all capacity indices (*CPI*) computed were lower than the limit value of 1.2. The *CPI* values computed for the moderately damaged buildings during the earthquake (Buildings 1 to 5) were slightly higher than those for severely damaged buildings (Buildings 6 to 10). Although, the difference was not so clear, in order to qualify the level of damage, all buildings were expected to be damaged (unsafe). Furthermore, since, this is a simplified procedure for ranking the vulnerable structures, further detailed assessments required for a reasonable vulnerability assessment for seismic damage.

In contrary with the Hassan & Sözen Procedure, this procedure requires not only the dimensions of the structure as input, but also accounts for strength (quality) of concrete, quality of construction, as-built properties (detailing), the negative effect of architectural features (soft story, short column, and vertical irregularity) and the quality of construction.

The max capacity index (CPI) was expected for the building 9 in X direction, where most of the vertical structural members were designed as structural walls in this direction. However, since the concrete strength which was used as 9.5 MPa, the computed value of base shear capacity, V_c, (which is approximated based on the concrete contribution) was lower than the design base shear, V_{code}. This situation was also valid for other buildings studied here.

7.2.3 Özcebe et al. (2004) Procedure

In general, recent post-earthquake investigations showed that the construction practice in Turkey does not successfully reflect the earthquake resistant design rules. Therefore, statistical analysis based on observations would provide more reliable results, especially for the regional assessments. After the 1999 earthquakes that shaked Marmara region of Turkey, another preliminary assessment procedure was proposed by Özcebe et al. (2004) based on statistical discriminant analysis of the observed damage in the city of Düzce and significant building attributes that are believed to affect the seismic performance. This preliminary assessment procedure was developed for low- to mid-rise RC buildings in order to provide more reliable and accurate results for regional assessments. The procedure was improved by inclusion of site characterisric effects, i.e. soil properties and distance to the source in the companion study (Yakut et al., 2006). In this sense, the procedure is the only preliminary assessment procedure that local site conditions and fault distance are considered.

According to the procedure, the existing buildings are classified as “safe”, “unsafe”, and “intermediate” by the damage scores that are obtained from the discriminant functions generated. The damage inducing parameters used in functions are given as number of stories (*N*), minimum normalized lateral stiffness index (*MNLSTFI*), minimum normalized lateral strength index (*MNLSI*), normalized redundancy score (*NRS*), soft story index (*SSI*) and overhang ratio (*OR*).

The index *MNLSTFI*, is defined as the indication of the lateral rigidity of the ground story, which is usually the most critical story. The columns and the structural walls at the ground story are considered and the index is computed as given in Equations (7.9) and (7.10).

$$MNLSTFI = \min(I_{nx}, I_{ny}) \tag{7.9}$$

$$I_{nx} = \frac{\sum (I_{col})_x + \sum (I_{sw})_x}{\sum A_f} \times 1000$$
$$I_{ny} = \frac{\sum (I_{col})_y + \sum (I_{sw})_y}{\sum A_f} \times 1000 \tag{7.10}$$

where,

I_{nx} and I_{ny} are total normalized moment of inertia of all members about x and y axes, respectively,

$(I_{col})_x$ and $(I_{col})_y$ are the moment of inertias of columns about x and y axes, respectively,

$(I_{sw})_x$ and $(I_{sw})_y$ are the moment of inertias of structural walls about x and y axes, respectively,

A_f is the total story area above ground level.

As the indication of the base shear capacity of the critical story, the index *MNLSI* is defined. For the calculation of index, masonry infill walls are also considered in addition to the columns and structural walls. The index *MNLSI* is calculated as given in Equations (7.11) through (7.12).

$$MNLSI = \min(A_{nx}, A_{ny}) \tag{7.11}$$

$$A_{ni} = \frac{\sum (A_{col})_i + \sum (A_{sw})_i + 0.1 * \sum (A_{mw})_i}{\sum A_f} \times 1000 \tag{7.12}$$

$$(A_{col})_i = k_i \cdot A_{col} \quad ; \quad (A_{sw})_i = k_i \cdot A_{sw} \quad ; \quad (A_{mw})_i = k_i \cdot A_{mw} \tag{7.13}$$

where,

i is the subcript representing each of x and y directions,

A_{col} is the effective cross sectional area of columns,

A_{sw} is the effective cross sectional area of structural walls,

A_{mw} is the effective cross sectional area of masonry infill walls,

k is the strength partitioning factor.

Here;

If x is the major axis of a rectangular column, k_x shall be equal to 2/3 for rectangular columns, and 1.0 for both structural walls and masonry infill walls. In all cases, $k_y = 1 - k_x$. For square and circular columns, $k_x = k_y = 1/2$.

The normalized redundancy score, *NRS*, is defined in order to indicate the degree of the continuity of multiple frame lines to distribute lateral forces throughout the structural system. For this purpose, firstly normalized redundancy ratio, NRR, is calculated by Equation (7.14).

$$NRR = \frac{A_{tr}(nf_x - 1)(nf_y - 1)}{A_{gf}} \quad \textbf{(7.14)}$$

where,

A_{tr} is the tributary area of a typical column,

nf_x and nf_y are number of continuos frame lines in x and y directions, respectively,

A_{gf} is the area of the ground (critical) story.

Here, the value of *Atr* depends on the number of continuous frame lines, nf_x and nf_y; where *Atr* is 25 m^2 if nf_x and nf_y are both equal or greater than 3, otherwise, in all other cases, *Atr* shall be taken as 12.5 m^2, as an additional penalty for such vulnerable buildings.

Depending on the *NRR* values calculated, the *NRS* scores are defined in Equation (7.15).

$$\begin{gathered} NRS = 1 \quad \text{for } 0 < NRR \leq 0.5 \\ NRS = 2 \quad \text{for } 0.5 < NRR \leq 1.0 \\ NRS = 3 \quad \text{for } 1.0 < NRR \end{gathered} \tag{7.15}$$

Soft story index, *SSI*, is the ratio of the height of the ground story, H_1, to the height of the second story, H_2 (Equation (7.16)). It is known that lack of infill walls in ground story is another factor for soft story, but it was taken into account in the calculation of *MNLSI*.

$$SSI = \frac{H_1}{H_2} \tag{7.16}$$

Lastly, overhang ratio, OR, is considered as a damage inducing parameter. In a typical floor plan, the area beyond the outermost frame lines on all sides is defined as the overhang area. Therefore, the OR is the ratio of the overhang area of a typical story, $A_{overhang}$, to the area of ground story, A_{gf}. (Equation (7.17))

$$OR = \frac{A_{overhang}}{A_{gf}} \tag{7.17}$$

Based on the parameters given above, a statistical model was proposed which is the result of the discriminant analysis. According to this statistical model, two distinct "Damage Index (or Damage Score)" functions were developed for "Life Safety (DI_{LS})" and "Immediate Occupancy (DI_{IO})" damage states, as given in Equations (7.18) and (7.19).

$$DI_{LS} = 0.620 \cdot N + 3.269 \cdot SSI + 2.728 \cdot OR - 0.246 \cdot MNLSTFI - 0.182 \cdot MNLSI - 0.699 \cdot NRS - 4.905 \quad \textbf{(7.18)}$$

$$DI_{IO} = 0.808 \cdot N + 0.508 \cdot SSI + 3.884 \cdot OR - 0.334 \cdot MNLSTFI - 0.107 \cdot MNLSI - 0.687 \cdot NRS - 2.868 \quad \textbf{(7.19)}$$

According to the proposed procedure, the number of story variable came out as the most significant parameter in both performance classifications. Thus, in order to classify the buildings, the cut-off values are defined based on the number of stories (CVR_{LS} and CVR_{IO}), as shown in Table 7.3.

Table 7.3 Number of story based cut-off values (*CVR*)

n	$\mathbf{CVR_{LS}}$	$\mathbf{CVR_{IO}}$
3	0.383	-0.425
4	0.430	-0.609
5	0.495	-0.001
6	1.265	0.889
7	1.791	1.551

The building is classified as “Safe (none or light damage – in low seismic risk group)”, if both damage indices are less than the corresponding cut-off values. If both damage indices are greater than the corresponding cut-off values, than it is judged that the building is “Unsafe (severe damage or collapse – in high seismic risk group)”. In case of the presence other than these situations, the building is classified as “requires further detailed evaluation (in moderate seismic risk group)”.

The procedure is emerged based on the statistical database of seismic damage compiled from Düzce city center after the November 12, 1999, Düzce Earthquake, where the soil conditions were uniform (quaternary alluvial deposits). Thus, the earthquake excitation was thought to be equivalent for all buildings in the site. The cut-off values recommended by Özcebe et al. (2004) are considered to be valid for damaging earthquakes and the regions that have similar distance to source and site conditions to that of the studied area in Düzce. In order to provide the applicability to other regions, the procedure was improved by introducing of site characteristics, i.e. soil conditions, site-to-source distance and the magnitude of the earthquake (Yakut et al., 2006). For this purpose, modified cut-off values were computed for different sites having different values of distance to source and different soil types.

Since the spectral displacement, S_d, is believed to be a well correlated response quantity with the structural damage, it was used in order to reflect the variation of ground motion and dynamic properties of the buildings. Considering various attenuation relationships proposed for North Anatolian Fault (NAF), and the soil types designated by Turkish Seismic Code (1997), S_d values were obtained for various period values representing different number of stories. Then, the S_d values computed were normalized by number of stories, and assuming that the change of the cut-off values follow an exponential trend the cut-off modification coefficients, *CMC*, were computed. Although, the cut-off modification coefficients, *CMC*, were computed for various magnitudes, i.e. 6.5, 7.0 and 7.4, the *CMC* values for moment magnitude of 7.4 are given in Table 7.4, since the August 17, 1999, earthquake is also covered.

The *CMC* computed for the distance (5-8 km) and soil type (V_s=201~400 m/s) representing Düzce as well, is unity, because of the normalization with respect to this site. As it can be seen in the *CMC* values increase by increasing distance as well as increasing shear wave velocity, which causes to decrease the number of buildings in high seismic risk group.

The modified cut-off values, *CV*, are obtained by multiplication of these *CMC* values by the reference cut-off values, *CVR*, that are given in Table 7.3.

Table 7.4 Cut-off modification coefficients, *CMC*, for $M_w = 7.4$.

V_s (m/s)	Distance (km)				
	0-4	**5-8**	**9-15**	**16-25**	**26+**
0-200	0.778	0.824	0.928	1.128	1.538
201-400	0.864	1.000	1.240	1.642	2.414
401-700	0.970	1.180	1.530	2.099	3.177
701+	1.082	1.360	1.810	2.534	3.900

The preliminary procedure summarized above was applied to the buildings studied. The damage inducing parameters for each of the buildings and accordingly calculated damage indices (*DI*) are given in Table 7.5. The damage indices computed were compared with the modified cut-off values (*CV*) for Sakarya/Adapazarı and the final decision about each of the building was set. The evaluation results are given in Table 7.6, including the corresponding cut-off values (*CVR*), modification factors (*CMC*), and modified cut-off values (*CV*). The information for the distance to fault and shear wave velocity at site can be found in Table 4.2, for each of the building.

In contrary with the results of preliminary assessments according to Hassan & Sözen Procedure, the assessment results of Özcebe et al Procedure for the severely damaged buildings were more accurate than for the moderately damaged buildings. High seismic risk was accurately estimated by the procedure, for all severely damaged buildings. Relatively low seismic risk of the moderately damaged buildings studied, on the other hand, were also estimated by the procedure. Seismic Risk was estimated as “low” to “moderate” for four out of five moderately damaged buildings. However, only the Building 1 was estimated as “Unsafe”, due to the effects of *SSI* and *NRS* indices which are the results of both plan and vertical irregularities in building. The seismic risk for Buildings 2 and 4 was underestimated by the preliminary assessment procedure. These buildings have less overhanging ratios and fewer irregularities than the others. Thus, they were evaluated as “Safe”.

Further detailed assessment is recommended for the buildings evaluated as "in moderate seismic risk group".

Table 7.5 Damage inducing parameters and corresponding Damage Indices

Building ID No	N	MNLSTFI	MNLSI	NRS	SSI	OR	DI_{LS}	DI_{IO}
1	4	0.063	2.034	1.0	1.679	0.10	2.239	0.664
2	5	0.060	2.438	3.0	0.893	0.00	-1.442	-0.716
3	4	0.136	4.365	2.0	1.429	0.11	0.331	-0.353
4	4	0.136	3.897	2.0	1.429	0.02	0.156	-0.674
5	5	0.110	3.215	2.0	0.857	0.09	-0.774	0.193
6	5	0.104	3.483	2.0	1.500	0.01	1.078	0.205
7	6	0.073	2.889	1.0	1.429	0.00	2.242	1.685
8	5	0.080	3.292	1.0	0.909	0.23	0.480	1.467
9	6	0.129	1.443	1.0	1.123	0.04	1.599	1.819
10	5	0.120	3.165	1.0	1.379	0.00	1.399	0.807

Table 7.6 The cut-off values and the evaluation results

Building ID No	CVR_{LS}	CVR_{IO}	CMC	CV_{LS}	CV_{IO}	Final Decision
1	0.430	-0.609	0.928	0.399	-0.565	High Seismic Risk
2	0.495	-0.001	0.928	0.459	-0.001	Low Seismic Risk
3	0.430	-0.609	0.928	0.399	-0.565	Moderate Seismic Risk
4	0.430	-0.609	0.928	0.399	-0.565	Low Seismic Risk
5	0.495	-0.001	0.928	0.459	-0.001	Moderate Seismic Risk
6	0.495	-0.001	1.240	0.614	-0.001	High Seismic Risk
7	1.265	0.889	1.240	1.569	1.102	High Seismic Risk
8	0.495	-0.001	0.928	0.459	-0.001	High Seismic Risk
9	1.265	0.889	1.240	1.569	1.102	High Seismic Risk
10	0.495	-0.001	1.240	0.614	-0.001	High Seismic Risk

The Özcebe et al Procedure, which is improved by inclusion of site characteristics by Yakut et al. (2006) was effective for the selection of buildings with high seismic vulnerability. The ranking of the buildings within this group was successful, since the buildings could be classified as severely and moderately damaged.

7.3 INTERPRETATIONS AND DISCUSSIONS

Since, the real damage states could not be obtained and the buildings could not be accurately qualified using none of the detailed assessment procedures (Section 6.6), considering the high effort given for the computation and post-process of the analyses results regardless of reliable evaluation results, global seismic performance of the buildings were assessed by preliminary assessment procedures. For this purpose, the preliminary assessment procedures of Hassan and Sözen (1997), Yakut (2004) and Özcebe et al. (2004) were employed.

In previous sections, the general features of the preliminary assessment procedures and their results are presented. The Hassan & Sözen procedure is effective for the selection of buildings with higher seismic vulnerability. The method requires only the dimensions of the structure as input. Yakut procedure requires also strength (quality) of concrete, quality of construction, as-built properties, the negative effect of architectural features (soft story, short column, and vertical irregularity) and the quality of construction. On the other hand, the seismic zone and the soil condition are implicitly considered by the computation of code required base shear (V_{code}), in Yakut (2004) procedure. The regional seismicity and type of underlying soil, on the other hand, are directly taken into consideration only by Özcebe et al procedure.

The damage states of the moderately damaged buildings during the earthquake were accurately assessed by Hassan & Sözen Procedure, in contrary with the detailed assessment results. For severely damaged buildings, on the other hand, the evaluation results generally underestimated the damage states. Yakut (2004) procedure evaluated all the buildings as “unsafe”, according to capacity indices (*CPI*) computed. Although, the difference was not so clear between moderate and severe damage states, all buildings were expected to be damaged (unsafe), which is consistent with the detailed assessment results. In contrary with the results of Hassan & Sözen procedure, all severely damaged buildings were accurately evaluated rather than the moderately damaged buildings by Özcebe et al. procedure.

However, the accuracy of Özcebe et al. procedure was relatively low for moderately damaged buildings studied.

The Özcebe et al procedure, which is improved by inclusion of site characteristics (Yakut et al., 2006) was effective for the selection of buildings with high seismic vulnerability. The ranking of the buildings within this group was successful, since the buildings could be classified as severely and moderately damaged.

The actual damage states of the buildings studied after the earthquake were not consistent with the detailed assessment results of both global and local scales, especially for the moderately damaged buildings. In contrary with the detailed assessment results, however, the vulnerable buildings studied could be evaluated successfully and qualified according to moderate or severe damage experienced during the earthquake by some preliminary assessment procedures. Therefore, especially in case of lack of reliable data related with the buildings and the expected seismic demand level at the site, assessments using preliminary procedures was quite enough for the buildings studied, considering the high effort given for the computation and post-process of the analyses results. It is believed that these conclusions about the application of assessment procedures are valid for the building inventory of Turkey, considering the construction practice in Turkey, since the buildings usually have different configurations and detailing than their design drawings.

CHAPTER 8

SUMMARY AND CONCLUSIONS

8.1 SUMMARY

Many new linear and nonlinear analysis procedures have been proposed for earthquake response determination of the structures, aiming to obtain the adequate knowledge level for a proper structural design for a stated objective of performance. Nonlinear Static Procedures (NSPs) come into prominence as a practical seismic response determination tool within these proposals, due to the complexities of Nonlinear Response History Analysis (NRHA) which is accepted as the most accurate source of information for nonlinear response, i.e. the inelastic deformations.

This study focused on the application of NSPs to the large building stocks in Turkey with the principal modality that to compare observed performance of buildings on the basis of field observations with estimates using nonlinear static procedures, initializing from the rhetorical question, “had we known one day in advance that this earthquake would occur, could we have estimated their global performance (the damage states) using the widely used NSPs?”

A number of NSPs as well as NRHA were applied to the damaged buildings in Adapazarı during the 1999 Marmara Earthquake. The approximate assessment procedures are compared with the global building performance of selected buildings. This way, the NSP Methods are evaluated and checked whether they have estimated the global damages suitably.

In addition to the global comparisons, the buildings were also examined using the detailed evaluation procedures of ASCE/SEI-41/06, TEC 2007 and EC-8-3, using both Nonlinear Static (NSA) and Nonlinear Dynamic (NDP) Assessment Procedures of the codes.

The global roof displacement value was used as the global performance parameter. The predictions of the NSPs were compared with the predictions of NRHA and with the observed damage level of the selected buildings. After this global comparison, the local deformations and strains of structural members at performance points predicted by NSPs and NRHA, were checked and compared with the acceptance criteria defined by the codes.

The study has focused on the application of NSPs to the large building stocks in Turkey. The approximate assessment procedures are applied to the selected buildings, which reflect the general structural features of the RC building inventory in Turkey, in order to evaluate the global building performance during the earthquake.

Due to the inaccurate results of the detailed assessment procedures, considering the high effort given for the computation and post-process of the analyses, preliminary assessment procedures were also carried out on the buildings. The vulnerable buildings studied could be evaluated successfully and qualified according to moderate or severe damage experienced during the earthquake by preliminary assessment procedures employed.

The assessment results are also summarized as follows;

- The buildings studied reflect the general deficiencies of the building stock in Turkey, such as non-ductile detailing and irregularities both in plan and height-wise. (Section 4.2)
- In general, torsional irregularity observed for the buildings, according to the modal analysis.
- Poor geotechnical condition of the Adapazarı was believed to amplify the effects of strong ground motion. In this sense, the site-specific ground motion was used for the analyses in this study.
- According to design documents the compressive strength of the concrete was low for the buildings studied.
- For most of the cases studied the expected mode of failure was flexural-type failure, rather than the shear-type brittle failure. There were also some exceptions, such as Building 8 and 9, and few columns for some other buildings. (Section 5.3)
- The shear capacity values of the columns were also investigated in comparison with the shear demand values obtained from the nonlinear analyses. Eventually, Building 9 was extremely vulnerable for shear in the X direction, as expected, and in Building 8, shear failure occurred in 3 columns in the X direction and 5 columns in the Y direction, in ground story. In the rest of the buildings, few columns failed due to the shear, and, there was no shear failure in Building 2, although it was expected in the "risky" group. In general, the vertical elements designed as structural walls experienced shear failure. (Section 6.2)

- According to the NRHA results, in general, larger lateral roof drift values were obtained for moderately damaged buildings. But, buildings having larger roof drift capacities performed better and experienced less damage during the earthquake.
- "Soft story behavior" was observed on the buildings analyzed, according to the results of max ISDR values, which are presented in Figure 5.24 and

Figure 5.25. Unlike the other buildings, for Building 2 the max ISDR values were obtained in second story, not in ground story, of the building. Because, all columns of the story have reduced dimensions, due to the decreasing vertical loads in upper stories. However, the comparison of these ISDRs with given acceptability limits of both ATC-40 and TEC-2007, would result inconsistent outcomes considering the observed damages.

- From the global roof drift ratio point of view, for moderately damaged buildings, the acceptability limits of ATC-40 for Life Safety (LS) performance level were exceeded either in X or Y direction of the building. This outcome is inconsistent with the observed damage state of the buildings. The LS limit of TEC-2007, however, was not exceeded. For severely damaged buildings, on the contrary, none of the buildings had a roof drift ratio exceeding 2 percent (Table 5.3). From this perspective, moderately damaged buildings would have experienced more serious damages than severely damaged buildings, which is not consistent with the observed global damage.

- According to the NSP results, the expected limit states according to each of the analysis procedures differ from each other. However, there is no clear and compelling evidence that any of the procedures used can identify the performance point suitably well for each condition.
- In addition, the results of the NSPs did not comply with the results of the NRHA most of the time. However, the results of the NRHA are more accurate while determining the global damage state than the NSPs.
- Especially considering the moderately damaged buildings, the DCM was the best performing approximate procedures for the performance point assessment. The CSM overestimated the performance point by means of the global roof drift parameter.

- Using these results it seems to be difficult to determine the seismic performance point and the corresponding damage state of the buildings before the occurrence of earthquake. Thus, detailed assessment of the seismic response is needed in structural elements level.

- The detailed evaluation procedures of ASCE/SEI-41/06, TEC 2007 and EC-8-3 were used.
- Although the detailed assessments resulted with varying degrees of damage levels for the columns, all buildings examined were evaluated as “severely damaged” or “collapsed” by all detailed assessment procedures of all codes considered, regardless of their actual damage state observed during the earthquake.
- Therefore, actual damage states could not be replicated, and the buildings could not be qualified, using any of these detailed assessment procedures.
- TEC-2007 was the most conservative, while ASCE/SEI-41 was the least conservative, according to the estimated damage on columns.
- Conservative results are thought to be related with the high safety margin of the codes, especially for the nonconforming transverse reinforcement condition. This high safety margin is a natural result of limited research on the seismic behavior of similarly constructed RC buildings.
- According to TEC-2007 assessment results, in general, the concrete material was reached to its ultimate strain value before the steel material, due to low material strength. Thus, the overall member damage state was controlled by concrete.
- In consequence of the damage parameter used (chord rotation) by EC8-3, the damage states of the columns in any story (given that the story height is constant) are more or less the same, especially if the torsional irregularity does not affect, since the rigid diaphragm constraint applied in building models.
- On the other hand, the detailed assessment results of all documents investigated, i.e. ASCE/SEI-41, TEC-2007 and EC8-3, are consistent with

the global damage indicator of ISDR. Even though the global acceptability limits proposed by only TEC-2007 and ATC-40, high interstory drift demands are correlated with the structural member deformations. Thus, all the buildings studied were evaluated as severely damaged, due to high deformation demands.

- The actual damage states of the buildings studied after the earthquake were not consistent with the assessment results of both global and local scales, especially for the moderately damaged buildings.

- The damage states of the moderately damaged buildings during the earthquake were accurately assessed by Hassan & Sözen Procedure, while all severely damaged buildings were accurately evaluated by Özcebe et al. procedure. All buildings were classified as “unsafe” using Yakut preliminary assessment procedure.

8.2 CONCLUSIONS

In general, the results of assessment procedures for the idealized building models may be satisfying. However, the results for the real buildings of same procedures are very misleading. The building assessment examples given in this study clearly show those misleading results. The results of the analyses are significantly affected by inadequate information about the soil effects and the approximations for the structural modeling. On the other hand, the workmanship effects and shear failure or bonding effects cannot be modeled definitely. Especially, if the building collapsed and the ruin has been lifted, the deficiency of information is more important.

In the research area, despite numerous studies, there are a few number of studies which compares the results of nonlinear analysis procedures with the real building performance observations from earthquakes. The nonlinear response history analysis results have been accepted as the "exact" solution, and widely used for the comparison issues. Or, the assessment results may be precise enough for the test structures in laboratories. However, the consistency of the damage expectations by the assessment procedures with the field observations is much less, due to the variability of actual properties of the existing buildings, as well as the ground motion at the site.

The valuable information about the seismic behavior of reinforced concrete buildings obtained from the tests should be supported with more data obtained from the field. This strikes a pessimistic tone because if the inconsistencies between field data and assessment procedures described in guidelines on account of fluctuations of material properties, geometries, ground motion variations and many other parameters considered then a clear need exists to be sanguine about the predictive powers of these methods.

Based on the available data and assumptions, the results were presented in the study. It is clearly known that each of the nonlinear analysis procedures have different levels of sensitivity for different building types. Each has several superiority or shortcomings. The results given in the figures, Figure 5.27 – Figure 5.36, support this information. There is no clear result that any of the procedures used can identify the performance point suitably for each condition.

The studied building experienced altered damage during the earthquake. However, most of the analyses results could not predict the level of damage accurately. Using these results seems to be difficult to determine the seismic response and the damage of the buildings before the occurrence of earthquake. The study has been concluded as; there is no safety for the compatibility of pushover procedures for the assessment of global damage states with field observations, yet. It is necessary to investigate the proposed assessment procedures in a detailed manner and to check the results for “real buildings”. The approximate nonlinear static assessment procedures should be improved for reliable damage estimation.

Unfortunately, there is no enough detailed information about the damage of the structural elements within each building. The given damage state information for the buildings in the database is so superficial, and given only globally. However, the results of the NSPs and the NRHA were studied in the scale of structural elements. Although there is no sufficient information, the local damages (i.e. structural element damages, interstory drift, etc.) were studied and the results were compared with the acceptance criteria defined by ASCE/SEI-41/06, TEC-2007 and EC-8-3. The damage states of the buildings were overestimated by the detailed assessment procedures of the codes.

Since, the real damage states could not be obtained and the buildings could not be accurately qualified using none of these detailed assessment procedures, considering the high effort given for the computation and post-process of the analyses results regardless of reliable evaluation results, global seismic performance of the buildings were assessed by preliminary assessment procedures. The damage states of the moderately damaged buildings during the earthquake were accurately assessed by Hassan & Sözen Procedure, while all severely damaged buildings were accurately evaluated by Özcebe et al. procedure. All buildings were classified as “unsafe” using Yakut preliminary assessment procedure.

In contrary with the detailed assessment results, the vulnerable buildings studied could be evaluated successfully and qualified according to moderate or severe damage experienced during the earthquake by some preliminary assessment procedures. Therefore, especially in case of lack of reliable data related with the buildings and the expected seismic demand level at the site, assessments using preliminary procedures was quite enough for the buildings studied, considering the high effort given for the computation and post-process of the analyses results.

It is believed that these conclusions about the application of assessment procedures are valid for the building inventory of Turkey, considering the construction practice in Turkey, since the buildings usually have different configurations and detailing than their design drawings.

It is clear that similar studies based on the field data are urgently needed, in order to improve the assessment procedures. The current Earthquake Code Specifications and their high safety margin should also be investigated.

8.3 RECOMMENDATIONS FOR FUTURE STUDIES

As mentioned above, there is no enough detailed information about the damage of the structural elements within each building in this study. The given damage state information for the buildings in the database is so superficial, and given only globally. In order to evaluate the damaged buildings in the scale of structural elements, similar studies are needed on the buildings that have adequate information.

In this study, the site-specific ground motion that was derived from the original ground motion record was excited to the buildings. Since the analysis results are affected by the ground motion significantly, the case studies which have close ground motion records should be done.

REFERENCES

Akkar, S., and Miranda, E., 2005. "Statistical Evaluation of Approximate Methods for Estimating Maximum Deformation Demands on Existing Structures", Journal of Structural Engineering, v. 131 (1), pp. 160–172.

Akkar, S., Sucuoğlu, H., and Yakut, A., 2005. "Displacement–Based Fragility Functions for Low and Mid–Rise Ordinary Concrete Buildings", Earthquake Spectra, v. 21 (4), pp. 901–927.

American Society of Civil Engineers (ASCE), 2007. "Seismic Rehabilitation of Existing Buildings", ASCE/SEI-41/06, Reston, Virginia.

American Society of Civil Engineers (ASCE), 2008. "Seismic Rehabilitation of Existing Buildings", ASCE/SEI-41/06 Supplement 1, Reston, Virginia.

Antoniou, S., and Pinho, R., 2004a. "Advantages and Limitations of Adaptive and Non-Adaptive Force-Based Pushover Procedures", Journal of Earthquake Engineering, v. 8 (4), pp. 497-522.

Antoniou, S., and Pinho, R., 2004b. "Development and Verification of a Displacement-Based Adaptive Pushover Procedure", Journal of Earthquake Engineering, v. 8 (5), pp. 643-661.

Applied Technology Council (ATC), 1996. "Seismic Evaluation and Retrofit of Concrete Buildings", Report No. SSC 96-01, ATC-40, Volume 1-2, Redwood City, California.

Applied Technology Council (ATC), 2005. “Improvement of Nonlinear Static Seismic Analysis Procedures”, Report No. FEMA-440, ATC-55 Project, Redwood City, California.

Aschheim, M., Tjhinb, T., Comartin, C., Hamburger, R., and Inel M., 2007. “The Scaled Nonlinear Dynamic Procedure”, Engineering Structures, v. 29 (7), pp. 1422-1441.

Aydinoglu, N.M., 2003. “An Incremental Response Spectrum Analysis Procedure Based on Inelastic Spectral Displacements for Multi-Mode Seismic Performance Evaluation”, Bulletin of Earthquake Engineering, v. 1, pp.3-36.

Bakır, B.S., Sucuoğlu, H., Yılmaz, T., 2002. “An Overview of Local Site Effects and the Associated Building Damage in Adapazarı during the 17 August 1999 İzmit EQ”, Bulletin of the Seismological Society of America, v. 92 (1), 509-526.

Bakır, B.S., Yılmaz, M.T., Yakut, A., Gülkan, P., 2005. “Re-examination of Damage Distribution in Adapazarı: Geotechnical Considerations”, Engineering Structures, v. 27, 1002-1013.

Beyen, K., Erdik, M., 2004. “Two-dimensional nonlinear site response analysis of Adapazarı plain and predictions inferred from aftershocks of the Kocaeli earthquake of 17 August 1999”, Soil Dynamics and Earthquake Engineering, v. 24 (3), pp. 261–279.

Bray, J., Sancio, R., Durgunoglu, T., Onalp, A., Youd, T., Stewart, J., Seed, R., Cetin, O., Bol, E., Baturay, M., Christensen, C., and Karadayilar, T., 2004. ”Subsurface Characterization at Ground Failure Sites in Adapazari, Turkey”, J. Geotechnical and Geoenvironmental Engineering, v. 130 (7), 673–685.

Bray, J., and Sancio, R., 2006. ”Assessment of the Liquefaction Susceptibility of Fine-Grained Soils”, J. Geotechnical and Geoenvironmental Engineering, v. 132 (9), 1165–1177.

Building Seismic Safety Council, 2000. “NEHRP Recommended Provisions for Seismic Regulations for New Buildings & Other Structures”, FEMA 368, Washington, DC.

Chamber of Civil Engineers (IMO), 2000. “Engineering Report of Marmara and Düzce Earthquakes”, (prepared by the members of Earthquake Engineering Research Center, EERC, METU), Ankara, Turkey. (In Turkish).

Chang, G., and Mander, J., 1994. "Seismic Energy Based Fatigue Damage Analysis of Bridge Columns: Part I – Evaluation of Seismic Capacity", NCEER Technical Report 94-0006.

Chintanapakdee, C., and Chopra, A.K., 2003. “Evaluation of Modal Pushover Analysis Using Generic Frames”, Earthquake Engineering and Structural Dynamics, v. 32, pp. 417-442.

Chintanapakdee, C., and Chopra, A.K., 2003. “Seismic Response of Vertically Irregular Frames: Response History and Modal Pushover Analyses”, Journal of Structural Engineering, ASCE, v. 130 (8), pp. 1177-1185.

Chopra, A.K., 2007. “Dynamics of Structures: Theory and Applications to Earthquake Engineering”, 3rd Edition, Pearson Prentice Hall, Upper Saddle River, N.J., 876 pp.

Chopra, A.K., Goel, R.K., 2000. “Evaluation of NSP to Estimate Seismic Deformation: SDF Systems”, Journal of Structural Engineering, v.126 (4), pp. 482-490.

Chopra, A.K., and Goel R.K., 2002. "A Modal Pushover Analysis Procedure for Estimating Seismic Demands for Buildings", Earthquake Engineering and Structural Dynamics, v. 31, pp. 561-582.

Chopra, A.K., Goel, R.K., Chintanapakdee, C., 2004. "Evaluation of a Modified MPA Procedure Assuming Higher Modes as Elastic to Estimate Seismic Demands", Earthquake Spectra, v. 20 (3), pp. 757-778.

Computers and Structures, Inc., 2005. SAP 2000 Nonlinear, Version 10.0.1, Structural Analysis Program, Berkeley, CA. http://www.comp-engineering.com/index.htm (last accessed in July 2008)

DRM (World Institute for Disaster Risk Management), 2003. "Microzonation for Earthquake Risk Mitigation – Background Report on Structural Damage – Development and Implementation of a Building Damage Survey for Adapazarı, Turkey: Interpretation and Soils Correlation".

Elnashai, A.S., 2000. "Analysis of the Damage Potential of the Kocaeli (Turkey) Earthquake of 17 August 1999", Engineering Structures, v. 22 (7), pp. 746–754.

European Committee for Standardization (EC), 2005. "Eurocode 8: Design of structures for earthquake resistance - Part 3: Strengthening and repair of buildings" European Standard, EC-8-3, BS EN 1998–3, Comité Européen de Normalisation, Brussels, Belgium.

Fajfar, P., and Fischinger, M., 1987. "Nonlinear Seismic Analysis of RC Buildings: Implications of a Case Study", European Earthquake Engineering, v. 1, pp. 31-43.

Fajfar, P., and Gaspersic, P., 1996. “The N2 Method for the Seismic Damage Analysis of RC Buildings”, Earthquake Engineering and Structural Dynamics, v. 25, pp. 31-46.

Federal Emergency Management Agency (FEMA), 1997. “Prestandard and Commentary for the Seismic Rehabilitation of Buildings”, FEMA-273 Washington, D.C.

Federal Emergency Management Agency (FEMA), 2000. “Prestandard and Commentary for the Seismic Rehabilitation of Buildings”, FEMA-356, Washington, D.C.

Federal Emergency Management Agency, 1988. “Rapid Visual Screening of Buildings for Potential Seismic Hazards: A Handbook”, FEMA 154 – ATC-21, Redwood City, CA.

Federal Emergency Management Agency, 1989. “A Handbook for Seismic Evaluation of Existing Buildings (Preliminary)”, FEMA 178 – ATC-22, Redwood City, CA.

Federal Emergency Management Agency, 1998, FEMA 310. “Handbook for the Seismic Evaluation of Buildings – A Prestandart”, American Society of Civil Engineers for the Federal Emergency Management Agency, Washington D.C.

Filippou, F. C., Popov, E. P., and Bertero, V. V., 1983. "Effects of Bond Deterioration on Hysteretic Behavior of Reinforced Concrete Joints". Report EERC 83-19, Earthquake Engineering Research Center, University of California, Berkeley, CA.

Freeman, S.A., Nicoletti, J.P., and Tyrell, J.V., 1975. “Evaluation of Existing Buildings for Seismic Risk - A Case Study of Puget Sound Naval Shipyard, Bremerton, Washington", Proceedings of the First U.S. National Conference on Earthquake Engineering, Berkeley, CA.

General Directorate of Disaster Affairs (GDDA), 2000. "17 Ağustos 1999 İzmit Körfezi Depremi Raporu", Ministry of Public Works and Resettlement, General Directorate of Disaster Affairs, Earthquake Research Department, Ankara, Turkey. Ed. Ramazan DEMİRTAŞ, (In Turkish).

General Directorate of Disaster Affairs (GDDA), 2004. "Seismic Microzonation for Municipalities – Pilot Studies", Ankara, Turkey.

Goel, R.K., and Chopra, A.K., 2004. "Evaluation of Modal and FEMA Pushover Analyses: SAC buildings", Earthquake Spectra, v. 20, pp. 225–254.

Gupta, B., and Kunnath, S. K., 2000. "Adaptive Spectra-Based Pushover Procedure for Seismic Evaluation of Structures", Earthquake Spectra, v. 16 (2), pp. 367-391.

Gülkan, P., and Sözen, M.A., 1974. "Inelastic Responses of Reinforced Concrete Structures to Earthquake Motions", Journal of the American Concrete Institute, v. 71, pp. 604-610.

Gülkan, P., and Sözen, M.A., 1999. "A Procedure for Determining Seismic Vulnerability of Building Structures", ACI Structural Journal, v. 96 (3), pp. 336-342.

Gülkan, P., 2000. "Building Code Enforcement Prospects: The Failure of Public Policy", Earthquake Spectra, Supplement A to Volume 16, Chapter 15 of Kocaeli, Turkey earthquake of August 17, 1999 Reconnaissance Report, pp. 351–367.

Hassan A.F. and Sözen M. A., 1997. “Seismic Vulnerability Assessment of Low-rise Buildings in Regions with Infrequent Earthquakes”, ACI Structural Journal, v. 94, pp. 31–39.

Jacobsen, L.S., 1930. “Steady Forced Vibrations as Influenced by Damping”, Transactions ASME, v. 52, pp. 169–181.

Jacobsen, L.S., 1960. “Damping in Composite Structures”, Proceedings of the 2WCEE, Tokyo and Kyoto, Japan, v. 2, pp.1029-1044.

Jennings, P.C., 1968. “Equivalent Viscous Damping for Yielding Structures”, Journal of Engineering Mechanics Division, ASCE, v. 94, pp. 103-116.

Kalkan, E., and Kunnath, S.K., 2006. “Adaptive Modal Combination Procedure For Nonlinear Static Analysis of Building Structures”, ASCE, Journal of Structural Engineering, v. 132 (11), pp. 1721-1731.

Kazaz, İ., Gülkan, P., and Yakut, A., 2012a. “Deformation Limits for Structural Walls with Confined Boundaries”, Earthquake Spectra, v. 28 (3), pp. 1019-1046, August.

Kazaz, İ., Gülkan, P., and Yakut, A., 2012b. “Performance Limits for Structural Walls: An Analytical Perspective”, Engineering Structures, v. 43, pp. 105-119, October.

Kent D.C. and Park R., 1971. “Flexural Members with Confined Concrete”, Journal the Structural Division, American Society of Civil Engineers, New York, v. 97, (ST7), pp. 1969-1990.

Krawinkler, H., and Seneviratna, G.D.P.K., 1998. “Pros and Cons of a Pushover Analysis of Seismic Performance Evaluation”, Engineering Structures, v. 20, pp. 452-464.

Mander, J.B., Priestley, M.J.N., and Park, R., 1988. “Observed Stress-Strain Behavior of Confined Concrete”, Journal of Structural Engineering, v. 114 (8), pp. 1827–1849.

Mazzoni, S., McKenna, F., Scott, M.H., and Fenves, G., 2009. “Opensees User’s Manual,” Available from http://opensees.berkeley.edu/wiki/ (last accessed in December 2012).

Miranda, E., and Ruiz-Garcia, J., 2002. “Evaluation of Approximate Methods to Estimate Maximum Inelastic Displacement Demands”, Earthquake Engineering and Structural Dynamics, v. 31, pp. 539-560.

Moehle, J.P., 1984. “Seismic Analysis of R/C Frame-Wall Structures”, Journal of Structural Engineering, ASCE, v. 110 (11), pp. 2619-2634.

Moehle, J.P., and Alarcon, I.F., 1986. “Seismic Analysis Methods for Irregular Buildings”, Journal of Structural Engineering, ASCE, v. 112 (1), pp. 35-52.

Mosalam, K. M., and Günay, M. S., 2010. “Seismic Retrofit of Non-Ductile Reinforced Concrete Frames Using Infill Walls as a Rocking Spine”. In Advances of Performance-Based Earthquake Engineering, Edited by: Fardis, M. N. Dordrecht: Springer. Ch. 33.

Ohkubo, M., 1991. “Current Japanese system on seismic capacity and retrofit techniques for existing reinforced concrete buildings and post-earthquake damage inspection and restoration techniques”, Report No. SSRP-91/02, Department of Applied Mechanics and Engineering Sciences, University of California, San Diego.

OpenSees, 2010, "Open System for Earthquake Engineering Simulation", Version 2.2.1, Pacific Earthquake Engineering Research Center, http://opensees.berkeley.edu, (last accessed in December 2012).

Ousalem, H., Kabeyasawa, T., and Tasai, A., 2004. "Evaluation of Ultimate Deformation Capacity at Axial Load Collapse of Reinforced Concrete Columns", Proceedings of 13th World Conference on Earthquake Engineering, Paper No. 370.

Özcebe, G., Yücemen, M. S., and Aydoğan, V., 2004, "Statistical Seismic Vulnerability Assessment of Existing Reinforced Concrete Buildings in Turkey on a Regional Scale", Journal of Earthquake Engineering, v.8 (5), pp.749-773.

Paret, T.F., Sasaki, K., Eilbeck, D.H., and Freeman S.A., 1996. "Approximate Inelastic Procedures to Identify Failure Mechanisms From Higher Mode Effect", 11th World Conference on Earthquake Engineering, Paper No. 966, Acapulco, Mexico.

Priestley M.J.N., Calvi G.M. and Kowalsky M.J., 2007. "Displacement-Based Seismic Design of Structures", IUSS Press, Pavia, Italy.

Rathje EM, Stokoe II KH., 2001. "Kocaeli and Duzce earthquakes—strong motion stations data from SASW testing", Pacific Earthquake Engineering Research Center Lifelines Quarterly Progress Meeting, Summary Notes. p. 1.

Rosenblueth, E., and Herrera, I., 1964. "On a Kind of Hysteretic Damping", Journal of Engineering Mechanics Division, ASCE, v. 90, pp. 37-48.

Saiidi, M., and Hudson, K.E.Jr., 1982. "Analytical Study of Irregular R/C Structures Subjected to In-Plane Earthquake Loads", College of Engineering, Report No. 59, University of Nevada, Reno.

Saiidi, M., and Sözen, M.A., 1981. “Simple Nonlinear Seismic Analysis of R/C Structures”, Journal of the Structural Division, ASCE, Vol. 107, No. ST5, pp. 937-952.

Sancio, R. B., Bray, J.D., Stewart, J.P., Youd, T.L., Durgunoglu, H.T., Önalp, A., Seed, R.B., Christensen, C., Baturay, M.B., Karadayılar, T., 2002. “Correlation between ground failure and soil conditions in Adapazari, Turkey”, Soil Dynamics and Earthquake Engineering, v.22 (9-12), pp. 1093–1102.

Sasaki, F., Freeman, S., and Paret, T., 1998. “Multi-Mode Pushover Procedure (MMP)-A Method to Identify the Effect of Higher Modes in a Pushover Analysis”, Proceedings of the 6th U.S. National Conference on Earthquake Engineering, Seattle, CD-ROM, EERI, Oakland.

Scott, B.D., Park, R., and Priestley, M.J.N., 1982. “Stress-Strain Behavior of Concrete Confined by Overlapping Hoops at Low and High Strain Rates”, ACI Structural Journal, v. 79 (1), pp. 13-27.

Sezen, H., Elwood, K.J., Whittaker, A.S., Mosalam, K.M., Wallace, J.W., Stanton, J.F., 2000. “Structural Engineering Reconnaissance of the August 17, 1999 Kocaeli (Izmit), Turkey Earthquake”. PEER 2000/09, Technical Report. Pacific Earthquake Engineering Research Center, University of California, Berkeley, CA.

Sezen, H., Whittaker, A.S., Elwood, K.J., Mosalam, K.M., 2003. “Performance of Reinforced Concrete Buildings during the August 17, 1999 Kocaeli, Turkey Earthquake, and Seismic Design and Construction Practice in Turkey”, Engineering Structures, v. 25 (1), pp. 103-114.

Sezen, H., and Moehle, J.P., 2006. “Seismic Tests of Concrete Columns with Light Transverse Reinforcement”, ACI Structural Journal, American Concrete Institute, v. 103 (6), pp. 842-849.

Shibata, A., and Sozen, M.A., 1976. “Substitute-Structure Method for Seismic Design in RC”, Journal of the Structural Division, ASCE, v.102, pp. 1-17.

State Institute of Statistics (SIS), 2000. “Building Census”, Ankara, Turkey.

Structural Engineers Association of California (SEAOC), 1999. “Seismic Recommended Lateral Force Requirements and Commentary, Blue Book”, Sacramento, CA.

Sucuoğlu, H., 2002. “Engineering Characteristics of the Near-Field Strong Motions from the 1999 Kocaeli and Düzce Earthquakes in Turkey”, Journal of Seismology, v.6, pp. 347-355.

Sucuoğlu, H., 2006. “The Turkish Seismic Rehabilitation Code”, First European Conference on Earthquake Engineering and Seismology, Geneva, Switzerland.

Sucuoğlu, H., Yazgan, U., and Yakut, A., 2007. “A Screening Procedure for Seismic Risk Assessment in Urban Building Stocks”, Earthquake Spectra, v.23 (2), pp.441-458.

TS 10465, 1992. “Test Method for Concrete- Obtaining Samples and Determination of Compesive Strength in Hardened Concrete in Structures and Components (Destructive Method)”, Turkish Standards Institute, Ankara.

TS 500 (Turkish Design Code), 2000. “Requirements for design and construction of reinforced concrete structures”, Turkish Standards Institute, Ankara.

Turkish Earthquake Code, 1975. “Specifications for the Buildings to be Constructed in Disaster Areas”, Ministry of Public Works and Resettlement, Ankara, Turkey.

Turkish Earthquake Code (TEC), 2007. “Specifications for the Buildings to be Constructed in Earthquake Regions”, Ministry of Public Works and Resettlement, Ankara, Turkey.

Vamvatsikos, D., and Cornell, C.A., 2002. “Incremental Dynamic Analysis”, Earthquake Engineering and Structural Dynamics, v. 31 (3), pp. 491–514.

Yakut A., 2004. “Preliminary Seismic Performance Assessment Procedure for Existing RC Buildings”, Engineering Structures, v. 26 (10), pp. 1447-1461.

Yakut, A., Ozcebe, G., and Yucemen, M. S., 2006. “Seismic Vulnerability Assessment Using Regional Empirical Data”, Earthquake Engineering and Structural Dynamics, v. 35, pp. 1187-1202.

Yassin, M.H.M., 1994. “Nonlinear analysis of prestressed concrete structures under monotonic and cyclic loads”, PhD thesis, University of California, Berkeley, CA.

Yoshimura, M., Takaine, Y., and Nakamura, T., 2004. “Axial Collapse of Reinforced Concrete Columns”, Proceedings of 13th World Conference on Earthquake Engineering, Paper No.1699.

APPENDIX A

LAYOUTS AND BLUEPRINTS OF BUILDINGS

The scanned copies of the blueprints of the buildings are given in the DVD enclosed. These blueprints include the typical floor plans, column application plans, and beam details. The figures are given in separate folders for each building studied. The folders of the moderately damaged buildings also contain the photographs taken from outside of the building at the site, during the visits to Adapazarı.

The names of the folders and the files are self explanatory.

APPENDIX B

ADAPAZARI MAPS OBTAINED BY GIS SURVEY

Some of the maps obtained from the Adapazarı survey using GIS tools which is discussed in Section 4.3 are shown in the following figures. The locations of the buildings selected for this dissertation are also shown on the maps.

Figure B.1 Adapazarı City Map. The borders of the 26 central districts of Adapazarı are shown in red.

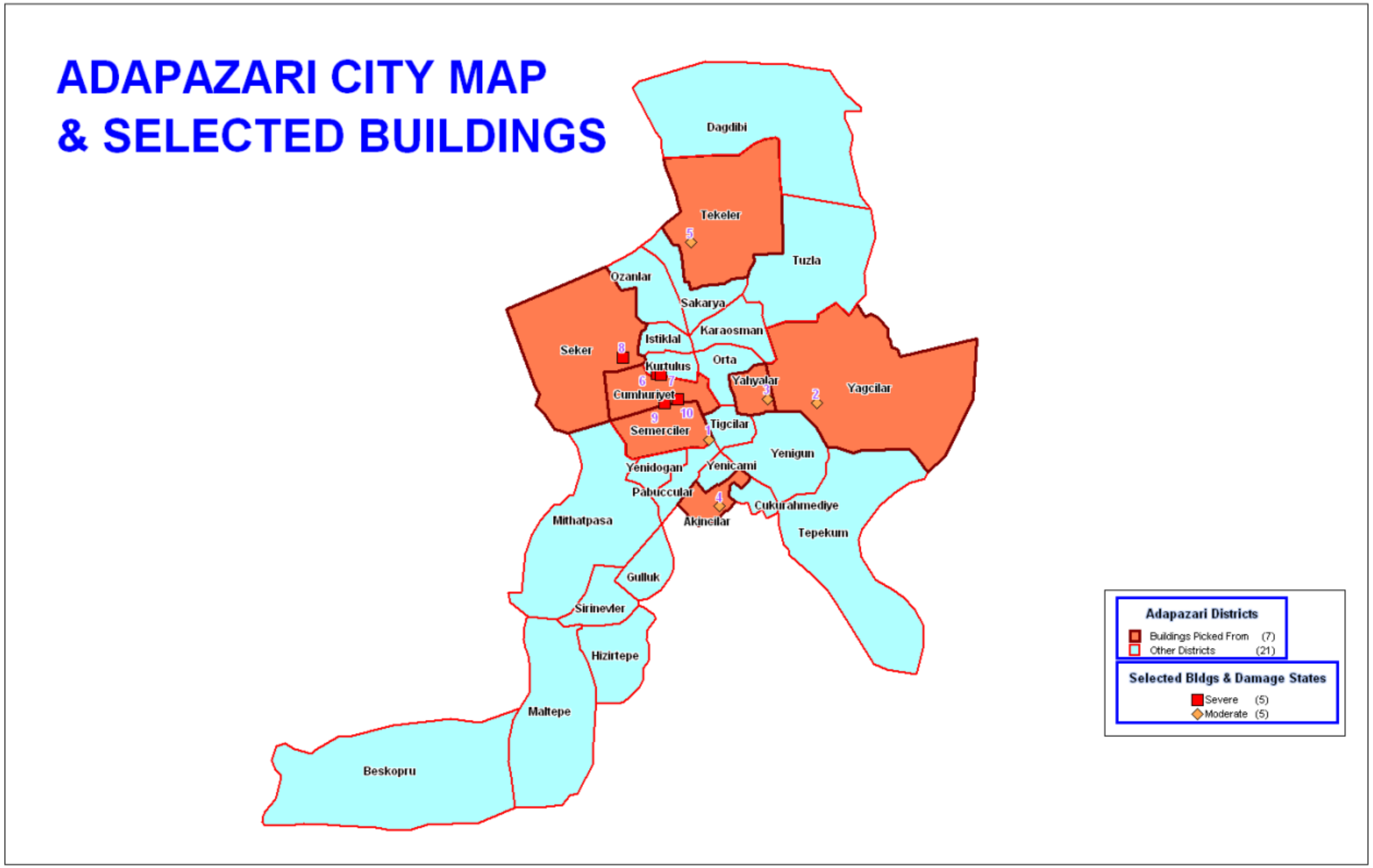

Figure B.2 The locations of the buildings studied. The districts where these buildings located are highlighted.

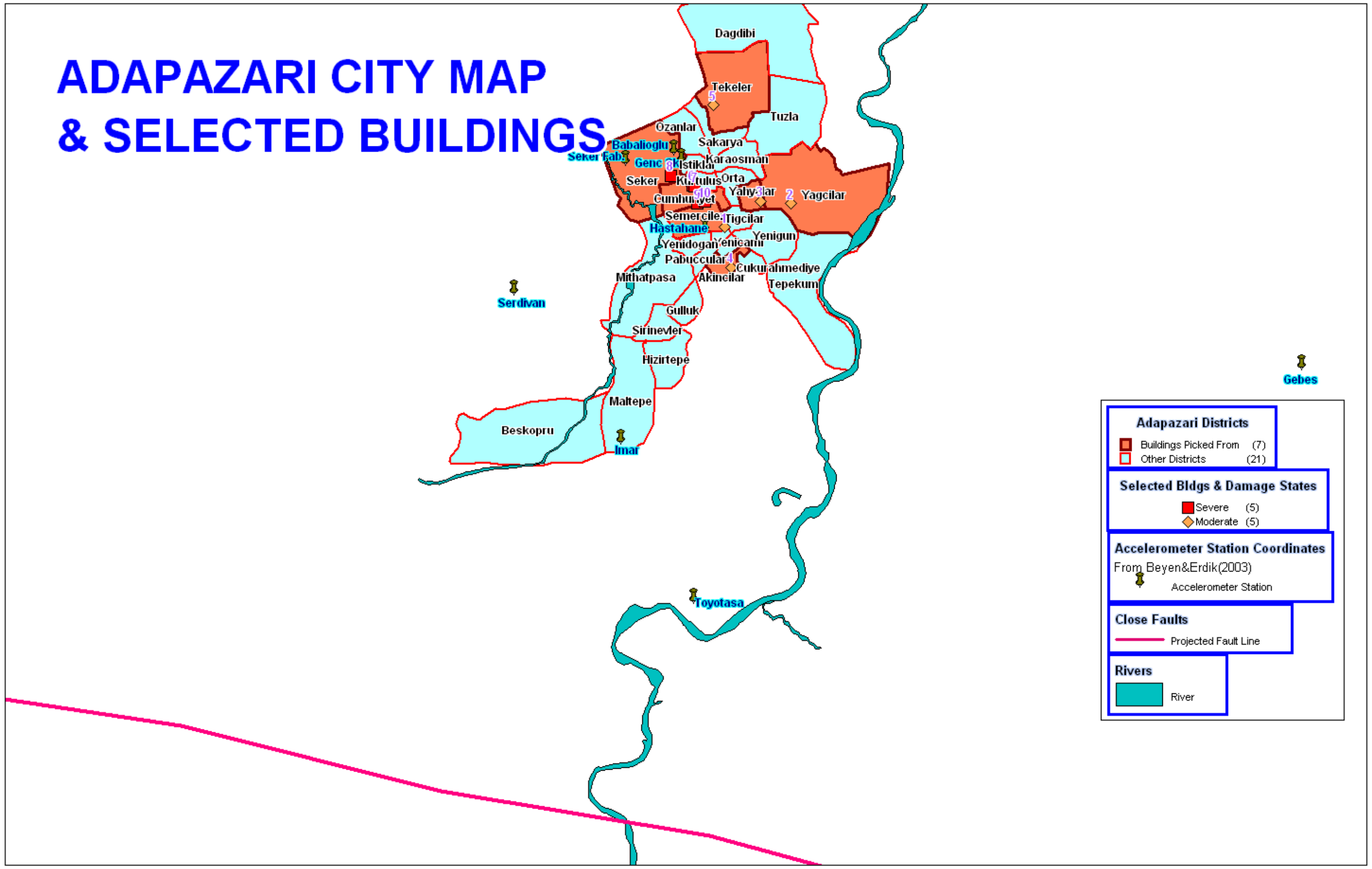

Figure B.3 The locations of the buildings studied and the temporary stations established after the earthquake. The projection of the NAF is also shown on the map.

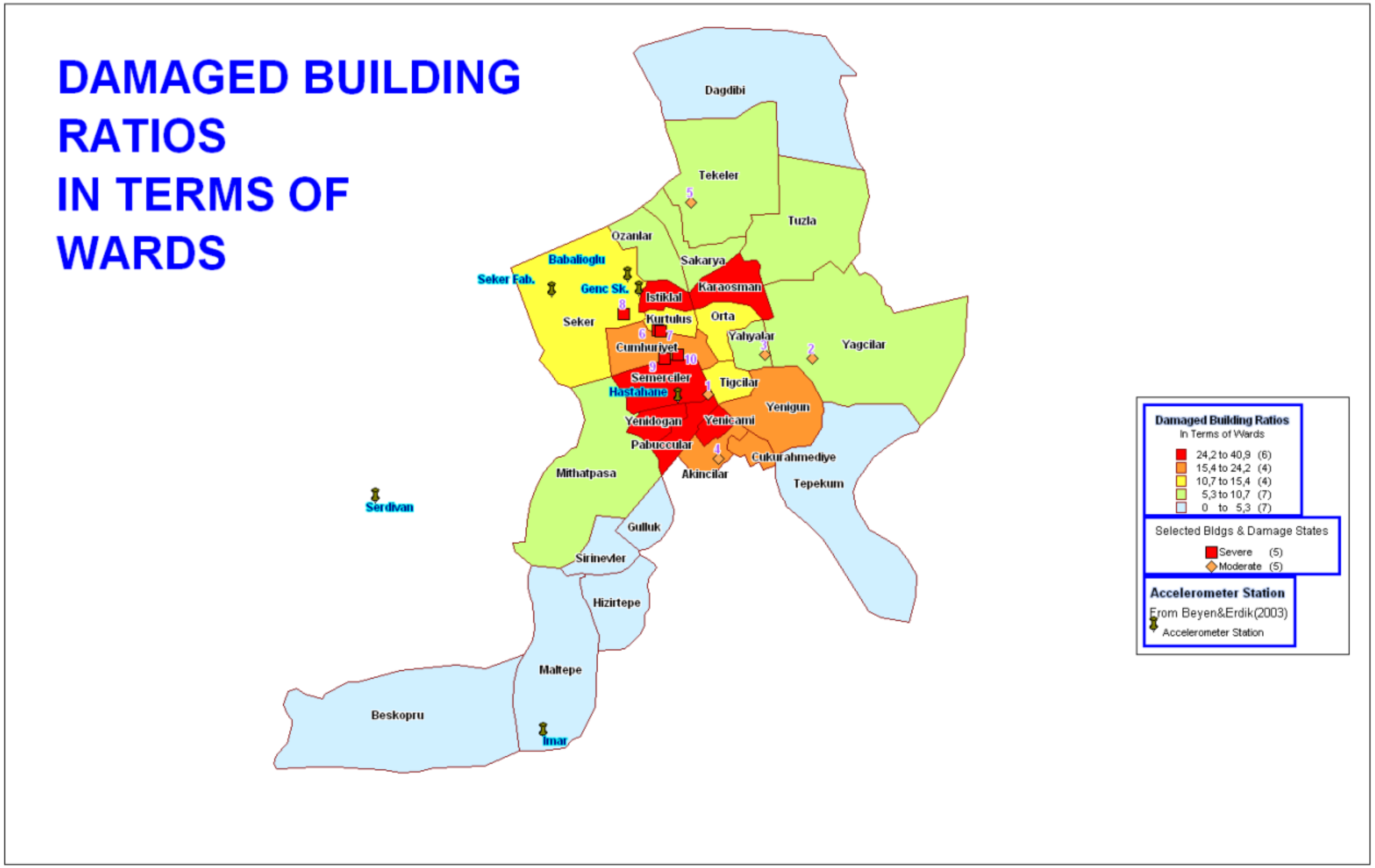

Figure B.4 The ratio of collapsed and heavily damaged buildings to the total number of buildings by central districts.

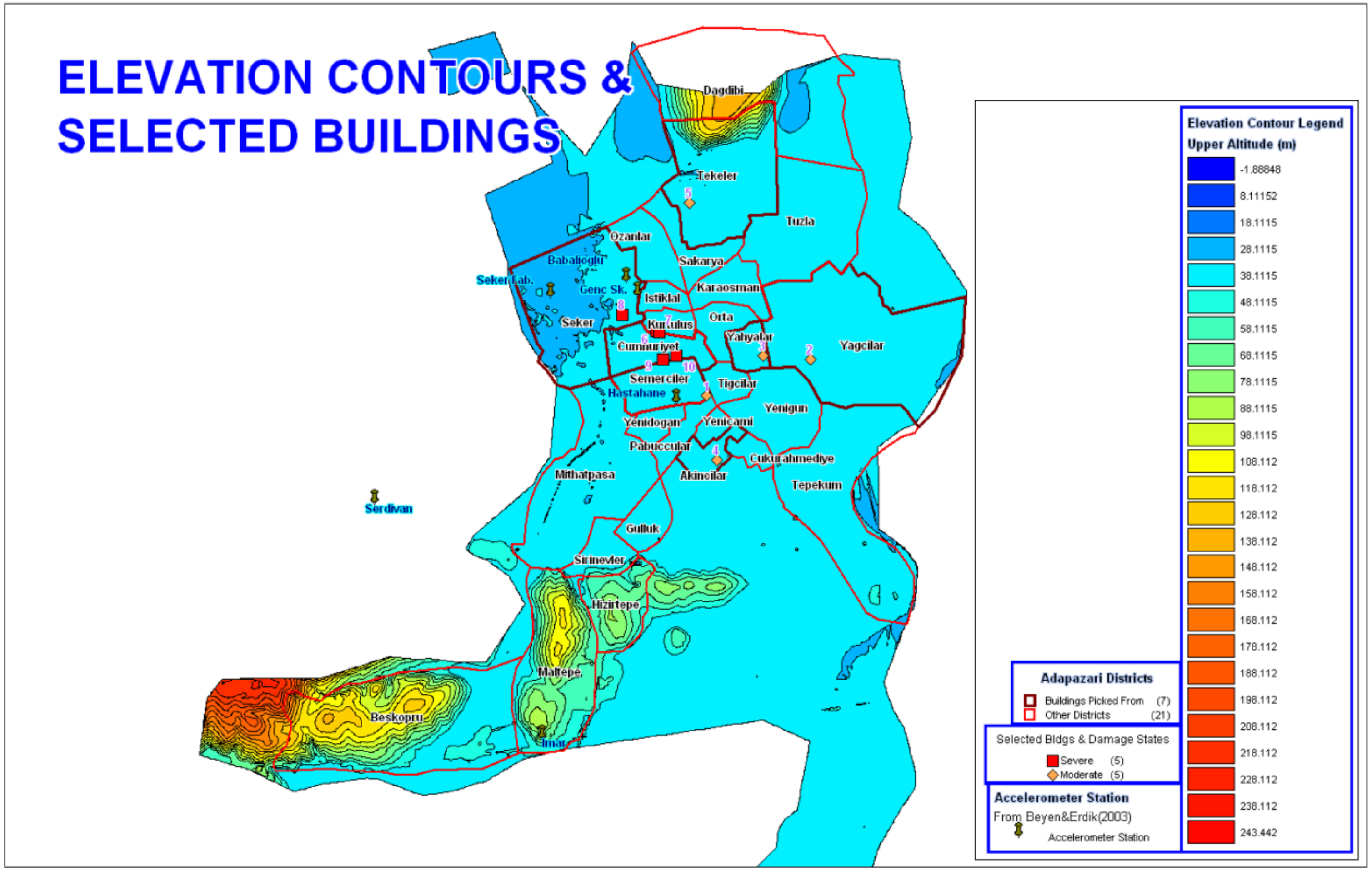

Figure B.5 The elevation of the 26 central districts in Adapazarı.

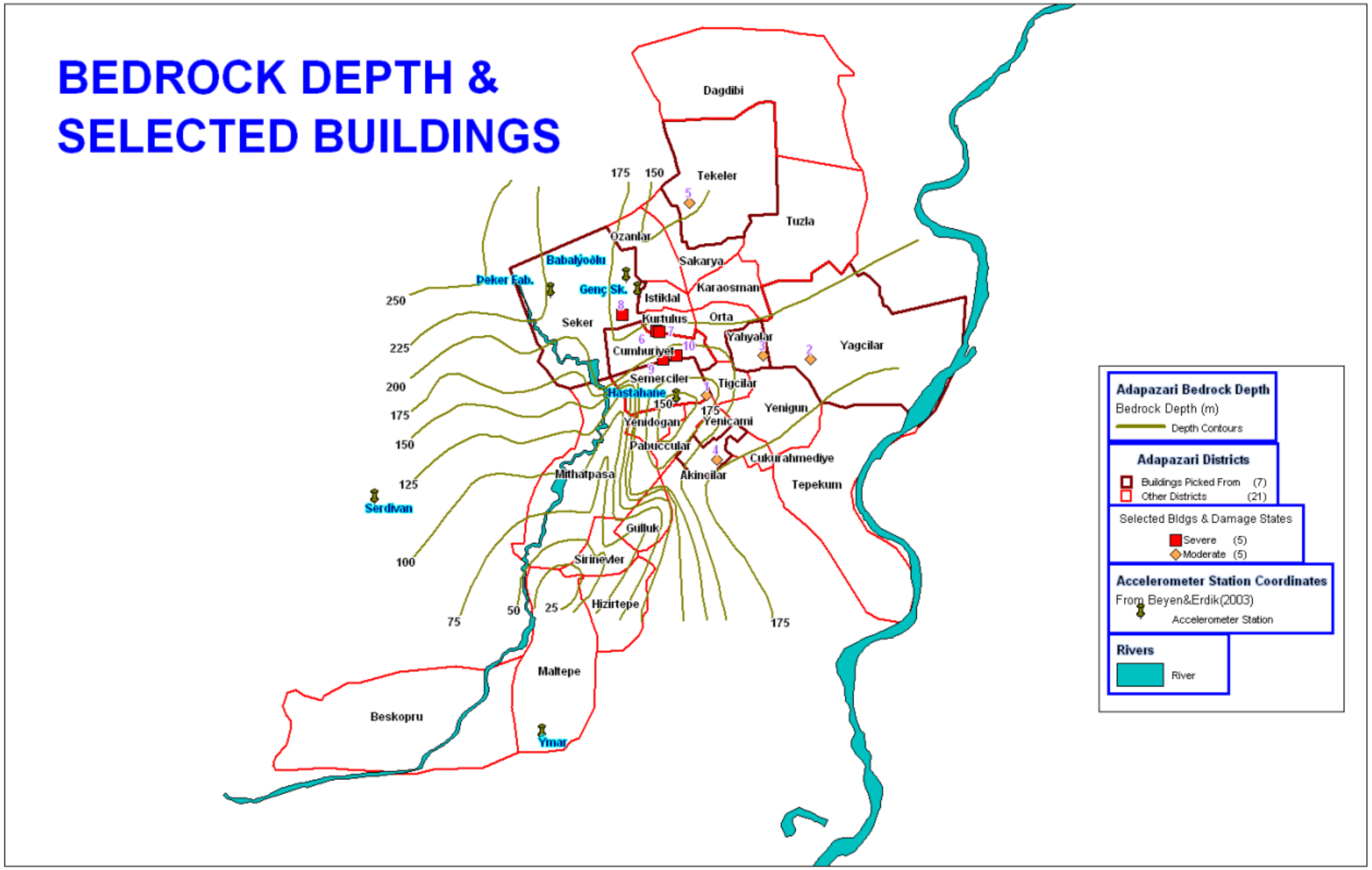

Figure B.6 Variation of the bedrock depth (Bakır et al. 2002)

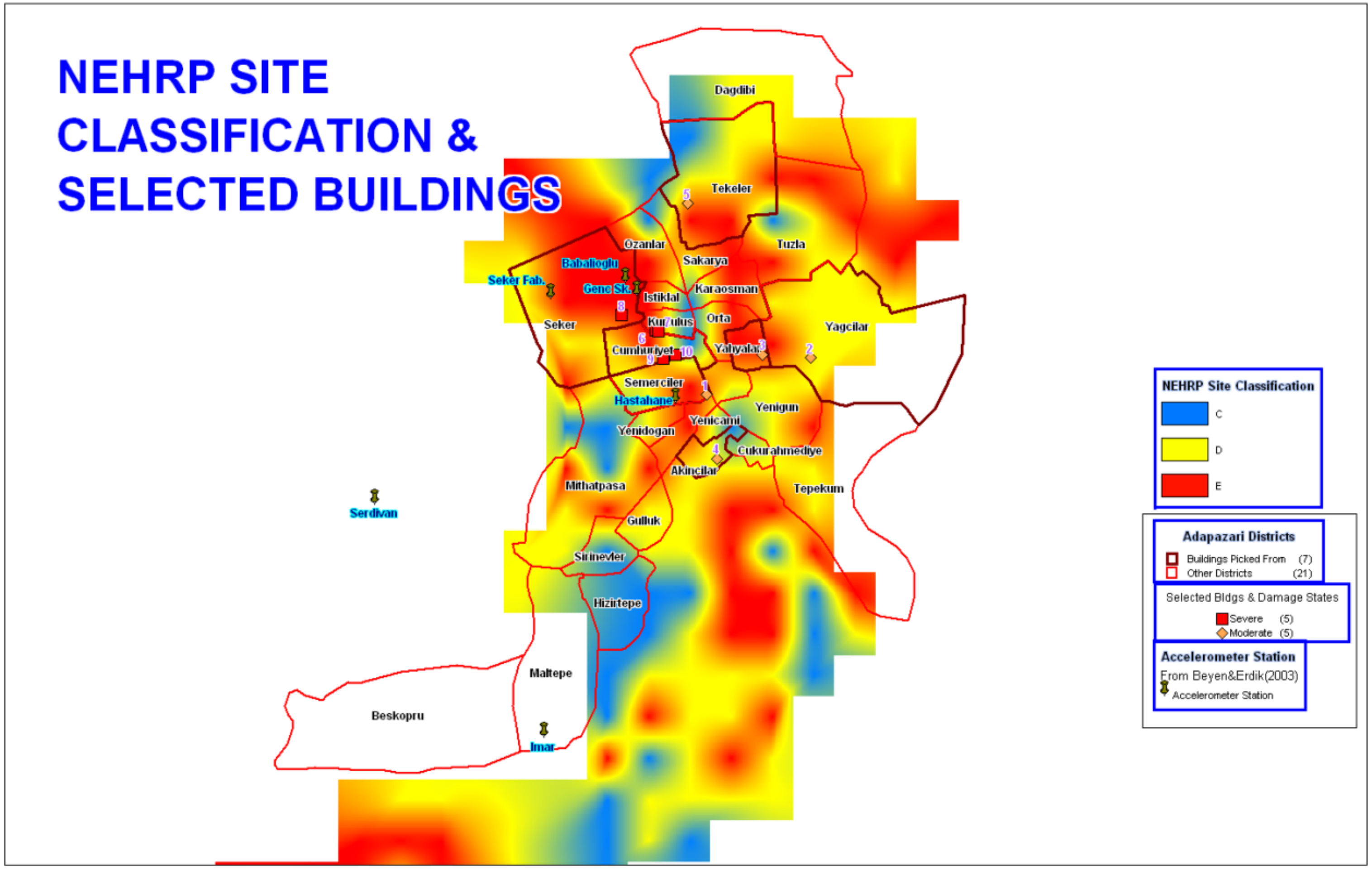

Figure B.7 NEHRP site classification in Adapazarı.

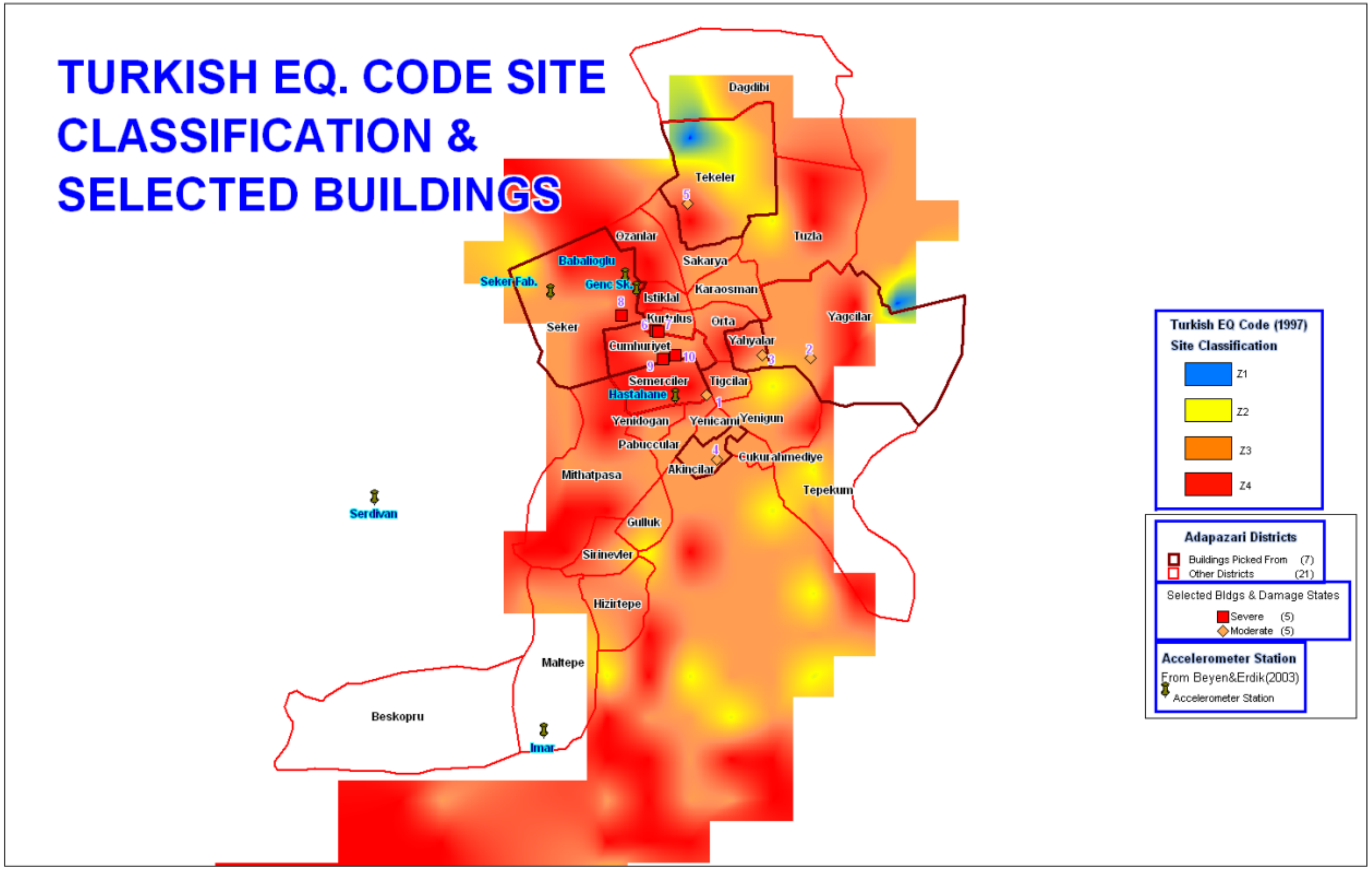

Figure B.8 Site classification according to TEC in Adapazarı.

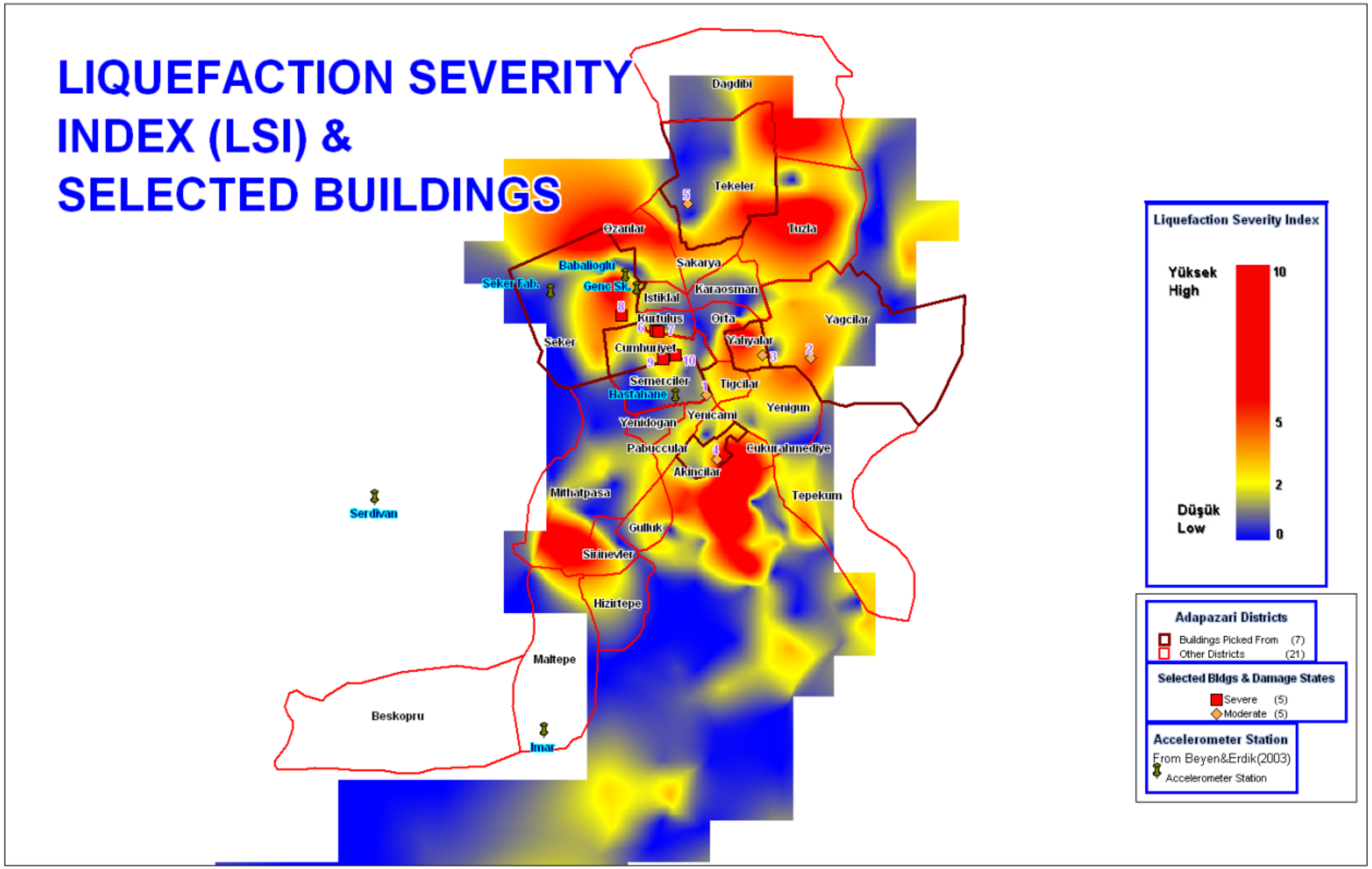

Figure B.9 The risk map of liquefaction in Adapazarı.

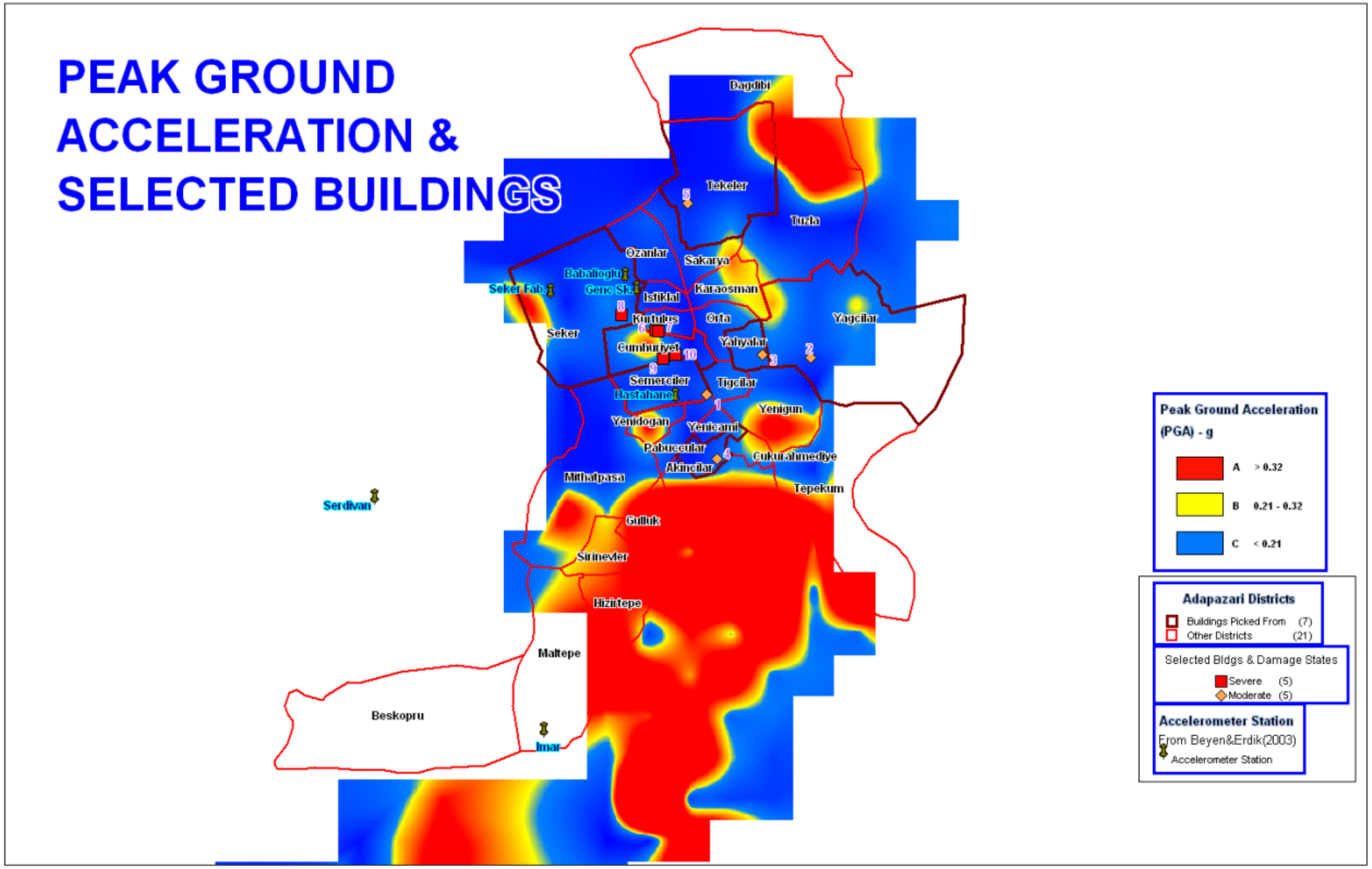

Figure B.10 Variation of PGA calculated by site response spectrum analysis in Adapazarı.

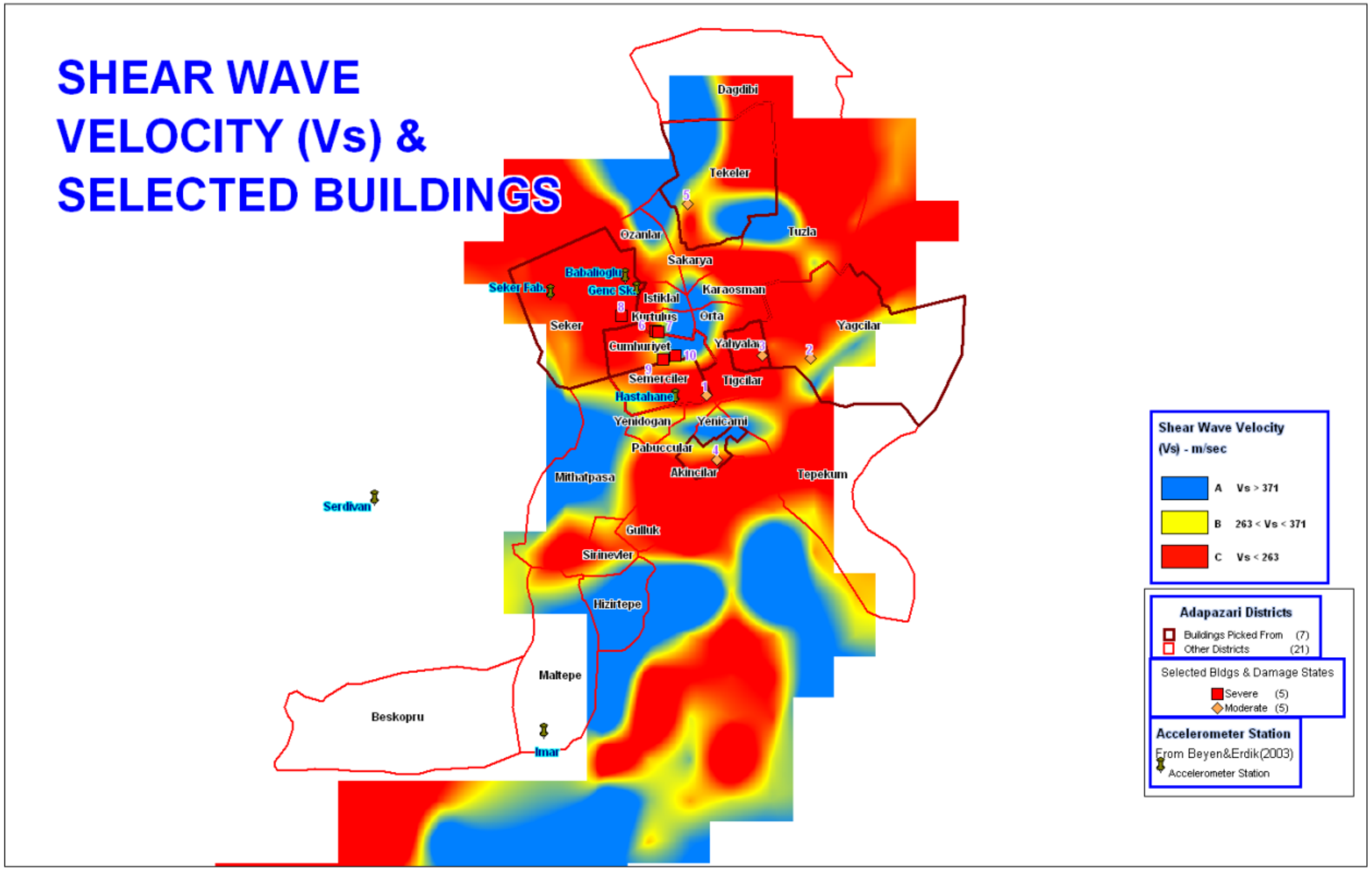

Figure B.11 Site classification according to equivalent shear wave velocity in Adapazarı

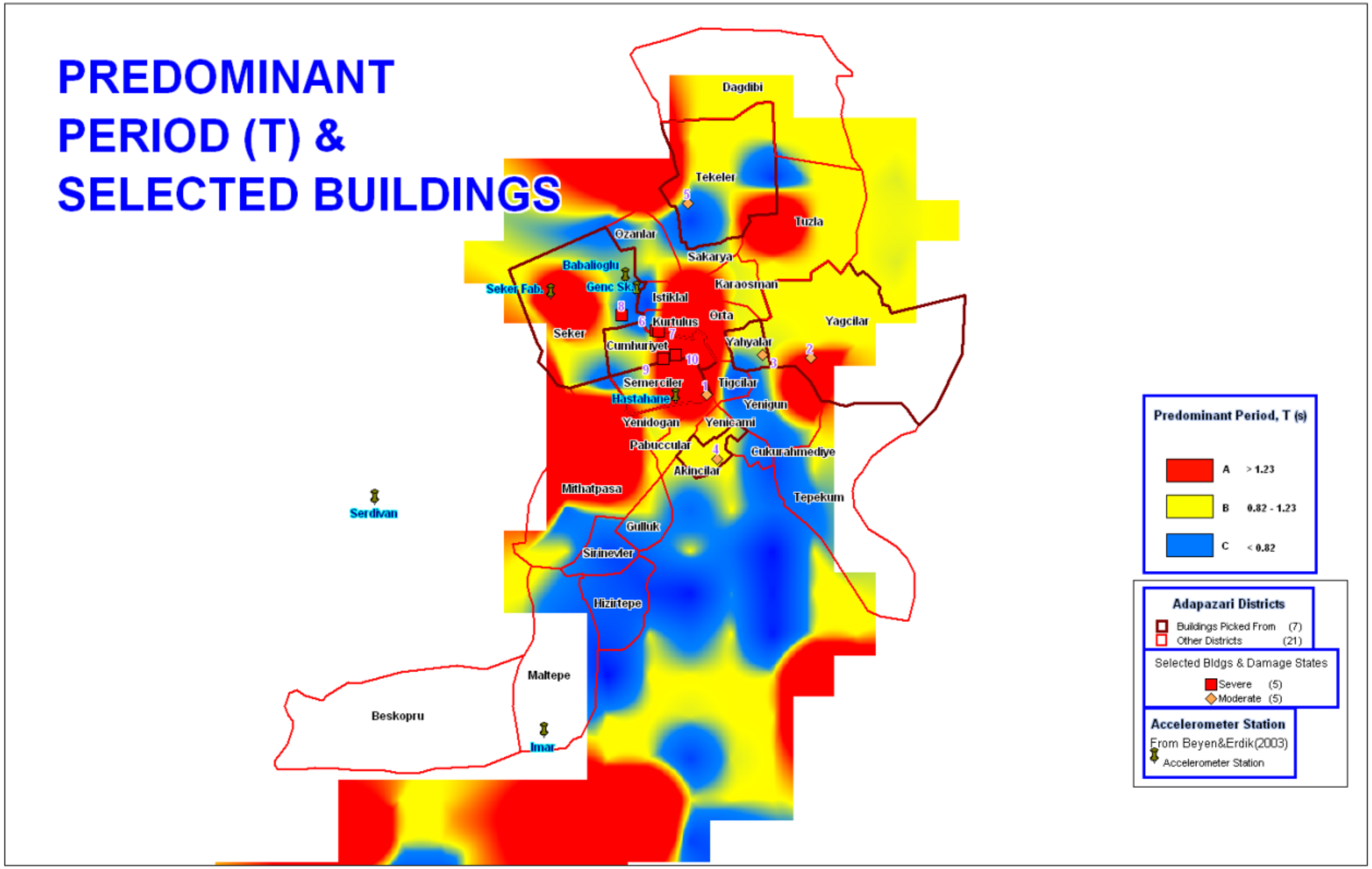

Figure B.12 Site classification according to predominant period in Adapazarı

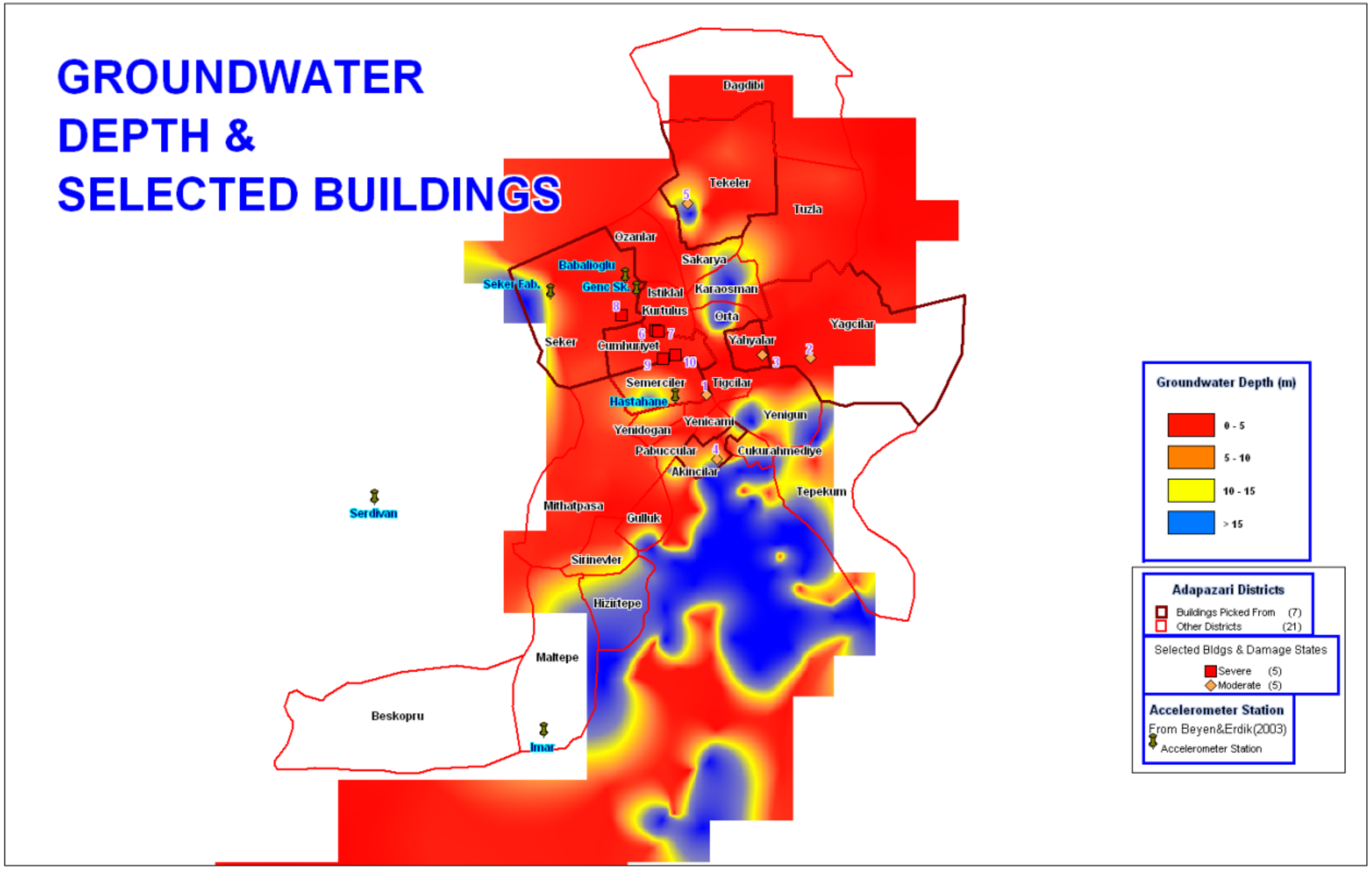

Figure B.13 Variation of the groundwater depth within Adapazarı basin

APPENDIX C

ANALYTICAL MODELS OF THE BUILDINGS

3D views of the analytical models constructed for the buildings studied are presented here. Additionally, ground story plans of the buildings are given in the DVD enclosed. The details of the analytical models were described in 5.3.

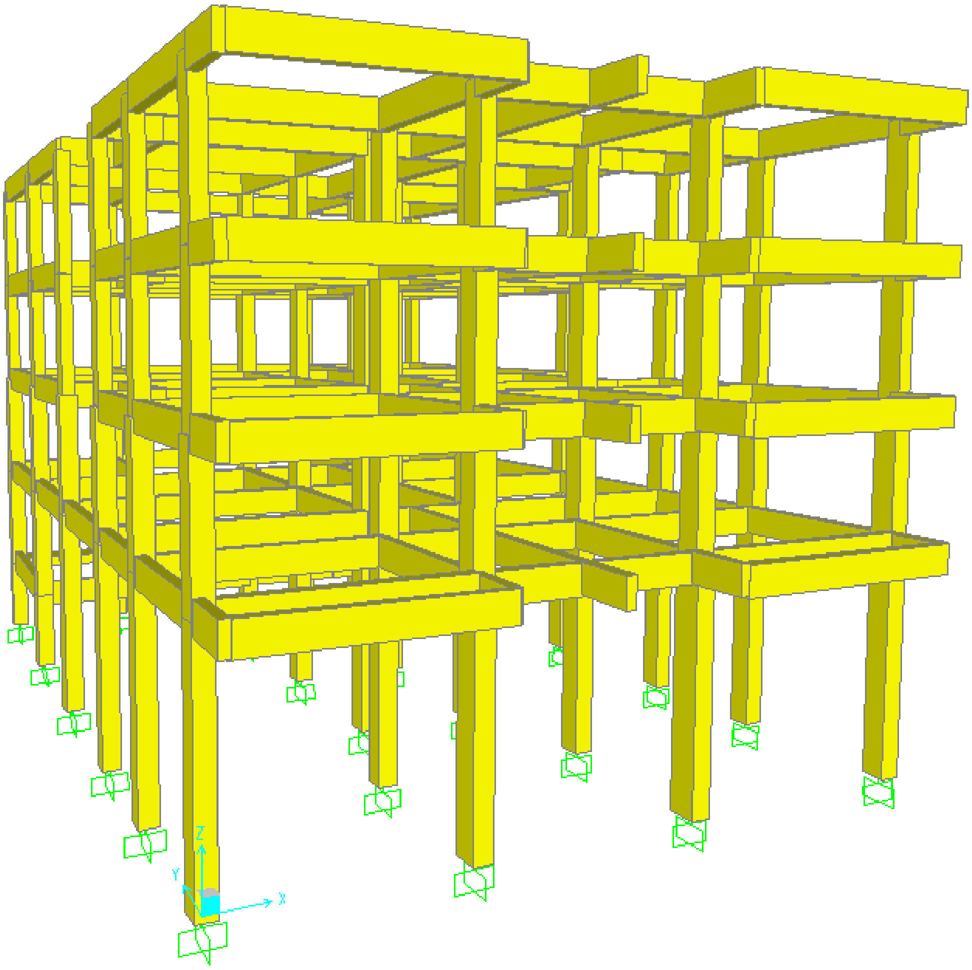

Figure C.1 3D view of the analytical model of the Building 1

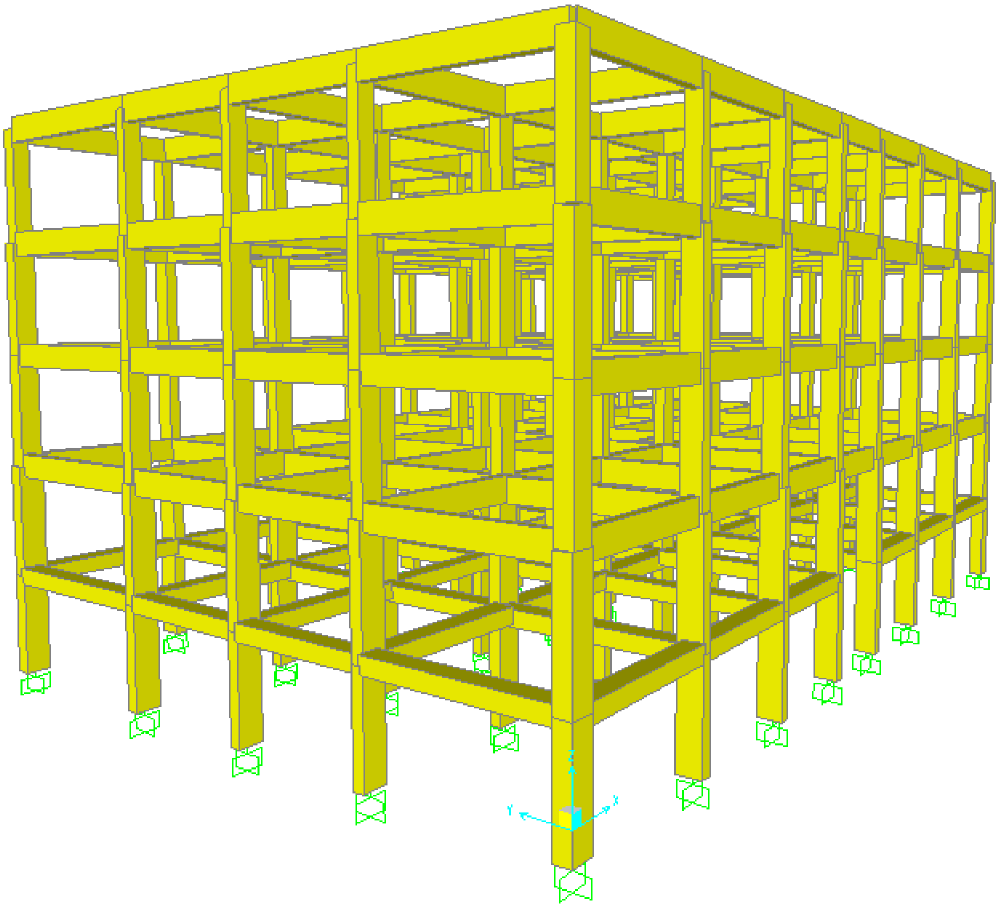

Figure C.2 3D view of the analytical model of the Building 2

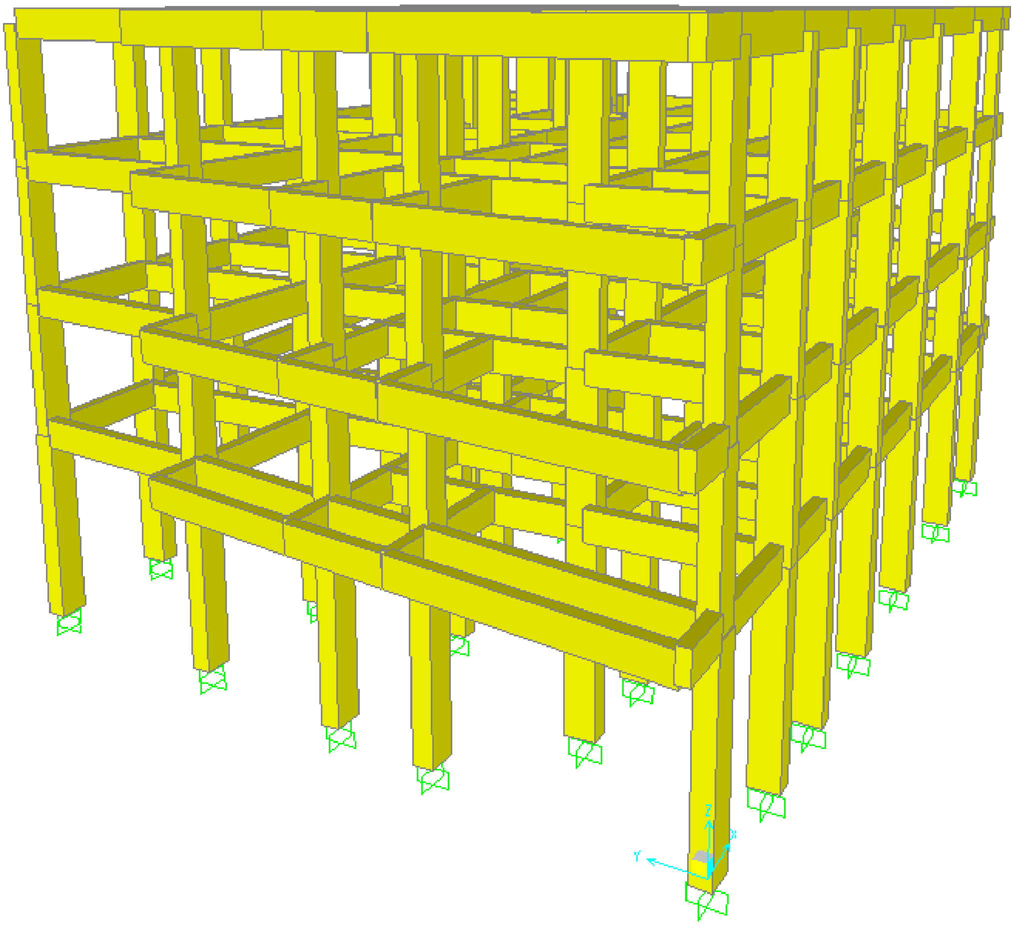

Figure C.3 3D view of the analytical model of the Building 3

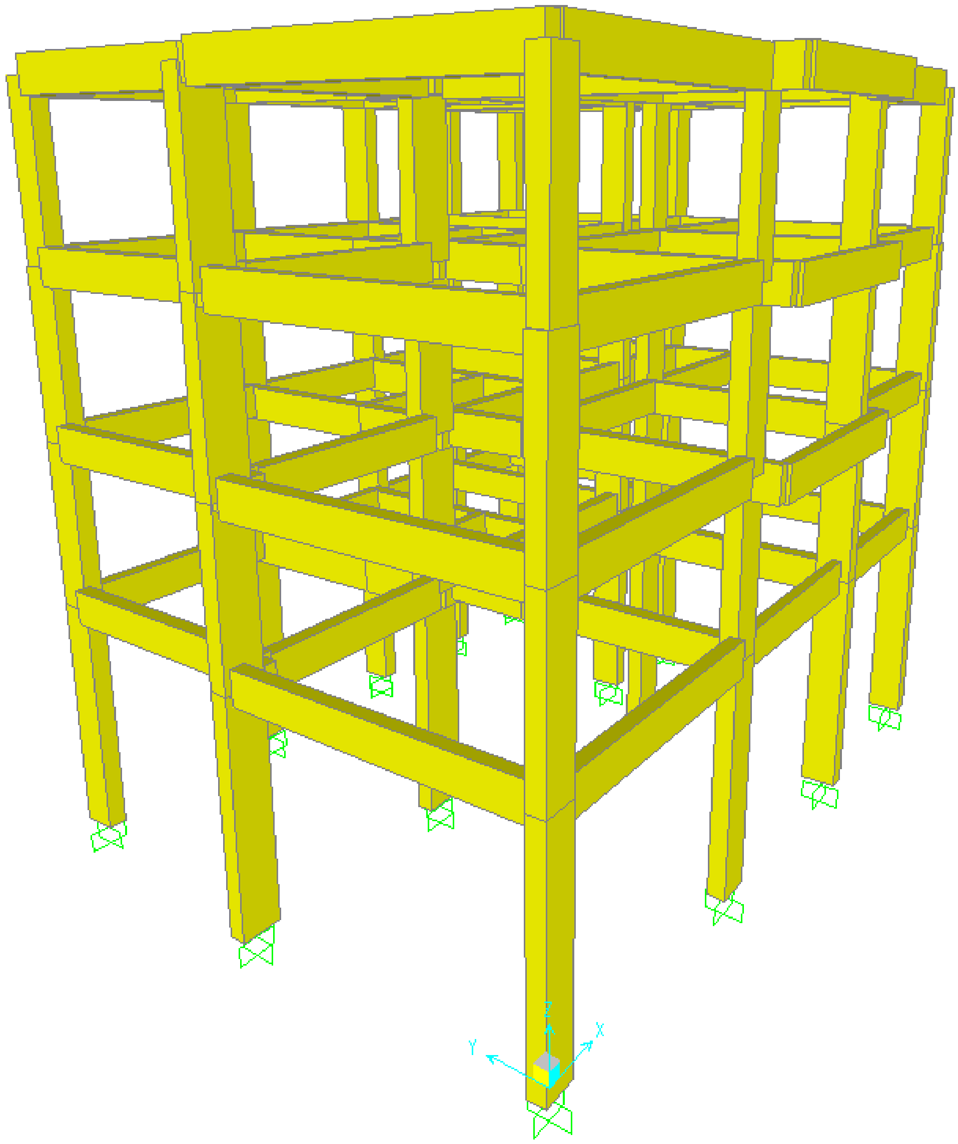

Figure C.4 3D view of the analytical model of the Building 4

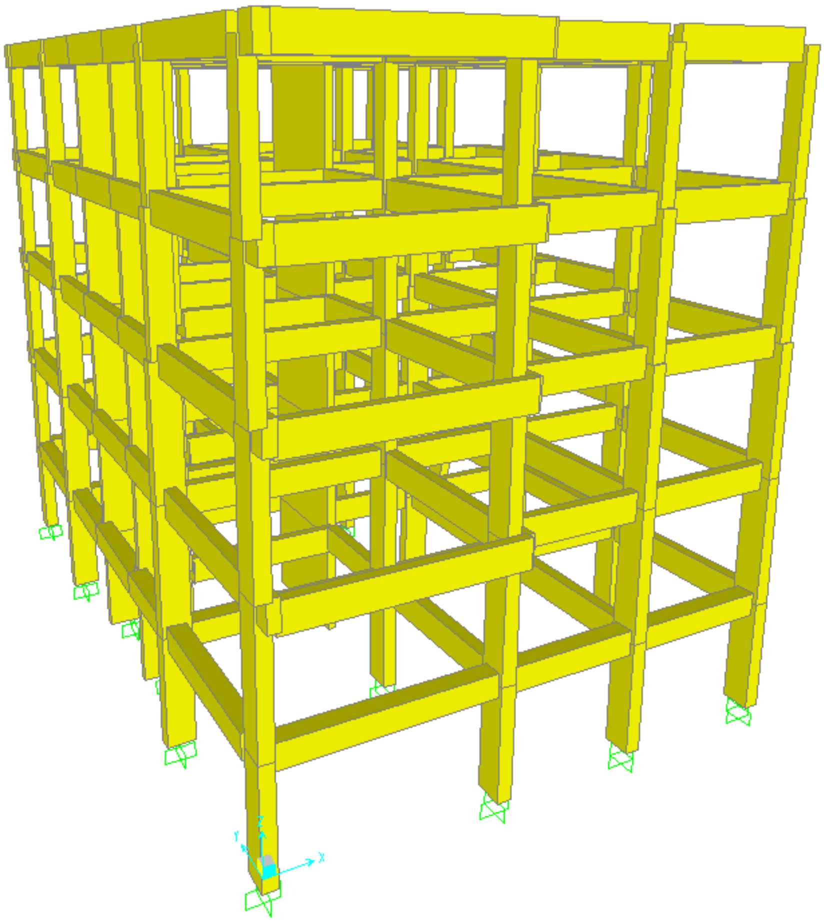

Figure C.5 3D view of the analytical model of the Building 5

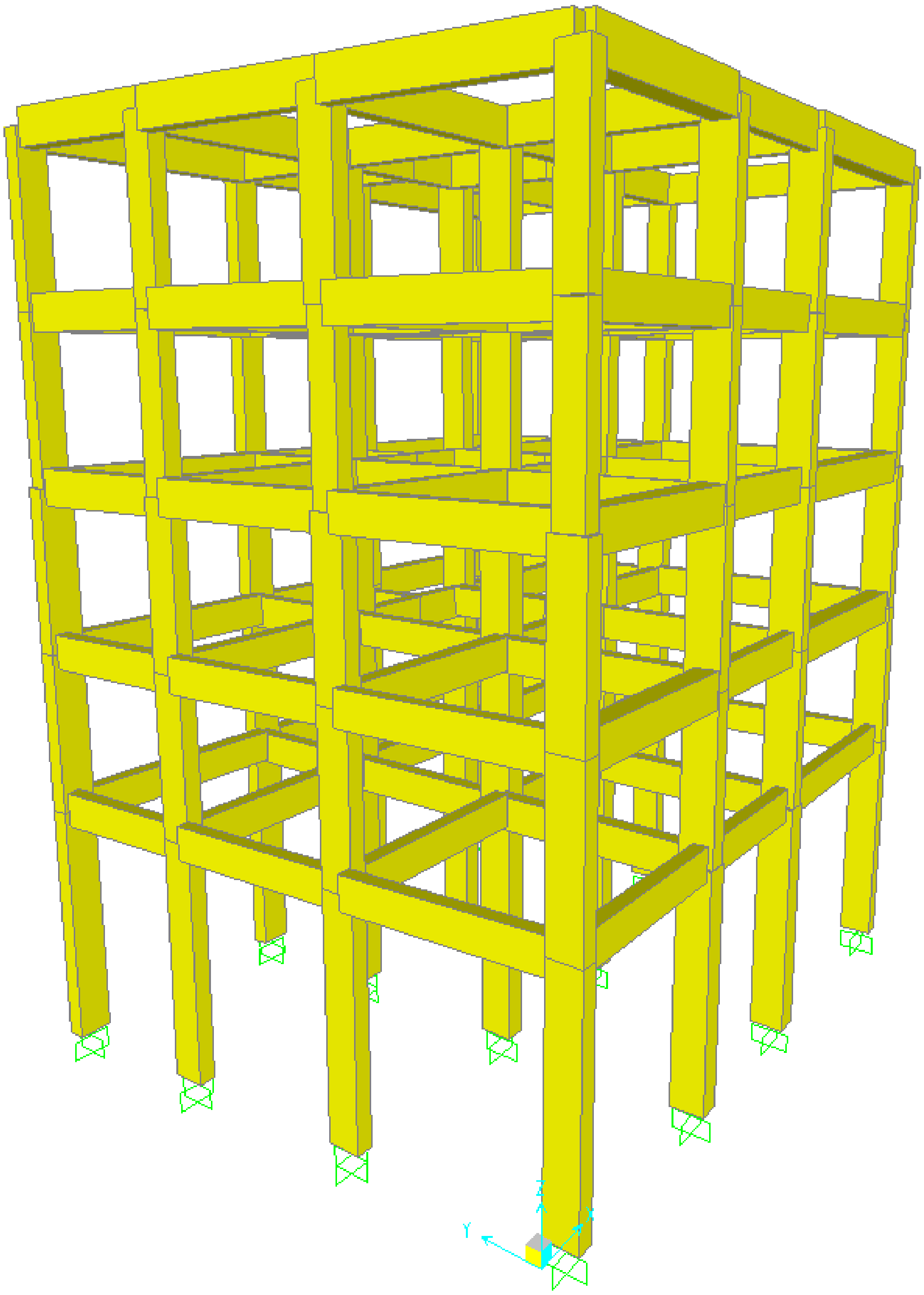

Figure C.6 3D view of the analytical model of the Building 6

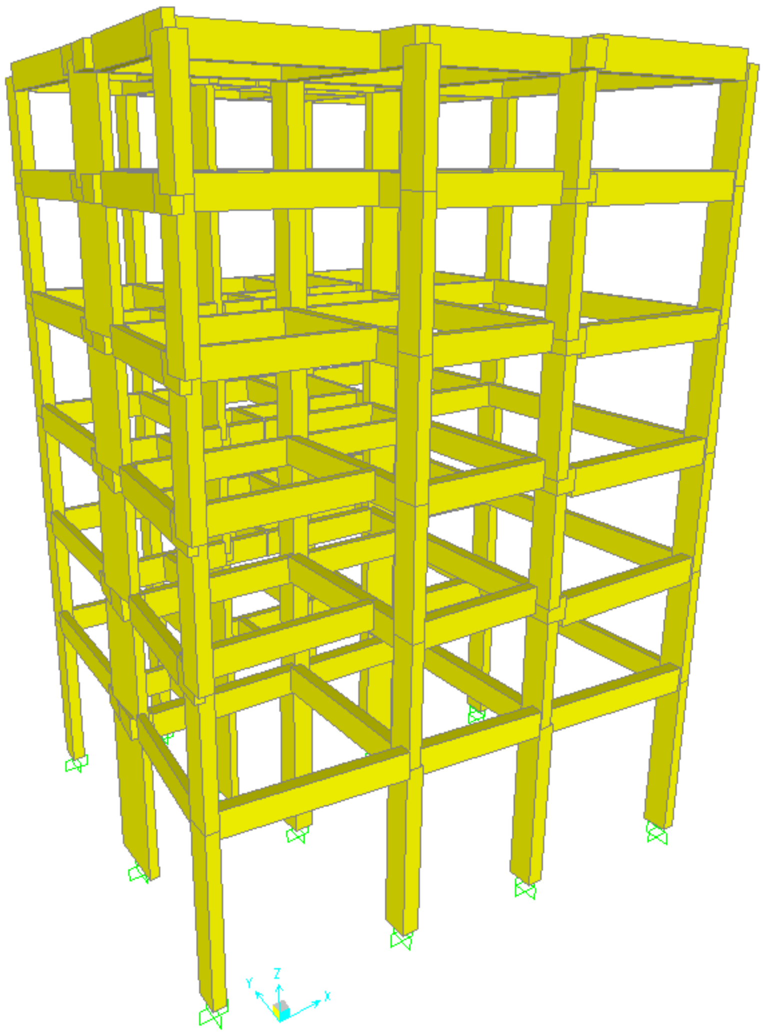

Figure C.7 3D view of the analytical model of the Building 7

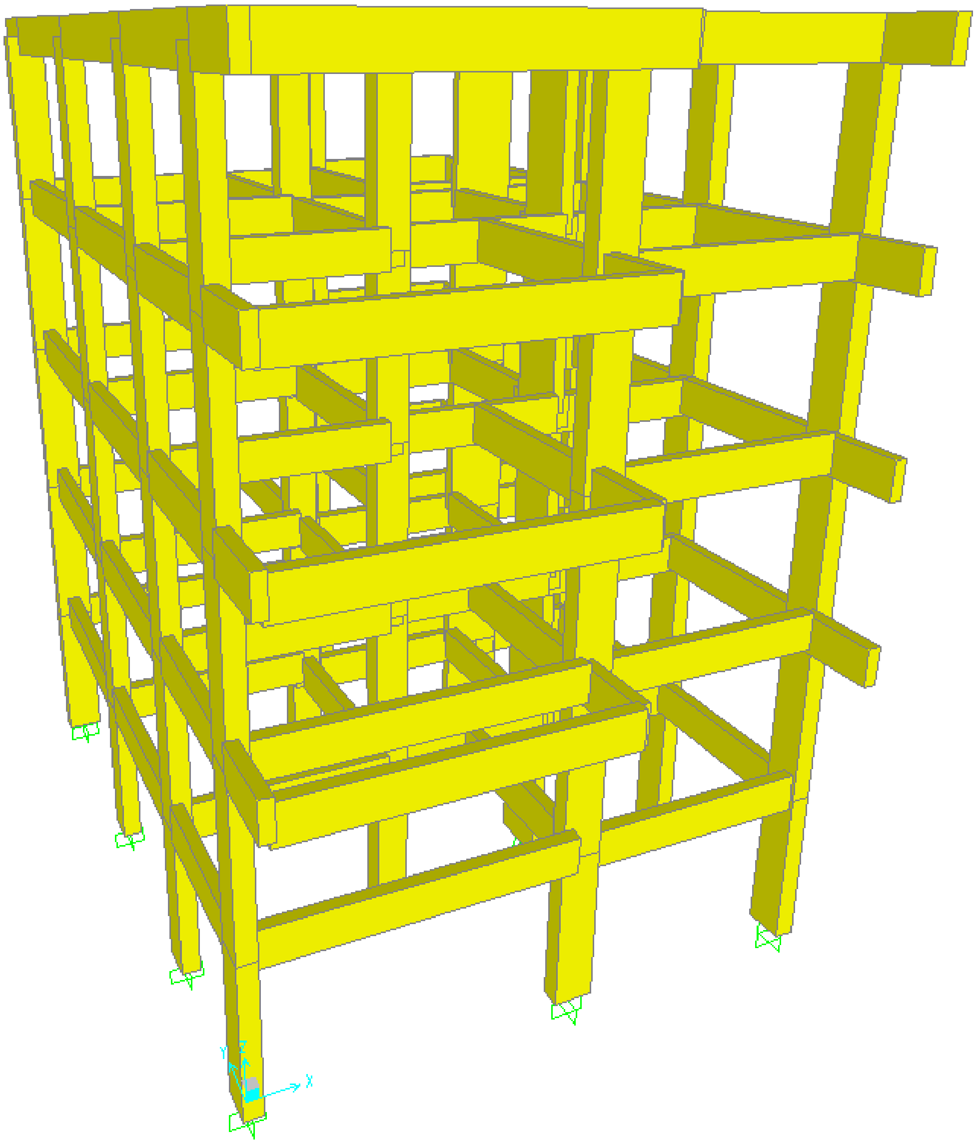

Figure C.8 3D view of the analytical model of the Building 8

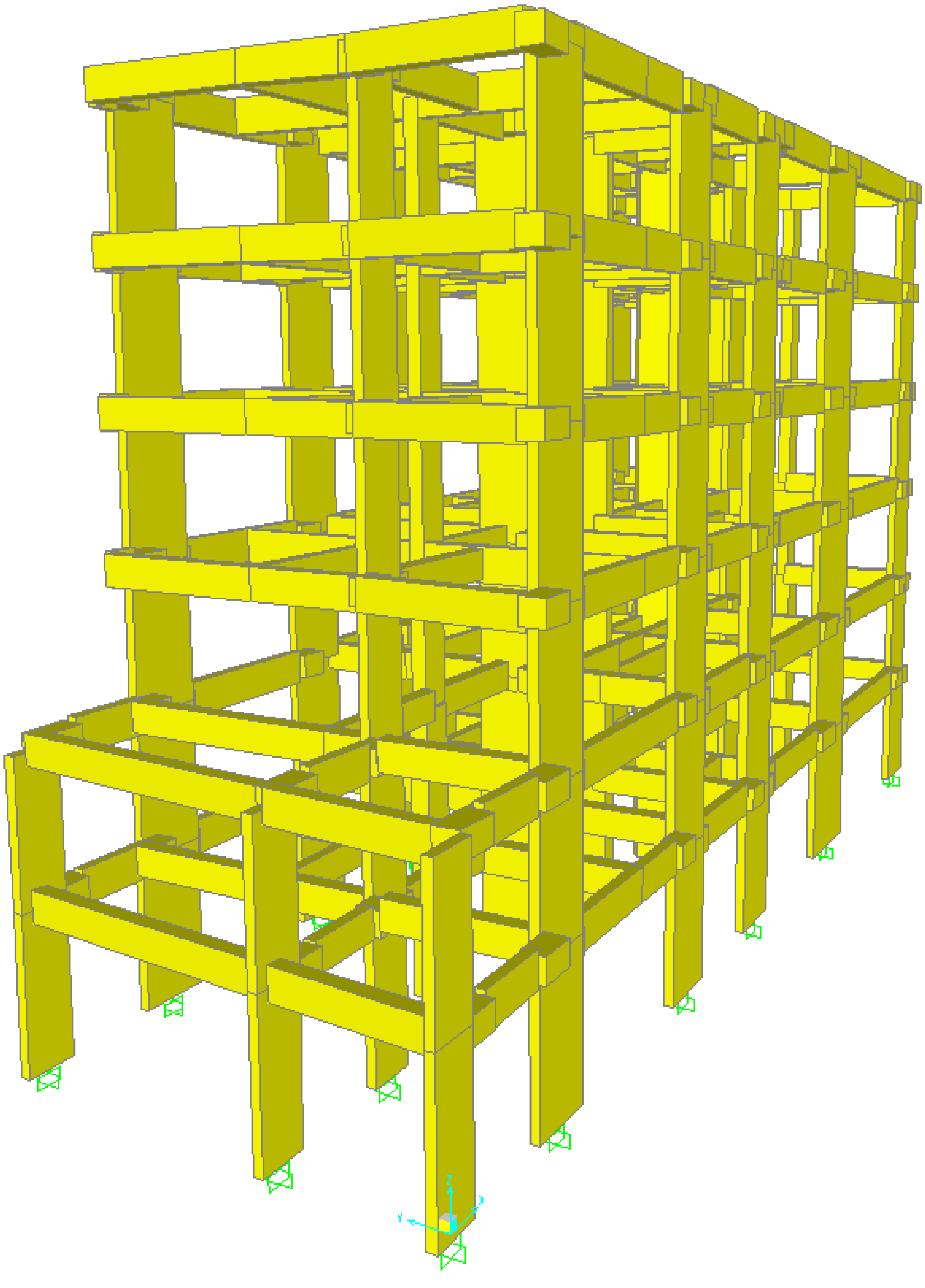

Figure C.9 3D view of the analytical model of the Building 9

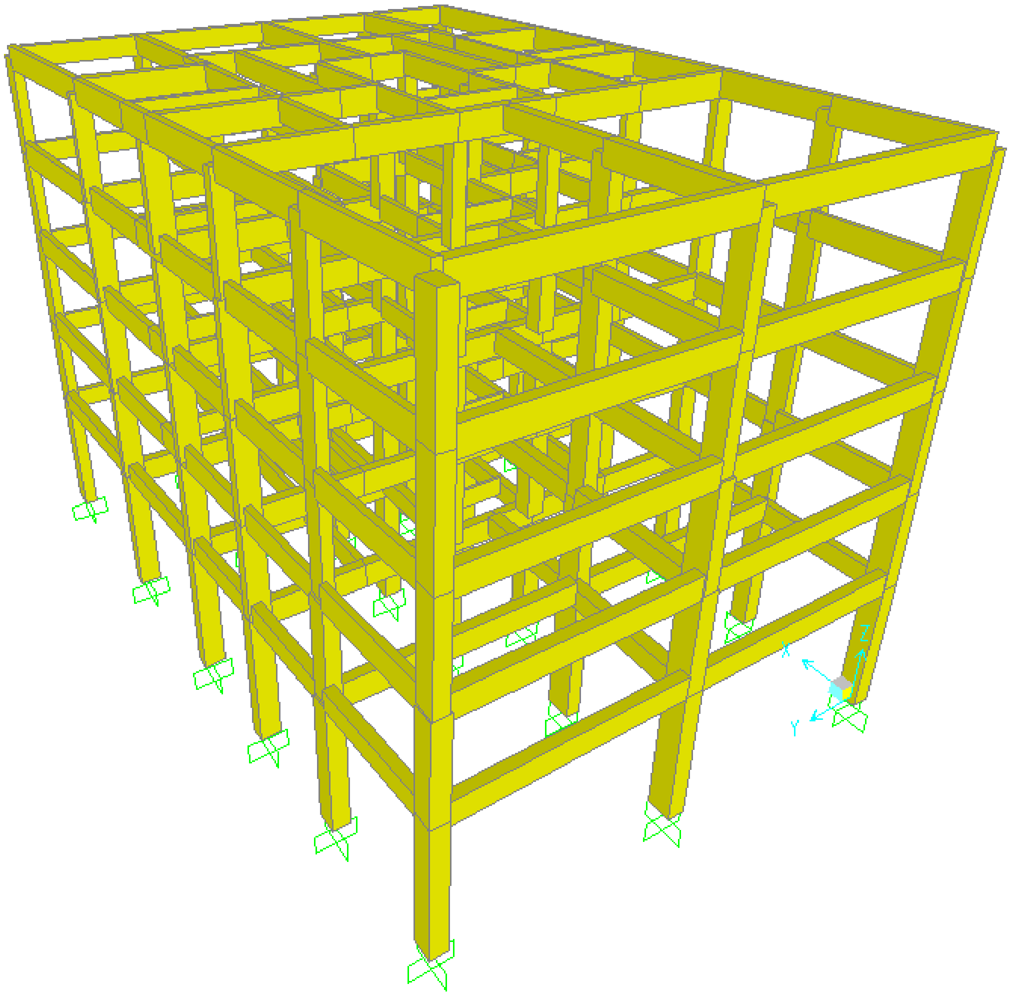

Figure C.10 3D view of the analytical model of the Building 10

APPENDIX D

AVAILABLE TECHNICAL REPORTS OF BUILDINGS

For the buildings studied, there are only two available technical reports for Building 2 and Building 5, as discussed in Section 4.2. These reports that are all in Turkish are presented here.

T.C.
SAKARYA ÜNİVERSİTESİ
MÜHENDİSLİK FAKÜLTESİ DEKANLIĞI
İNŞAAT MÜHENDİSLİĞİ BÖLÜM BAŞKANLIĞI

Sayı : B.30.2 saü.0.45.00.80-/ 15/11/2001

Konu : Hasar Tespiti Hk.

Tespit İsteyen: **Petek Evler Yapı Koop. Başkanlığı**

17 AĞUSTOS 1999'DA MEYDANA GELEN MARMARA DEPREMININ YAPIDA SEBEP OLDUĞU HASARLARLA İLGİLİ TETKİK VE TESBİT RAPORU

Yapının Adresi : Sakarya Adapazarı Yağcılar Mahallesi Alçak Tarla Mevkii,50 pafta ,955 ada ve 438 parsel Adapazarı.

Yapının Cinsi : A, C ve G bloklardan oluşan Bodrum+4 katlı Betonarme Karkas yapılar

Deprem Sebebiyle Yapıda Meydana Gelen Hasarlar:

15.11.2001 Tarihli dilekçeli başvurunuz üzerine Adapazarı Yağcılar Mahallesi Alçak tarla mevkii ve tapunun 50 pafta ,955 ada ve 438 nolu parselde bulunan Petek Evler Yapı Kooperatifine ait A.C ve G bloklardan oluşan inşaatlara gidilerek binalar yerinde gezilerek incelenmiştir.

Yapılan incelemelerde her biri bodrum+4 kattan oluşan Betonarme karkas yapılı A,C ve G Blok inşaatların 17.08.1999 da meydana gelen Marmara depreminden ve bugüne kadar oluşan münferit depremlerden dolayı taşıyıcı sistemlerinin (kolon, kiriş ve perdelerin) herhangi bir hasar görmediği ve zeminde batmaların olmadığı saptanmıştır. Ayrıca beton kalitesini belirlemek amacıyla daha önce alınan beton karot numunelerin değerlendirilmesinden beton kalitesinin de BS16 olduğu belirlenmiştir.

Bina halihazır durumuyla hasarsız bir binadır. Ancak binanın kullanılması için Zemin Etütlerinin yapılması ve mevcut projenin 1998 Deprem yönetmelikleri çerçevesinde yeniden değerlendirilmesi gerekir.

Bilgilerinize rica ederiz. 15/11/2001

İnş.Müh. Müfit Camcı

Yrd.Dr. Mansur SÜMER
Yapı Malz. Ana Bilim Dalı Bşk.

T.C
SAKARYA ÜNİVERSİTESİ
MÜHENDİSLİK FAKÜLTESİ DEKANLIĞINA
İNŞAAT MÜHENDİSLİĞİ BÖLÜM BAŞKANLIĞI

Sayı :B.30.2 SAÜ.0.45.00./ 08 /10 /2001
Konu : Karot Alma

TEKNİK RAPOR

Petek Evler Konut Yapı Başkanlığına

ADAPAZARI

Adapazarı Yağcılar Mahallesi Petek Evler Sitesi A.C ve G Blok İnşaatlarından alınan beton karot numuneler üzerinde yapılan basınç deneyleri sonuçları aşağıda verildiği gibi bulunmuştur.

Numune No	Numunenin Alındığı Yer	Numune Çapı (cm2)	Kesit Alanı (cm2)	Kırılma Yükü (kg)	Eşdeğer Küb Basınç Dayanımı (kg/cm2)	Beton Sınıfı
1	A Blok	7,6	45,34	8075	178	BS16
2		7,6	45,34	9370	207	
3		7.6	45,34	10200	225	
4		7,6	45,34	6950	154	
5		7,6	45,34	8385	185	
1	C Blok	7,6	45,34	9570	211	BS16
2		7,6	45,34	9820	217	
3		7,6	45,34	7980	176	
4		7,6	45,34	9380	207	
5		7,6	45,34	7950	175	
1	G Blok	7,6	45,34	9250	204	BS16
2		7,6	45,34	6950	154	
3		7,6	45,34	8750	193	
4		7,6	45,34	8920	197	
5		7,6	45,34	9570	211	

Bilgilerinize Rica Ederiz

Tek.Recai Şenyurt İnş.Müh Müfit CAMCI

Yrd.Doç.Dr. Mansur SÜMER
SAÜ, Müh. Fak, İnşaat Müh. Böl.
Yapı Malz. Anabilim Dalı Başkanı

Proje Kontrol Müşavirliği
Geçici Belgesi Uygulama Esasları
5.Maddesi Gereğince Sorumluluk
Proje Kontrol Müşavirine Ait Olmak
Üzere Tasdik Edilmiştir.

TEKNİK RAPOR

Tekeler mahallesi, 107 Pafta, 783 Ada, 442 Parseldeki Dostlar Yapı Kooperatifi'ne ait A2, B2 ve C2 blokları 17 AĞUSTOS 1999 depreminde orta hasarlı duruma gelmiştir.

Ruhsatlı projesine göre, Bodrum + 4 katlı ve betonarme olarak inşa edilmiştir. İnşaatın temeli radye temel olarak yapılmıştır. Binada dolgu malzemesi olarak, yatay delikli tuğla kullanılmıştır. *Bina ruhsatlı projesine uygun olarak yapılmıştır.*

Yapılan zemin etütleri neticesinde, zeminde sıvılaşma olmadığı tespit edilmiştir. Zemin emniyet gerilmesi 0,62 kg/cm^2 dır.

Projesinde görüldüğü gibi uygun yerlere deprem perdeleri konularak 1998 Deprem Yönetmeliğine uygun hale getirilmiştir.

Deprem perdeleri mevcut elemanlara ankraj çubukları ve epokxi malzemeleri ile ankrajlanacaktır. Ankraj delikleri tozdan tamamen arındırıldıktan sonra epoxi malzemesi uygulanacaktır.

Binada mevcut malzeme BS 16 ST I 'dir. Yeni kullanılacak malzeme BS 20ST III olacaktır.

Onarım ve güçlendirme denetimim altında yapılmaktadır.

Arif TAŞLICA
İNŞ. MÜH. PM:479
Oda sicil no:21387

Fahrettin KEKLİK
Ruhsat Müdür V.

Mehmet Cesim AKTAŞ
İnşaat Mühendisi

ONANDI
Adapazarı Belediyesi
İmar İşleri Müd.
Tarih :
12 ARALIK 2001

CURRICULUM VITAE

PERSONAL INFORMATION

Surname, Name: Dilsiz, Abdullah

Nationality: Turkish (TC)

Date and Place of Birth: 23.06.1978, Kırıkkale

Marital Status: Married

Email: adilsiz@yahoo.com

EDUCATION

2004-2013	Ph.D., Civil Engineering, METU
2001-2004	MS, Civil (Earthquake) Engineering, Istanbul Technical University
1996-2001	BS, Civil Engineering, Kırıkkale University
1993-1996	Kırıkkale Science Lycee

WORK EXPERIENCE

2005-2013	Research Assistant, Department of Civil Engineering, METU
2003-2004	Project Director, Istanbul Metropolitan Municipality, Transportation Department, İstanbul.
2001-2002	Civil Engineer, Istanbul Metropolitan Municipality, Transportation Department, İstanbul.

PUBLICATIONS

Dilsiz, A., "A CRITICAL EVALUATION OF PERFORMANCE ASSESSMENT PROCEDURES IN THE LIGHT OF FIELD DATA", The 9th U.S. National and 10th Canadian Conference on Earthquake Engineering, Toronto / Canada, July 25 – 29, 2010.

Dilsiz, A., Gülkan, P., “PERFORMANS TAHMİN METOTLARININ SAHA VERİLERİYLE DEĞERLENDİRİLMESİ”, Sakarya International Symposium of Earthquake Engineering, Kartepe / Kocaeli / Turkey, October 1 – 2, 2009.

Dilsiz, A., Gülkan, P., “A CASE STUDY: EFFECTS OF SELECTED MODELING PARAMETERS ON PERFORMANCE ESTIMATES OF BUILDINGS”, International Earthquake Symposium Kocaeli 2009, Kocaeli / Turkey, August 17 – 19, 2009.

Türer, A., Dilsiz, A., “TÜRKİYE’DE YIĞMA BİNALAR İÇİN DEPREMSEL RİSK HARİTASI OLUŞTURULMASI (Forming a Seismic Risk Map for the Masonry Buildings in Turkey)”, Deprem Sempozyumu Kocaeli 2005, Kocaeli / Turkey, March 23 – 25, 2005.

Dilsiz A., “Evaluation of the Seismic Resistance of Existing Reinforced Concrete Buildings”, Master Thesis, İstanbul Technical University, 2004.